

# NOTE TO USERS

This reproduction is the best copy available.

**UMI**<sup>®</sup>



**STUDY OF DISTRIBUTED OCCUPANT-SEAT INTERACTIONS AS AN  
OBJECTIVE MEASURE OF SEATING COMFORT**

Anthony Tarczay

A Thesis  
in  
the Department  
of  
Mechanical Engineering

Presented in Partial Fulfillment of the Requirements

For the Degree of Master of Applied Science at

Concordia University

Montreal, Quebec, Canada

April 2005

© Anthony Tarczay, 2005



Library and  
Archives Canada

Bibliothèque et  
Archives Canada

Published Heritage  
Branch

Direction du  
Patrimoine de l'édition

395 Wellington Street  
Ottawa ON K1A 0N4  
Canada

395, rue Wellington  
Ottawa ON K1A 0N4  
Canada

*Your file* *Votre référence*

*ISBN: 0-494-04432-2*

*Our file* *Notre référence*

*ISBN: 0-494-04432-2*

#### NOTICE:

The author has granted a non-exclusive license allowing Library and Archives Canada to reproduce, publish, archive, preserve, conserve, communicate to the public by telecommunication or on the Internet, loan, distribute and sell theses worldwide, for commercial or non-commercial purposes, in microform, paper, electronic and/or any other formats.

The author retains copyright ownership and moral rights in this thesis. Neither the thesis nor substantial extracts from it may be printed or otherwise reproduced without the author's permission.

#### AVIS:

L'auteur a accordé une licence non exclusive permettant à la Bibliothèque et Archives Canada de reproduire, publier, archiver, sauvegarder, conserver, transmettre au public par télécommunication ou par l'Internet, prêter, distribuer et vendre des thèses partout dans le monde, à des fins commerciales ou autres, sur support microforme, papier, électronique et/ou autres formats.

L'auteur conserve la propriété du droit d'auteur et des droits moraux qui protègent cette thèse. Ni la thèse ni des extraits substantiels de celle-ci ne doivent être imprimés ou autrement reproduits sans son autorisation.

---

In compliance with the Canadian Privacy Act some supporting forms may have been removed from this thesis.

Conformément à la loi canadienne sur la protection de la vie privée, quelques formulaires secondaires ont été enlevés de cette thèse.

While these forms may be included in the document page count, their removal does not represent any loss of content from the thesis.

Bien que ces formulaires aient inclus dans la pagination, il n'y aura aucun contenu manquant.

  
**Canada**

## **ABSTRACT**

### **STUDY OF DISTRIBUTED OCCUPANT-SEAT INTERACTIONS AS AN OBJECTIVE MEASURE OF SEATING COMFORT**

Anthony Tarczay

The automotive interior is characterized as a confined workspace into which the occupants are required to adapt in order to perform the normal driving and vehicular control tasks. As part of the interface between the driver and the automobile, the automotive seat must provide the occupant with a comfortable environment in which driving can be performed in a safe and comfortable manner. Prolonged exposure to excessive loading on the body in the seated position is related to discomfort and pain. Seating comfort has been found to be a complex function of the occupant anthropometry, the seated posture and many seat design factors. The characterization of the interactions between the occupant and the seat under various conditions thus constitutes an important goal for enhancing the knowledge of essential design factors that could yield improved seating comfort.

The occupant-seat interactions are investigated through measurement and analysis of the generalized and distributed contact forces and pressures at the body-seat-pan and body-backrest interfaces of a total of three different automotive seats. The contact force, contact area, and peak and mean pressure responses are analyzed as a function of the occupant anthropometry, the seated posture and the seat design features. Single and multi-factor statistical analyses are performed for the response data to identify the significance of the experimental factors considered in this study.

Those include posture related factors, such as seat height, the knee angle and the backrest angle, while the seat design factors are quantified by the cushion static stiffness over the entire subject weight range as well as the cushion contouring. Multiple linear regression functions are formulated to describe the relative contribution of the significant factors to the measured responses. The results of the comprehensive statistical analyses reveal that the alleviation of high interface pressures in some areas of the body pose conflicting contact effects on other body segments also known to be sensitive to pressure loading. Investigations into the cushion properties have shown that adequate cushion contouring and appropriate static stiffness also provide efficient methods for the alleviation of pressure loading.

## **ACKNOWLEDGMENTS**

I would thank my supervisors, Dr. Subhash Rakheja and Dr. Ali Akgunduz, for initiating this project as well as for their technical, financial and motivational support throughout the completion of this thesis work.

I would also like to thank Mr. José Esteves for his technical support and criticism during my work at CONCAVE. His constant input has extended this learning experience far beyond the scope of the work presented in this thesis.

I wish to thank all the students at CONCAVE who have volunteered their help during the experimental and analytical stages of the thesis.

## **TABLE OF CONTENTS**

LIST OF FIGURES	ix
LIST OF TABLES	xiii
LIST OF ABBREVIATIONS AND SYMBOLS	xv

### **CHAPTER 1**

#### **INTRODUCTION AND SCOPE OF RESEARCH**

1.1	Introduction	1
1.2	Review of Literature	3
1.2.1	Biomechanics of Comfort	3
1.2.2	Seat Design	10
1.2.3	Cushion Materials: Properties and Behavior	15
1.2.4	Comfort Assessment: Subjective Measures	19
1.2.5	Comfort Assessment: Objective Measures	22
1.2.6	Review of Pressure Measurement Technology	29
1.3	Scope and Objectives of the Dissertation	31
1.4	Organization of the Dissertation	34

### **CHAPTER 2**

#### **EXPERIMENTAL METHODOLOGY AND CUSHION CHARACTERIZATION**

2.1	Introduction	35
2.2	Body Pressure Distribution Measurement Methodology	36
2.2.1	Test Matrix	36
2.2.2	Experimental Setup	38
2.2.3	Data Acquisition of Body Pressure Distribution	39



2.3	Characterization of Static Properties of Test Seats	40
2.3.1	Cushion Characterization Methodology	41
2.3.2	Test Setup and Data Acquisition of Force-Deflection Characteristics	47
2.4	Test Seat Comparison	50
2.5	Static Properties of Test Seats	52
2.6	Summary	64

### **CHAPTER 3**

#### **GENERALIZED CONTACT FORCES AND PRESSURE ANALYSIS AT THE HUMAN-SEAT INTERFACE OF AUTOMOTIVE SEATS**

3.1	Introduction	65
3.2	Data Analysis	66
3.3	Analysis of Seat-Pan Contact Force and Peak Contact Pressure	67
3.3.1	Relationship between Seat-Pan Contact Force and Posture	78
3.3.2	Relationship between Peak Pressure and Posture	86
3.3.3	Postural Effects on Contact Area and Mean Pressure	89
3.4	Regression Model Diagnostics and Best Subset Regressor	94
3.5	Summary of Seat-Pan Analysis	96
3.6	Total Backrest Contact Forces and Pressures	98
3.6.1	Relationship between the Backrest Contact Force and Seated Posture	106
3.6.2	Relationship between Interface Pressure and Posture	113
3.7	Summary of Backrest Analysis	114
3.8	Summary of Generalized Seat-Pan and Backrest Analyses	115

## **CHAPTER 4**

### **DISTRIBUTED CONTACT PRESSURE ANALYSIS AT THE HUMAN-SEAT INTERFACE OF AUTOMOTIVE SEATS**

4.1	Introduction	116
4.2	Analysis of Distributed Seat-Pan Forces and Pressures	117
4.2.1	Postural Effects on the Distribution of Seat-Pan Contact Forces	119
4.2.2	Distribution of Seat-Pan Contact Pressure	125
4.3	Analysis of Distributed Backrest Contact Forces and Pressures	129
4.3.1	Postural Effects on the Distribution of Backrest Contact Forces	131
4.3.2	Distribution of Backrest Contact Pressure	139
4.4	Distribution of Total Body Weight	142
4.5	Summary	145

## **CHAPTER 5**

### **CONCLUSIONS AND RECOMMENDATIONS FOR FUTURE WORK**

5.1	Highlights of the Study	148
5.2	Conclusions	150
5.3	Recommendations for Future Work	153
	REFERENCES	154
	APPENDIX A: Seat-Pan Data Plots	159
	APPENDIX B: Sample Statistical Output from SPSS	180

## LIST OF FIGURES

- Figure 1.1: Lateral view of the spine in its natural shape
- Figure 1.2: Lateral view of spine in poorly supported posture [5]
- Figure 1.3: Lateral view of the spine in a properly supported posture [5]
- Figure 1.4: Reference dimensions for automotive seat design
- Figure 1.5: SAE J826 2D H-point template [12]
- Figure 1.6: 3-D H-point Machine defined by SAE J 826 [12]
- Figure 1.7: Vehicle interior dimension envelops [13]
- Figure 1.8: Stress-strain relationship of PUF [16]
- Figure 1.9: Percent weight distribution for three different car seats over predefined seat zones [31].
- Figure 1.10: Schematic diagram of common pressure measurement system.
- Figure 2.1: Static test stand for BPD measurements
- Figure 2.2: Baseline goniometer
- Figure 2.3: Angular protractor
- Figure 2.4: Schematic diagram of the *Novel* pressure sensing mat
- Figure 2.5: SAE J1051 recommended force indenter [51]
- Figure 2.6: Tekken type indenter used by [52]
- Figure 2.7: Load application points for the “Tekken” type indenter [52]
- Figure 2.8: Typical hysteresis loop for PUF seat cushions [52]
- Figure 2.9: Test stand for load-deflection characterization of test seat cushions.
- Figure 2.10: Data flow chart for DDE and DMA blocks used in the acquisition of the load-deflection data
- Figure 2.11: Test seats selected for the study

Figure 2.12: Spring element linearization process. [55]

Figure 2.13: Comparison of force-deflection characteristics of seat 3 attained using the SAE J1051 and JASO B407 methods

Figure 2.14: Seat-pan load-deflection characteristics of the test seat

Figure 2.15: Backrest load-deflection characteristics of the test seats

Figure 2.16: Comparison of load-deflection curves of the seat-pan and backrest: (a) Seat 1; (b) Seat 2; (c) Seat 3

Figure 2.17: Seat-pan cushion stiffness as a function of subject weight

Figure 2.18: Backrest cushion stiffness as a function of subject weight

Figure 2.19: Seat-pan cushion deflection as a function of subject weight

Figure 2.20: Backrest cushion deflection as a function of subject weight

Figure 3.1: Seat-pan pressure profiles for a 76 kg subject seated on seats 1, 2 and 3

Figure 3.2: Effect of backrest angle on the seat-pan pressure distribution for a 76 kg subject seated on seat 1

Figure 3.3: Effect of knee angle on the seat-pan pressure distribution for a 76 kg subject seated on seat 1

Figure 3.4: Effect of seat height on the seat-pan pressure distribution for a 76 kg subject seated on seat 1

Figure 3.5: Correlation between the measured and estimated mean contact force at the seat- pan for the three test seats

Figure 3.6: Variations in the CFR of the seat-pan of seat 1 as a function of knee angle:  
◆ K1 - 95°; ■ K2 - 115 °; ▲ K3 - 135°.

Figure 3.7: Variations in the CFR of the seat-pan of seat 2 as a function of knee angle:  
◆ K1 - 95°; ■ K2 - 115 °; ▲ K3 - 135°.

Figure 3.8: Variations in the CFR of the seat-pan of seat 3 as a function of knee angle:  
◆ K1 - 95°; ■ K2 - 115 °; ▲ K3 - 135°.

Figure 3.9: Correlations between the measured and estimated seat-pan mean peak pressures for the three test seats.

Figure 3.10: Correlations between the measured and estimated seat-pan mean contact area for the three test seats.

Figure 3.11: Correlations between the measured and estimated seat-pan mean pressure for the three test seats.

Figure 3.12: Contact pressure profiles measured at the backrest of seats 1, 2 and 3 for a 76 kg subject.

Figure 3.13: Effect of seat height on the pressure distribution at the backrest of seat 1 for a 76 kg subject

Figure 3.14: Effect of knee angle on the pressure distribution at the backrest of seat 1 for a 76 kg subject.

Figure 3.15: Effect of backrest angle on the pressure distribution at the backrest of seat 1 for a 76 kg subject.

Figure 3.16: Correlations between the measured and estimated backrest mean contact force for the three candidate seats

Figure 3.17: Variations in the CFR of the backrest of seat 1: ♦ K1 - 95°; ■ K2 - 115 °; ▲ K3 - 135°.

Figure 3.18: Variations in the CFR of the backrest of seat 2: ♦ K1 - 95°; ■ K2 - 115 °; ▲ K3 - 135°.

Figure 3.19: Variations in the CFR of the backrest of seat 2: ♦ K1 - 95°; ■ K2 - 115 °; ▲ K3 - 135°.

Figure 4.1: Zone definitions for the seat-pan cushion.

Figure 4.2: Effect of seat height, knee angle and backrest angle on the zonal CFR variations of the seat-pan of seat 1  
(■ 5° ■ 15° ■ 25° backrest angle)

Figure 4.3: Effect of seat height, knee and backrest angle on the zonal CFR variations on the seat-pan of seat 2 (■ 15° ■ 25° backrest angle)

Figure 4.4: Effect of seat height, knee and backrest angle on the zonal CFR variations on the seat-pan of seat 3 (■ 15° ■ 25° backrest angle)

Figure 4.5: Comparisons of seat-pan contours of seats 1 (a), 2 (b) and 3 (c)

Figure 4.6: Zone definitions for the backrest cushion

Figure 4.7: Comparison of the backrest contouring of seats 1 (a), 2 (b) and 3 (c)

Figure 4.8: Effect of seat height, knee and backrest angle on the zonal CFR variations on the backrest of seat 1

( 5°  15°  25° backrest angle)



Figure 4.9: Effect of seat height, knee and backrest angle on the zonal CFR variations on the backrest of seat 2 ( 15°  25° backrest angle)



Figure 4.10: Effect of seat height, knee and backrest angle on the zonal CFR variations on the backrest of seat 3 ( 15°  25° backrest angle)

Figure 4.11: Percentage of total body weight on the seat-pan and backrest of seats 1, 2 and 3 (Mean  $\pm$  1 standard deviation)

## LIST OF TABLES

- Table 1.1: Reported dimensional ranges for postures of *least discomfort*
- Table 1.2: Percent load distribution over defined seat zones and their standard deviations after a 128 km (80 mile) drive [32].
- Table 1.3: Rate of contribution of various sensations to overall comfort [34].
- Table 1.4: Rate of contribution of various sensations to overall comfort. [35].
- Table 2.1: Weight, height and BMI of the 8 male test subjects selected for the study
- Table 2.2: BPD Test matrix
- Table 2.3: Comparison of SAE and JASO static stiffness coefficients for the seat-pan of seat 3
- Table 2.4: Deflection, static spring constant and coefficient of hysteresis loss for seat 1, 2 and 3
- Table 2.5: Seat-pan and Backrest cushion deflection and static stiffness
- Table 3.1: Mean values and standard deviations of seat-pan contact force
- Table 3.2: Mean values and standard deviations of seta-pan peak pressure
- Table 3.3: Mean values and standard deviations of seta-pan contact area
- Table 3.4: Mean values and standard deviations of seta-pan mean pressure
- Table 3.5: Contribution of seat stiffness, body weight, seat height, knee and backrest angles to seat-pan contact force
- Table 3.6: Regression coefficients for the prediction of seat-pan CFR
- Table 3.7: Contribution of seat stiffness, body weight, seat height, knee and backrest angles to seat-pan peak pressure
- Table 3.8: Contribution of seat stiffness, body weight, seat height, knee and backrest angles to seat-pan contact area
- Table 3.9: Contribution of seat stiffness, body weight, seat height, knee and backrest angles to seat-pan mean pressure

Table 3.10: Best subset regression for seat-pan contact force

Table 3.11: Best subset regression for seat-pan peak pressure

Table 3.12: Best subset regression for seat-pan contact area

Table 3.13: Best subset regression for seat-pan mean pressure

Table 3.14: Mean and standard deviation of backrest contact force

Table 3.15: Mean and standard deviation of backrest peak pressure

Table 3.16: Mean and standard deviation of backrest peak pressure

Table 3.17: Mean and standard deviation of backrest mean pressure

Table 3.18: Regression coefficients and correlation factors for contact force for seats 1,2 and 3

Table 3.19: Regression coefficients and correlation factors for peak pressure for seats 1,2 and 3

Table 3.20: Regression coefficients and correlation factors for peak pressure for seats 1,2 and 3

Table 3.21: Regression coefficients and correlation factors for contact area for seats 1,2 and 3

Table 4.1: Regression coefficients for the zonal contact force ratios for seats 1, 2 and 3

Table 4.2: Zonal mean peak pressure and standard deviations (SD) variations for seat 1

Table 4.3: Zonal mean peak pressure and standard deviations (SD) variations for seat 2

Table 4.4: Zonal mean peak pressure and standard deviations (SD) variations for seat 3

Table 4.5: Summary of ANOVA results for the backrest zonal CFR for 99.9% and 95% Confidence Intervals (CI)

Table 4.6: Regression and correlation coefficients for the backrest CFR

Table 4.7: Zonal peak pressure variations for seat 1

Table 4.8: Zonal peak pressure variations for seat 2

Table 4.9: Zonal peak pressure variations for seat 3



## LIST OF ABBREVIATIONS AND SYMBOLS

IT	Ischial Tuberosities
BDP	Body Pressure distribution
A	Hip Angle
B	Knee Angle
C	Ankle Angle
D	Pedal plane Angle
E	Backrest Angle
F	Seat Pan Angle
L1	Distance between Accelerator Heel Point and Leading Edge of Seat
L2	Length of Seat Cushion
H-30	H-point Height
Psi	Pressure – Pounds per Square Inch
Hz	Frequency of Vibration Measured in Hertz
g	Acceleration due to gravity
SgRP	Seating Reference Point
kg	mass
$X_i$	Horizontal location of the H-point
Z	Height of the H-point
PUF	Polyurethane Foam
K	Seat Coefficient of Static Stiffness
$\epsilon$	Strain
BMI	Body Mass Index

## CHAPTER 1

### INTRODUCTION AND SCOPE OF RESEARCH

#### 1.1 Introduction

The interior environment of the automobile can be characterized as a confined workstation into which drivers and passengers are required to adapt in order to perform the driving tasks. The function of the interior therefore is to provide the occupant with a suitable workspace in which the driving and control tasks can be performed in a safe and comfortable manner. The human sensation of short and long-term comfort is strongly dependent on the seat design together with the placement of controls. The presence of extreme vibration as in off-road vehicles, and poor workstation configuration design that encourages inadequate posture, could contribute to physiological symptoms of discomfort and pain. The design of automotive seats with enhanced comfort therefore necessitates careful consideration of the relationship between the seated occupant and the vehicle. Due to the unnatural posture in a seated position, body parts including the buttocks, thighs, lower legs and feet act as mechanical levers that help stabilize the body. It has been reported that prolonged exposure to an insufficiently supported posture leads to excessive static loads on the body, which result in a sensation of discomfort [1]. The occurrence of localized high pressures at the human-seat interface is known to cause soft tissue deformation leading to restricted blood and nutrient flow to the lower extremities resulting in human discomfort [2]. Furthermore, prolonged exposure to vibrations induced by the road surface irregularities and automotive components has been found to cause chronic health problems including: low back pain, spinal disorders, abdominal pain and vision disorders in the 0.5 - 80 Hz frequency range [3]. The combination of

prolonged sitting and the adverse physiological effects of exposure to vibration create an uncomfortable, and in some cases painful environment that may decrease the level of performance resulting in unsafe driving.

The comfort provided by an automotive seat is related to many design factors including: adjustability, weight distribution, seat geometry, seat cushion properties, vibration isolation, and aesthetic appeal. The sensation of sitting comfort is related to all these factors in a highly complex manner, and is difficult to quantify due to extreme variabilities in individuals' perceptions and preferences. Designing for comfort therefore requires an in depth understanding of the relationship between the behavior of the human body in the seated position and these factors. Considerable efforts have been attempted to develop effective guidelines to help design more comfortable seats. Early comfort assessments consisted in surveying sample populations on their perception of comfort in an automotive seat. This allowed seat designers and manufactures to obtain feedback on the level of comfort provided by a specific seat feature relative to the overall comfort of the seat. This approach, while necessary in the assessment of comfort, is laborious and requires a large number of subjects to obtain valid results and can also only be applied after a seat has been manufactured. Furthermore, such an approach can yield helpful design information, when relative assessments of different seats or features are involved. In an attempt to streamline the design of seats, considerable efforts are now being directed to define objective measures of the seat comfort performance. The objective is to develop quantitative tools, such as seat cushion models, that could provide insight regarding the comfort of a specific seat or feature in terms of support characteristics and vibration isolation. Very little progress, however, has been made and is mostly due to the

lack of well correlated measures of comfort, measurement analysis methods, and extreme variabilities among the individuals' perception and preference.

In this research dissertation, the occupant-seat support characteristics are investigated in terms of human-seat interface pressure distributions. The dependence of the anthropometric factors, the seat geometry, the seat height, and the resilient properties of the seat cushions and the backrests, are explored in an attempt to identify fundamental relations between interface pressure and the factors considered.

## **1.2 Review of Literature**

The ability to predict the level of comfort provided by an automotive seat requires an in depth understanding of the biomechanics of the seated posture as well as the effects of seat geometry, seat properties and vehicle environment on perceived comfort. To further study the issue of seat comfort, knowledge of the past and current assessment and measurement techniques is warranted. Thus, the following literature review highlights the relevant research pertaining to the biomechanics of comfort, current seat design methodology, and various comfort assessment techniques, in order to define the scope and objectives of the present research thesis.

### **1.2.1 Biomechanics of Comfort**

In order to make seats more comfortable, knowledge of what constitutes discomfort is of fundamental importance. The argument is that if a seat feature is known to cause discomfort, then it can be removed or modified in the design process to yield a better seat. The biomechanics pertaining to comfort in the seated position then refers to

the interactions at the human-seat interface, which could yield information relevant to body behavior while performing the driving tasks. During sitting, the primary supporting members of the body are the spine, pelvis, legs and feet, which act as a system of mechanical levers that help stabilize the body. The natural curvature of the spine, shown in Figure 1.1, is the shape in which the pressure distribution over the cervical discs and the level of static loading on the inter-vertebral muscles is optimum [1].

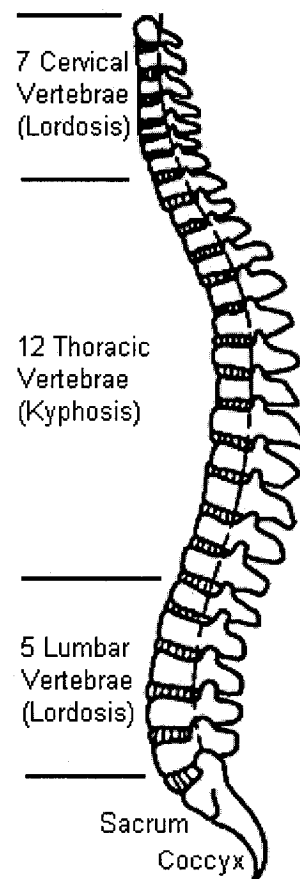


Figure 1.1: Lateral view of the spine in its natural shape

A posture that does not allow the spine to maintain its natural shape is thus assumed to eventually cause discomfort. This is explained by the fact that the muscles and tendons surrounding the spine help maintain its natural shape, and any deviation from this shape increases the stress on the surrounding muscles and tendons. The biomechanics related to the seated position can thus be further examined in three ways: first, from an orthopedic perspective which relates to the seat features that may cause the spine to adopt an “unnatural posture”, secondly, from a muscular aspect related to the energy expansion required to maintain stability in the seated posture from the muscles, and finally, from a behavioral aspect that is related to the physiological perception of comfort [1]. The deviation from the natural posture could thus yield an increase in the muscle activity required to maintain the posture; if this posture is sustained without any external support, the static loading on the spine increases encouraging muscular fatigue and spinal deformation, which could cause reduced comfort and increased stress on the spine [1]. Therefore, providing sufficient support to the back will inevitably reduce the stress on the spine and its supporting muscles and tendons. Figure 1.2 illustrates how the lack of proper support leads to excessive deformation of the spine, particularly in the thoracic and lumbar regions where both the kyphotic and lordotic curves of the spine are hyper-extended [5]. The lack of lower back support also allows the pelvis to rotate counter-clockwise towards the rear into an unstable position also leading to an increase in stress in its surrounding muscles and tendons. Thus the lack of proper back support can also affect the comfort perception in the IT and sacro-iliac region of the body.

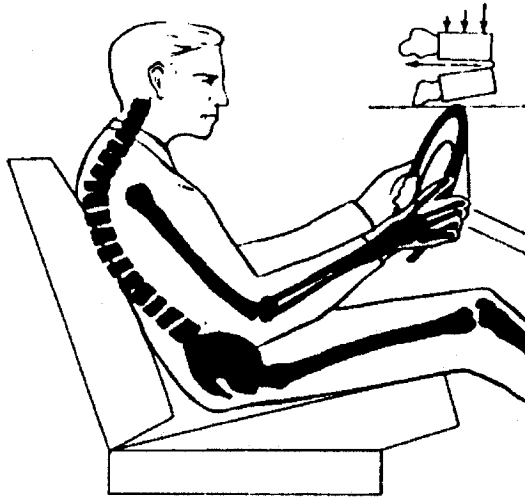


Figure 1.2: Lateral view of spine in poorly supported posture [5]

Figure 1.3, on the other hand, clearly shows how strategically placed back support can reduce the amount of spinal deformation by supporting its natural shape and reducing the amount of pelvic rotation. Much work has been done to define seat configurations that provide a minimum level of discomfort. Figure 1.4 and Table 1.1 summarize the dimensional values that have been reported to provide postures of *least discomfort* [4-9].

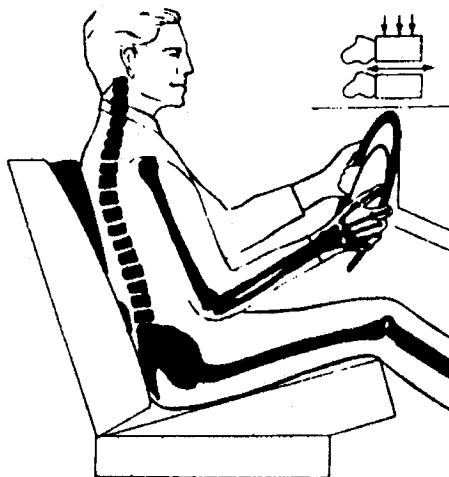


Figure 1.3: Lateral view of the spine in a properly supported posture [5]

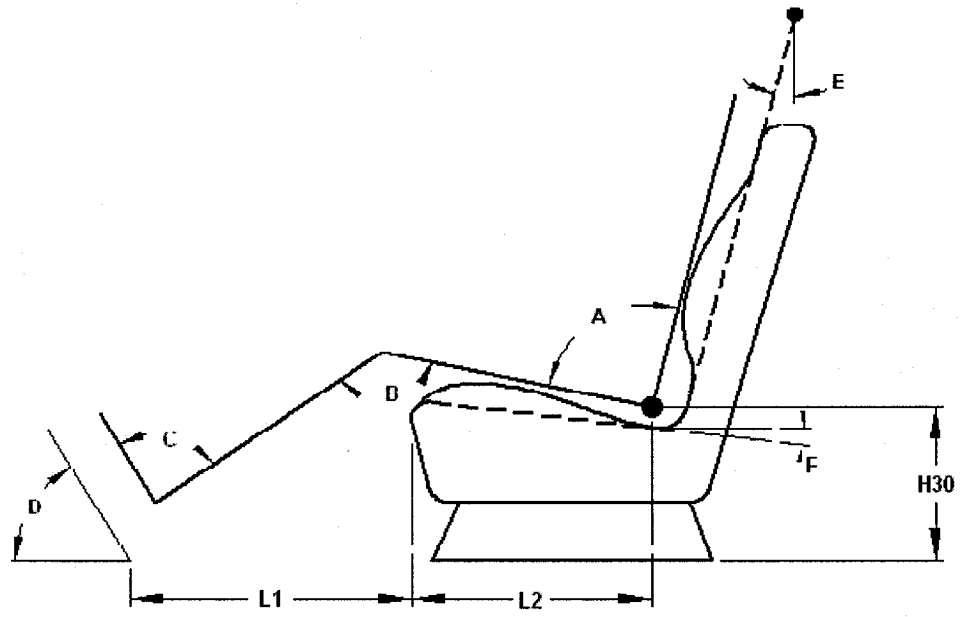


Figure 1.4: Reference dimensions for automotive seat design

Table 1.1: Reported dimensional ranges for postures of *least discomfort*

MEASURE	A (deg.)	B (deg.)	C (deg.)	D (deg.)	E (deg.)	F (deg.)	L1 (cm)	L2 (cm)	H-30 (cm)
Dempsey [4]	80 – 106	–	–	–	5 – 21	5 – 15	95 ± 9	–	27 ± 6
Sanders & McCormick [5]	95 – 120	95 – 135	90 – 110	–	20 – 30	–	–	–	–
Woodson & Conover [6]	100 – 105	–	–	35 – 40	–	6 – 8	28 – 38	43 – 46	–
Domey & McFarland [7]	112 ± 5	–	–	–	–	7	–	–	–
Judic <i>et al.</i> [8]	95 – 120	95 – 135	78 – 105	40 – 70	20 – 30	12 – 25	–	–	–
Weichenreider [9]	90 – 122	90 – 143	73 – 113	–	10 – 34	–	–	–	–



While a number of studies have proposed the ranges of seat dimensions to realize postures of least discomfort, considerable variations exist among different studies, as evident from the tabulated results. In addition to the spine, both the pelvis and the Ischial Tuberosities (IT) are under a considerable amount of stress, since both are the primary weight bearing structures of the body, in the seated position. The IT carry up to 75% of the body weight over an area of approximately  $25.8 \text{ cm}^2$  ( $4 \text{ in.}^2$ ) [4]; when the body first settles into a seated posture, the fatty tissues and the muscles surrounding the IT move away from under the bony area thereby reducing the distance between the skin of the buttocks and the bones. This results in an increase in pressure on the skin surrounding the IT, and, if no action is taken to relieve or reduce the pressure, the loading will continue to increase until it reaches the capillary pressure of 5.03 kPa (0.73 psi) where blood circulation is cut-off and skin cells begin to die (necrosis). Failure to alleviate these localized high pressures, will lead to the onset of a burning sensation and the pain threshold of 56 kPa (8.2 psi) is reached in about 30 minutes [10]. This raises the issue of cushion compliance and the properties of the cushion materials and the requirement to have some knowledge on their contribution in reducing the magnitude and distribution of pressure at the human-seat interface.

Moreover, the automobile represents a dynamic environment where the whole-body vibrations arising from irregular road profiles and various components are transmitted to the occupant through the seat. The soft tissue organs within the body may undergo significantly higher or lower deformations depending on the applied frequency and magnitude of vibration. It has been reported that under vibration at frequencies below 2 Hz, the body behaves similar to a mass and the dynamics of the seat have very little

influence. The presence of vibration in the range of 4 – 5 Hz, however, is known to excite the vertical resonant deformations of the spine and its supporting structure, and may cause extreme discomfort. Automotive seats have also been found to reduce vibrations at frequencies above 10 Hz [3]. The effects of vibration on health, motor performance and vision have also been reported in a number of studies [1,3]. Of greater significance to seat designers however, are the effects of vibration on the perception of comfort. Exposure to vibrations of rms accelerations above 0.06 – 0.09g in the 4 to 20 Hz frequency range has been reported to cause discomfort among transport passengers [11]. Based on the findings reported in [1,3] the body posture can be considered to have a significant effect on the manner in which vibration is transmitted to the body. Designing an automotive seat thus requires careful consideration of both the seat characteristics as well as the body posture in order to minimize vibration-induced discomfort. The design process would therefore require complete knowledge of the effects of the different seat parameters, such as cushion geometry, cushion stiffness, foam density, backrest geometry and contact characteristics. In order to minimize the adverse effects of poor seated posture, based on biomechanics alone, a good automotive seat must provide:

- The presence of adequate adjustable support and some freedom of mobility inside the vehicle in order to enhance driving efficiency.
- The seat features must allow for adjustability in the longitudinal direction as well as angular adjustability of the back support to accommodate users of various stature.
- An appropriate adjustable backrest support is vital to maintain the natural curvature of the spine.
- Good cushion support is essential to reduce the magnitudes of peak pressure surrounding the sensitive parts of the body, specifically near the IT and the thighs just above the knees.

- Poly-Urethane Foam (PUF) material and the seat construction must aid in reducing the magnitudes of vehicular vibrations transmitted to the human body.

### 1.2.2 Seat design methodology

Automotive seat design in North America generally follows the guidelines established by the Society of Automotive Engineers (SAE) standard J826 for road vehicles [12]. This standard defines a two-dimensional (2D) H-point template and a three-dimensional (3D) H-point machine, which are used to define and measure vehicle seating accommodations. The H-point is the pivot center of the torso and the upper thigh on the recommended 2D and 3D devices. Apart from this, a seating reference point (SgRP) defines the design reference point of a specific for seat which [12]:

1. establishes the rearmost normal design driving or riding position for each designated seating position, upon consideration of all modes of adjustments (horizontal, vertical and tilt).
2. utilizes established X, Y and Z coordinates relative to the designed vehicle structure.
3. simulates the position of the pivot center of the human torso and thigh.
4. defines the reference point employed to position 2D drafting template with the 95<sup>th</sup> percentile leg as outlined in SAE J826 [12].

The devices defined by the standards are used to obtain passenger compartment dimensions using a deflected seat rather than a free seat contour to define seating space. Figure 1.5 shows the 2D H-point template used in the preliminary design phase of automotive interiors. The template represents the profile of an adult male with shoes, and consists of separate torso, thigh, lower-leg and foot segments with locking pivot joints. Reference bars are also located at all articulated joints so that the angular relationship

between body segments can be determined. The standardized 2D template is used to display [12]:

1. Passenger compartment space and seating attitude during conceptual, engineering, and development stages of a new vehicle.
2. Passenger compartment space and seating attitude for comparison and reporting purposes.
3. Data obtained from checks made with the 3D H-point machine.

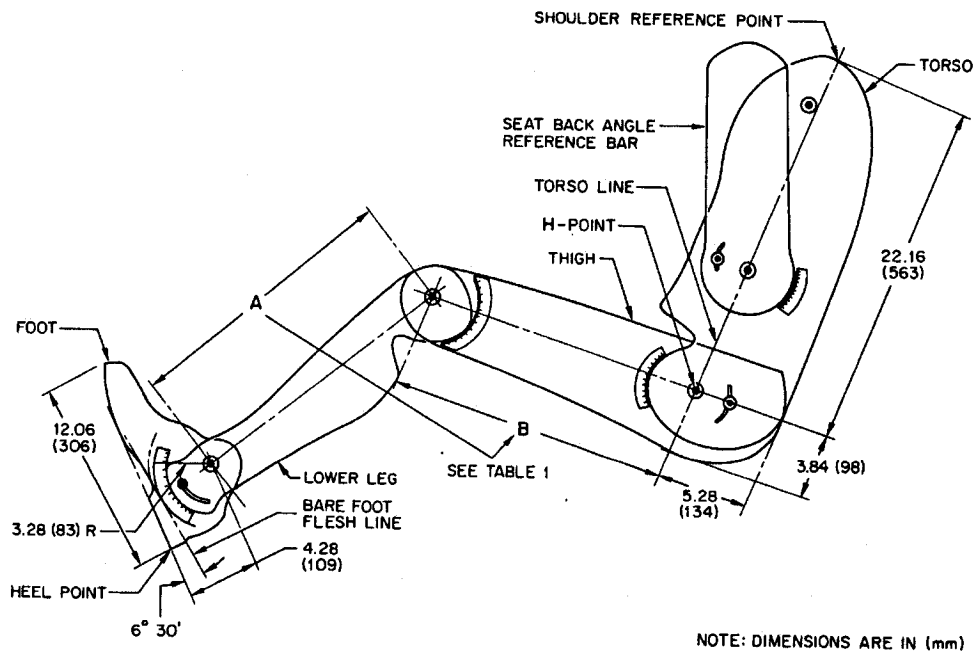


Figure 1.5: SAE J826 2D H-point template [12]

The 3D H-point machine, on the other hand, is used to define the actual H-point on any seat in any position. The 3D machine is made of reinforced plastic and metal pans, which simulates the torso and thighs hinged at the H-point. As shown in Figure 1.6, body segment weights are placed at the center of gravity locations to provide seat penetration equivalent to a 50<sup>th</sup> percentile male occupant weighing 76 kg. The functions of the 3D H-

point machine are to aid in the design and development of seats and seat materials and, also to check for conformance to seat design specifications provided by the 2D template [12].

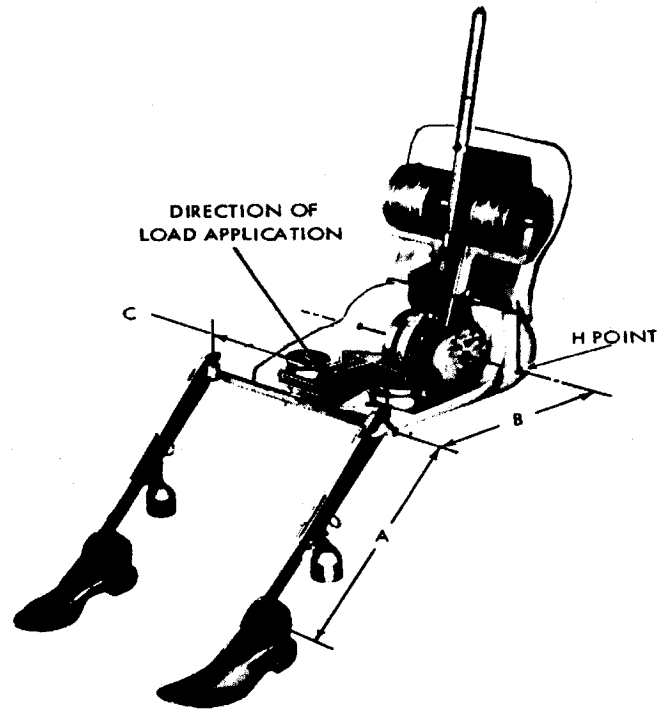


Figure 1.6: 3-D H-point Machine defined by SAE J 826 [12]

The standardized seat design methodology is defined by SAE J1517 [13], which consists in placing manikins of the 5<sup>th</sup>, 50<sup>th</sup> and 95<sup>th</sup> percentile populations in a chosen posture of *least discomfort* to define the seat dimensions. SAE J1517 is a design tool developed to describe where the percentages of drivers position their adjustable seats in various vehicle interiors. It consists of a set of second-degree polynomials that describe the horizontal location of the H-point as a function of the H-point height. These equations, define curves that represent the range of for-aft seat adjustability ranges for the 2.5<sup>th</sup>, 5<sup>th</sup>, 10<sup>th</sup>, 50<sup>th</sup>, 95<sup>th</sup>, 97.5<sup>th</sup> percentile body dimensions based on the a selected H-

point height, shown in Figure 1.6. For class A vehicles, which includes passenger cars, the horizontal distance,  $X_i$ , in millimeters of the  $i^{\text{th}}$  percentile H-point behind the ball of foot reference point, which is located on the inclined plane of the accelerator pedal is computed from [13] where  $z$  refers to the desired H-point height.

$$X_{2.5} = 687.1 + 0.895336z - 0.00210494z^2 \quad (1.1)$$

$$X_5 = 692.6 + 0.981427z - 0.00226230z^2 \quad (1.2)$$

$$X_{10} = 715.9 + 0.968793z - 0.00228674z^2 \quad (1.3)$$

$$X_{50} = 793.7 + 0.903387z - 0.00225518z^2 \quad (1.4)$$

$$X_{90} = 885.0 + 0.735374z - 0.00201650z^2 \quad (1.5)$$

$$X_{95} = 913.7 + 0.672316z - 0.00195530z^2 \quad (1.6)$$

$$X_{97.5} = 936.6 + 0.613879z - 0.00186244z^2 \quad (1.7)$$

Figure 1.7 further illustrates the relationship between the seat geometry and the vehicle interior. Simply put, the location of the seat, irrespective of the point of reference used to define the interior, affects the design and location of the steering wheel (driver hand control reach SAE J287 [14]) and the also the height of the vehicle roof which further relates to vision (Motor vehicle driver eye range SAE J941 [15]).

Although the standards are widely used in the design of automotive seats in terms of accommodating passengers of various stature, they do not represent dimensions associated with a specific level of comfort. The SAE standards [12,13] thus define the dimensional relationships only for the automotive interior to accommodate a predefined range of users. Since comfort has become an important issue in automotive seating, the current methodology proves insufficient and the need to incorporate comfort from a

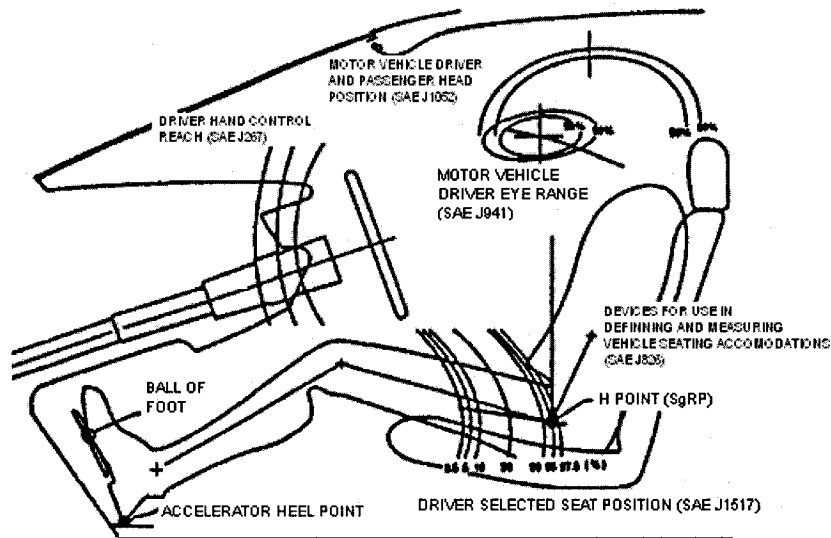


Figure 1.7: Vehicle interior dimension envelopes [13]

sensory perspective into preliminary vehicle design has become increasingly interesting to vehicle researchers and designers.

Kumar *et al.* [2] highlighted the deficiencies of the design procedures outlined by [12,13] and have developed a four step design process, which incorporates biomechanical tools developed for the characterization of seat comfort through mapping of contact pressure and subjective evaluations during the design process, this includes:

1. **Benchmarking for best-in-class**

Defines the type of vehicle in which the seat will be used; then finds and evaluates the best seat features of competing cars in the same category. The features are based on Original Equipment Manufacturer (OEM) marketing input; subjective showroom comfort and long term ride and drive jury evaluations. This step helps define the best in-class seat features, which set the target for the new seat. The seats are then pressure mapped using people from the 5<sup>th</sup> percentile female to the 95<sup>th</sup> percentile male populations; the results are then correlated to the occupant subjective evaluations

2. **Hard points evaluation**

The hard points of the seats are eliminated in this step by using both subjective jury evaluations and static pressure distributions

### 3. **Foam and trim development**

In this step, the foam and the trim of the seat are developed, and subjective ride and drive evaluations, occupant pressure mapping and seat contour checks are conducted.

### 4. **Consumer comfort confirmation**

The final step of the design process is the confirmation of comfort by the consumers, which is conducted in, ride and drive consumer clinics. Again both subjective and objective evaluations are used to confirm expected comfort.

The contact pressure and the perception of comfort of a seat are strongly dependent upon the properties of the PUF material, contouring of the cushion and the backrest, and the seat geometry. Only minimal efforts, however, have been made to quantify the relationship among these factors.

#### **1.2.3 Cushion Materials: Properties and Behavior**

It has been reported that proper dimensioning and adequate support of the seated body leads to a more comfortable experience in the seat [1, 4-10]. These biomechanical factors alone, however, do not provide sufficient guidelines for effective design of comfortable seats. The assessment of comfort necessitates an investigation into the contribution of the seating materials, specifically their mechanical properties. Polyurethane Foam (PUF) has become the cushion material of choice, largely due to the lightweight and ease of manufacturability when compared to the combined foam steel spring seat system. The behavior of PUF under compression is best described by the stress-strain curve shown in Figure 1.8. At small loads, mainly for strains between  $0 < \epsilon < 0.05$ , the stiffness of PUF behaves like most linear-elastic materials [16]. As the loading increases, the elastic buckling of the PUF cells progresses and a softening of the foam occurs, identified from the plateau on Figure 1.8. Further increases in the load



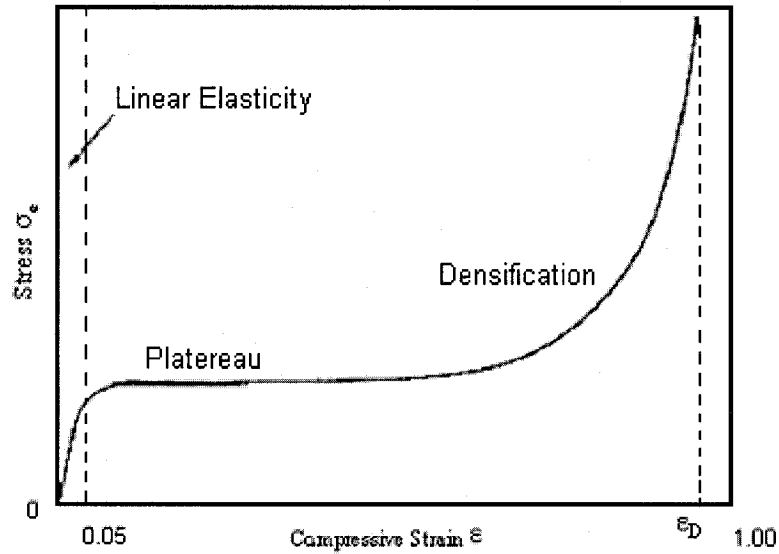


Figure 1.8: Stress-strain relationship of PUF [16]

causes the cells to completely buckle resulting in a densification of the PUF and a rapid increase in the stiffness, referred to as bottoming. The stiffness properties of the PUF seat would thus differ with the seated body weight. A PUF cushion must therefore be designed to provide sufficient cushioning for a wide range of occupant weights; it must be soft enough to deflect under lighter subjects, and be sufficiently stiff to not bottom out under heavier subjects. Furthermore, the vibration attenuation properties of a seat strongly rely upon its stiffness. Most importantly, the stiffness properties of a PUF cushion affect the contact pressure distribution at the body-seat interface and thus the comfort sensation, although only a few studies have attempted to correlate the peak pressures with the material properties. The majority of the reported studies have focused on the wheelchair cushion and pressure sores caused among paraplegics due to sustained contact pressure.

Apatsidis *et al.* [17] compared the difference between viscoelastic foams and polymeric gels with respect to their ability to reduce and redistribute the peak pressure surrounding the IT for custom molded wheelchair seats. The study showed that viscoelastic foams were more efficient at reducing and redistributing peak pressure around the IT compared to polymeric gels. Ebe [18] investigated the effect of changing the cushion thickness of PUF on the static properties as well as the vibration transmissibility of the cushion. Samples of the same PUF ranging from 50mm to 120mm in thickness were tested to determine their load-deflection characteristics. Thicker foams exhibited greater deflection and smaller gradients on the load-deflection curves; thicker foams behaved more like softer foams relative to the thinner samples. Furthermore, the hysteresis loss for the thicker samples was smaller than that of the thinner samples. The thicker samples of PUF, however, resulted in higher transmissibility due to low hysteresis and stiffness. In the frequency range above 5 Hz, thinner foams had higher transmissibility compared to thicker foams. Conversely, the thicker foam samples had higher transmissibility below 3 Hz. The magnitude of vibration transmissibility of a PUF cushion is affected by its damping property or hysteresis. At vibration frequencies below the human body's natural frequency, in the vicinity of 5 Hz, a thin cushion exhibits higher hysteresis loss and thus lower transmissibility. At vibration frequencies above the body's natural frequency, thick foam cushions provide better vibration isolation. The 50 mm sample used in the study revealed a hysteresis loss similar to the 70 mm sample, but resulted in much lower transmissibility caused by bottoming of the cushion. Pneumatic damping must also be considered due to the airflow escaping the foam cells during compression. It was also found that varying the thickness of the PUF had a greater effect

on the vibration transmissibility as opposed to changing the chemical composition of the PUF. Thus, foam thickness was found to be a useful way to change the static and dynamic mechanical properties of the seat. However, it was found that this was only beneficial for thicknesses between 50 and 100 mm for the same foam composition.

Gurram and Vézitz [19] investigated the role of seat cushion deflection and its relation to improving the ride comfort of automotive seats. The study also attempted to determine seat cushion deflection patterns that maximize occupant comfort. The cushion deflection characteristics were determined using a 95<sup>th</sup> percentile male buttock indenter. The study concluded that seats, with linear load-deflection patterns, could yield more comfort under simulated driving conditions. The increase comfort comes from the reduced accelerations at the human-seat interface of seats with linear load-deflection characteristics when compared to seats with non-linear deflection characteristics.

Hostens *et al.* [20] tested various seats used in the agricultural industry for their static pressure distribution characteristics. The study compared 4 commercially available foam seats to a new air based cushion seat under static conditions. Mean and maximum pressures for multiple sitting durations of 2 minutes were recorded at three different hip angles (110°, 130° and 145°). The results showed that the magnitude of the pressure around the buttocks decreased as the backrest angle increased and that the mean pressure increased linearly with Body Mass Index (BMI). The study reported that the new air-based cushion reduced the peak pressure by half for all subjects, when compared to those measured on the foam seats. The study aimed to use these results in a future study to design an intelligent, automatic pre-programmed pressure controller that could passively

or actively change the pressure in different sections of the cushion to provide pressure relief for the occupants.

A study by Blair *et al.* [21] investigated the effect of PUF chemistry on the static and dynamic response of seat cushions. Some cushions were found to have good static properties but exhibited unacceptable vibration characteristics. Also, the vibration analysis of the seats indicated that cushions with high thickness; moderate hardness and foam core densities provide the best response under dynamic conditions, namely low natural frequency and low vibration transmissibility at the resonant frequency. Cushions with the same geometry but different foam formulations revealed different vibration transmissibility. The accurate characterization of the mechanical properties of automotive seats clearly provides a solid foundation upon which predictions of comfort can be made. For example, a very stiff seat undergoes very little deformation and tends to cause higher pressures, while a softer seat deforms with the body and as a result redistributes the body weight over a larger area, which in turn may reduce the magnitudes of peak pressure and enhance comfort.

### **1.2.3 Comfort Assessment: Subjective Measures**

The concept of comfort is extremely subjective in nature because it varies from subject to subject and each subject has pre-conceived expectations of what comfort or discomfort is. The subjective measures evaluate seat comfort by means of a questionnaire or survey in which subjects usually rate the seat features. Subsequent statistical analyses attempt to derive an overall comfort rating based on the results of the survey. Ratings of individual features are also derived relative to the overall comfort. The aim of the seat

designer is to identify specifically the features and attributes of a seat that enhance comfort or eliminate discomfort or pain related factors. The comfort sensation of a seated occupant has been defined quite differently in many studies, mostly in very general terms that could be applied in seating dynamics. Some of these are summarized below:

- a feeling of relief or contented well-being [22];
- affording or enjoying physical comfort [22];
- some state of well being or being at ease [23];
- a state of conscious well-being [24];
- occupant's empirical perception of being at ease [25]; and
- absence of discomfort [26].

Bower-Carnahan et al. [27] conducted a survey on the preferences of heavy truck drivers in the United-States regarding seat design. Among the drivers that responded to the survey, 64.6% experienced lower back pain and 52.6% complained of neck pain, while 51.5% and 51.4% of the respondents also expressed muscle stiffness and sore buttocks, respectively, at the end of a typical driving day. The respondents were also asked to rate the importance of certain seat features on a scale of 1 ("Not at all Important") to 5 ("Very Important"). Overall driver comfort and adjustable suspension damping were the most important features rated at 4.86 and 4.58, respectively. The importance of adjustable lumbar, kidney and thigh support was also highlighted, obtaining scores of 4.56, 4.5 and 4.12, respectively. Another important contribution from this study was the identification of areas of physical discomfort, which were illustrated on a discomfort point plot. Five areas in particular were highly related to seating discomfort:

1. Discomfort in the upper neck and back; most probably caused by the stress of driving all day and the requirement to maintain the head in a proper position for extended durations.
2. Discomfort in the shoulders; largely caused by the improper positioning of the seat with respect to the steering wheel and steering wheel angle.
3. Discomfort in the lower back caused by insufficient and improper lumbar support.
4. Discomfort in the buttocks attributed to unevenly distributed pressure at the human-seat interface.
5. Discomfort in the back of the thighs just above the back of the knees resulting again from improper pressure distribution.

While the geometry and workstation configuration of heavy trucks is different from that of an automobile, the issues of seat comfort remain the same and general conclusions pertaining to the alleviation of the sensation of discomfort can be universally applied; specifically, by providing adequate adjustable lumbar support, sufficient cushion contouring with appropriate seat padding to reduce the magnitudes of peak pressure and evenly redistribute interface pressure.

The review of literature pertaining to the evaluation of seat comfort by the subjective measures has shown that it is an essential tool for identifying seat features that provide comfort or discomfort. The major disadvantage of this approach is that it can only be performed once a seat has been manufactured and, owing to the large inter-subject variability regarding comfort, accurate results require a large sample population. Many studies, particularly on the vibration-related comfort performance, have however used this approach along with the objective measures in an attempt to correlate subjective comfort ratings to measurable parameters. Moreover, the subjective assessments are not suited for relative evaluations of a group of seats or features. The knowledge gained from

a favorable or positive subjective response could be applied in conjunction with some of the objective measures, such as Body Pressure Distribution (BPD) or cushion deformation contours, to establish design target values to which a known level of comfort can be associated.

### **1.2.5 Comfort Assessment: Objective Measures**

Objective measures regarding seat comfort refer to quantitative measures obtained from experiments that are used as comfort predictors. The BPD has been suggested as one of the objective measures in more recent studies [28,29,30], while the rms acceleration due to vibration at the body-seat interface has been widely applied to assess the vibration related comfort performance of seats [31,32]. As highlighted in section 1.2.1, the presence of high pressure around the IT eventually leads to high levels of discomfort and pain. An understanding of the pressure changes with anthropometric and seat features could thus provide the seat designers with effective tools and guidelines to define a comfortable seat. Furthermore, conducting pressure distribution studies in conjunction with subjective studies enables researchers to associate specific pressure profiles to specific seat features. The pressure distribution at the human-seat interface has been characterized in many clinical studies to evaluate the effectiveness of wheelchair cushions to provide pressure relief for disabled or paraplegic patients. Brienza *et al.* [33] investigated the relationship between pressure ulcer incidence and buttock-seat interface pressure in elderly wheelchair users. They reported that the incidence of pressure ulcers was significantly higher among patients who experienced peak pressure greater than 7.99 kPa. Kernozek *et al.* [34] studied the effects of BMI on peak pressure on an

institutionalized elderly population. The BMI is a measure of obesity related to a person's height and weight, such that:

$$BMI = \frac{Weight(kg)}{[Height(m)]^2} \quad (1.8)$$

the study observed lower peak pressure with subjects of higher BMI. This result suggests that taller and leaner subjects were more at risk of developing pressure sores.

Frusti and Hoffman [35] attempted to correlate pressure maps to the results of a subjective survey to predict comfort. The study was conducted on 140 subjects who had recently purchased a mid-sized car in the United-States. The study involved a questionnaire, which defined the seat surface into a number of predetermined zones, and the respondents were asked to rate the importance of each seat zone in view of their overall comfort. The pressure mapping was further conducted inside each subject's own vehicle, where the seat was considered to be adjusted as per the user's preference. In addition to correlating pressure maps to the subjective results of the survey, the study established the ideal pressure ranges for each individual seat zone based on the subjective response. The percentages of the seated body weight supported by particular zones, which correlated to favorable subjective responses, were obtained as 58% - 64% in the zone surrounding the IT, 21% - 28% under the thighs, 58% - 65% at the lumbar area, 25% - 32% on the thoracic area and a maximum of 6% on the cervical area. The authors emphasized that these values were representative of a specific seat and the generalization of the results may be inappropriate for other seat types.

Gross *et al.*[28] have similarly attempted to relate subjective and objective comfort with the seat design parameters. The subjects were asked to rate 12 aspects of the seats after they had been adjusted to their preferred setting. The study involved pressure



mapping of seats employed in economy, sport and luxury automobiles. The study concluded that it was possible to predict comfort ratings from patterns of weight distribution over the cushion area. Figure 1.9 summarizes the reported weight distribution data for both the seat-pan and backrest. The results show that 71.3% of the body weight is supported around the IT for an economy automobile seat compared to the 51 – 53 % range for sport and luxury vehicle seats. The study, however, did not report the static and dynamic properties of the seats.

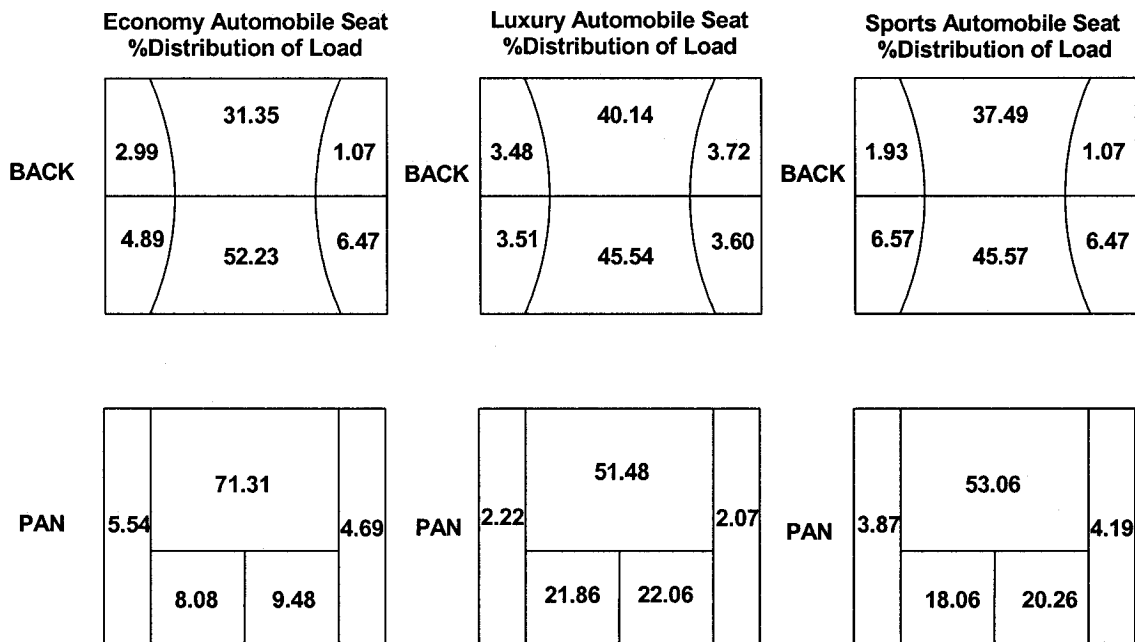


Figure 1.9: Percent weight distribution for three different car seats over predefined seat zones [28].

In a similar study, Thakurta *et al.* [29] compared the results from pressure maps at both the seat pan and the backrest for short and long term sitting with the response of a subjective survey administered before and after the 128 km (80-mile) driving test. After the driving tests, the subjects remained in their seats and a pressure measurement mat was

inserted between the seat and the subject. Table 1.2 shows the mean percent load distribution and the standard deviations. Although the quantitative values of the load distribution differ considerably from those reported by Gross *et al.* [28], the two studies suggest comparable patterns. The study concluded that the pressure distribution is strongly related to the subjective comfort sensation, while the lumbar and IT supports are more significant than the shoulder and thigh support. While the effect of time of measurement was observed to be significant, the five seats considered in the study revealed significantly different results, suggesting strong contributions of the seat geometry and material properties.

Table 1.2: Percent load distribution over defined seat zones and their standard deviations after a 128 km (80 mile) drive [29].

Vehicle and Seat	Lumbar Mean (SD)	Shoulder Mean (SD)	Thigh Mean (SD)	IT Mean (SD)
1	7 (3)	7 (3)	15 (5)	45 (10)
2	9 (3)	10 (3)	13 (5)	45 (10)
3	10 (3)	10 (3)	10 (4)	46 (5)
4	9 (3)	8 (3)	12 (5)	47 (10)
5	10 (4)	9 (4)	11 (5)	42 (7)

the study highlighted the importance of assessing overall comfort for both short and long term sitting conditions, and that seating comfort is a complex function of pressure distribution, posture, time of measurement, occupant anthropometry and seat features.

Oudenhuijzen *et al.* [36] investigated the relationship between the seat pressure distribution and comfort and attempted to identify seat features that contribute the most to seat comfort. They also attempted to identify target pressure distributions leading to maximized perception of comfort. The pressure measurements were taken on two

different seats with fixed geometry. Comfort was reported to depend more on the pressure distribution rather than the pressure values. While there was no preference with regard to a firm seat and a medium-soft seat, the firm seats could be assessed as less comfortable due to a poorer fit than a softer seat. The significant conclusion of the study was that the backrest contributes considerably more to the overall comfort than the seat pan. It was suggested that an uneven pressure distribution at the back will be less comfortable, but that an even pressure distribution is not necessarily desirable. Thus, they concluded that the ideal pressure distribution for optimum comfort should be similar at the lower and middle back and gradually diminishing from the middle of the back to no pressure at the upper back.

Demontis and Giacoletto [30] conducted a combined subjective and objective assessment of comfort on various automotive seats and developed linear regressive models for the contribution of the seat pan and the backrest to the overall comfort performance. The objective measures were based on BPD, and the comfort evaluations were based on three considerations:

**1. Postural Comfort Rating (PCR)**

To increase postural comfort ratings, it is necessary to reduce loaded weight over the popliteal zone (under the thighs just above the knee), reduce the contact surface in the lateral cushion zone near the thighs and increase the load on the lumbar area and reduce the load on the upper back.

**2. Stiffness Rating (STF)**

Best perceived stiffness evaluation is attained by reducing the loaded weight at the popliteal zone. Increase in the contact area surrounding the IT and also to increase the mean pressure at the dorsal and lateral cushion areas.

**3. Wrapping Rating (WRP)**

The wrapping rating depends on the ratio between the peak and mean pressure in the anterior popliteal zone and in the back rest, and is inversely proportional to the standard deviation of pressure values in the lateral ischiatic zone as well as the percentage of contact surface in the superior backrest area.

Contrarily to [36], the contribution of the seat pan to the overall comfort rating of the automotive seats was found to be more important than that of the backrest. Table 1.3 shows the weights of the multiple linear regression models used for seat-pan and backrest contributions.

Table 1.3: Rate of contribution of various sensations to overall comfort [30].

Parameters	Postural Comfort	Stiffness	Wrapping
Cushion	0.6	0.55	0.55
Backrest	0.4	0.45	0.45

Kamijo *et al.* [37] conducted a sensory evaluation of 43 different car seats, and on the basis of the statistical analysis, concluded that the sensation of body pressure distribution and driving posture are the most important factors contributing to overall seat comfort. Table 1.4 summarizes the contributing factors and the corresponding contribution rates. The study further suggested that the symmetric pressure distributions for both the seat-pan and the backrest could yield enhanced comfort.

Table 1.4: Rate of contribution of various sensations to overall comfort [37]

Factor of Seating Comfort	Contribution Rate (%)
The sensation of body pressure distribution	44
The sensation of driving posture	44
The sensation of having ample room	30
The sensation of being cushioned	24
The sensation of being held	17

The peak pressure at the IT was measured as 5.88 kPa, which decreases almost linearly decreasing almost linearly with the distance away from the IT. Similar trends were also observed at the backrest except that the peak pressure occurred in the lumbar region ranging from 2.35 to 2.65 kPa. The study also reported the pressure maps for an uncomfortable seat, where the pressure maps were characterized by low values of peak pressure 1.18 – 1.37 kPa with an asymmetric distribution. The pressure at the seat pan was also found to be asymmetric and the peak pressure was located at the femoral joint. The difference in pressure distribution between the comfortable and uncomfortable seats is mostly associated with the lack of body support by the uncomfortable seat. The study further proposed the following design recommendations for comfortable seats:

- Mean pressure levels of 1.47 – 2.35 kPa in the lumbar support region, which should be located 60 mm to either side of the center.
- The quality of the seat backrest is directly related to its pressure distribution.
- The seat pan can be qualified as good if the pressure distribution shows variance of pressure along the body's shape away from the IT.
- Lower static stiffness and lower seat natural frequency generally provide a better sensation of being cushioned.

Gyi and Porter [38] reported that the method of pressure distribution was an unsatisfactory method for predicting comfort because of the high inter-subject variability. Two different subjects produced different pressure maps yet reported the same amount of discomfort. It was further stated that the reported studies on pressure distribution provide only few details regarding the experimental design and data analysis. Based on the reported conclusions of the objective studies [26-38], the evidence supporting a correlation between the pressure distribution alone and the comfort is somewhat

contradictory. However, more studies have reported that pressure distribution did correlate well with subjective measures and was successfully used as a predictor of comfort [26-37]. While the pressure values vary significantly from source to source, the reviewed studies strongly suggest that a symmetric, uniform distribution of pressure away from the IT provides good comfort ratings. Similarly for the backrest, symmetric uniform pressure distributions are desirable. Further investigations into pressure distribution at the human-seat interface as a function of anthropometry, seat properties and posture are thus desirable in order to obtain more conclusive results on the assessment of automotive seating comfort and to establish more effective design guidelines.

#### **1.2.6 Review of Pressure Measurement Technology**

The increased interest in BPD as a means of quantifying seat comfort by the automotive industry has led to rapid advances in pressure measurement technology. Many techniques have been used in the past to record pressure at the human-seat interface. Swearingen *et al.* [39] used absorbent paper placed over ink soaked corduroy cloth to measure the intensity and distribution of pressure. Dempsey [4] used a *buttockscope*, which used edge lighting and changes in light reflection caused by compression of a soft latex type material. A mirror placed beneath the layer of latex made it possible to measure the area and pressure distribution patterns on the flesh around the IT. Lindan *et al.* [40] used a “bed of nails and springs” to measure the pressure distribution through deflections of the springs. Current pressure measurement techniques are numerous and varied, but generally fall into three categories: electronic, pneumatic and electro-pneumatic [41]. While these systems may vary from manufacturer to

manufacturer, they are generally available in similar formats; they include a pressure-sensing device, a data acquisition/conversion system and data analysis software, as schematically illustrated in Figure 1.10.

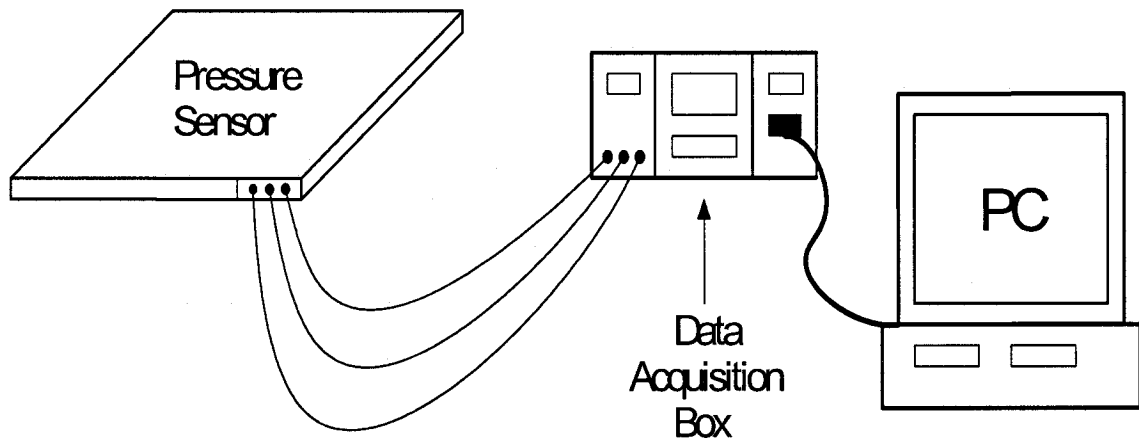


Figure 1.10: Schematic diagram of common pressure measurement system.

Electronic pressure sensing devices are based upon three different principles and employ either capacitive or resistive sensors or strain gauges [41]. The sensing elements are arranged in a matrix enveloped by a thin elastomeric mat which allows the sensors to comply well with irregular profiles, such as the curved surfaces of automotive seats. It has been reported that the output of the capacitive type sensors are generally less sensitive to temperature and humidity [42,43], this would suggest a better suitability of capacitive type sensors for pressure measurements over extended durations where variations due to increased sensor temperature caused by body heat become less pronounced. The resistive sensors, on the other hand, are reported to cause large hysteresis error [43].

Pneumatic pressure sensors are air cells connected to an air reservoir, to fill the air cells, the air pressure in the reservoir must be greater than the pressure applied to the sensor. As the pressure in the air cell rises above the applied pressure, the volume of air in the cell suddenly increases, leading to a quick decrease in the rate of inflation of the air cell. The instant at which this change in rate of inflation occurs is recorded as the interface pressure [41]. Electro-pneumatic sensors work much like the pneumatic type except that the inside surface of the air cell is lined with an electrical contact; when the pressure inside the cell is equal to the applied pressure the contact breaks and the pressure is recorded as interface pressure.

Regardless of the pressure measurement system being used, Ferguson-Pell [42,44] and Grant [43] have established useful selection guidelines for measurements at the human-seat interface. It is suggested that the sensing element be flexible, small and thin, less than 1 mm thick and with a diameter of 10 mm. The sensors and the signal conditioning should have continuous output and be capable of measuring shear as well as normal load. The measurement error must be low when used over curved surfaces. Gross *et al.* [28] further suggested that the sensing matrix must be durable and flexible to adapt to contoured surfaces, while the sensors should be repeatable with low sensitivity to vibration, noise and temperature. Many studies emphasize the need for low hysteresis sensing and elastomers to ensure high repeatability of the measurements.

### **1.3 Scope and Objectives of the Dissertation**

From the relevant literature, it is evident that the seating comfort depends on the seat dimensions, mechanical properties, driving conditions, seated posture, contact



pressure and its distribution in a highly complex manner. The current seat design methodology outlined by the SAE standards [12,13] does not take into consideration the issues of comfort but only defines the dimensional ranges believed to yield *least discomfort*. The motivation to develop effective quantitative tools to predict comfort has become vital for automotive designers, since the showroom comfort of the seat is considered as a significant marketing factor.

The comfort characteristics of seats have been mostly evaluated on the basis of subjective responses, which tend to be extremely demanding on the financial and human resources and yield extremely high inter-subject variability and poor repeatability. The need to identify effective objective measures has been widely emphasized to achieve more consistent assessments of comfort and to establish design guidelines. The objective measures based on acceleration due to vibration transmitted to the occupant-seat interface has been widely applied to assess and design seats with enhanced vibration related comfort. The objective measures relating the overall seating comfort, specifically the postural support and showroom comfort under static environments, have not been adequately quantified. The reported studies, however, suggest that occupant-seat interface pressure could serve as an effective objective measure of the comfort. The BPD however is strongly dependent upon many seat and anthropometry related factors. The correlations between the comfort, BPD, anthropometry and seat design factors have not yet been established. The reported studies have attempted to correlate the BPD with the subjective responses with respect to comfort. Furthermore, analyzing the BPD as a function of anthropometry and posture may eventually provide more solid foundations against which more advanced techniques, such as finite element analysis can be validated.

In light of the evidence supporting the use of BPD to study and predict comfort characteristics of seats, the scope of this research thesis is formulated to conduct fundamental investigations into variations in the BPD as a function of occupant anthropometry, seat geometry and seated posture. The effects of posture will be studied by varying the seat height, the knee and the backrest angles. The resulting BPD could provide important trends in the peak pressure, location of peak pressures and pressure distributions as a function of the anthropometry, posture and seat geometry. The scope is further extended to include an investigation into the contribution of cushion stiffness in an attempt to provide an additional basis for comparing the different automotive seats and their associated BPDs.

The overall objectives of this research thesis are to analyze the BPD at the human-seat interface as a function of the anthropometry, seat height, knee angle and the backrest angle. This is accomplished through structured experimental measurements of the BPD under static conditions. This investigation into seat comfort therefore includes:

- (a) The characterization of the mechanical properties of the seat-pan and the backrest of the three different automotive seats.
- (b) Investigation of the variations in the seat-pan and the backrest cushion stiffness as a function of subject weight.
- (c) Measurements of BPD at the occupant seat-pan and the occupant backrest interfaces for each subject as functions of the seat height, knee angle, backrest angle and static stiffness.
- (d) Study of the role of seat-pan and backrest stiffness on the pressure loading and distribution with respect to posture and subject anthropometry.
- (e) Identification of the seat configurations that generate the highest/lowest peak pressures and determining the areas of the body on which they occur.
- (f) Study of the behavior of the pressure distributions in the zones subjected to higher pressure and the zones known to be more sensitive to pressure loading.

- (g) Attempt to derive general trends in pressure distribution as a function of cushion properties, subject anthropometry and seated posture.
- (h) Deriving guidelines for the design of automotive seats with enhanced occupant comfort based on BPD.

#### **1.4 Organization of the Dissertation**

This dissertation is organized into 5 chapters describing the systematic realization of the above objectives. The literature is reviewed in the appropriate chapters highlighting the research contributions on the various topics related to BPD and comfort studies on automotive seats. Chapter 2 highlights the experimental procedures followed to perform the cushion characterization and the acquisition of the BPD data. An analysis and discussion of the results of the cushion characterization is also presented. Chapter 3 presents the generalized results of the BPD measurements at the seat-pan and backrest, respectively. Statistical analyses are then performed on the data to identify the parameters that most significantly cause variations of pressure distribution at the human-seat interface. A multiple linear regression is also performed on the data to investigate the relative contribution of each significant parameter with respect to one-another. A zonal analysis of the same pressure data is performed in chapter 4 to identify the zones of peak pressure and to investigate the variations in the peak pressures, contact forces and contact areas, as a function of the cushion stiffness, subject weight and seated postures within the defined zones. The interpretations and discussions of results from both the statistical and zonal analyses are presented in chapter 5. Conclusions and guidelines regarding seat testing and design with enhanced subject comfort are also presented. Finally, recommendations for future studies in seat comfort testing are also discussed.

## CHAPTER 2

### EXPERIMENTAL METHODOLOGY AND CUSHION CHARACTERIZATION

#### 2.1 Introduction

Automotive driver/passenger seating comfort is strongly influenced by the interactions at the human-seat interface. The measures based on BPD have been widely suggested to obtain objective comfort assessment of automotive seats. While BPDs have successfully been correlated to a subjective comfort rating [29,37,46-49], they have been found to vary significantly with anthropometry and the seated posture. The comfort assessment of automotive seats can further be assessed through the accurate characterization of the seat mechanical properties. PUF is widely used in the seat cushion and backrest; the properties are reported to exhibit highly non-linear load deflection characteristics. Furthermore, these characteristics are significantly affected by the load applied, the thickness of the foam and by the foam chemistry. The design of automotive seats with enhanced comfort therefore necessitates the consideration of the anthropometry of the target populations, the dimensional and postural ranges intended for the seat and finally the mechanical properties of the seat itself. The seat properties can be determined in the laboratory through the measurement of the load deflection characteristics under appropriate conditions.

In this chapter, the test methodology and laboratory equipment used to acquire body pressure distributions at the seat-pan and the backrest with human subjects is presented. The test procedures followed for the characterization of the seat properties for the seat-pan and the backrest cushions are briefly described and the results are discussed.

## 2.2 Body Pressure Distribution Measurement Methodology

### 2.2.1 Test matrix

To investigate the interactions at the human-seat interface, BPD measurements at the seat-pan and backrest were acquired for 8 male subjects under static conditions. Table 2.1 summarizes the weight, height and BMI of each test subject selected for the experiments. The BPDs were measured for three combinations of seat height (H1 – 318 mm, H2 – 368 mm and H3 – 419 mm), knee angle (K1 – 95°, K2 – 115° and K3 – 135°) and backrest angle (B1 – 5°, B2 – 15° and B3 – 25°). The ranges of test conditions are selected on the basis of the recommended dimensions for *least discomfort* in different studies as summarized in Table 1.1 [4-9].

Table 2.1: Weight, height and BMI of the 8 male test subjects selected for the study.

Subject	1	2	3	4	5	6	7	8	Mean	SD
Mass (kg)	60.6	66.8	67.8	73.8	75.4	86.0	90.2	108.0	78.6	15.43
Height (m)	1.73	1.87	1.77	1.73	1.79	1.83	1.84	1.81	1.80	0.05
BMI (kg/m <sup>2</sup> )	20.3	19.0	21.8	24.6	23.5	25.7	26.8	33.0	24.3	4.4

The experimental design involved three different seats to study the role of stiffness and contouring on the BPD. The selected seats are referred to a ‘seat 1’, seat 2 and seat 3. The ‘seat 1’ represents the type of seat typically employed in sports vehicles, while ‘seat 2’ represents those employed in economy vehicles. The ‘seat 3’ represents those typically employed in economy to luxury vehicles. Table 2.2 presents the test variations considered for all seats. As evident from the table, the seats 2 and 3 could not

be adjusted to realize a backrest inclination of 5° because their respective minimum backrest angles were limited to 12° and 14°. The BPD measurements for these two seats were thus acquired for backrest inclinations corresponding to 15° and 25° only.

Table 2.2: BPD test matrix

Seat	Seat Height (mm)	Knee Angle (deg.)	Backrest Angle (deg.)		
			5	15	25
1	318	95	X	X	X
		115	X	X	X
		135	X	X	X
	368	95	X	X	X
		115	X	X	X
		135	X	X	X
	419	95	X	X	X
		115	X	X	X
		135	X	X	X
2	318	95	-	X	X
		115	-	X	X
		135	-	X	X
	368	95	-	X	X
		115	-	X	X
		135	-	X	X
	419	95	-	X	X
		115	-	X	X
		135	-	X	X
3	318	95	-	X	X
		115	-	X	X
		135	-	X	X
	368	95	-	X	X
		115	-	X	X
		135	-	X	X
	419	95	-	X	X
		115	-	X	X
		135	-	X	X

### 2.2.2 Experimental setup

The test stand used for the BPD measurements is schematically shown in Figure 2.1. Each of the test seats were mounted and fixed to a static test stand and set to the highest seat height position ( $H3 - 419$  mm). The seat height was changed by adding platforms beneath the feet to raise the floor, thus simulating a lower seat height ( $H2 - 368$  mm) and again to achieve the lowest setting ( $H1 - 318$  mm). The knee angle measurements were confirmed with a 30 cm BASELINE dial type steel goniometer with a tolerance of  $\pm 5^\circ$ , as shown in Figure 2.2. The horizontal distance  $L1$  between the Accelerator Heel Point (AHP) and the forward edge of the cushion, was also recorded to investigate its behavior as a function of anthropometry and the seated posture. A dial type protractor, shown in Figure 2.3, with a tolerance of  $\pm 2^\circ$ , was placed on the surface of the backrest to achieve the desired backrest inclination.

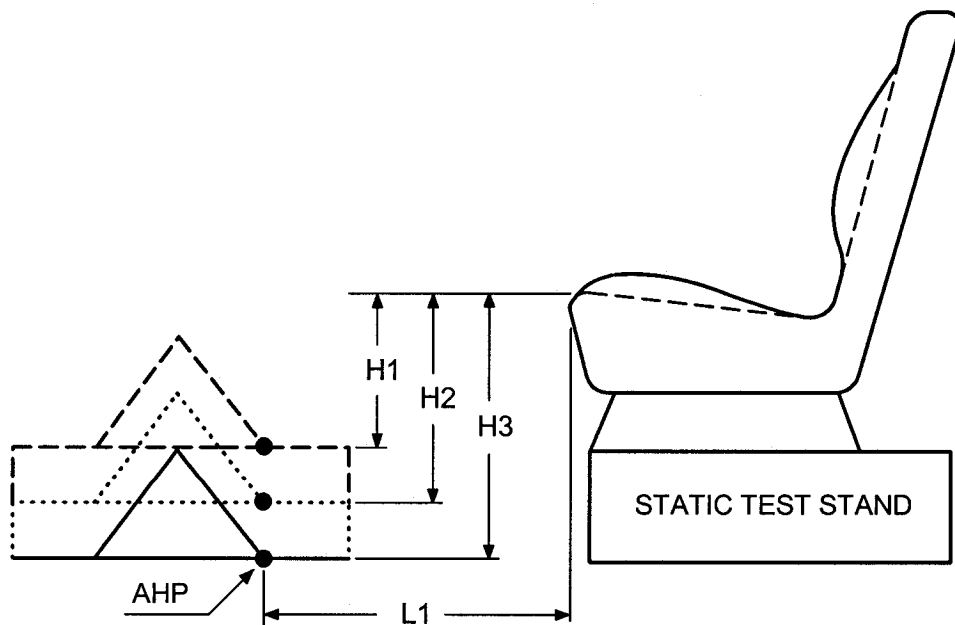


Figure 2.1: Static test stand for BPD measurements

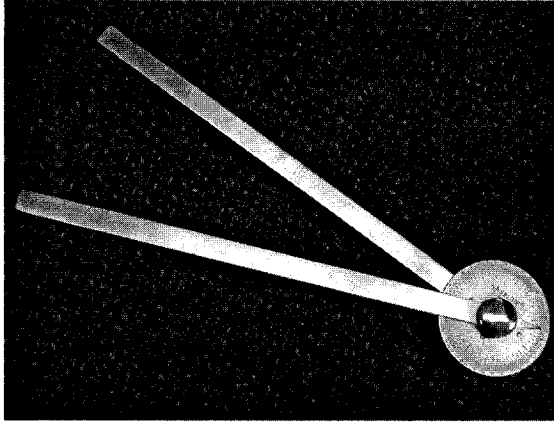


Figure 2.2: Baseline goniometer



Figure 2.3: Angular protractor

### 2.2.3 Data acquisition of body pressure distribution

The BPD measurements at the human-seat interface were acquired using the *EMED* measurement system manufactured by *NOVEL Electronics*. The pressure measurement system consists of a flexible capacitive type sensor matrix and a *PLIANCE* mobile data conditioning and acquisition system. The pressure-sensing device, schematically shown in Figure 2.4, consists of a 16X16 sensor matrix molded into a 2 mm thick elastomeric mat. Each sensor has an area of  $2.54 \times 2.54 \text{ cm}^2$  and a total of 256 sensors cover an effective area of  $1651.61 \text{ cm}^2$ . The threshold values of the pressure were set to  $0.25 \text{ N/cm}^2$  and  $0.125 \text{ N/cm}^2$  for the seat-pan and the backrest, respectively. The flexibility of the sensing mat allowed the mat to conform and follow the contour of the cushions of the seat-pan and the backrest. The resulting measurements thus represent the normal forces and pressures acting at the human-seat interface. Each measurement was taken twice at a rate of 5 Hz for 10 seconds to ensure good repeatability of the data. The measured data was simultaneously displayed in color-coded graphics, which were subsequently stored on a computer for post-processing.



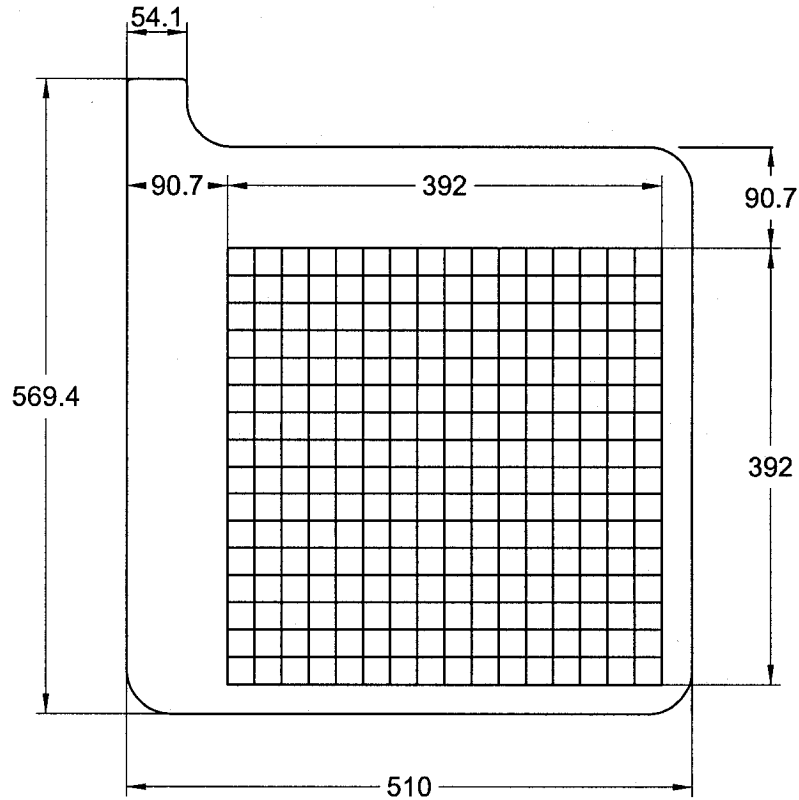


Figure 2.4: Schematic diagram of the *Novel* pressure sensing mat (all dimensions in mm)

### 2.3 Characterization of Static Properties of Test Seats

The comfort performance of seats is dependent upon the mechanical properties of the seat cushion and the backrest. The vibration attenuation performance and thus the vibration related comfort of seat cushions have been directly related to the static and dynamic stiffness and the hysteresis loss of the PUF cushions in a number of studies [18,21,51]. The role of mechanical properties on the BPD, however, has not yet been investigated. Owing to the non-linear force-deflection properties of PUF, the mechanical properties and thus the BPD may also depend upon subject weight and the sitting posture. The force-deflection characteristics of the PUFs used in the manufacturing of automotive

seats have been found to be highly non-linear [16-21, 50-52]. In addition to the visible geometric differences between test seats, such as seat-pan and backrest cushion contours, the characterization of stiffness and hysteresis loss of the respective cushions provides additional parameters upon which the seats are compared. The characterization of the test seats was conducted in accordance with the standards and practices recommended by both the SAE and the Japanese Automobile Standards Organization (JASO).

### **2.3.1 Cushion characterization methodology**

The characterization of the test seats was conducted in accordance with the procedures outlined in SAE J1051 [53] and JASO B-407 [54]. These standards provide specifications regarding the test conditions, loading levels and points of application of loads required for the determination of the mechanical properties of automotive seat cushions. SAE J1051 is a proposed standard for the determination of the load-deflection characteristics for finished cushioned seats found in off-road work machinery. The data obtained from these tests may be useful in determining seat comfort characteristics and maintaining quality control during seat manufacturing; the standard however does not intend to establish any acceptance criteria based on its results. The test specifications are outlined as follows:

#### **Test Conditions**

The specimen shall be conditioned, un-deflected and un-distorted at  $22^{\circ}\text{C} \pm 2.8^{\circ}\text{C}$  and relative humidity of  $50\% \pm 2\%$  for at least 12 hours before being tested. The test shall be performed at least 96 hours after it has been manufactured.

#### **Test Specimen**

The test specimen shall consist of a seat cushion, a back cushion and any other components in an un-used condition.

### Apparatus

1. A 200 mm diameter, rigid, flat, or curved indenter, as shown in Figure 2.5, is used to apply a force through a rigid or a swivel joint capable of accommodating the seat-pan angle of the test seat.
2. A platform capable of positioning the top surface of the test seat parallel to and centered with the jointed indenter and not to restrict the normal breathing or deformation of the test seat.
3. An apparatus capable of applying forces and measuring the deflections of the indenter into the test seat.

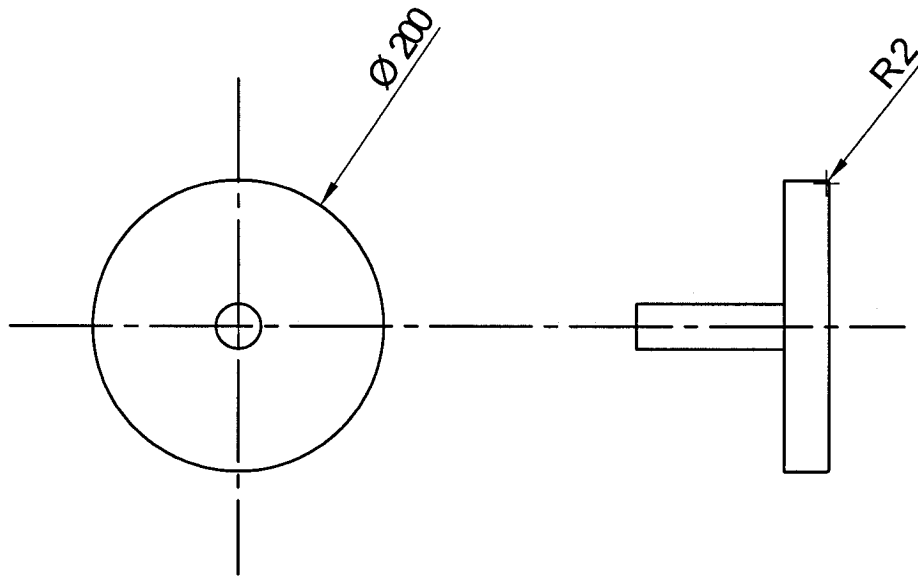


Figure 2.5: SAE J1051 recommended force indenter [53] (all dimensions in mm)

### Procedure

1. Mount the specimen with the top surface parallel to and centered with the indenter. The 200 mm diameter indenter shall be used for both the seat-pan and backrest cushion tests.

2. Pre-flex the test seat 3 times by compressing and releasing the force at a rate of 100mm/min. the specimen shall be compressed as follows.
  - Seat-pan cushion: 1335 N
  - Backrest cushion: 665 N
  - All other components shall be compressed to 20 % of the original thickness
  - Allow 10 min.  $\pm$  5 min. for the specimen to stabilize after preflexing before continuing with the test.
3. Apply a 45 N pre-load to the 200 mm diameter indenter and set the deflection to zero.
4. For the 200 mm indenter, apply an incremental load (no greater than 220 N) slowly to minimize shock. Allow the test seat to stabilize for 1 minute then measure the deflection. Continue this incremental procedure without removing the previous force until the maximum load of 1335 N and 665 N is attained for the seat-pan and backrest, respectively. When incremental thickness is used, the specimen shall be compressed to no less than 20% of its original thickness.
5. After reaching the maximum force, reduce the force slowly in the same increments used in step 4 and allow the cushion to stabilize for 1 min. before measuring the deflection at each increment.

Due in large part to the differences between operating conditions of off-road machinery and automobiles, the maximum loads applied to the respective seat-pan and backrest cushions were modified. The application of 1335 N and 665 N to the seat-pan and backrest, respectively, to the automotive seats would most certainly cause excessive deflection of the cushion and seat sub-frame, and perhaps cause failure of the seat's outer covering. In addition, automotive seat cushions are subjected to approximately 70 –76 % and 24 – 30 % of the total body weight for the seat-pan and backrest, respectively [4,55]. Therefore the maximum load to which the cushions were loaded was limited to 850 N and 300 N for the seat-pan and backrest, respectively. Furthermore, the incremental

values of force were reduced from 220 N to 50 N to facilitate the characterization of the cushion at loads representative of the subjects seated mass.

JASO B-407 [54] on the other hand prescribes test methods for the evaluation of seat parameters specifically with respect to the assessment of comfort performance of automotive seats. The test methodology is outlined as follows:

### **Test Conditions**

This standard does not provide specifications for the conditioning of test seats prior to cushion characterization.

### **Test Specimen**

Shall be any automotive seat for which the characterization is desired.

### **Apparatus**

For the Tekken type indenter, shown in Figure 2.6 the point of application of the indenter force shall be through the center of the indenter located at a distance of 130 mm forward of the B point on the seat pan and 170 mm above the B point for the backrest. The method used to determine the location of the B point is shown in Figure 2.7.

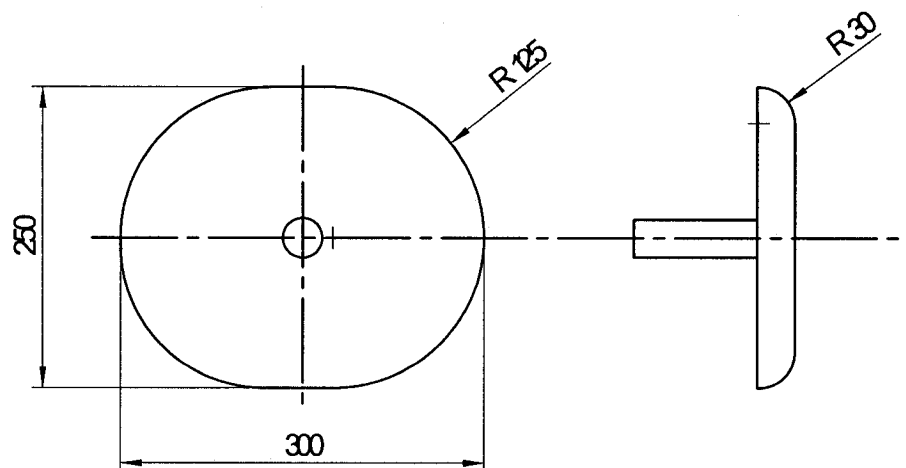


Figure 2.6: Tekken type indenter used by [52] (all dimensions in mm)

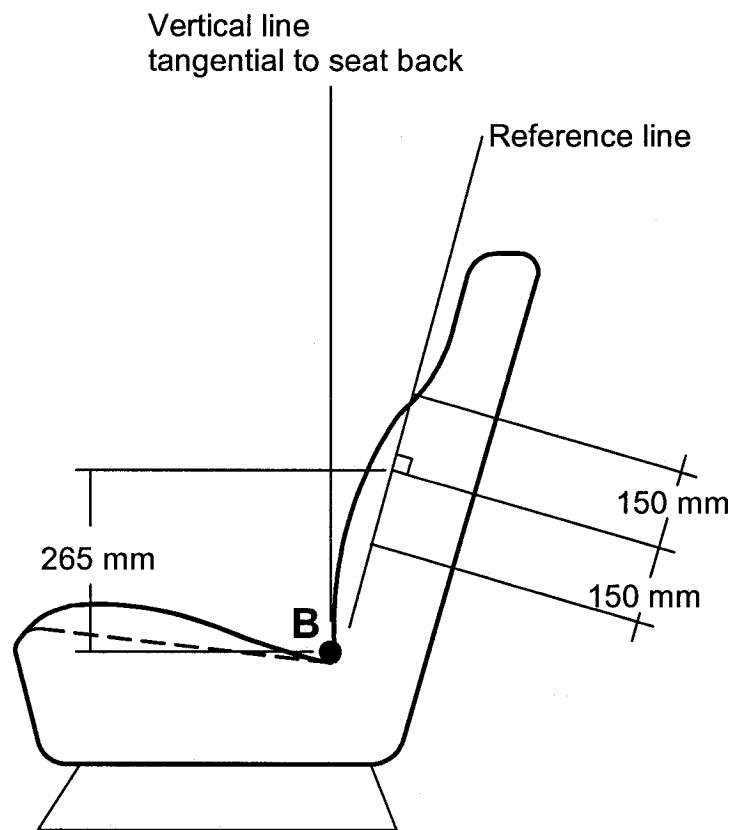


Figure 2.7: Load application points for the “Tekken” type indenter [54]

**Procedure**

1. This standard specifies that seats must be pre-loaded at least two times to a load of 700 N at the seat-pan and 300 N at the backrest. However, if the seat has previously been loaded to similar magnitudes, the pre-loading may be omitted.
2. Pre-load the cushion to 5 N at the specified point of application. Load and unload the test seat at a rate of 150 – 300 mm/min and restricting the switchover time from load to unload to no more than 2 seconds until the maximum load is reached (700 N and 300 N for the seat-pan and the backrest, respectively).
3. Record the loading rate and obtain the loading curves for the test seats.
4. From the load-deflection curve, obtain and record the deflection, in mm, corresponding to loads of 450 N and 150 N for the seat-pan and the backrest, respectively.

5. Derive the static spring constant, which is defined as the slope of the tangent to the load-deflection curve at a point corresponding to 450 N and 150 N loads for the seat-pan and backrest, respectively.
6. Obtain the coefficient of hysteresis loss by measuring the area inside the load-deflection curve and dividing this value by the area under the loading curve. The ratio defines the coefficient of hysteresis loss ( $\alpha$ ) expressed in percent, and can be expressed as:

$$\alpha = \frac{\text{Area } 0 \text{ } abcd \text{ } 0}{\text{Area } 0 \text{ } abe \text{ } 0} \quad (2.1)$$

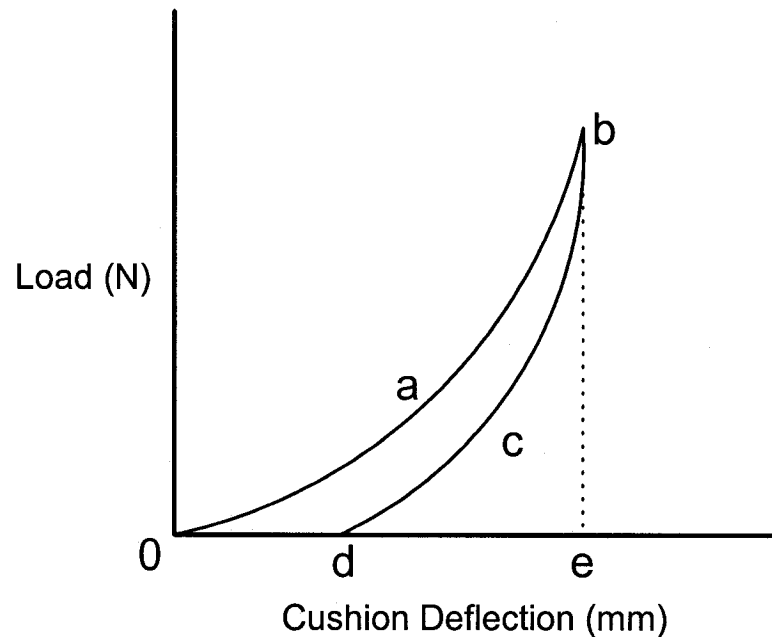


Figure 2.8: Typical hysteresis loop for PUF seat cushions [54]

The fundamental difference between the methods outlined by SAE [53] and JASO [54] is the manner in which the load is applied. For the practices recommended by the SAE, the loading is discrete and from a physical perspective yields truly static values of cushion stiffness by allowing the PUF to completely relax before the incremental load is changed. The JASO, on the other hand, use a continuous triangular function to deflect the

cushion and obtain a more realistic value of the cushions properties in-light of the dynamic environment of the automobile, which may not allow for complete cushion relaxation. The test methods outlined in [53,54] both use different load indentors and points of application. While the use of different indentors would inevitably yield different results, the same 200 mm diameter SAE indenter, shown in Figure 2.5, was used in this study for both characterization methods. Furthermore, the point of application for the loads was taken as the aggregate center of pressure for all the subjects for each seat.

### **2.3.2 Test setup and acquisition of force-deflection characteristics**

Three different automotive seats were selected for the static characterization. The force-deflection characteristics of the seats were acquired using a 4500 N Sensotek load cell, a built-in Schaevitz LVDT and a Magnatek string potentiometer. The displacement measured by the built-in LVDT however was used for the data analysis. Figure 2.9 shows a schematic of the hardware for the experimental setup. An analog Direct Memory Access (DMA) block of a PC connected to a 4-channel data acquisition board PC-1-204228W-1 acquired the sensor signals. The DMA block was linked to a Dynamic Data Exchange (DDE) server block, schematically shown in Figure 2.10, which contains a Visual Designer Analog to Digital conversion (A/D) code that exports the data directly into a Microsoft Excel spreadsheet. The data is acquired at a rate of 360 Hz and is further manipulated by Excel to display the force-deflection diagrams.



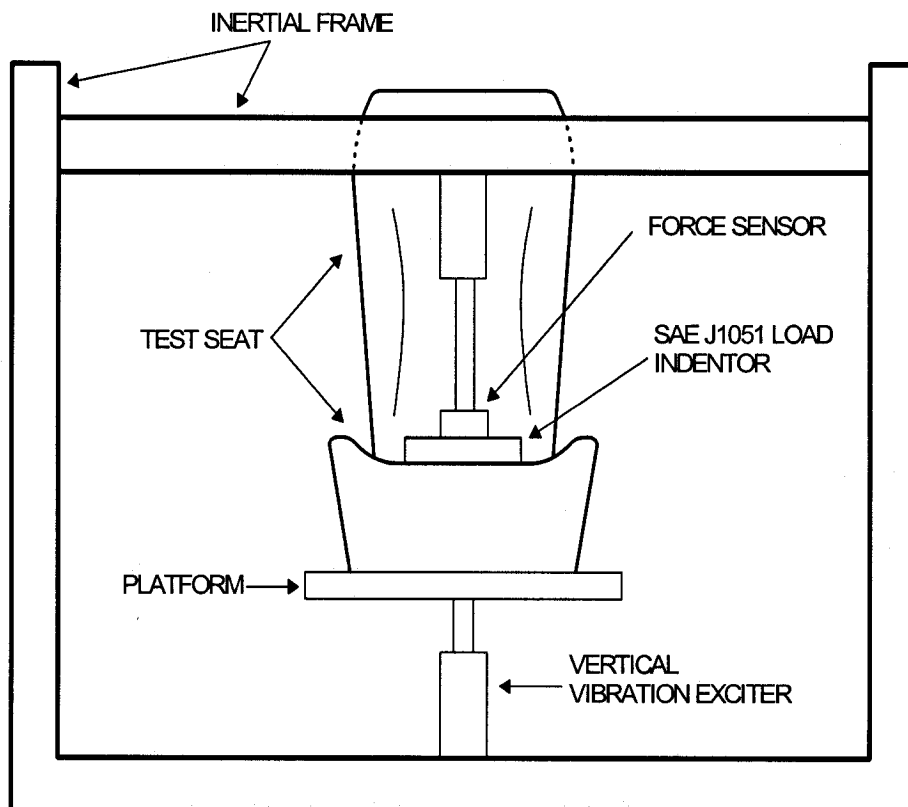


Figure 2.9: Test stand for load-deflection characterization of test seat cushions.

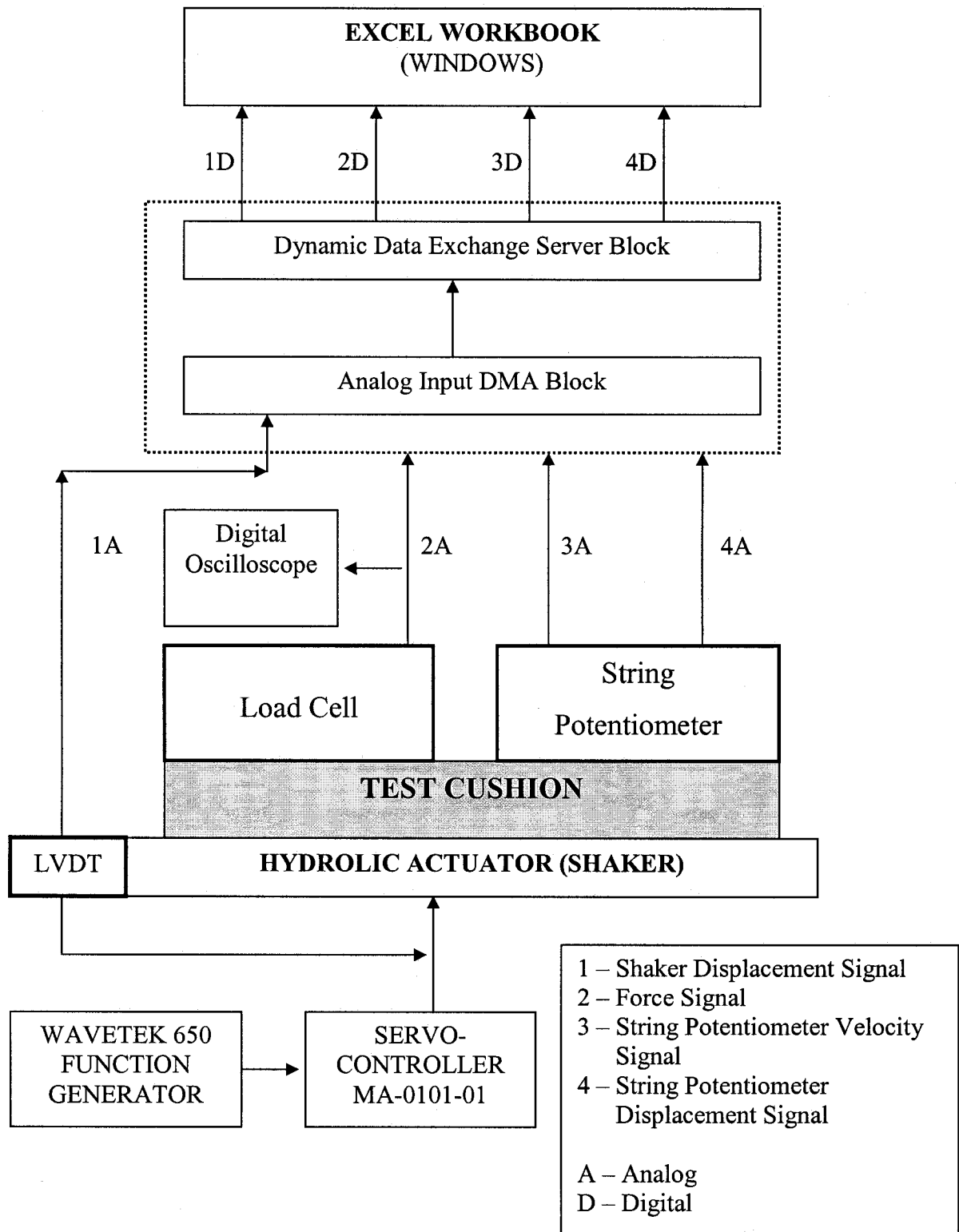
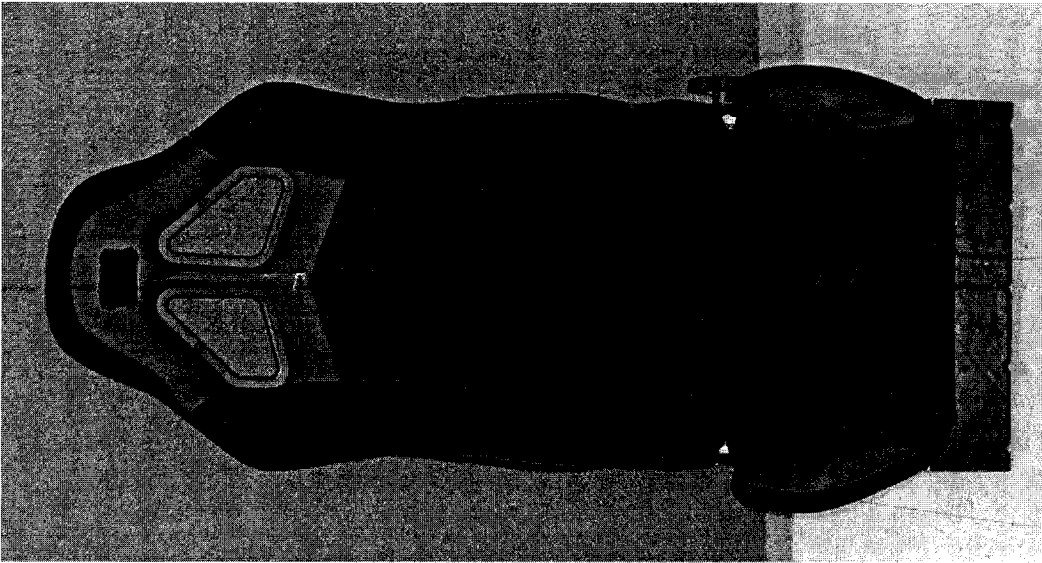


Figure 2.10: Data flow chart for DDE and DMA blocks used in the acquisition of the load-deflection data

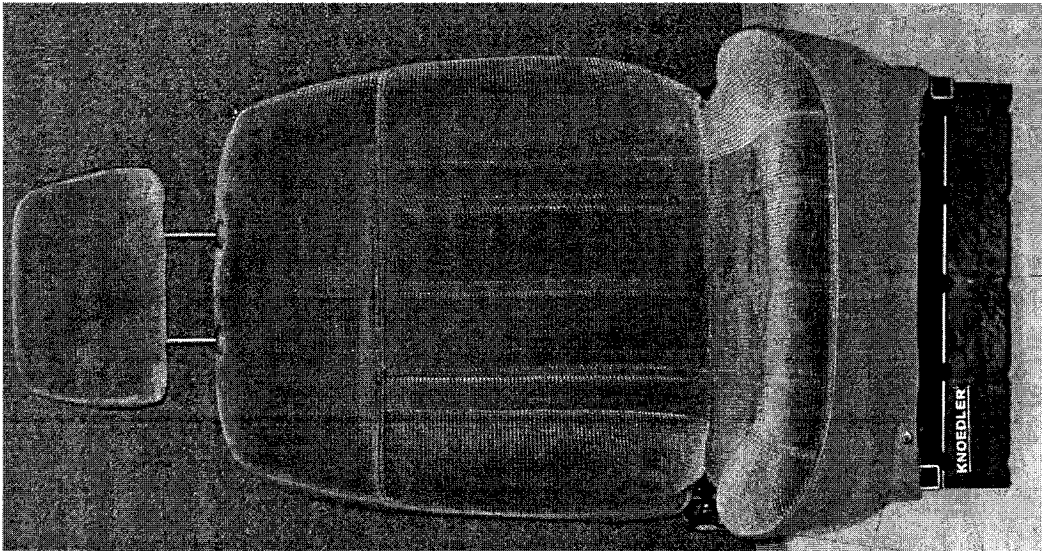
## 2.4 Description of Test Seats

The effects of pre-load and deflection amplitudes on the cushion properties and the pressure variations resulting from these property changes have been reported [19,48, 56]. Figure 2.11 shows the three test seats used in this study, each seat can be categorized based on the vehicle it was taken from. Seat 1 is a high-end after market racing seat that has narrow seat-pan and backrest cushions, and high wings located on both the seat-pan and the backrest. The wings on seat 1 are much larger than those of seats 2 and 3, and are typical of racing type seats, which must provide greater lateral support to the body resulting from cornering at higher speeds. It is anticipated that these wings will provide a higher level of wrapping leading to increased loading and potentially higher peak pressures in these areas. Seats 2 and 3 are OEM seats that fall into the economy and sport seat categories, respectively. Seat 2 has very little variation in the seat-pan cushion contour and is typical of seats that are intended to accommodate a wider range of occupants. The wider seat-pan and smaller wings reduces the likelihood of localized high pressure for the heavier subjects. Seat 3 shows similar characteristics to those of seat1 with respect to the wings located on both the seat-pan and backrest but still offers wider distance between the wings. Figure 2.11 further illustrates the differences in seat-pan and backrest cushion contours, which are also anticipated to have a significant effect on the variations of the BPD.

**SEAT 1**



**SEAT 2**



**SEAT 3**



Figure 2.11: Test seats selected for the study

## 2.5 Static Properties of the Test Seats

The candidate seats are characterized in terms of the static stiffness of the cushions, defined in the vicinity of a specific pre-load, as illustrated in the force deflection curve in Figure 2.12.

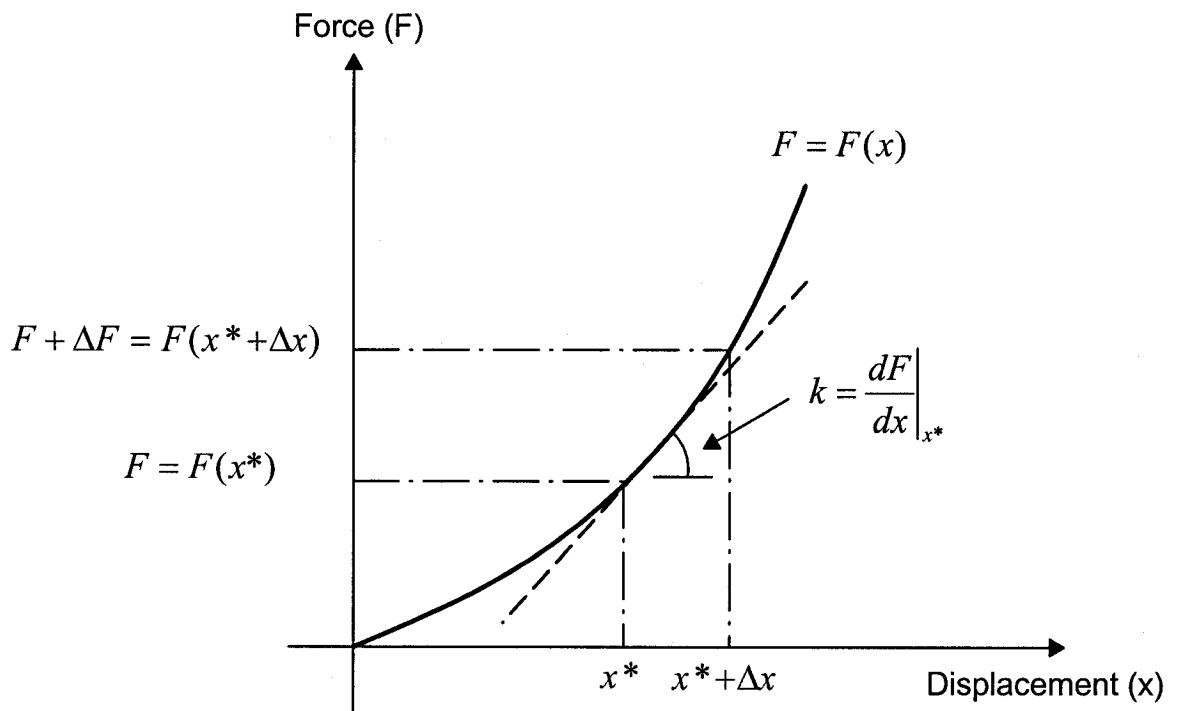


Figure 2.12: Spring element linearization process. [57]

for a given static load,  $F$ , representing the occupant weight supported by the seat cushion, the cushion undergoes a static deflection  $x^*$ , the application of an incremental load,  $\Delta F$ , causes the cushion to further deflect by  $\Delta x$ . The static stiffness of the seat cushion about a

given pre-load can be derived from the Taylor's Series expansion and neglecting the higher order terms, such that:

$$K_i = \left. \frac{dF}{dx} \right|_{x^*} \quad (2.2)$$

where  $K_i$  is the linear static stiffness of the cushion about the operating point  $x^*$ . The force-deflection characteristics were obtained for the candidate seats using both characterization methods and independent trials. The experiments were repeated to obtain the static force-deflection characteristics of the seat-pans and the backrests. Figure 2.13 shows, as an example, the force deflection curves for the seat-pan of seat 3, measured using the JASO and the modified SAE test guidelines. Both methodologies yield significantly different characteristics for the entire load range considered. In addition, the results show poor repeatability of the SAE method above 50 mm deflection, while the JASO standard showed excellent repeatability. The poor repeatability of the SAE method is most likely attributed to the differences in the relaxation duration at each step of loading.

To derive the equivalent stiffness of the cushions, the force-deflection curves are fitted with a fourth order best-fit polynomial. Evaluating the slope of the curves at any desired pre-load (subject weight) derives the equivalent stiffness for the cushion. Equations (2.3) and (2.4) define the best-fit polynomials describing the force-deflection data acquired using the JASO and SAE test methodologies, respectively.

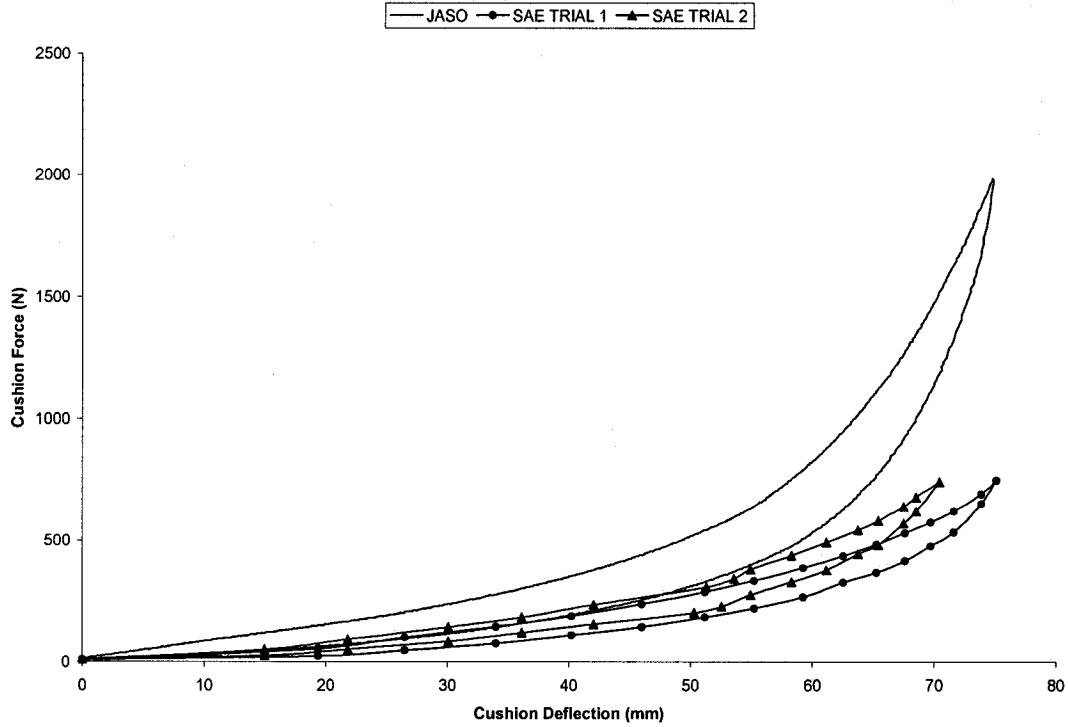


Figure 2.13: Comparison of force-deflection characteristics of seat 3 attained using the SAE J1051 and JASO B407 methods

$$F(x) = 0.0002x^4 - 0.0169x^3 + 0.5246x^2 + 2.1832x + 13.01; \text{ for } x > 0 \quad (2.3)$$

$$F(x) = 7 \times 10^{-5} x^4 - 0.0008x^3 + 0.372x^2 - 1.8304x + 9.9511; \text{ for } x > 0 \quad (2.4)$$

Both the above functions revealed  $R^2$  values in the order of 0.999. The equivalent static stiffness about an operating point  $F(x^*)$  is computed using Equation (2.2), such that:

$$K_i = 0.0008x^3 - 0.0507x^2 + 1.0492x + 2.1832; \text{ for the JASO data} \quad (2.5)$$

$$K_i = 2.8 \times 10^{-4} x^3 - 0.0024x^2 + 0.744x - 1.8304; \text{ for the SAE data} \quad (2.6)$$

The equivalent stiffness of the cushions over the entire weight range of the subject population considered in the study is determined from Equations (2.5) and (2.6) by considering the appropriate pre-load. Table 2.5 summarizes the results obtained for both characterization methods for seat-pan pre-loads corresponding to 76 % of the total body

weight of each subject selected in this study. The results show significant differences between the two methods for both deflection and stiffness. For the same load, the cushion deflection is significantly higher for the SAE method, when compared to the JASO method. This is attributed to the relaxation of the cushion in the SAE method and possible bottoming of the foam cells under high loads in the JASO method. Inspection of the cushion stiffness reveals that the stiffness evaluated by the JASO methodology is up to 1.4 times higher than that evaluated by the SAE method. In both cases however, the results show an increasing trend in deflection and stiffness with an increase in the pre-load. Table 2.3 further illustrates that SAE J1051 is not able to provide enough information to characterize the cushion over the entire weight range due to high deformations of the relaxed PUF. Owing to its poor repeatability, the data obtained from the SAE J1051 standard was dropped and further characterizations were performed using the JASO test methodology.

Table 2.3: Comparison of SAE and JASO static stiffness coefficients for the seat-pan of seat 3

Seat	Subject	Pre-Load (N)	SAE [51]		JASO [52]	
			Cushion Deflection (mm)	Static Stiffness (N/m)	Cushion Deflection (mm)	Static Stiffness (N/m)
3	1	452	61.2	17994	46.6	21888
	2	498	63.6	20485	49.0	26038
	3	506	64.0	20893	49.5	26825
	4	550	66.2	23439	51.5	31043
	5	562	66.7	24109	52.1	32271
	6	641	69.8	28376	55.1	40006
	7	673	70.8	29834	56.2	42872
	8	805	X	X	59.48	53566



The measured force-deflection characteristics of the cushions and backrests of the candidate seats are analyzed to compute the static stiffness values corresponding to the pre-load of 450 N and 150 N, respectively, as outlined in the JASO standard. The coefficients of the hysteresis loss for the candidate seat-pans and backrests are further analyzed using equation (2.1). The results attained for the three seats are summarized in Table 2.4 together with the deflections corresponding to specified pre-loads. The results suggest that the seat-pan cushion of seat 3 (21735 N/m) is more than 5 times stiffer than that of seat 1 (4267 N/m) and seat 2 (12422 N/m) is almost 3 times stiffer than that of seat 1 corresponding to a pre-load of 450 N. The behavior of the backrest cushions, however, are significantly different; in addition to being stiffer than both seats 2 and 3, the backrest of seat 1 (7999 N/m) is also stiffer than its seat-pan cushion. The backrest of seat 3 is 53 % stiffer than seat 2. The coefficient of hysteresis loss of seat 3 for both the seat-pan and backrest are significantly higher than those of seat 1 and 2, which in large part is due to the seat construction and to the different foam chemistry.

Table 2.4: Deflection, static spring constant and coefficient of hysteresis loss for seat 1, 2 and 3

SEAT		Pre-Load (N)	Foam Deflection (mm)	Static Spring Constant (N/m)	Coefficient of Hysteresis Loss (%)
1	Seat-Pan	450	54.51	4267	30.9
	Backrest	150	26.73	7999	18.5
2	Seat-Pan	450	44.01	12422	24.5
	Backrest	150	32.01	5015	43.1
3	Seat-Pan	450	46.47	21735	63.9
	Backrest	150	20.23	7656	49.6

Figure 2.14 further illustrates the comparisons of load-deflection characteristics of the seat-pans of the candidate seats. The pan of seat 3 exhibits highly non-linear characteristics, and bottoming of the foam cells under deformations near 60 mm. the seat-pan cushions of seats 1 and 2 show comparable behavior in the 0 – 450 N pre-load range; above which the foam characteristics become highly non-linear, while the bottoming seems to occur under deformations exceeding 90 mm. Seat 1 exhibits typical PUF deflection characteristics where the softening of the cushion material becomes visible between 40 mm – 75 mm deflection, and rapid stiffening (densification) above 80 mm deflection.

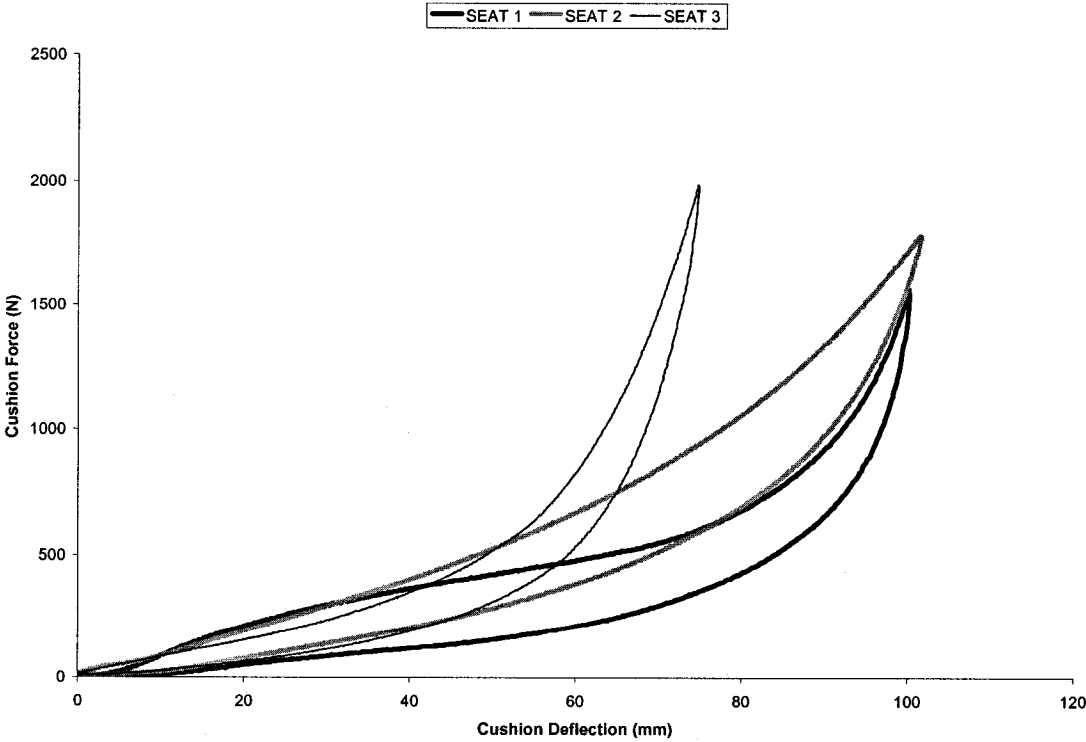


Figure 2.14: Seat-pan load-deflection characteristics of the test seat

Figure 2.15 similarly shows a comparison of the backrest load-deflection characteristics of the candidate seats. The backrest of seat 1 is stiffer than that of seat 2 over the entire weight range, while seat 3 is only stiffer than seat 1 above approximately 175 N pre-load. Furthermore, the backrest of seat 2 permits larger deformation, while that of seat 3 allows for least deformation prior to bottoming. Figure 2.16 illustrates comparisons of the load-deflection between the seat-pan and backrest for the three seats; seats 1 and 2 show significant differences between the seat-pan and backrest properties, while seat 3 shows almost identical behavior below 450 N for both the seat-pan and the backrest. The backrest of seat 1 reveals higher stiffness than its seat-pan, while the backrest of seat 2 is softer than its seat-pan.

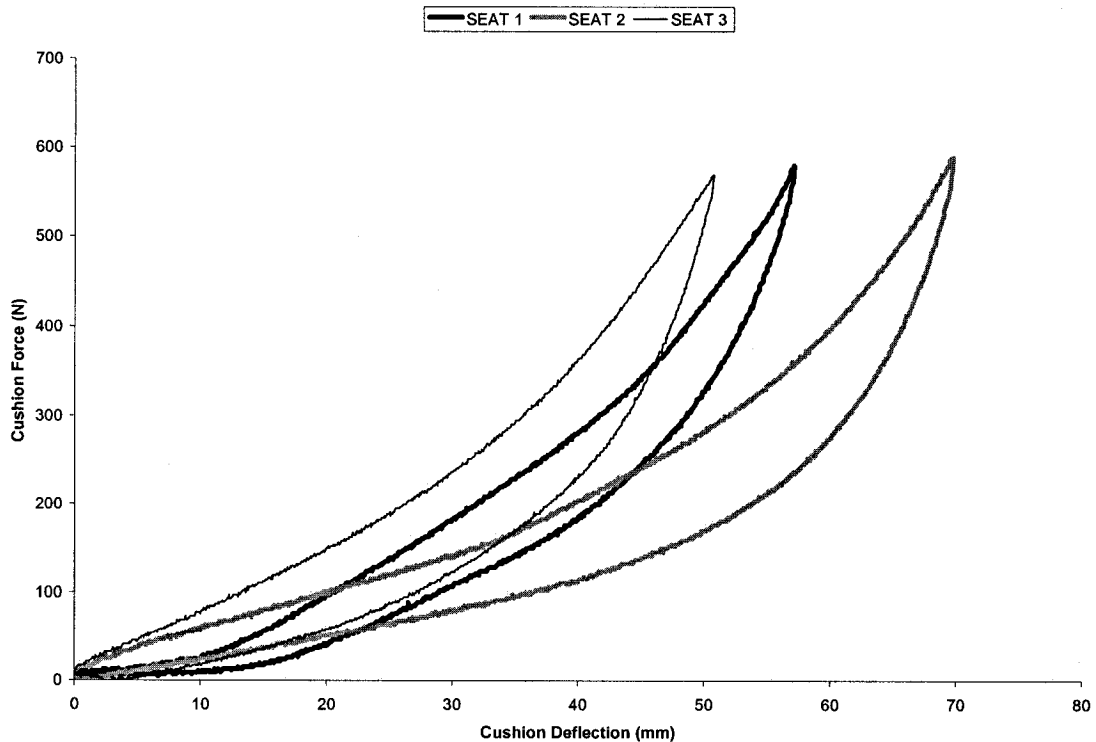
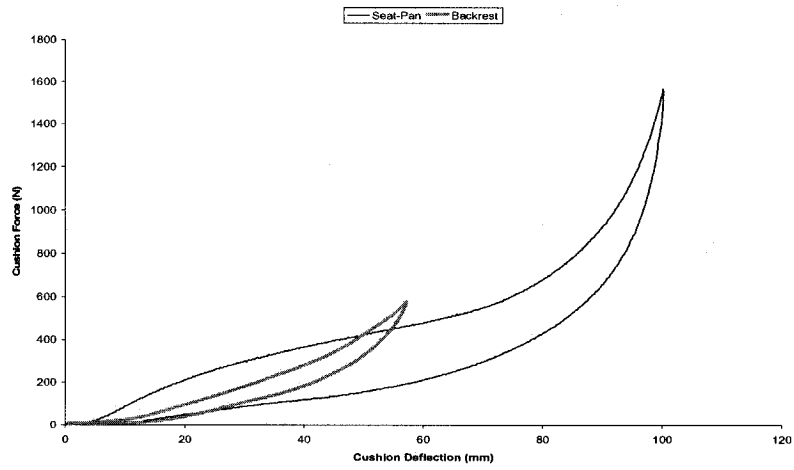
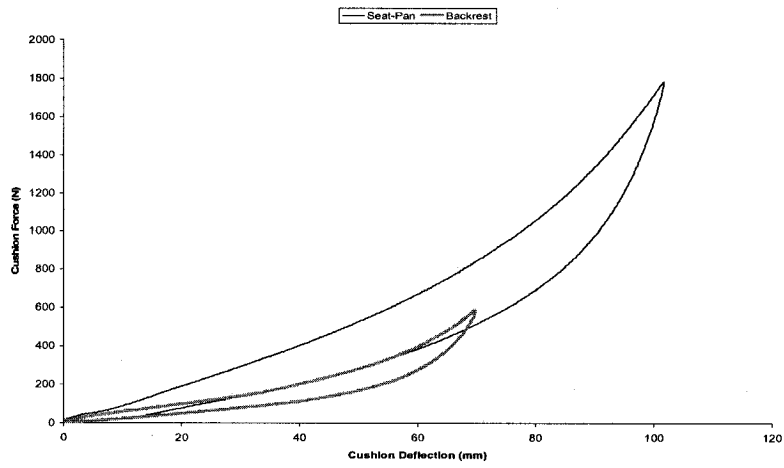


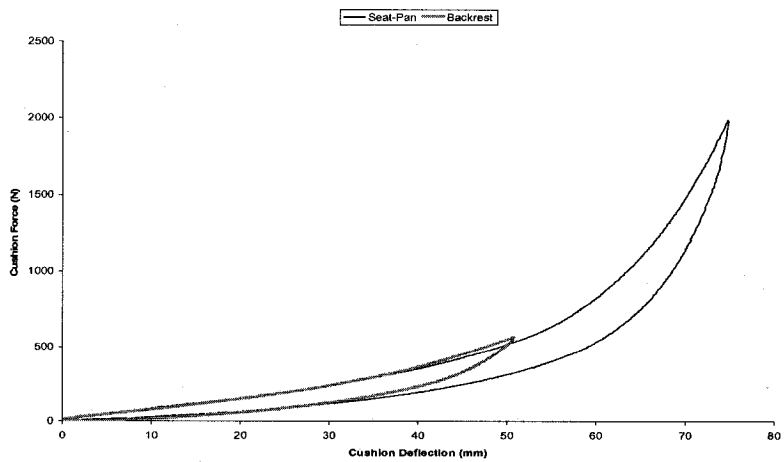
Figure 2.15: Backrest load-deflection characteristics of the test seats



(a)



(b)



(c)

Figure 2.16: Comparison of load-deflection curves of the seat-pan and backrest: (a) Seat 1; (b) Seat 2; (c) Seat 3

The measured data are further analyzed to derive the static stiffness and deflections of the seat-pans and backrests corresponding to pre-loads due to the 8 subjects employed in the study. Table 2.5 summarizes the seat properties corresponding to the selected pre-loads. For the seat-pan, seat 3 is more than 5 times stiffer than seat 1, as observed earlier in Table 2.6. but as pre-load increases the difference in stiffness becomes smaller as the pre-load increases. The seat-pan cushion of seat 3 approaches only 1.8 times that of seat 1 for a pre-load of 805 N. A similar trend is also observed for the pans of seats 2 and 1, where the pan of seat 2 is almost 3 times stiffer than that of seat 1 for 450 N pre-load but becomes slightly softer than seat 1 at pre-loads above 640 N. The difference between seat 3 and 2 however show different trends. For the entire weight range, seat 3 is between 1.7 and 2.7 times stiffer than seat 2.

Table 2.5: Seat-pan and Backrest cushion deflection and static stiffness

SEAT	Subject	Seat-Pan		Backrest	
		Cushion Deflection (mm)	Static Stiffness (N/m)	Cushion Deflection (mm)	Static Stiffness (N/m)
1	1	54.88	4277	25.65	7958
	2	62.89	5726	27.36	8022
	3	64.08	6174	27.50	8027
	4	69.93	9422	29.15	8084
	5	71.31	10466	29.42	8094
	6	77.71	16879	32.04	8210
	7	79.54	19229	33.04	8270
	8	85.98	29545	37.40	8702
2	1	44.10	12436	30.42	4836
	2	47.79	13049	33.49	5208
	3	48.34	13151	33.89	5264
	4	51.76	13858	35.75	5552
	5	52.51	14030	36.38	5659
	6	58.76	15749	39.89	6358
	7	60.25	16241	41.22	6670
	8	67.83	19318	46.82	8299
3	1	46.57	21888	19.03	7437
	2	49.03	26038	21.15	7843
	3	49.45	26825	21.39	7895
	4	51.51	31043	23.28	8338
	5	52.06	32271	23.68	8442
	6	55.14	40006	26.44	9243
	7	56.15	42872	27.75	9681
	8	59.48	53566	31.72	11245

The relationship between stiffness and pre-load for the seat-pan and the backrest cushions are further illustrated in Figures 2.17 to 2.18, respectively. The seat-pan and backrest stiffness shows good linear relationships with subject weight, as evident from the  $R^2$  values, where  $R^2 > 0.99$  and  $R^2 > 0.93$  for the seat-pan and the backrest cushions, respectively. Figure 2.17 further suggests that the seat-pan stiffness of seat 2 is less sensitive to pre-load when compared to seats 1 and 3, while Figure 2.18 suggests that the backrest stiffness of seat 1 is less sensitive to pre-load when compared to the backrest of seats 2 and 3. Figure 2.19 and 2.20 also show that the static deflection of the cushions exhibits a good linear relationship with pre-load, as observed by the  $R^2$  values, where  $R^2 > 0.93$  and  $R^2 > 0.99$  for the seat-pans and the backrests, respectively. Figure 2.19 shows that the seat-pan cushions of seats 2 and 3 undergo significantly smaller static deflections than those of seat 1 over the entire weight range considered. Seats 2 and 3 exhibit similar static deflections up to approximately 800 N pre-load, above which seat 2 undergoes slightly higher deflections. Figure 2.20 shows that the backrest cushions of all test seats have similar relationships with the pre-load, and that the static deflections of seat 2 are higher than those of seat 1 and that the deflections of seat 1 are greater than those of seat 3 over the entire weight range considered in this study. The stiffness properties of the seat-pan and backrest yield considerable insight into the behavior of the seat under loading. While the characterization of the candidate seats has established both a quantitative and qualitative relationship between the three test seats, it is anticipated that the differences in seat-pan and backrest cushion contours will also account for significant differences in the measured responses.

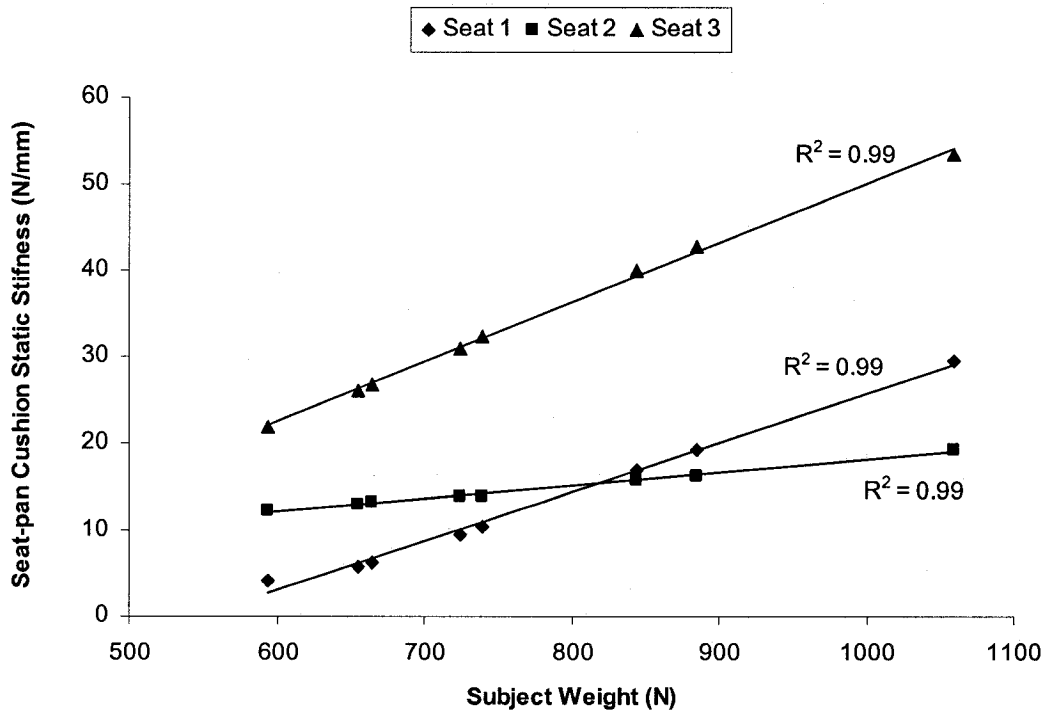


Figure 2.17: Seat-pan cushion stiffness as a function of subject weight

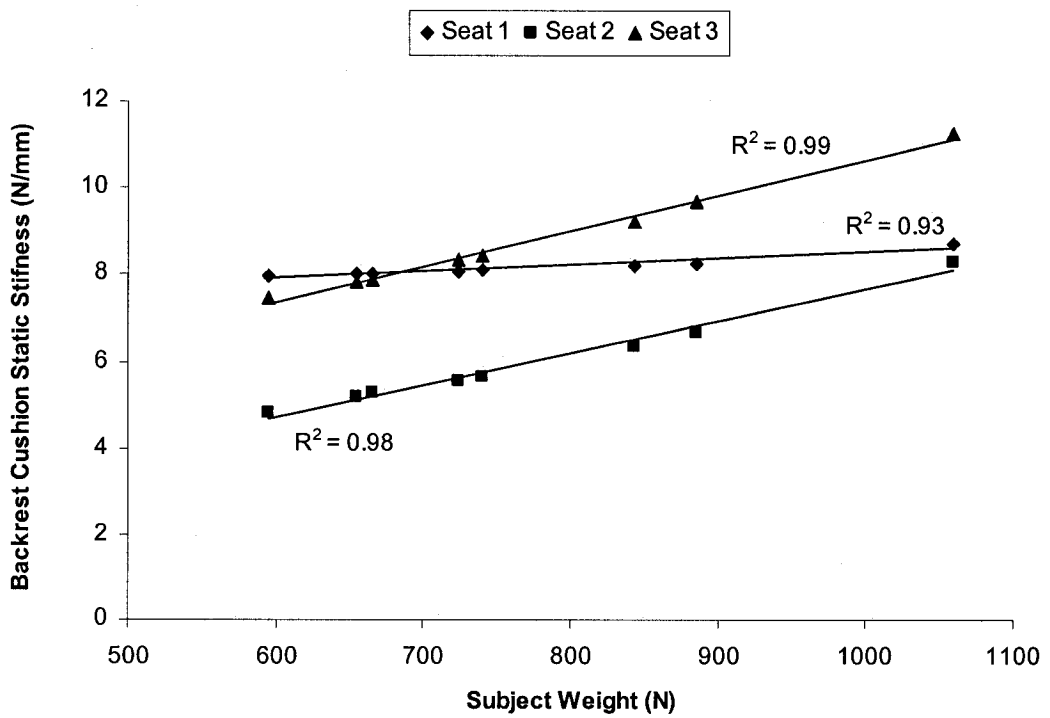


Figure 2.18: Backrest cushion stiffness as a function of subject weight

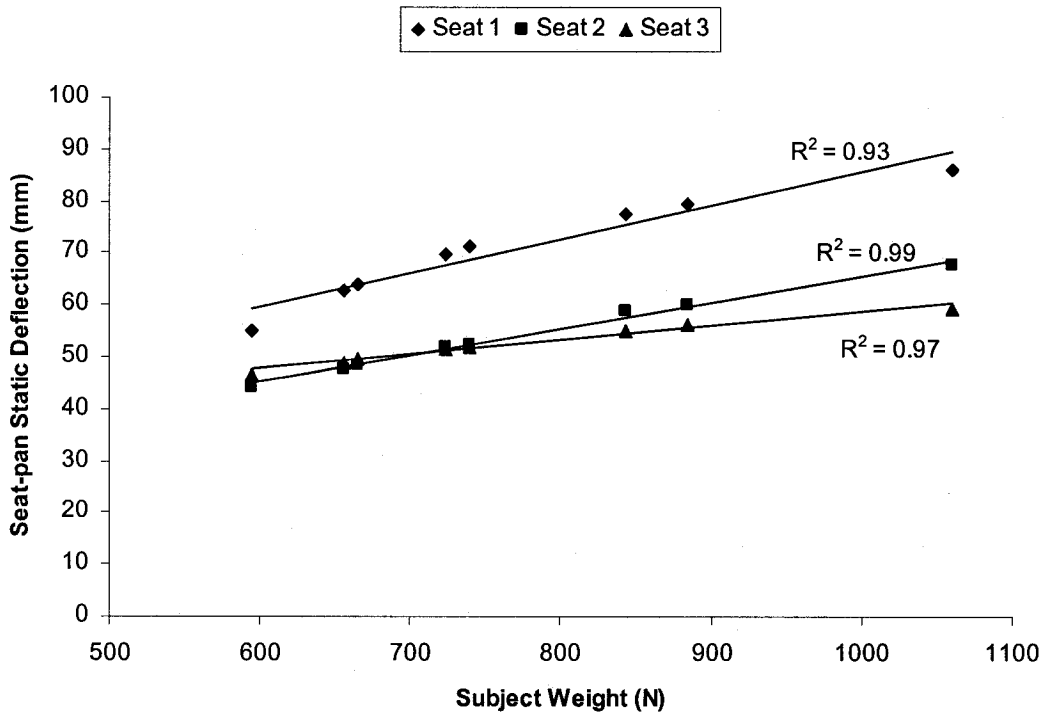


Figure 2.19: Seat-pan cushion deflection as a function of subject weight

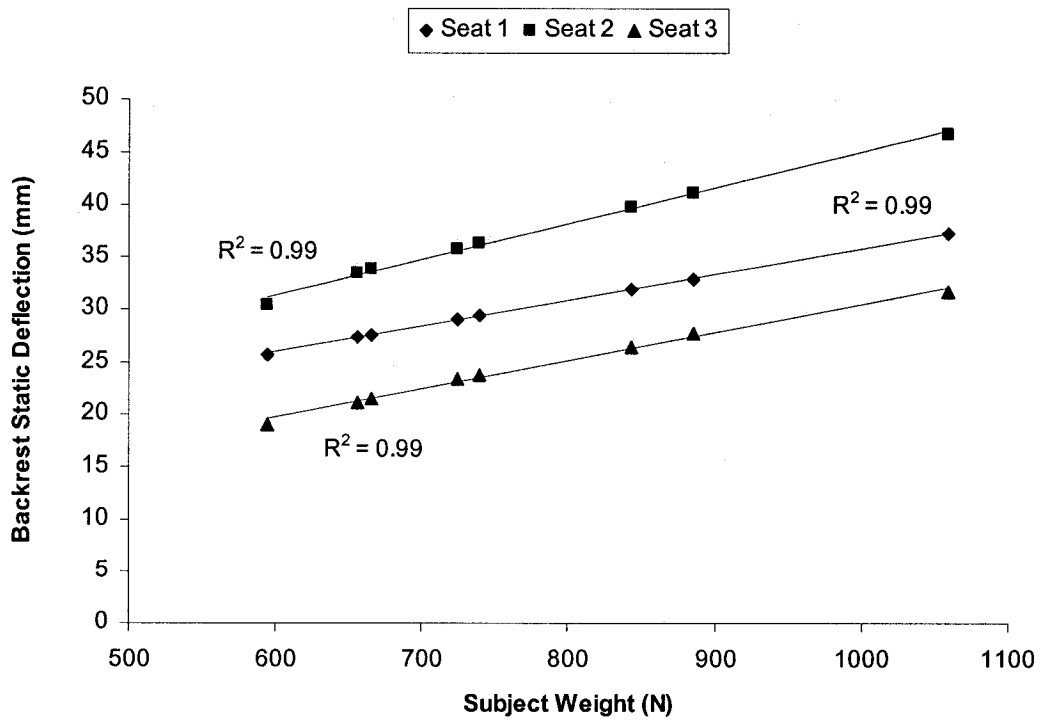


Figure 2.20: Backrest cushion deflection as a function of subject weight



## 2.6 Summary

In this chapter, the methodology and test setup used for the acquisition of BPD has been presented. The equipment used and standards followed for the characterization of the test seats has also been presented. Two proposed cushion characterization standards, one from the SAE and the other from the JASO, have been investigated and compared. It was found that the SAE method showed poor repeatability and yielded considerably lower stiffness results when compared to the JASO standard. The load-deflection characteristics of the three test seats showed highly non-linear behavior for both the seat-pan and the backrest cushions. Consequently, the force-deflection curves were fitted with a fourth order best-fit polynomial to determine the static stiffness of the cushions. Both the seat-pan and backrest cushion stiffness were found to have a strong dependence on pre-load. The cushion stiffness and deflections obtained by the methods outlined in this chapter are used simply to compare the test seats to one-another. Based on the results from the JASO standard, it is concluded, for the purposes of this study that: the seat-pan cushion of seat 3 is stiffer than that of seats 1 and 2 over the entire weight range, while seat 2 is stiffer than seat 1 up to 800 N pre-load, above which seat 1 becomes slightly stiffer than seat 2. For the backrest stiffness, seat 2 is softer than both seats 1 and 3 over the entire weight range considered, and seat 1 is stiffer than seat 3 up to approximately 550 N pre-load above which seat 1 is slightly softer.

## CHAPTER 3

### GENERALIZED CONTACT FORCES AND PRESSURE ANALYSIS AT THE HUMAN-SEAT INTERFACE OF AUTOMOTIVE SEATS

#### 3.1 Introduction

The reported studies on comfort performance characteristics of automotive seats have suggested that the contact pressure at the body-seat interface could serve as an effective and important measure [20,21,26]. The peak pressures and local concentrations of high pressures at the interface could be related to the discomfort and/or pain [28,33,34]. Both the peak pressures and their concentrations, however, depend upon many subject and seat design related factors in a complex manner. The pressure data, therefore, could not be directly interpreted to design guidelines in a quantitative manner. The need for further efforts to develop quantitative tools has been emphasized to enhance the understanding of the contact forces and the effects of various seat design features on the comfort performance of automotive seats.

The pressure distributions acquired at the body-seat interface for the seat-pans backrests of the three candidate seats are analyzed in this chapter to build the essential knowledge on the role of different seating variations, such as posture as determined by the backrest inclinations, the knee angles, the seat heights, as well as the mechanical properties of the seats, and the various anthropometric factors such as: body weight and build. The data are analyzed to study the effective contact area, peak contact pressures, and locations of peak pressures and contact force magnitudes as functions of the seated posture, as well as the various seat design and anthropometric factors.

### 3.2 Data Analysis

The total contact force developed over the entire surface is derived through integration of the localized pressures over the effective seat-pan and backrest contact areas. Since each sensor area is constant, and, assuming a uniform pressure distribution over the relatively small sensor area, the overall contact force  $F_c$  can be estimated by:

$$F_c = \Delta A_c \sum_{i=1}^n p_i \quad (3.1)$$

Where  $\Delta A_c$  is the surface area of a single sensor equal to  $6.45 \text{ cm}^2$ ,  $p_i$  is the pressure measured by sensor  $i$  and  $n$  is the total number of active sensors for which the pressure exceeds the preset threshold value. The pressure thresholds for the seat-pan and the backrest were selected as  $0.25$  and  $0.125 \text{ N/cm}^2$ , respectively, to reduce the signal noise.

The effective contact area between the body and the seat is further derived upon consideration of the number of active sensors, such that:

$$A_c = n\Delta A_c \quad (3.2)$$

where  $A_c$  is the total effective contact area. The data were acquired for 8 male adult subjects for each seat-height-knee-back combination. Each measurement was repeated twice and the data were examined to ensure repeatability of the measurements. The subjects were asked to stand up and move away from the seat before assuming the desired sitting posture for the next trial to account for the small differences in the posture, and also to allow the mat to be re-positioned to its reference position in case it had shifted. The data acquired from the two trials showed good within subject repeatability and very little variations in the magnitudes and locations of peak pressures and the contact force. As a result of the good repeatability, the subsequent force and pressure analyses, as well as the statistical analyses, are performed on the basis of the mean values

of the two trials. The mean values of the contact force, peak contact pressure and the effective contact area are thus analyzed to investigate the influence of subject anthropometry, seated posture and seat properties on the behavior of the interactions at the human-seat interface.

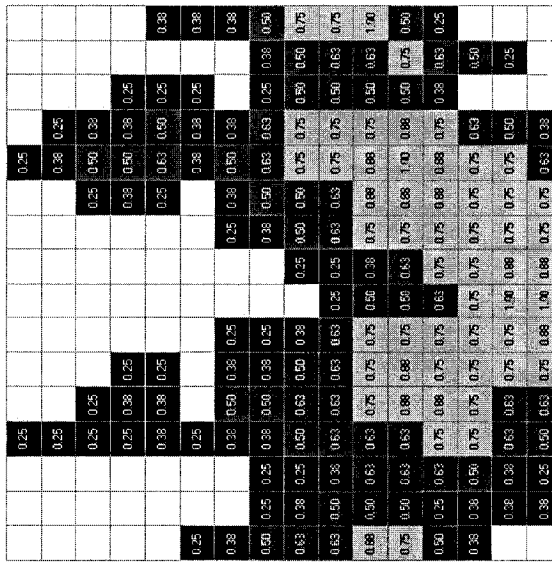
### **3.3 Analysis of Seat-Pan Contact Force and Peak Contact Pressure**

The BPD acquired for the selected subject-seat-posture combinations are analyzed using the *PLIANCE* software to derive total contact force and effective contact area on the basis of equations (3.1) and (3.2). The peak and mean contact pressures are further derived from the measured data for each test combination. Figure 3.1 shows, as an example, the seat-pan pressure profiles for a 76 kg subject assuming the same sitting posture on seats 1, 2 and 3. The concentration of higher pressure is clearly seen to be in the vicinity of the IT and surrounding buttocks for all seats with peak pressures ranging from 0.75 – 1.00 N/cm<sup>2</sup>, 1.125 – 1.375 N/cm<sup>2</sup> and 0.75 – 0.875 N/cm<sup>2</sup>, respectively, for seats 1, 2 and 3. The body/seat-pan contact forces and peak pressures are directly influenced by the effective contact between the seat and the human body, which appears to further be affected by the seat design and the seated posture. A lower contact area could generate higher contact force and magnitude of peak pressure. The relationship between contact area ( $A_c$ ) contact force ( $F_c$ ) and peak pressure (PP) is also directly related to the anthropometry and the cushion's ability to deform under the weight of the subject. Softer seats tend to reduce the likelihood of hard points and the associated localized high pressures. Analyses of the pressure distribution data acquired for the same

Posture: H2 - 368 mm / K2 - 115° / B2 - 15°

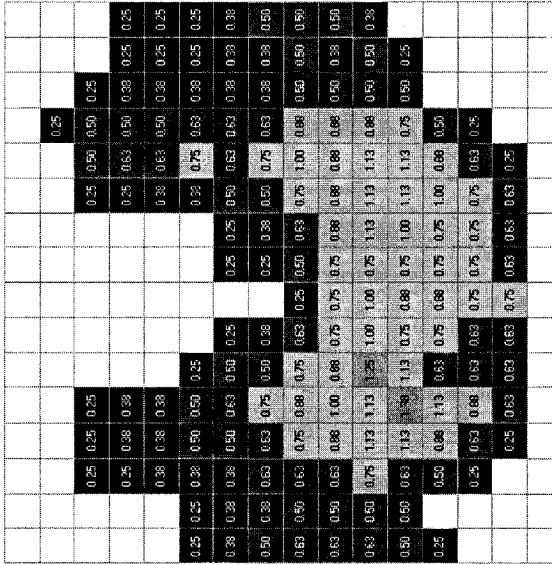
**SEAT 1**

F<sub>c</sub>: 554.0 N  
 PP: 1.00 N/cm<sup>2</sup>  
 A<sub>c</sub>: 1129.0 cm<sup>2</sup>  
 MP: 0.54 N/cm<sup>2</sup>



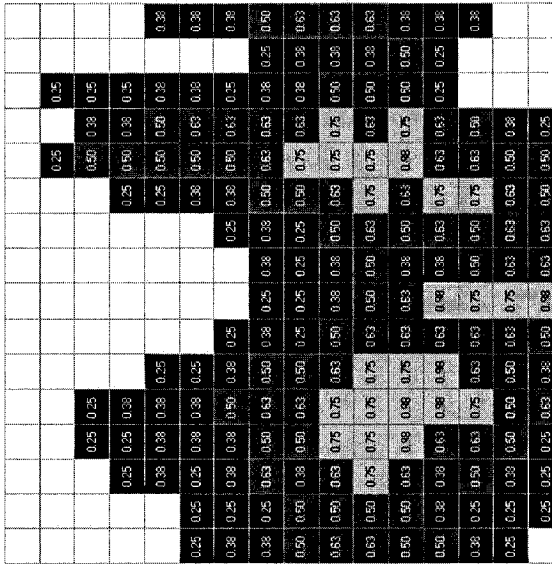
**SEAT 2**

F<sub>c</sub>: 587.9 N  
 PP: 1.375 N/cm<sup>2</sup>  
 A<sub>c</sub>: 1096.8 cm<sup>2</sup>  
 MP: 0.58 N/cm<sup>2</sup>



**SEAT 3**

F<sub>c</sub>: 517.7 N  
 PP: 0.875 N/cm<sup>2</sup>  
 A<sub>c</sub>: 1174.2 cm<sup>2</sup>  
 MP: 0.49 N/cm<sup>2</sup>



**P ≥ 3.75   P ≥ 2.75   P ≥ 1.875   P ≥ 1.25   P ≥ 0.75   P ≥ 0.5   P ≥ 0.25**  
 N/cm<sup>2</sup>

Figure 3.1: Seat-pan pressure profiles for a 76 kg subject seated on seats 1, 2 and 3

subject and posture could thus yield considerable insight into the differences attributed to the cushion features of each seat. The pressure profiles in Figure 3.1 suggest that seat 3 behaves more like a softer seat providing a smoother pressure gradient away from the IT and a higher effective contact area, while seat 2 behaves as the hardest seat with the lowest contact area and the highest contact force and peak pressure. Seat 1, on the other hand, as anticipated, yields asymmetric pressure distribution attributed the high wings, while the contact area and force magnitudes are between those of seats 2 and 3. Based on the cushion characterization and the seat-pan stiffness derived in section 2.5, the results suggest that for a pre-load of 562 N (76 kg subject), seat 3 is observed to be stiffer than seat 2 and that seat 2 is observed to be stiffer than seat 1. Comparing the pressure profiles obtained for seats 1 and 2, the results indeed suggest that a stiffer seat undergoes significantly lower deflection causing leading to lower interface contact area and higher magnitudes of contact force and peak contact pressures as shown in Figure 3.1. A subsequent physical inspection of the seta-pan of seat 3 revealed that the seat-pan actually had a very thin layer of PUF supported by steel bars running along the width of the seat-pan. This would explain why the pressure profile of seat 3 behaves more like a soft seat but that the effective static stiffness of the seat-pan is greater than that of seats 1 and 2.

As a result of the differences in pressure profiles between test seats, each seat was analyzed separately to investigate the variations in the pressure profiles and to identify relationships as functions of the anthropometry and the seated posture. The results of the individual analyses are then compared to one-another in an attempt to explain the differences in the cushion stiffness and seat contouring. Tables 3.1 to 3.4 summarize the mean values of contact force ( $F_c$ ), contact area ( $A_c$ ), peak pressure (PP) and mean

pressure (MP), and the standard deviations of the means for each seat-posture combination. The results show considerable variations as indicated by the large standard deviations, which are attributed to the large inter-subject variability associated with differences in subject anthropometry and preferred sitting postures. While these variations are expected, the mean values show clear trends with respect to the experimental factors considered, namely, seat height (H), knee angle (K) and the backrest angle (B).

Table 3.1: Mean and standard deviation (SD) of seat-pan contact force,  $F_c$

Seat Height (mm)	Knee Angle (deg.)	Back Angle (deg.)	Seat-Pan Contact Force, $F_c$ (N)					
			Seat 1		Seat 2		Seat 3	
			Mean	SD	Mean	SD	Mean	SD
318	95	5	544.9	86.0	X	X	X	X
		15	517.9	88.1	523.7	87.9	516.9	99.5
		25	460.5	79.9	485.2	84.1	468.9	82.4
	115	5	569.1	84.7	X	X	X	X
		15	534.3	73.7	545.4	99.9	523.1	100.4
		25	470.6	88.3	488.3	77.6	464.5	95.5
	135	5	600.7	92.4	X	X	X	X
		15	558.3	101.8	561.1	95.9	533.9	103.9
		25	520.7	90.5	506.5	80.9	485.5	101.1
368	95	5	561.0	94.1	X	X	X	X
		15	519.9	88.3	527.7	95.4	508.4	87.0
		25	451.7	71.4	478.1	88.5	463.4	104.2
	115	5	569.8	87.5	X	X	X	X
		15	529.1	94.6	541.7	89.4	523.7	93.2
		25	471.0	64.4	478.8	88.3	475.8	107.1
	135	5	579.6	108.7	X	X	X	X
		15	565.5	120.7	555.4	83.6	559.1	91.4
		25	504.5	109.2	512.1	81.8	496.0	115.7
419	95	5	558.8	68.1	X	X	X	X
		15	538.5	104.5	528.2	111.4	528.3	101.8
		25	464.6	62.5	490.0	76.1	472.1	113.7
	115	5	574.1	71.4	X	X	X	X
		15	557.9	91.0	541.0	106.3	543.5	95.5
		25	501.1	81.8	506.2	80.8	488.3	104.5
	135	5	590.7	106.0	X	X	X	X
		15	547.1	108.8	562.1	87.9	564.8	90.2
		25	513.5	119.5	520.5	73.2	515.4	102.1

X – Data not acquired for the combination

Table 3.2: Mean and standard deviation (SD) of seat-pan peak pressure, PP

Seat Height (mm)	Knee Angle (deg.)	Back Angle (deg.)	Seat-Pan Peak Pressure, PP (N/cm <sup>2</sup> )					
			Seat 1		Seat 2		Seat 3	
			Mean	SD	Mean	SD	Mean	SD
318	95	5	1.50	0.12	X	X	X	X
		15	1.28	0.09	1.43	0.27	1.35	0.30
		25	1.24	0.16	1.30	0.21	1.22	0.24
	115	5	1.39	0.19	X	X	X	X
		15	1.27	0.17	1.26	0.25	1.18	0.30
		25	1.17	0.20	1.18	0.22	1.03	0.24
	135	5	1.33	0.21	X	X	X	X
		15	1.16	0.26	1.07	0.21	1.02	0.23
		25	1.08	0.26	1.08	0.22	0.89	0.17
368	95	5	1.45	0.11	X	X	X	X
		15	1.23	0.14	1.32	0.22	1.21	0.24
		25	1.19	0.12	1.26	0.19	1.12	0.13
	115	5	1.37	0.24	X	X	X	X
		15	1.17	0.14	1.21	0.27	1.09	0.29
		25	1.14	0.18	1.09	0.18	0.99	0.20
	135	5	1.33	0.25	X	X	X	X
		15	1.18	0.23	1.08	0.24	1.01	0.27
		25	1.08	0.21	1.03	0.20	0.85	0.11
419	95	5	1.38	0.20	X	X	X	X
		15	1.19	0.20	1.26	0.31	1.10	0.22
		25	1.09	0.14	1.16	0.18	0.96	0.10
	115	5	1.32	0.26	X	X	X	X
		15	1.13	0.18	1.15	0.24	0.97	0.16
		25	1.07	0.18	1.08	0.18	0.90	0.10
	135	5	1.34	0.29	X	X	X	X
		15	1.15	0.27	1.04	0.16	1.01	0.19
		25	1.05	0.19	1.02	0.15	0.91	0.18

Table 3.3: Mean and standard deviation (SD) of seat-pan contact area, A<sub>c</sub>

Seat Height (mm)	Knee Angle (deg.)	Back Angle (deg.)	Seat-Pan Contact Area, A <sub>c</sub> (cm <sup>2</sup> )					
			Seat 1		Seat 2		Seat 3	
			Mean	SD	Mean	SD	Mean	SD
318	95	5	883.8	166.4	X	X	X	X
		15	875.8	179.9	839.2	170.5	950.0	165.5
		25	804.0	174.1	799.2	178.9	913.0	164.8
	115	5	1025.5	161.4	X	X	X	X
		15	997.8	155.9	917.3	180.6	1037.6	176.3
		25	922.7	177.4	922.2	171.4	985.9	182.3
	135	5	1160.0	153.1	X	X	X	X
		15	1135.4	157.5	1117.9	180.2	1146.3	161.2
		25	1112.4	160.0	1053.2	205.0	1118.0	179.7
368	95	5	977.0	181.0	X	X	X	X
		15	922.8	181.7	898.6	189.0	994.5	178.1
		25	854.9	163.5	842.3	194.5	937.4	190.9
	115	5	1089.9	161.2	X	X	X	X
		15	1046.3	202.5	1010.1	178.7	1093.1	202.9
		25	991.6	161.1	952.5	200.1	1048.8	222.2
	135	5	1148.6	180.0	X	X	X	X
		15	1149.1	204.2	1111.8	149.7	1200.3	156.1
		25	1101.1	199.2	1101.8	173.9	1163.8	187.6
419	95	5	1036.1	138.4	X	X	X	X
		15	1028.5	205.8	970.3	205.6	1080.7	195.7
		25	962.8	162.8	926.5	172.2	1024.8	214.8
	115	5	1132.0	125.3	X	X	X	X
		15	1130.8	160.3	1072.6	170.8	1181.9	178.6
		25	1103.9	145.5	1059.3	177.1	1126.0	192.8
	135	5	1134.2	163.3	X	X	X	X
		15	1128.5	177.0	1134.0	117.5	1228.3	136.4
		25	1101.0	208.9	1112.6	155.8	1204.1	143.0

X – Data not acquired for the combination



Table 3.3: Mean and standard deviation (SD) of seat-pan mean pressure, MP

Seat Height (mm)	Knee Angle (deg.)	Back Angle (deg.)	Seat-Pan Mean Pressure, MP (N/cm <sup>2</sup> )					
			Seat 1		Seat 2		Seat 3	
			Mean	SD	Mean	SD	Mean	SD
318	95	5	0.62	0.04	X	X	X	X
		15	0.60	0.04	0.63	0.04	0.54	0.04
		25	0.58	0.04	0.61	0.05	0.51	0.02
	115	5	0.56	0.04	X	X	X	X
		15	0.54	0.04	0.58	0.04	0.51	0.05
		25	0.51	0.05	0.55	0.05	0.47	0.04
	135	5	0.52	0.02	X	X	X	X
		15	0.49	0.03	0.50	0.04	0.47	0.04
		25	0.47	0.02	0.49	0.04	0.43	0.04
368	95	5	0.58	0.04	X	X	X	X
		15	0.57	0.05	0.59	0.03	0.51	0.03
		25	0.53	0.04	0.57	0.04	0.50	0.03
	115	5	0.52	0.04	X	X	X	X
		15	0.51	0.04	0.54	0.04	0.48	0.03
		25	0.48	0.05	0.51	0.05	0.45	0.03
	135	5	0.50	0.03	X	X	X	X
		15	0.49	0.03	0.50	0.04	0.46	0.03
		25	0.46	0.03	0.46	0.04	0.42	0.04
419	95	5	0.54	0.04	X	X	X	X
		15	0.53	0.03	0.54	0.02	0.49	0.03
		25	0.49	0.04	0.53	0.04	0.46	0.03
	115	5	0.51	0.02	X	X	X	X
		15	0.49	0.03	0.50	0.03	0.46	0.04
		25	0.45	0.03	0.48	0.04	0.43	0.03
	135	5	0.52	0.03	X	X	X	X
		15	0.48	0.03	0.49	0.04	0.46	0.04
		25	0.46	0.03	0.47	0.04	0.42	0.04

X – Data not acquired for the combination

The most significant factor affecting the magnitudes of the measured responses is the backrest angle. For each combination of seat height and knee angle, increasing the backrest angle from 5° to 15° to 25° systematically reduces the magnitude of the seat-pan contact force and contact area, while also significantly reducing the magnitudes of peak pressure surrounding the IT. The higher backrest angles cause the upper body to recline more and therefore reduce the percentage of total body weight supported by the seat-pan. This trend has also been reported in a recent study on the biodynamic behavior of the seated occupants exposed to vertical vibration [55]. Figure 3.2 shows the pressure profiles measured on the pan of seat 1 as a function of backrest angle for a 76 kg subject. Higher backrest inclination reduces the contact beneath the thighs and transfers the body weight towards the rear of the seat away from the IT onto the sacrum and lower lumbar

area. For the same subject, increasing the backrest angle results in a reduction of the peak pressure around the IT from 1.0 – 1.125 N/cm<sup>2</sup> to 0.875 – 1.0 N/cm<sup>2</sup> to 0.75 – 0.875 N/cm<sup>2</sup> for 5° to 15° to 25° backrest angles, respectively. The transfer of weight towards the rear of the seat is clearly visible from the last two rows of each pressure map; higher backrest angles generate higher peak pressures and higher concentrations of peak pressure near the sacrum and lower lumbar area.

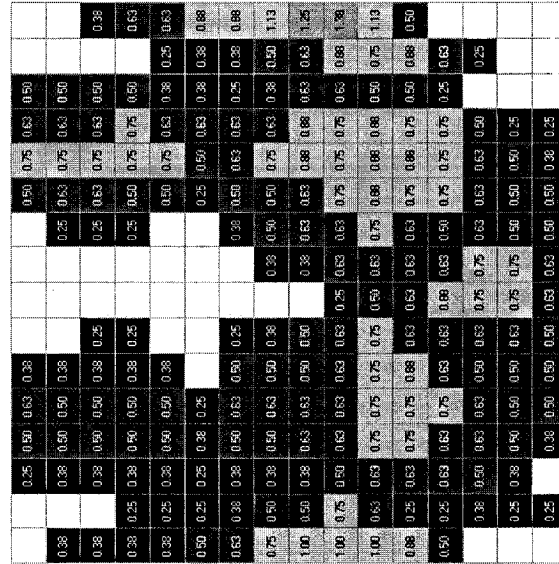
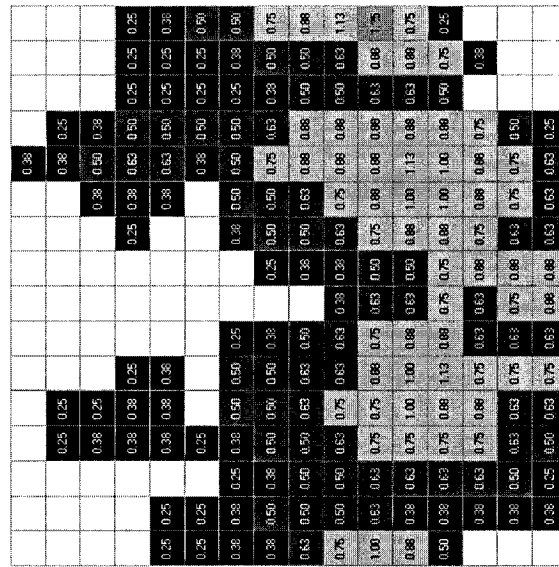
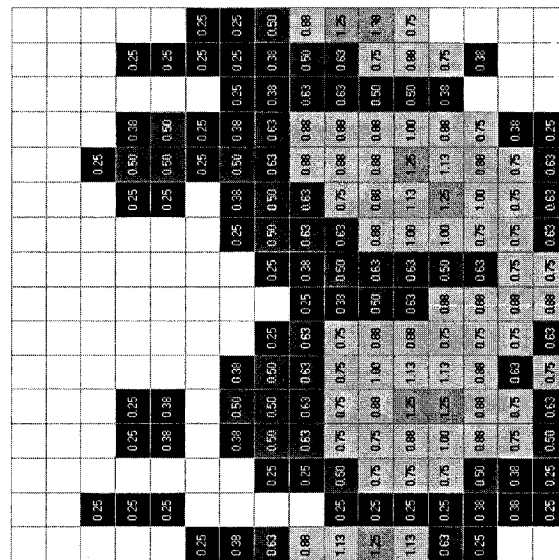
While an increase in the backrest angle generally leads to a decrease in the total contact force and contact area, the effect of increasing the knee angle is opposite. As seen in Figure 3.3, increasing the knee angle from 95° to 115° and to 135° increases the contact force from 607.5 N to 636.3 N and finally to 720.2 N, respectively. The corresponding peak pressure around the IT, however, tends to benefit as it decreases from 1.25 – 1.125 N/cm<sup>2</sup> to 1.125 – 1.00 N/cm<sup>2</sup> to 0.875 – 0.75 N/cm<sup>2</sup> for 95° to 115° and to 135° knee angles, respectively. The decrease in the pressure around the IT, however, results in a significant increase in the contact pressure beneath the thighs just above the knees, which may encourage reduced blood flow to the legs and rapid fatigue. A higher knee angle, however, tends to reduce the concentration of high pressure around the IT and generates a smoother pressure gradient surrounding the IT. Moreover, higher knee angles create increased contact between the lower body and the seat-pan, as evident from the increase in contact area from 1071.1 cm<sup>2</sup> to 1193.5 cm<sup>2</sup> to 1348.4 cm<sup>2</sup> for 95°, 115° and 135° knee angles, respectively. A higher contact area ensures that the body weight is distributed over a larger area, and thereby reducing the magnitudes of peak pressure. The results thus suggest that sitting postures with higher knee angles may be sustained for longer periods of time without discomfort or pain.

### SEAT 1

**Posture: H2 - 368 mm / K1 - 95° / B1 - 5°**  
**F<sub>c</sub>: 606.5 N**  
**PP: 1.375 N**  
**A<sub>c</sub>: 1071.0 cm<sup>2</sup>**  
**MP: 0.62 N/cm<sup>2</sup>**

**Posture: H2 - 368 mm / K2 - 115° / B1 - 5°**  
**F<sub>c</sub>: 636.3 N**  
**PP: 1.25 N/cm<sup>2</sup>**  
**A<sub>c</sub>: 1193.5 cm<sup>2</sup>**  
**MP: 0.58 N/cm<sup>2</sup>**

**Posture: H2 - 368 mm / K3 - 135° / B1 - 5°**  
**F<sub>c</sub>: 720.2 N**  
**PP: 1.375 N/cm<sup>2</sup>**  
**A<sub>c</sub>: 1348.4 cm<sup>2</sup>**  
**MP: 0.56 N/cm<sup>2</sup>**



**P ≥ 3.75   P ≥ 2.75   P ≥ 1.875   P ≥ 1.25   P ≥ 0.75   P ≥ 0.5   P ≥ 0.25**  
**N/cm<sup>2</sup>**

Figure 3.3: Effect of knee angle on the seat-pan pressure distribution for a 76 kg subject seated on seat 1

## SEAT 1

**Posture: H1 - 318 mm / K2 - 115° / B2 - 15°**  
**F<sub>c</sub>: 546.0 N**  
**PP: 1.125 N/cm<sup>2</sup>**  
**A<sub>c</sub>: 1064.5 cm<sup>2</sup>**  
**MP: 0.57 N/cm<sup>2</sup>**

**Posture: H2 - 368 mm / K2 - 115° / B1 - 5°**  
**F<sub>c</sub>: 554.0 N**  
**PP: 1.00 N/cm<sup>2</sup>**  
**A<sub>c</sub>: 1129.0 cm<sup>2</sup>**  
**MP: 0.54 N/cm<sup>2</sup>**

**Posture: H3 - 419 mm / K3 - 115° / B1 - 5°**  
**F<sub>c</sub>: 586.3 N**  
**PP: 1.125 N/cm<sup>2</sup>**  
**A<sub>c</sub>: 1238.7 cm<sup>2</sup>**  
**MP: 0.52 N/cm<sup>2</sup>**

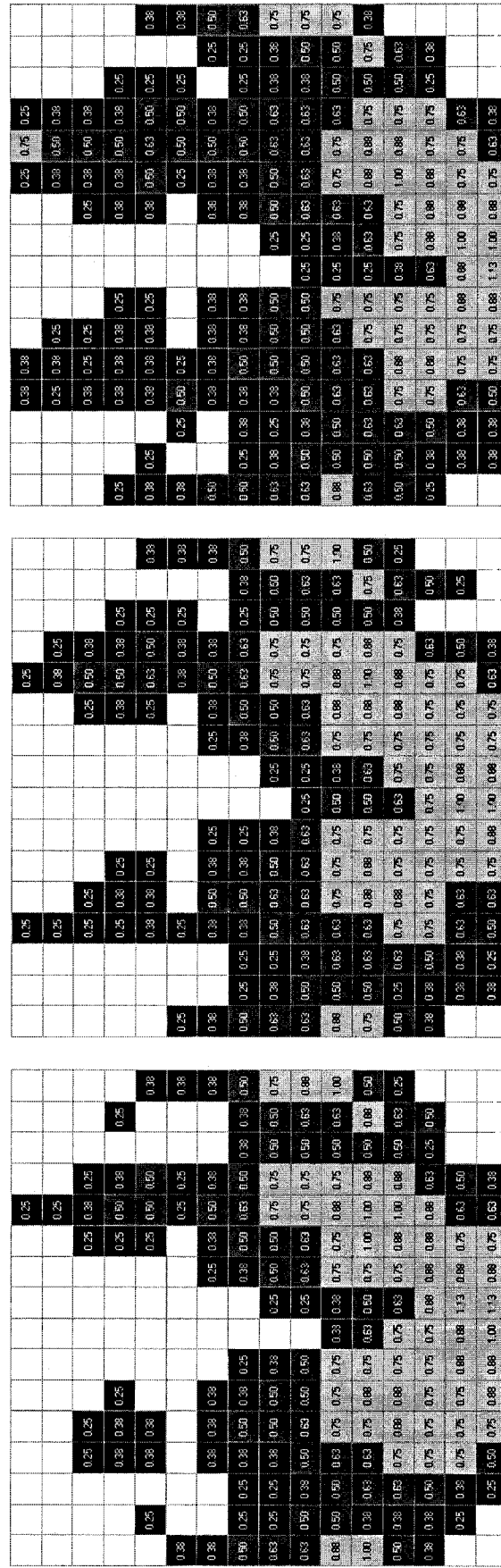


Figure 3.4: Effect of seat height on the seat-pan pressure distribution for a 76 kg subject seated on seat

The effect of seat height on the seat-pan pressure distribution is shown in Figure 3.4, for the same seat-knee-backrest combination to study the effect of seat height alone. An increase in the seat height results in higher contact force and contact area beneath the thighs just above the knees. The effect of seat height shows very little effect on reducing the magnitudes of peak pressure surrounding the IT,  $0.625 - 1.00 \text{ N/cm}^2$  and  $0.625 - 1.00 \text{ N/cm}^2$  to  $0.875 - 1.00 \text{ N/cm}^2$  for seat heights H1 – 318 mm, H2 – 368 mm and H3 – 419 mm, respectively. The higher contact force with a relatively higher seat is attributed to increased body mass supported by a higher seat-pan. A few studies have shown that the body weight supported by the seat increases with seat height [52,55,56]. Increased contact between the thighs and the pan is mostly caused by the subject's tendency to stabilize the desired knee angle. The variations in the measured parameters attributed to changes in the seat height, however, show much smaller significance compared to those due to the variations in the backrest and knee angle settings. In light of the observed variations in  $F_c$ ,  $A_c$ , PP and MP with respect to the three experimental factors, a multi-factor within subject ANalysis Of VAriance (ANOVA) is performed on the data to verify the statistical significance of the different factors, namely: the seat (S); seat height (H); knee angle (K); and the backrest angle (B); on the measured responses. The Statistical Package for the Social Sciences (SSPS) software is used to perform the analyses. The ANOVA is further applied to identify and verify the significance of any interactions between the experimental factors considered. While significant variations in the contour shape exist between the three candidate seats, the parameter designated as S, is quantified by the static stiffness of the cushion as derived in section 2.5 for the appropriate pre-loads.

### 3.3.1 Relationship between seat-pan contact force and posture

The results attained from the ANOVA revealed that the factors K and B have very significant effect on the total contact forces ( $p < 0.001$ ), while the effects of H and the two-way interaction between H and K ( $H * K$ ) as well as the three-way interactions between S, H, K ( $S * H * K$ ) and S, K, B ( $S * K * B$ ) are fairly significant ( $p < 0.05$ ). Figures A1.1 to A1.9, presented in appendix A1, show the variations in the seat-pan contact force for each seat-posture combination as a function of the subject weight. The contact forces exhibit fairly linear relationships between the subject weight, backrest angle (Figures A1.1 to A1.3), knee angle (Figures A1.4 to A1.6) and seat height (Figures A1.7 to A1.9). A sample output for the ANOVA is shown in Table B1-1 in Appendix B. Seat 1 in this study offered an advantage over seats 2 and 3, where it was possible to acquire BPD measurements for a third angular setting, B1 - 5°, representing a more erect sitting posture. The results clearly suggest that both the backrest and knee angles have strong effects on the variations in the contact force, when compared to the seat height.

A multiple linear regression analysis was further performed to illustrate the relationship between the contact force and the experimental factors, S, H, K, B using the SPSS software. The model also included the significant two and three-way interactions revealed by the ANOVA as well as the subject weight (W). The resulting regression analysis reveals the following relationship between the experimental factors and the predicted values of contact force.

$$F_c = \beta_0 + \beta_1(W) + \beta_2(K) + \beta_3(B) + \beta_4(H) + \beta_5(H * K) + \beta_6(S * H * K) + \beta_7(S * K * B) \quad (3.2)$$

The coefficients  $\beta_0, \beta_1, \beta_2, \beta_3, \beta_4, \beta_5, \beta_6,$  and  $\beta_7,$  represent the contributions due to the individual factors and their interactions which are summarized in Table 3.5.

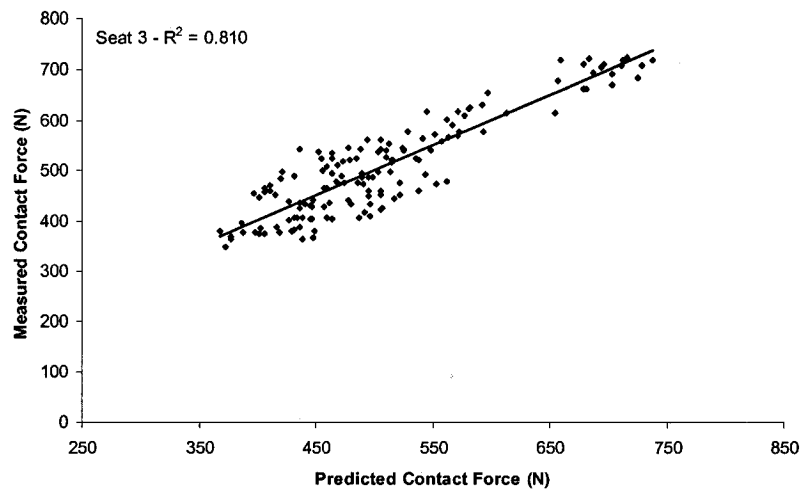
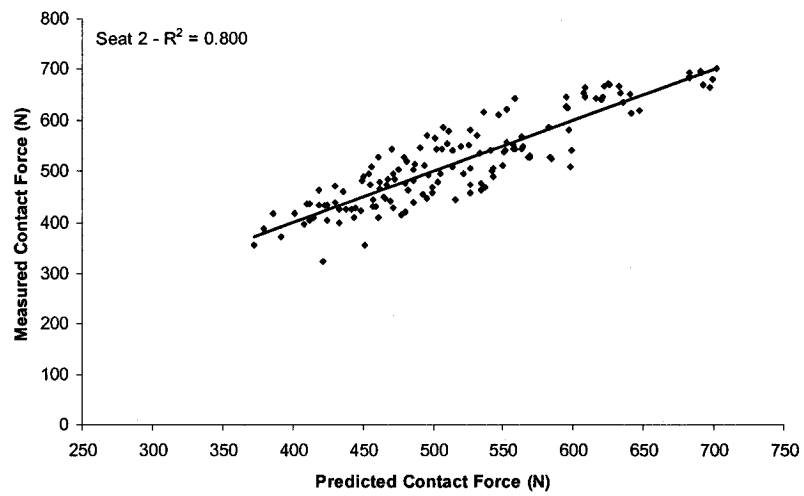
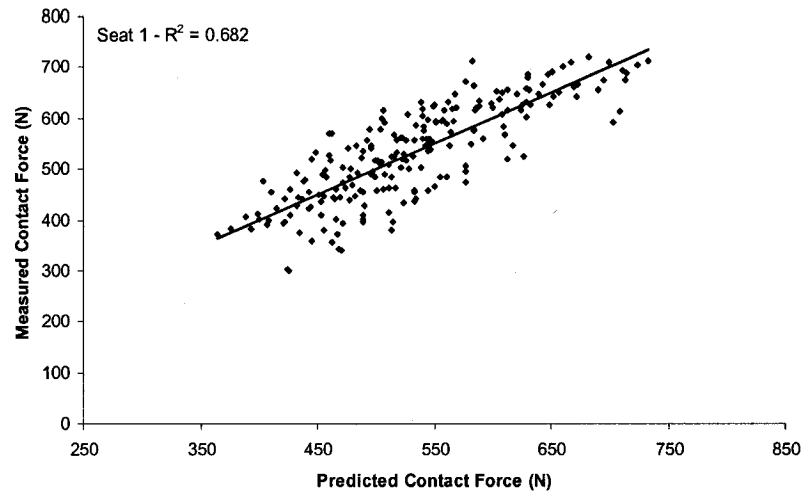


Figure 3.5: Correlation between the measured and estimated mean contact force at the seat- pan for the three test seats

The regression model provides an acceptable prediction of the actual measured seat-pan contact force values as shown in Figure 3.5. The correlation coefficients,  $R^2$ , of 0.68, 0.80 and 0.81 were obtained for seats 1, 2 and 3, respectively. A sample output from the SPSS software is shown in Figure B2-1 in Appendix B.

Table 3.5: Regression coefficients for the prediction of total seat-pan contact force

Seat	$R^2$	$\beta_0$	$\beta_1$	$\beta_2$	$\beta_3$	$\beta_4$	$\beta_5$	$\beta_6$	$\beta_7$
1	0.682	-255.7	0.62	3.0	-4.5	0.71	-0.005	$-6.3 \times 10^{-8}$	$7.1 \times 10^{-8}$
2	0.800	-205.4	0.86	1.15	-1.0	-0.02	0.007	$-4.3 \times 10^{-7}$	$-2.2 \times 10^{-6}$
3	0.810	344	0.463	-1.40	-6.0	-0.45	0.006	$-9.4 \times 10^{-10}$	$7.1 \times 10^{-8}$

The results indicate, as anticipated, that the total contact force increases proportionally with the subject weight ( $W$ ). The coefficients of  $B$ ,  $\beta_3$ , clearly show the decreasing trend in contact force with higher backrest angles for all seats. The regression model further suggests that a higher knee angle for seat 3 would reduce the contact force, while higher contact forces would be attained for seats 1 and 2. Similarly, seat height has a positive effect on the contact force of seat 1, while higher seat settings contribute to reductions in the contact force on seats 2 and 3. The coefficients of the two and three way interactions show very little contribution to the of seat pan contact force, but further suggest that contact force is sensitive to the postural variations.

The regression analysis of the contact force shows good linear relationship with the subject weight and the individual experimental factors. Owing to the most obvious effect of the body weight and the considerable variations in the body weights of different subjects, the measured contact force is normalized with the body weight to study the



effects of the other factors alone. The normalized contact force, referred to as the Contact Force Ratio (CFR), is expressed as:

$$CFR = \frac{F_c}{W_i} \quad (3.3)$$

where  $F_c$  is the total contact force measured at the seat-pan for a given posture and  $W_i$  represents the total body weight of the subject. The CFR is a direct indication of the amount of total body weight supported by the seat-pan cushion, which may further depend upon various seat-posture related factors. Figures 3.6 – 3.8 illustrate the variations in CFR for seats 1, 2 and 3, respectively, as a function of the backrest angle, knee angle and the seat height. The regression model, presented in Equation 3.2, is further simplified to describe the CFR, and by neglecting the contributions due to the three-way interactions S\*H\*K and S\*K\*B, such that:

$$CFR = \beta_0 + \beta_1(H) + \beta_2(K) + \beta_3(B) + \beta_4(H * K) \quad (3.4)$$

Table 3.6: Regression coefficients for the prediction of seat-pan CFR

Seat	R <sup>2</sup>	$\beta_0$	$\beta_1$	$\beta_2$	$\beta_3$	$\beta_4(10^{-6})$
1	0.945	0.232	0.00111	0.004477	-0.00589	-8.8
2	0.814	0.663	-0.00011	0.000824	-0.00552	1.85
3	0.970	0.926	-0.00067	-0.001755	-0.00721	7.75

Table 3.6 summarizes the results of a stepwise forward regression analysis used to verify the contribution of each parameter to the CFR. The results presented in Figure 3.6 to 3.8, show strong coupled effects of the backrest and knee angles with little clear trends

for all the tree seats. The backrest angle, however, appears to be most instrumental in reducing the ratio of the body weight supported by the seat pan as shown by the coefficient  $\beta_1$ . A lower knee angle also tends to reduce the CFR considerably, irrespective of the seat height and seat type considered. Seat height shows a negative effect on the seat-pan CFR where the higher seats caused more significant decreases in contact force for seats 2 and 3, while higher knee angles generated higher contact at the seat-pan for the same two seats. Seat height and knee angle however, do not have the same effect on the CFR of seat 3, which shows relatively higher dependence on the two-way interaction between H and K, where the coupled increase in height and knee angle cause the CFR to increase, while seat 1 was observed to behave in an opposite fashion.

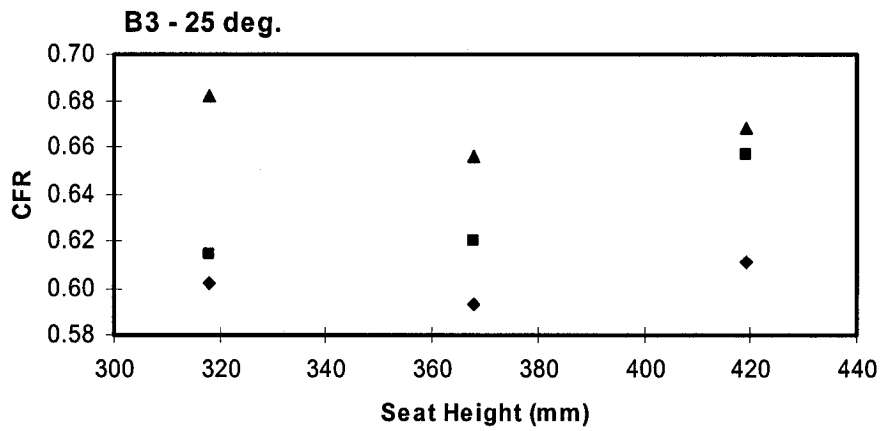
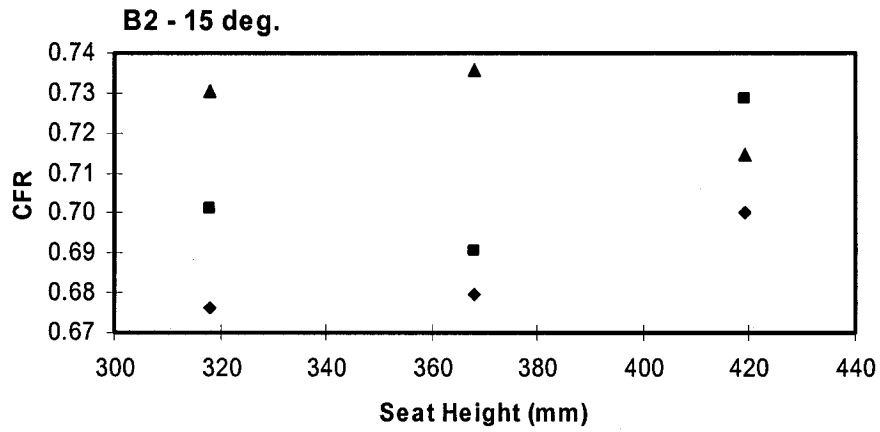
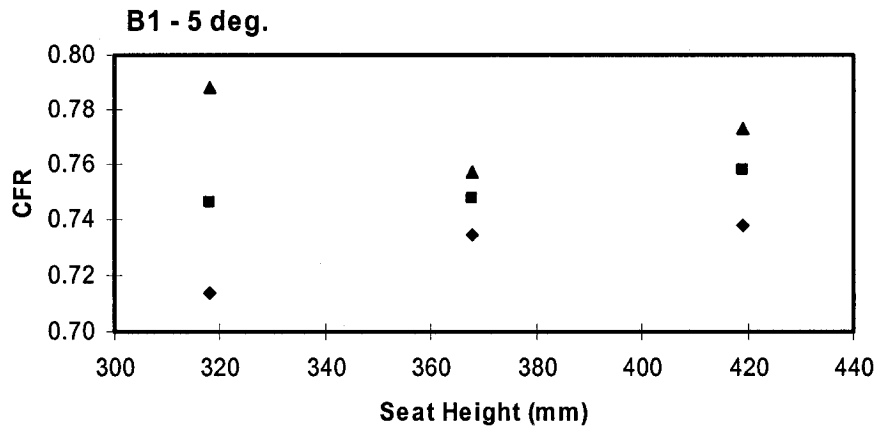


Figure 3.6: Variations in the CFR of the seat-pan of seat 1 as a function of knee angle:  
 ◆ K1 - 95°; ■ K2 - 115°; ▲ K3 - 135°.

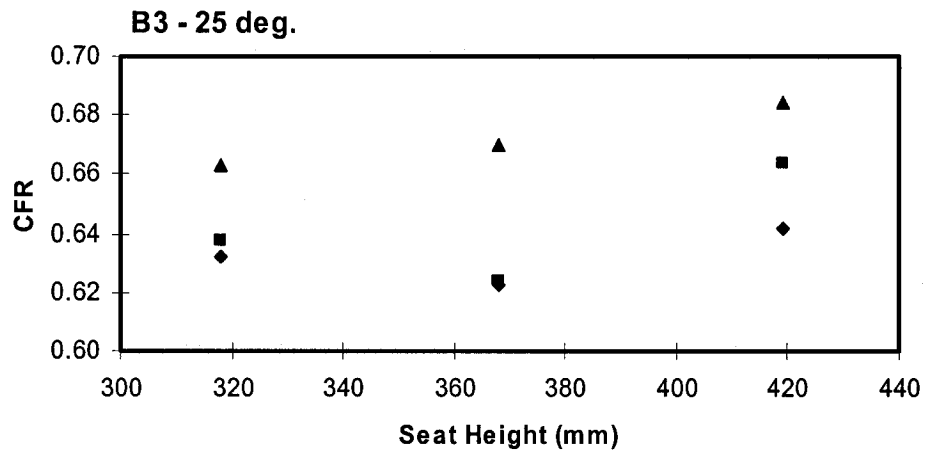
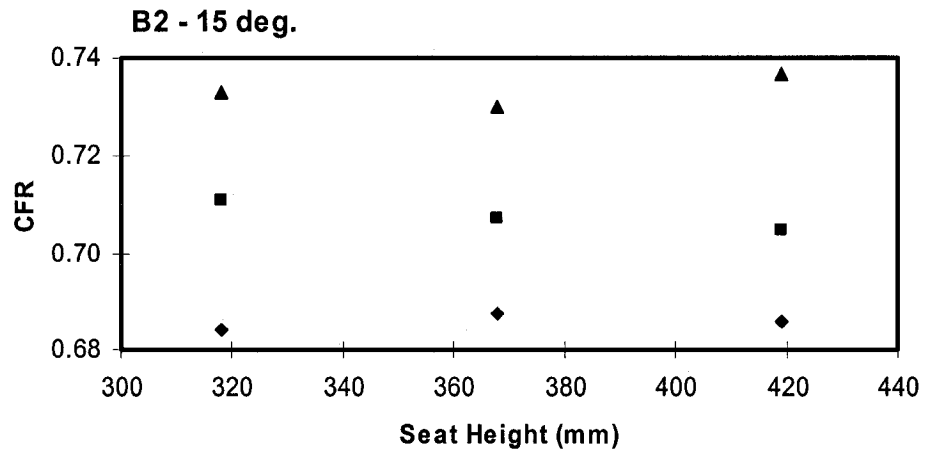


Figure 3.7: Variations in the CFR of the seat-pan of seat 2 as a function of knee angle:  
 ◆ K1 - 95°; ■ K2 - 115 °; ▲ K3 - 135°.

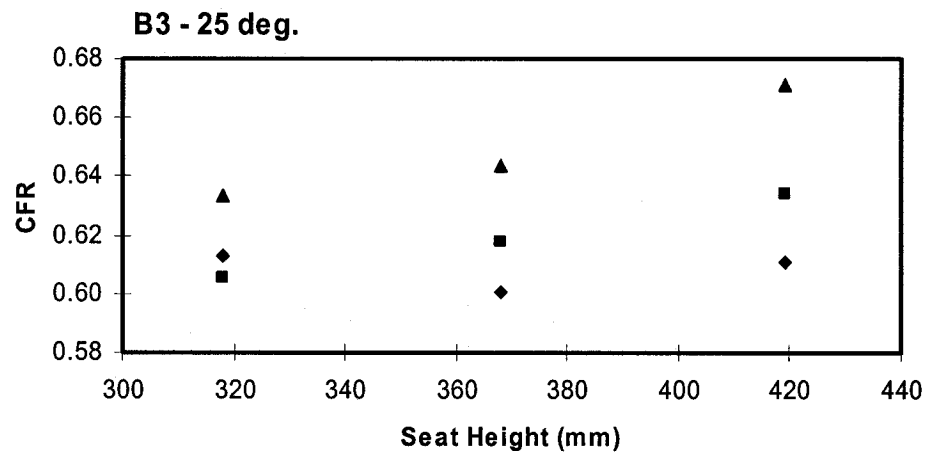
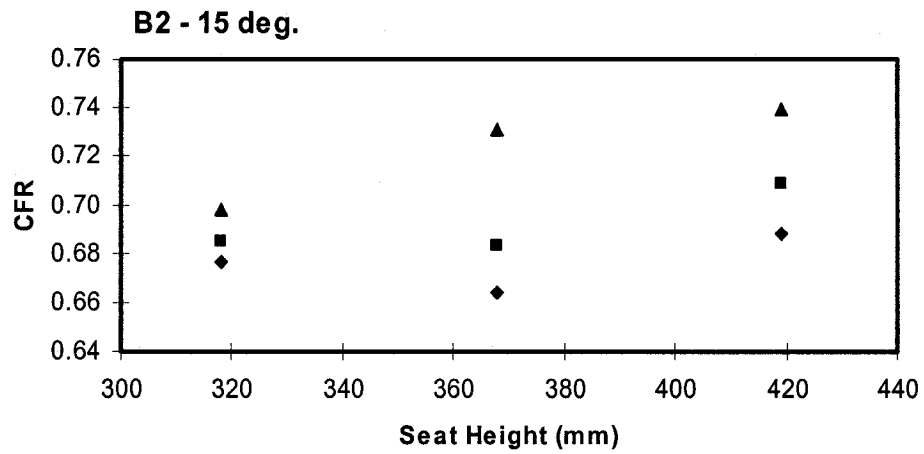


Figure 3.8: Variations in the CFR of the seat-pan of seat 3 as a function of knee angle:  
 ◆ K1 - 95°; ■ K2 - 115 °; ▲ K3 - 135°.

### 3.3.2 Relationship between peak pressure and posture

The ANOVA of the peak pressure data revealed that the factors K and the two-way interactions between H and K (H\*K) are most significant ( $p < 0.001$ ), while H, K, B and the two-way interaction between S and K (S\*K) are fairly significant ( $p < 0.05$ ). The variations in the peak pressures measured on the candidate seats as functions of the subject weight and the different experimental factors are presented in Figures A2.1 to A2.9, presented in Appendix A2. Similar to the contact force data, a multiple linear regression analysis was performed to study the relationship of the peak pressure with the experimental factors considered. The regression model for peak pressure is obtained as:

$$PP = \beta_0 + \beta_1(W) + \beta_2(K) + \beta_3(B) + \beta_4(H) + \beta_5(H * K) + \beta_6(S * K) \quad (3.5)$$

where the coefficients,  $\beta_0$  to  $\beta_6$ , are summarized in Table 3.7 for all the test seats.

Table 3.7: Contributions of seat stiffness, body weight, seat height and knee and backrest angles to the seat-pan peak pressure.

Seat	R <sup>2</sup>	$\beta_0$	$\beta_1$	$\beta_2$	$\beta_3$	$\beta_4$	$\beta_5$	$\beta_6$
1	0.314	1.89	0.002	-0.009	-0.013	-0.004	$2.9 \times 10^{-5}$	$-2.7 \times 10^{-7}$
2	0.448	5.42	-0.002	-0.031	-0.007	-0.004	$2.7 \times 10^{-5}$	$1.0 \times 10^{-6}$
3	0.343	5.56	-0.001	-0.029	-0.012	-0.009	$6.3 \times 10^{-5}$	$3.2 \times 10^{-9}$

The regression coefficients suggest that increasing the knee angle ( $\beta_2$ ), back angle ( $\beta_3$ ) and seat height ( $\beta_4$ ) leads to a reduction in the peak pressure surrounding the IT for all three seats. Seats 2 and 3 reveal lower peak pressures for heavier subjects, while seat 1 shows an opposite trend. This is directly attributed to the construction of the seat and the cushion contours. Seat 1 has a significantly narrower seat-pan and is confined on both sides by high lateral wings, which tends to generate high pressures for heavier subjects

who generally have larger, thicker and longer legs. Seats 2 and 3, on the other hand, are much wider than seat 1 and comprise much smaller lateral wings, and therefore can accommodate larger subjects without generating localized high pressures. The coefficients  $\beta_2$  suggests that knee angle has higher influence in reducing seat-pan peak pressures for seats 2 and 3 than it does for seat 1, which further illustrates the effect of high lateral wings, where higher knee angles for seat 1 caused increased contact between the thighs and the lateral wings. While the regression model results in trends that are observed from the measured peak pressure, relatively poor correlations exist between the predicted and measured peak pressures as shown in Figure 3.9. The correlation coefficients obtained for the three seats are also reported in Table 3.7. The poor correlations observed for all seats are believed to be attributed to large inter-subject variability related to large variations in the anthropometric dimensions of the lower limbs. Apart from this, the variations in peak pressure are mostly caused by the poor resolution of the 16 X 16 sensing matrix in detecting the exact magnitude and location of the hard points. Sustained exposure to excessive pressure loading has been reported to restrict blood flow to the lower limbs and increase the sensation of discomfort in the seated position. Therefore, based on the pressure analysis of the seat-pan, higher knee angles and backrest angles provide efficient mechanisms for the alleviation of pressure loading surrounding the IT. Furthermore, wider, flatter seat-pans generally are more efficient in accommodating passengers of greater stature while reducing the occurrence of high localized pressures associated with a higher degree of cushion contouring.

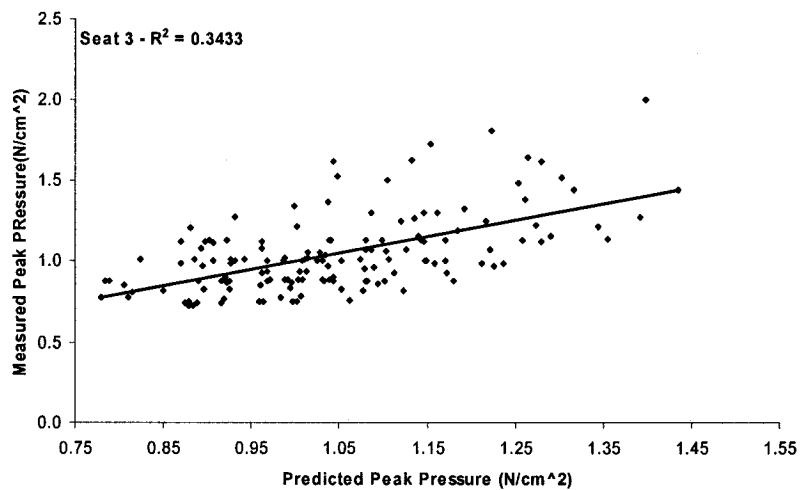
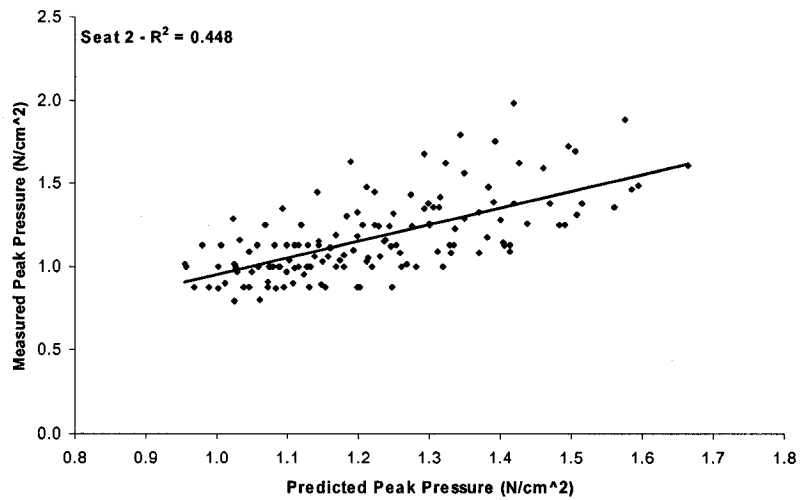
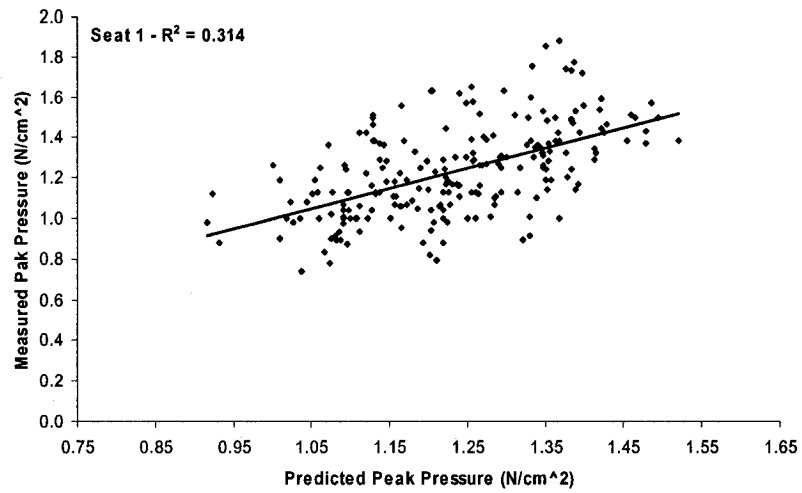


Figure 3.9: Correlations between the measured and estimated seat-pan mean peak pressures for the three test seats.



### 3.3.3 Postural effects on the contact area and mean pressure

The measures of contact area and mean pressure were also subjected to a multi-factor within subject ANOVA involving the experimental factors. The results revealed that the factors S, H, K and B, as well as the two-way interaction between H and K (H\*K) are very significant ( $p < 0.001$ ) while the three-way and four-way interactions (S\*H\*K) (S\*H\*K\*B) are fairly significant ( $p < 0.05$ ). Equation (3.6) shows the regression model derived from the analysis that describes the relationship between the contact area and each significant factor. Table 3.8 summarizes the respective regression coefficients for seats 1, 2 and 3. Higher levels of body weight (W), knee angle (K) and seat height (H) tend to cause higher contact area at the body-seat interface while a higher backrest angle yields lower seat-pan contact area. The regression model provides an accurate prediction of the actual contact area developed at the seat-pan for the ranges of postural settings considered in this study, as evident from Figure 3.10

$$A_c = \beta_0 + \beta_1(W) + \beta_2(K) + \beta_3(B) + \beta_4(H) + \beta_5(S) + \beta_6(H * K) + \beta_7(S * H * K) + \beta_8(S * H * K * B) \quad (3.6)$$

Table 3.8: Contribution of seat stiffness, body weight, seat height, knee and backrest angles to seat-pan contact area

Seat	R <sup>2</sup>	$\beta_0$	$\beta_1$	$\beta_2$	$\beta_3$	$\beta_4$	$\beta_5$	$\beta_6$	$\beta_7$	$\beta_8$
1	0.784	-2465.5	1.1	20.4	-4.9	5.7	0.003	-0.04	$-1.7 \times 10^{-7}$	$2.5 \times 10^{-9}$
2	0.872	-1877.7	3.5	13.9	-9.65	3.6	-0.11	-0.03	$-1.5 \times 10^{-6}$	$1.0 \times 10^{-8}$
3	0.893	-1115.9	1.2	8.2	-5.9	2.2	0.001	0.008	$-2.4 \times 10^{-8}$	$3.8 \times 10^{-10}$

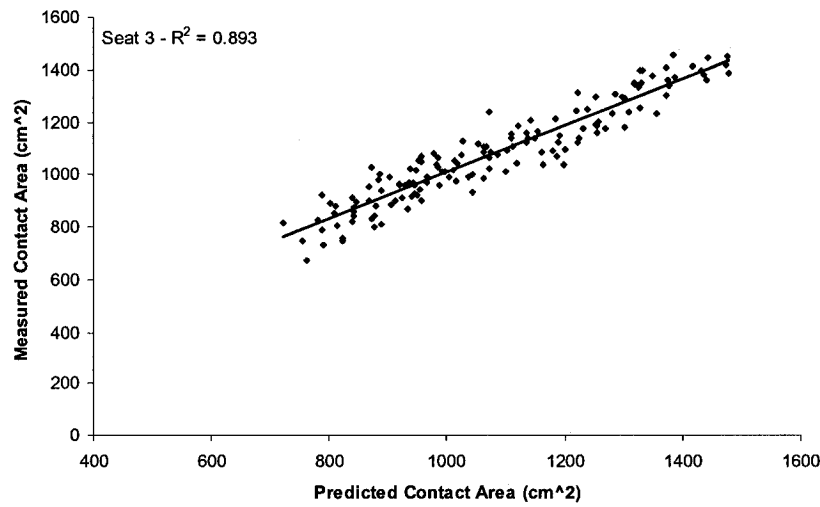
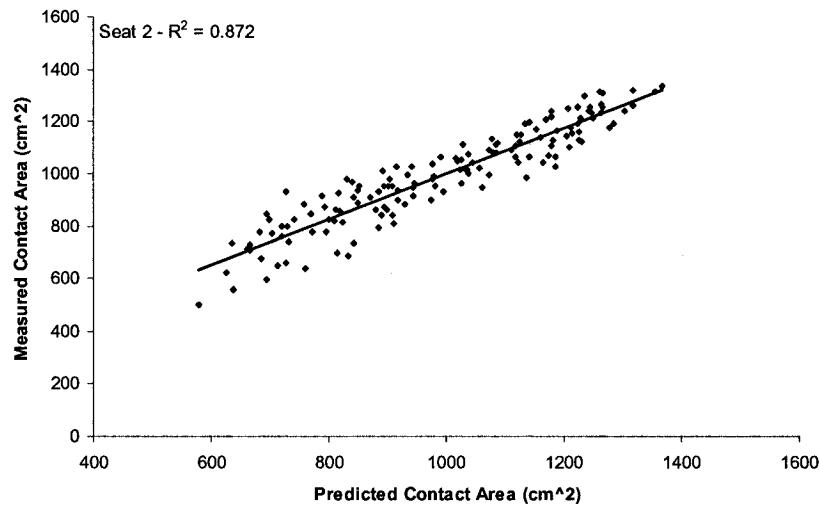
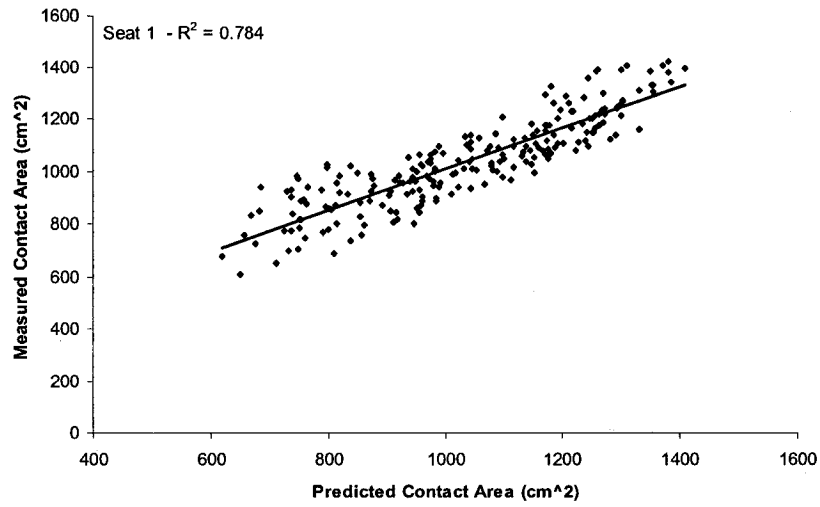


Figure 3.10: Correlations between the measured and estimated seat-pan mean contact area for the three test seats.

As indicated in section 3.2, a higher contact area implicitly increases the interface contact force, but beneficially reduces the magnitudes of peak pressure surrounding the IT. The effective contact area is also significantly affected by the cushion design, which includes both the stiffness properties of the PUF and the cushion contouring. The variations in the coefficient  $\beta_5$  suggest that seats with a higher level of contouring and stiffness generate higher contact area, while a stiffer seat with less contouring could yield lower contact area.

The results attained from the ANOVA of the mean pressure data revealed high significance of all factors, namely, S, H, K and B ( $p < 0.001$ ). The interactions between the seat height and the knee angle (H\*K) was also observed to be as significant ( $p < 0.001$ ), while the two-way interactions, S\*H and S\*K, and the three-way interaction, S\*H\*K, S\*K\*B and H\*K\*B were observed to be fairly significant ( $p < 0.05$ ). The contribution due to the large number of parameters may suggest that the measure of mean pressure is not sensitive to any particular factor, which can be observed from the variations in the coefficients summarized in Table 3.9 for the regression model given below:

$$MP = \beta_0 + \beta_1(W) + \beta_2(K) + \beta_3(B) + \beta_4(H) + \beta_5(S) + \beta_6(H * K) + \beta_7(S * H) + \beta_8(S * K) + \beta_9(S * K * B) + \beta_{10}(S * H * K) + \beta_{11}(H * K * B) \quad (3.6)$$

Table 3.9: Contribution of seat stiffness, body weight, seat height, knee and backrest angles to seat-pan mean pressure.

Seat	R <sup>2</sup>	$\beta_0$	$\beta_1$	$\beta_2$	$\beta_3$	$\beta_4$	$\beta_5(\times 10^{-5})$	$\beta_6(\times 10^{-5})$	$\beta_7(\times 10^{-9})$	$\beta_8(\times 10^{-7})$	$\beta_9$	$\beta_{10}$	$\beta_{11}$
1	0.72	1.27	0.001	-0.01	-0.002	-0.003	-4.1	2.0	2.5	1.3	$1.2 \times 10^{-10}$	$-1.2 \times 10^{-10}$	$-1.7 \times 10^{-8}$
2	0.66	1.75	-0.001	-0.01	0.002	-0.002	2.3	-	-5.5	-1.0	$-3.6 \times 10^{-9}$	$1.1 \times 10^{-9}$	$4.5 \times 10^{-8}$
3	0.62	1.34	$-8.4 \times 10^{-5}$	-0.006	-0.001	-0.002	-0.012	1.1	-0.026	-0.0045	$2.5 \times 10^{-11}$	$8.1 \times 10^{-12}$	$-4.3 \times 10^{-8}$

The regression model also shows acceptable accuracy in the prediction of seat-pan mean pressure, as evident from Figure 3.11. The results suggest similar magnitudes of coefficients of B, H and W, while those of the two and three-way interactions suggest very little contribution on behalf of their parameters. The interactions between the experimental factors show that changing a single factor will create a noticeable difference in the mean pressure. The measure of the mean pressure is also observed to vary significantly from seat to seat, which further suggests that contouring and stiffness properties strongly influence the interactions at the human-seat interface.

The measures of contact area and mean pressure were found to vary significantly with respect to the experimental factors, namely; the seat height, the knee angle and the backrest angle. Significant differences were observed between the three candidate seats, which further suggests that contouring and stiffness properties strongly influence the interactions at the human-seat interface. This would further suggest that more suitable measures to compare the seat design factors of automotive seats would significantly improve the significance of pressure studies related to the assessment of comfort performance of automotive seats.

While the regression models developed in the section 3.3 account for the significant inter-subject variability, as shown by the regression coefficients, variations in peak pressure and their locations are also attributed to intra-subject variability. Since each subject was asked to stand up and sit back down between each measurement, variations in seated posture with respect to the position during the previous measurement would cause some variations in the measured responses for the same posture.

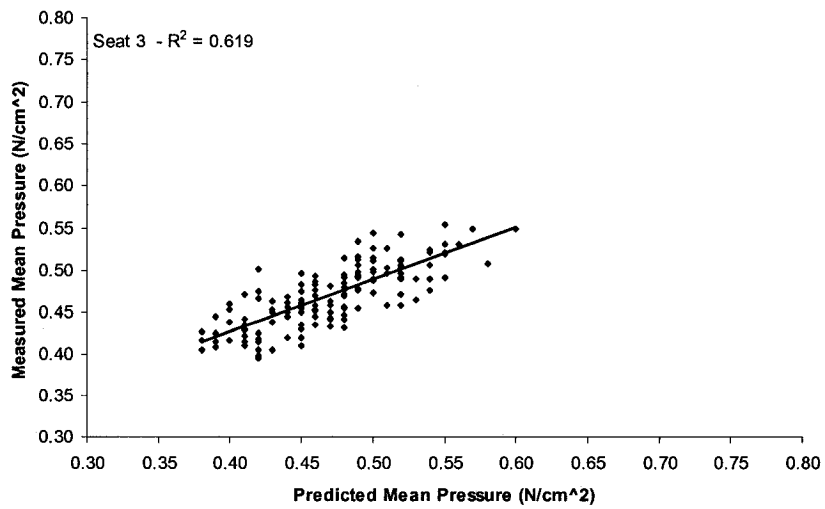
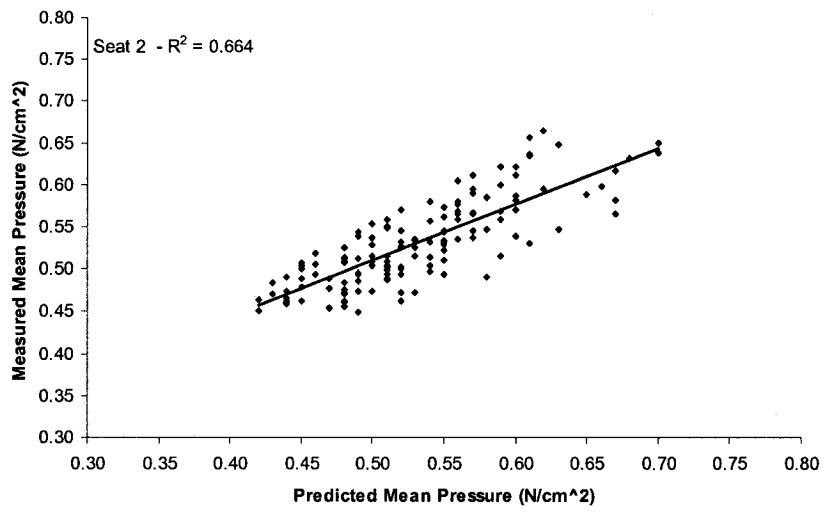
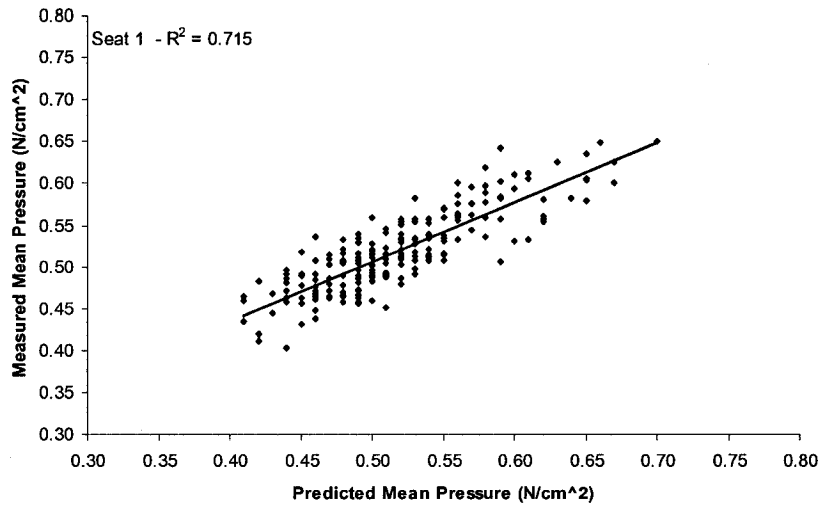


Figure 3.11: Correlations between the measured and estimated seat-pan mean pressure for the three test seats.

### 3.4 Regression Model Diagnostics and Best Subset Regressor

The interpretation of the regression coefficients as measuring the change in the expected value of the response variable (force, area and pressure) when the given predictor variable is increased by one unit while all other variables are held constant is not fully applicable when multicollinearity exists [58-61]. When the regression variables are strongly correlated, the interpretation of the regression analysis may become ambiguous. There are generally three problems associated with multicollinearity [61]; first, the importance and the effects of individual regressor variables cannot be estimated; secondly, the estimates of the regressor variables are very sensitive to slight changes in the data and to the addition or deletion of regressor variables in the equation; finally, the estimated regression coefficients have large sampling error that affect both inferences concerning the regression model and the forecasts based on the model. The occurrence of multicollinearity is detected by the Variance Inflation Factor (VIF) and the Condition Index (CI) as well as the correlation matrix of the experimental factors obtained from the SPSS software package [60]. Owing to the existence of multicollinearity of the measures, a best subset regression is performed on the data to eliminate the correlated variables and to obtain a more accurate regression model representing the variations in the predicted measures. A stepwise forward selection method was performed with the SPSS to identify the best subset regressor having the smallest change in the overall correlation factor,  $R^2$ . The resulting predictor equations for the contact force, peak pressure, contact area and mean pressure are expressed below:

$$F_c = \beta_0 + \beta_1(W) + \beta_2(B) + \beta_3(K) + \beta_4(S * K * B) \quad (3.7)$$

$$PP = \beta_0 + \beta_1(W) + \beta_2(B) + \beta_3(K) + \beta_4(S * K) + \beta_5(H * K) \quad (3.8)$$

$$A_c = \beta_0 + \beta_1(W) + \beta_2(B) + \beta_3(K) + \beta_4(H) + \beta_5(S) + \beta_6(S * H * K) \quad (3.9)$$

$$MP = \beta_0 + \beta_1(W) + \beta_2(B) + \beta_3(K) + \beta_4(H) + \beta_5(S) + \beta_6(S * K) + \beta_7(S * H * K) + \beta_8(H * K) + \beta_9(S * H * K) + \beta_{10}(S * K * B) + \beta_{11}(H * K * B) \quad (3.10)$$

The coefficients of the above regression models in  $F_c$ , PP,  $A_c$  and MP are summarized in Tables 3.10 to 3.13, respectively.

Table 3.10: Best subset regression for seat-pan contact force

Seat	$R^2$	$\beta_0$	$\beta_1$	$\beta_2$	$\beta_3$	$\beta_4$
1	0.68	114.4	0.48	-4.39	1.01	-
2	0.79	127.5	0.52	-4.68	0.77	-
3	0.79	268.0	0.45	-5.91	-	$6.1 \times 10^{-8}$

Table 3.11 Best subset regression for seat-pan peak pressure

Seat	$R^2$	$\beta_0$	$\beta_1$	$\beta_2$	$\beta_3$	$\beta_4$	$\beta_5$
1	0.26	1.68	-0.001	-0.013	-	-	$-6.0 \times 10^{-6}$
2	0.38	2.34	-	-0.007	-0.001	$-3.9 \times 10^{-7}$	-
3	0.29	2.30	-	-0.012	-	$3.1 \times 10^{-9}$	$-1.33 \times 10^{-5}$

Table 3.12 Best subset regression for seat-pan contact area

Seat	$R^2$	$\beta_0$	$\beta_1$	$\beta_2$	$\beta_3$	$\beta_4$	$\beta_6$	$\beta_5$
1	0.76	-978.5	1.37	-3.51	5.86	1.36	-	$-1.7 \times 10^{-4}$
2	0.87	-1936.7	3.49	-3.36	13.01	3.33	-	$-1.35 \times 10^{-6}$
3	0.89	-825.8	1.15	-4.34	5.42	1.32	0.001	$-1.66 \times 10^{-8}$

Table 3.13 Best subset regression for seat-pan mean pressure

Seat	$R^2$	$\beta_0$	$\beta_1$	$\beta_2$	$\beta_3$	$\beta_4$	$\beta_5$	$\beta_6$	$\beta_7$	$\beta_8$	$\beta_9$	$\beta_{10}$	$\beta_{11}$
1	0.71	1.27	0.001	-0.002	-0.01	-0.003	$-3.2 \times 10^{-5}$	$8.5 \times 10^{-8}$	-	-	-	-	-
2	0.55	0.79	-	-	-	-	-	-	-	$-4.9 \times 10^{-5}$	-	$1.4 \times 10^{-9}$	-
3	0.59	1.3	$-8.4 \times 10^{-5}$	-	-0.006	-0.002	-	-	$5.5 \times 10^{-11}$	$1.3 \times 10^{-5}$	$5.5 \times 10^{-11}$	-	$-8.7 \times 10^{-8}$

The best subset regressor model based on the forward selection process establishes a hierarchical order among the significant factors beginning with the most significant and ending with the least. Therefore, Equations (3.7) to (3.10) not only show the contributions of the respective experimental factors to the measured response but also show which experimental factor is more significant relative to the others. From the results of the best subset regression, it is clear that the subject weight (W), backrest angle (B) and the knee angle (K) have the most significant effect on the variations of the contact force, the contact area and the peak and mean pressures. Heavier subjects and higher knee angles generally caused higher overall responses, while backrest angle was instrumental in reducing the magnitudes of contact force and peak pressure at the seat-pan.

### **3.5 Summary of Seat-Pan Analysis**

The pressure distributions at the human-seat interface of three different automotive seats were measured using a flexible pressure sensing mat under static conditions. The seat-pan pressure profiles for each seat were compared to one-another, the effects of anthropometry and posture on the variations in pressure distribution were investigated in terms of contact force, contact area, and peak and mean pressures. The study revealed that the pressure distribution was significantly affected by the subject weight and seated posture, which is a complex function of the seat height, knee angle and the backrest inclination. Heavier subjects tend to generate higher values of contact force, which also leads to a higher ratio of body weight supported by the seat-pan. Similarly, heavier subjects also cause higher effective contact area of the seat-pan mainly due to longer, larger and heavier legs. Heavier subjects, in general, tend to have larger muscles



and more fatty tissue surrounding the buttocks and thighs, and, while these subjects generated higher values of contact force and area, they benefited from significantly lower values of peak interface pressure which is attributed to a higher amount of soft tissue deformation of the surrounding the lower limbs. The analyses further reveals that the backrest angle is the most significant factor that leads to a systematic reduction in the magnitudes of contact force, contact area and peak pressure for all the test seats. Subject weight and knee angle on the other hand, had an opposite effect on contact force and area, while higher levels of knee angle generated significantly lower levels of peak pressure surrounding the IT.

The regression analysis also revealed significant two and three-way interactions between the seat, seat height, and the knee and the backrest angles for the peak and mean pressures. These interactions clearly suggest that the construction and contour of the seat-pan cushion is of considerable importance. In this study, the factor designated as seat (S) was quantified by the cushion static stiffness, derived in chapter 2; these interactions clearly suggest that stiffness alone does not provide sufficient information regarding the characteristics of the seat-pan cushion and more measures to compare the stiffness and cushion contours in different locations are required. It can, however, be concluded that higher cushion stiffness generates higher magnitudes of interface pressure in the IT region. It was also found that the amount of body weight supported by the seat-pan was a function of the backrest angle, knee angle and the cushion stiffness.

### 3.6 Analysis of Backrest Contact Forces and Pressures

The pressure profiles measured at the backrests of the candidate seats were also analyzed using the *PLIANCE* software to derive overall values of contact force, contact area, and peak and mean pressures. Figure 3.12 shows, as an example, the variations in the pressure distribution for a 76 kg subject assuming identical seated posture on seats 1, 2 and 3. The variations in the pressure distributions are largely due to the differences in the contouring and stiffness of the backrest. Seat 1 exhibits an almost symmetric distribution about the vertical central axis of the backrest. The peak pressures range between 0.375 – 0.5 N/cm<sup>2</sup> in the lower lumbar area, while seat 2 reveals higher magnitudes of peak pressure, approaching 0.625 N/cm<sup>2</sup>, as well as a higher concentration of pressure at points well above the lumbar region along the vertical axis of the backrest. Seat 3 again shows much smoother pressure gradients away from the centerline of the backrest cushion. The location of the high pressure zone is considerably lower than those observed for seats 1 and 2, while the magnitudes of peak pressures similar are similar to those obtained for seat 1.

Figures 3.13, 3.14 and 3.15 illustrate the effects of variations in the backrest angle, knee angle and the seat height, respectively, on the pressure distributions measured at the backrest of seat 1 for a 76 kg subject. These distributions suggest that the most significant factor affecting the pressure distribution is again the backrest angle, as observed for the seat-pan. The effect however, is opposite to that observed for the seat-pan pressure distribution. Higher backrest angles cause higher loads on the backrest, and thus significantly higher contact area and pressure. Figure 3.16 clearly shows an almost symmetric distribution of contact pressure about the vertical axis where both the

Posture: H2 - 368 mm / K2 - 115° / B2 - 15°

**SEAT 1**

F<sub>c</sub>: 220.2 N  
 PP: 0.875 N/cm<sup>2</sup>  
 A<sub>c</sub>: 1400 cm<sup>2</sup>  
 MP: 0.21 N/cm<sup>2</sup>

**SEAT 2**

F<sub>c</sub>: 208.9 N  
 PP: 0.625 N/cm<sup>2</sup>  
 A<sub>c</sub>: 1225.8 cm<sup>2</sup>  
 MP: 0.21 N/cm<sup>2</sup>

**SEAT 3**

F<sub>c</sub>: 195.2 N  
 PP: 0.625 N/cm<sup>2</sup>  
 A<sub>c</sub>: 1432.3 cm<sup>2</sup>  
 MP: 0.18 N/cm<sup>2</sup>

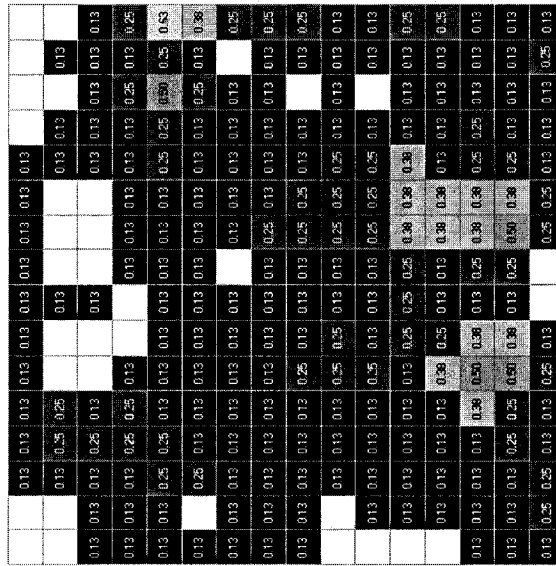
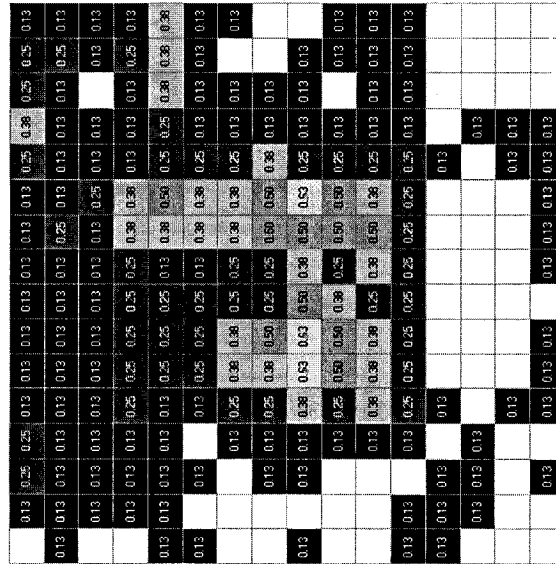
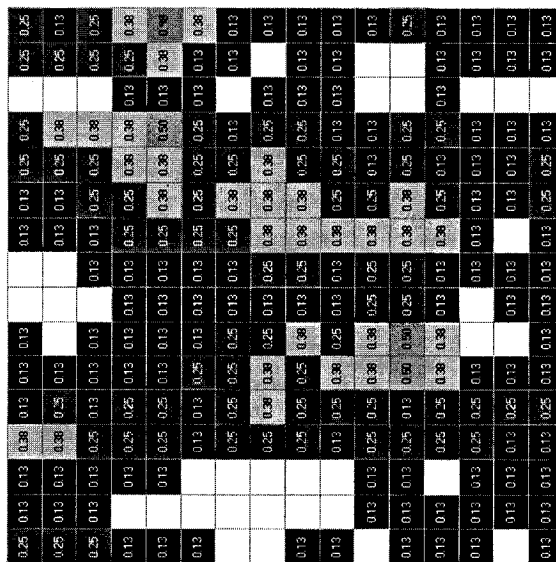
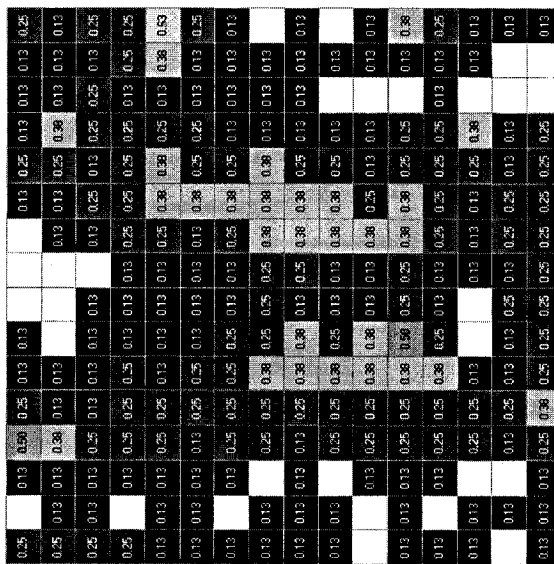


Figure 3.12: Contact pressure profiles measured at the backrest of seats 1, 2 and 3 for a 76 kg subject.

## SEAT 1

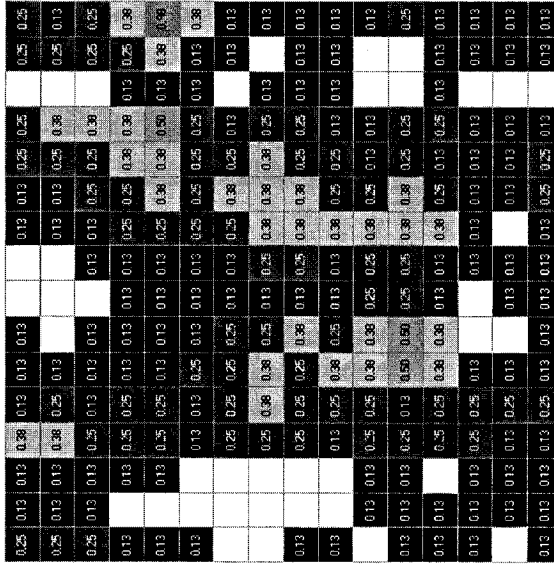
Posture: H1 - 318 mm / K2 - 115° / B2 - 15°

F<sub>c</sub>: 228.2 N  
 PP: 0.625 N/cm<sup>2</sup>  
 A<sub>c</sub>: 1458.1 cm<sup>2</sup>  
 MP: 0.21 N/cm<sup>2</sup>



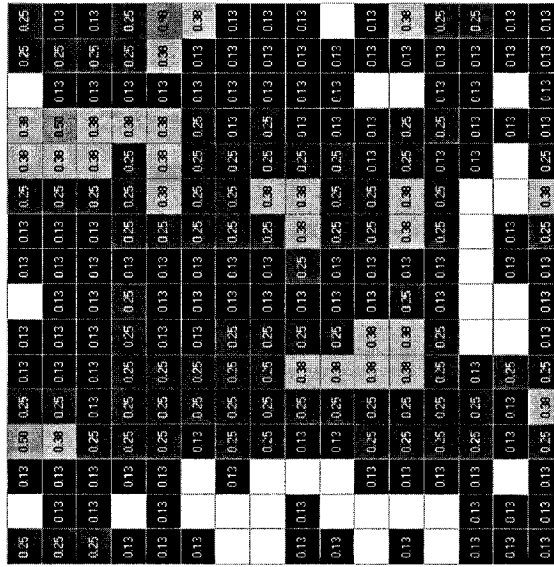
Posture: H2 - 368 mm / K2 - 115° / B2 - 15°

F<sub>c</sub>: 220.2 N  
 PP: 0.875 N/cm<sup>2</sup>  
 A<sub>c</sub>: 1400 cm<sup>2</sup>  
 MP: 0.21 N/cm<sup>2</sup>



Posture: H3 - 419 mm / K2 - 115° / B2 - 15°

F<sub>c</sub>: 228.2 N  
 PP: 0.875 N/cm<sup>2</sup>  
 A<sub>c</sub>: 1438.7 cm<sup>2</sup>  
 MP: 0.21 N/cm<sup>2</sup>



**P ≥ 0.875   P ≥ 0.75   P ≥ 0.625   P ≥ 0.5   P ≥ 0.375   P ≥ 0.25   P ≥ 0.125**  
 N/cm<sup>2</sup>

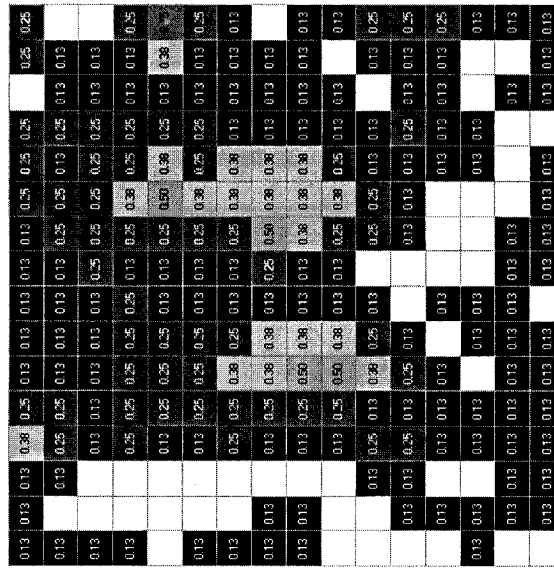
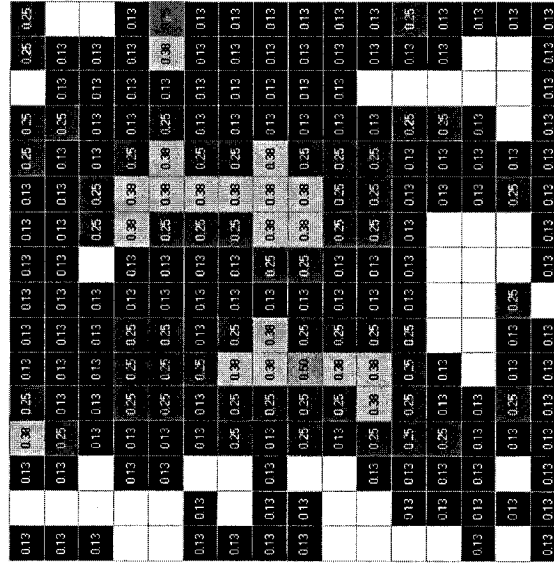
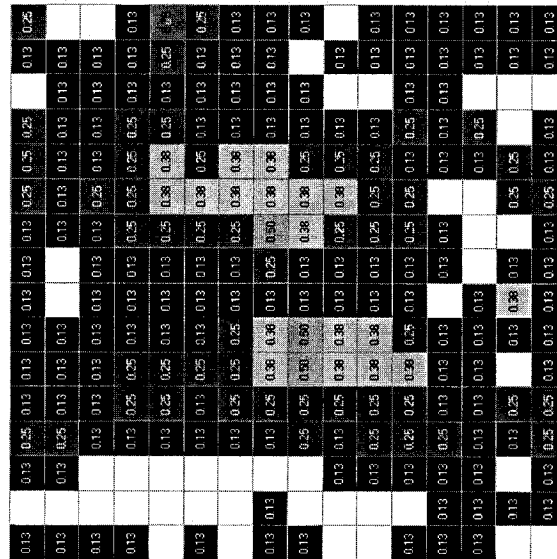
Figure 3.13: Effect of seat height on the pressure distribution at the backrest of seat 1 for a 76 kg subject.

## SEAT 1

**Posture:** H2 - 368 mm / K1 - 95° / B2 - 15°  
**F<sub>c</sub>:** 190.3 N  
**PP:** 0.75 N/cm<sup>2</sup>  
**A<sub>c</sub>:** 1361.3 cm<sup>2</sup>  
**MP:** 0.19 N/cm<sup>2</sup>

**Posture:** H2 - 368 mm / K2 - 115° / B2 - 15°  
**F<sub>c</sub>:** 183.9 N  
**PP:** 0.75 N/cm<sup>2</sup>  
**A<sub>c</sub>:** 1361.3 cm<sup>2</sup>  
**MP:** 0.18 N/cm<sup>2</sup>

**Posture:** H2 - 368 mm / K3 - 135° / B2 - 15°  
**F<sub>c</sub>:** 200.8 N  
**PP:** 0.750 N/cm<sup>2</sup>  
**A<sub>c</sub>:** 1329.0 cm<sup>2</sup>  
**MP:** 0.19 N/cm<sup>2</sup>



**P ≥ 0.875   P ≥ 0.75   P ≥ 0.625   P ≥ 0.5   P ≥ 0.375   P ≥ 0.25   P ≥ 0.125**  
**N/cm<sup>2</sup>**

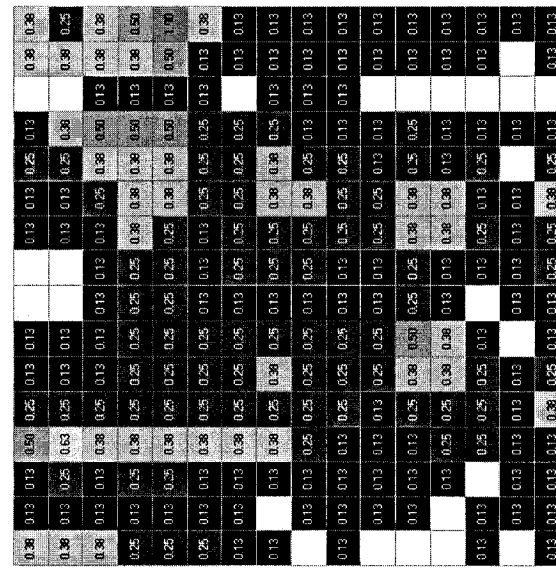
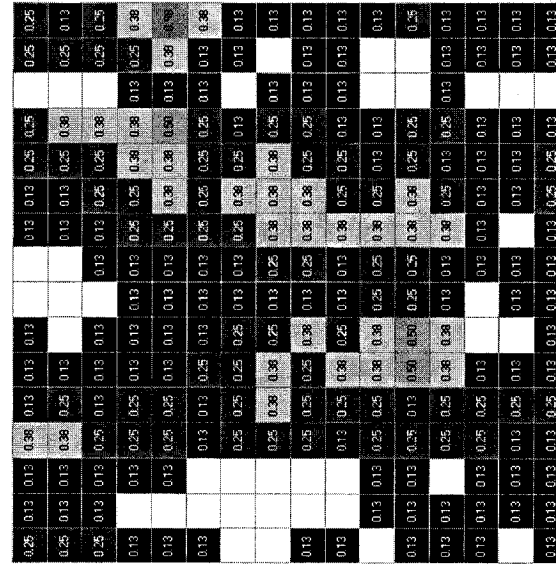
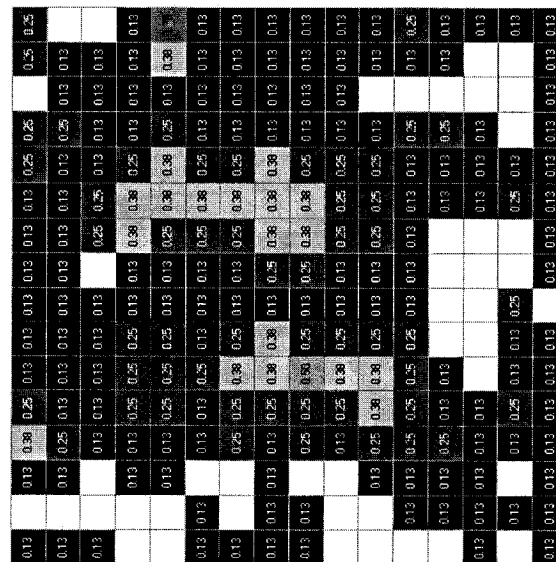
Figure 3.14 Effect of knee angle on the pressure distribution at the backrest of seat 1 for a 76 kg subject.

### SEAT 1

Posture: H2 - 368 mm / K2 - 115° / B1 - 5°  
**F<sub>c</sub>: 183.9 N**  
**PP: 0.750 N/cm<sup>2</sup>**  
**A<sub>c</sub>: 1361.3 cm<sup>2</sup>**  
**MP: 0.18 N/cm<sup>2</sup>**

Posture: H2 - 368 mm / K2 - 115° / B2 - 15°  
**F<sub>c</sub>: 220.2 N**  
**PP: 0.875 N/cm<sup>2</sup>**  
**A<sub>c</sub>: 1400.0 cm<sup>2</sup>**  
**MP: 0.21 N/cm<sup>2</sup>**

Posture: H2 - 368 mm / K2 - 115° / B3 - 25°  
**F<sub>c</sub>: 267.0 N**  
**PP: 1.00 N/cm<sup>2</sup>**  
**A<sub>c</sub>: 1490.3 cm<sup>2</sup>**  
**MP: 0.22 N/cm<sup>2</sup>**



**P ≥ 0.875   P ≥ 0.75   P ≥ 0.625   P ≥ 0.5   P ≥ 0.375   P ≥ 0.25   P ≥ 0.125**  
**N/cm<sup>2</sup>**

Figure 3.15: Effect of backrest angle on the pressure distribution at the backrest of seat 1 for a 76 kg subject.

magnitudes of peak pressure 0.75 N/cm<sup>2</sup>, 0.875 N/cm<sup>2</sup> and 1.00 N/cm<sup>2</sup> and the higher concentration of pressure generate higher magnitudes of contact force 183.9 N, 220.2 N and 267 N for backrest inclinations of 5°, 15° and 25°, respectively. Figure 3.14 shows that knee angle has very little effect on the variations of pressure at the backrest. The difference is mainly in the amount of contact in the lower lumbar region where higher knee angles reduce the contact between the lower lumbar region and the seat. This is attributed to the rotation of the pelvic link away from the backrest for higher knee angles. Figure 3.15 indicates that seat height also has very little effect on the pressure variations when compared to backrest angle. The values of contact force, contact area, peak and mean pressure measured on the backrest are virtually unchanged as a function of seat height.

Tables 3.14 to 3.17 summarize the mean values and the standard deviations of the contact force, contact area, and peak and mean pressure, respectively, as a function of posture related factors for each seat. The extremely large standard deviations are mainly attributed to the radically different contours of the backrest cushions as well as the differences in upper body anthropometry and the preferred sitting postures of the test subjects. The preferred sitting posture relates to the instinctive position that each subject adopts when they sit; while some subjects feel more comfortable in a slouched posture, others prefer to sit in a more erect posture. These qualitative measures are not as easily quantifiable as the knee or backrest angles and imply that both heavy and lighter subjects alike may have similar backrest pressure profiles. The characterization of the backrest has determined that the backrests of seats 1 and 3 are stiffer than that of seat 2 over the entire weight range, and that seat 3 is stiffer than seat 1 for loads above 550 N. the results

presented in Tables 3.14 – 3.17 suggest that a softer backrest generates higher magnitudes of contact force and contact area, irrespective of the seated posture, while it also reduces the magnitudes of peak pressure over the entire contact area.

Table 3.14: Mean and standard deviation (SD) of backrest contact force,  $F_c$

Seat Height (mm)	Knee Angle (deg.)	Back Angle (deg.)	Backrest Contact Force, $F_c$ (N)					
			Seat 1		Seat 2		Seat 3	
			Mean	SD	Mean	SD	Mean	SD
318	95	5	119.9	33.3	X	X	X	X
		15	130.4	37.2	171.6	64.4	146.9	31.2
		25	158.5	39.6	197.0	58.8	167.2	27.8
	115	5	123.2	36.5	X	X	X	X
		15	138.4	41.3	164.5	56.1	148.8	35.1
		25	158.3	51.4	196.4	56.0	159.7	33.5
	135	5	128.5	38.4	X	X	X	X
		15	149.7	44.3	166.1	50.5	155.1	34.3
		25	163.2	48.3	182.6	57.6	161.6	36.9
368	95	5	113.0	35.1	X	X	X	X
		15	135.1	40.9	163.1	42.1	139.8	38.9
		25	141.9	59.3	189.1	56.4	154.9	38.7
	115	5	96.4	46.1	X	X	X	X
		15	122.6	50.1	153.6	40.0	138.6	42.8
		25	146.2	54.2	183.7	53.0	150.7	37.6
	135	5	115.4	32.9	X	X	X	X
		15	139.1	42.7	154.8	41.0	143.1	36.7
		25	152.3	46.5	181.9	46.9	158.6	38.1
419	95	5	118.7	54.8	X	X	X	X
		15	132.7	41.7	155.2	46.5	138.8	30.6
		25	140.3	39.6	182.3	58.5	154.3	36.2
	115	5	111.3	47.9	X	X	X	X
		15	135.2	48.7	152.7	48.0	136.9	31.9
		25	140.2	44.5	173.1	51.8	143.7	33.4
	135	5	110.5	46.0	X	X	X	X
		15	131.4	40.0	145.0	39.9	142.2	33.5
		25	147.7	43.9	163.7	47.7	147.4	27.6

X – Data not acquired for the combination



Table 3.15: Mean and standard (SD) deviation of backrest peak pressure, PP

Seat Height (mm)	Knee Angle (deg.)	Back Angle (deg.)	Backrest Peak Pressure, PP (N/cm <sup>2</sup> )					
			Seat 1		Seat 2		Seat 3	
			Mean	SD	Mean	SD	Mean	SD
318	95	5	0.62	0.12	X	X	X	X
		15	0.66	0.16	0.63	0.12	0.60	0.09
		25	0.69	0.28	0.66	0.13	0.66	0.13
	115	5	0.67	0.13	X	X	X	X
		15	0.66	0.15	0.61	0.08	0.59	0.08
		25	0.70	0.21	2.60	5.49	0.66	0.12
	135	5	0.62	0.11	X	X	X	X
		15	0.66	0.13	0.64	0.12	0.59	0.09
		25	0.71	0.23	0.66	0.13	0.65	0.07
368	95	5	0.67	0.18	X	X	X	X
		15	0.67	0.16	0.61	0.10	0.59	0.13
		25	0.71	0.28	0.65	0.10	0.61	0.10
	115	5	0.63	0.11	X	X	X	X
		15	0.63	0.18	0.61	0.12	0.60	0.09
		25	0.75	0.29	0.61	0.07	0.62	0.11
	135	5	0.57	0.13	X	X	X	X
		15	0.64	0.16	0.60	0.08	0.59	0.10
		25	0.73	0.27	0.64	0.15	0.65	0.11
419	95	5	0.59	0.13	X	X	X	X
		15	0.61	0.14	0.62	0.13	0.55	0.09
		25	0.70	0.27	0.67	0.14	0.60	0.06
	115	5	0.58	0.13	X	X	X	X
		15	0.61	0.15	0.62	0.14	0.58	0.10
		25	0.74	0.27	0.62	0.10	0.62	0.09
	135	5	0.56	0.13	X	X	X	X
		15	0.59	0.19	0.59	0.13	0.58	0.11
		25	0.68	0.20	0.62	0.15	0.61	0.10

Table 3.16: Mean and standard deviation (SD) of backrest contact area, A<sub>c</sub>

Seat Height (mm)	Knee Angle (deg.)	Back Angle (deg.)	Backrest Contact Area, A <sub>c</sub> (cm <sup>2</sup> )					
			Seat 1		Seat 2		Seat 3	
			Mean	SD	Mean	SD	Mean	SD
318	95	5	622.5	203.0	X	X	X	X
		15	675.1	248.5	814.7	301.9	785.2	192.9
		25	785.9	247.0	882.0	237.0	877.4	165.0
	115	5	630.4	230.3	X	X	X	X
		15	675.2	249.5	761.7	266.9	790.2	193.8
		25	767.5	264.8	869.0	245.4	812.7	163.0
	135	5	624.9	186.4	X	X	X	X
		15	698.1	215.3	760.1	210.5	798.2	205.1
		25	764.2	230.7	767.0	231.4	811.0	187.4
368	95	5	605.7	222.2	X	X	X	X
		15	690.9	236.7	787.6	194.6	752.3	172.8
		25	711.9	334.3	863.9	257.9	818.9	202.0
	115	5	482.3	271.5	X	X	X	X
		15	612.7	291.6	734.5	186.7	747.6	206.6
		25	721.5	283.1	840.9	229.7	817.1	189.4
	135	5	593.5	180.2	X	X	X	X
		15	663.2	216.6	720.1	167.0	777.3	175.2
		25	688.4	197.9	832.5	206.4	829.0	181.8
419	95	5	633.1	308.4	X	X	X	X
		15	670.6	270.2	752.3	230.4	762.3	181.1
		25	719.1	265.9	836.4	267.2	797.6	202.6
	115	5	593.4	277.9	X	X	X	X
		15	685.9	303.8	732.9	209.7	745.4	190.0
		25	684.9	239.4	824.5	263.7	757.2	177.3
	135	5	564.9	263.9	X	X	X	X
		15	646.9	215.7	711.6	191.7	766.4	185.6
		25	684.2	169.6	758.3	224.6	794.0	181.7

X – Data not acquired for the combination

Table 3.17: Mean and standard deviation (SD) of backrest mean pressure, MP

Seat Height (mm)	Knee Angle (deg.)	Back Angle (deg.)	Seat-Pan Mean Pressure, MP (N/cm <sup>2</sup> )					
			Seat 1		Seat 2		Seat 3	
			Mean	SD	Mean	SD	Mean	SD
318	95	5	0.58	0.13	X	X	X	X
		15	0.56	0.17	0.58	0.11	0.57	0.08
		25	0.66	0.26	0.59	0.11	0.62	0.12
	115	5	0.60	0.18	X	X	X	X
		15	0.63	0.18	0.60	0.08	0.57	0.08
		25	0.67	0.25	2.19	4.42	0.60	0.10
	135	5	0.57	0.11	X	X	X	X
		15	0.58	0.15	0.59	0.09	0.53	0.09
		25	0.65	0.24	0.62	0.14	0.61	0.08
368	95	5	0.59	0.16	X	X	X	X
		15	0.62	0.16	0.57	0.08	0.52	0.13
		25	0.65	0.25	0.58	0.13	0.55	0.12
	115	5	0.56	0.09	X	X	X	X
		15	0.58	0.19	0.58	0.10	0.51	0.09
		25	0.69	0.31	0.56	0.07	0.54	0.08
	135	5	0.52	0.12	X	X	X	X
		15	0.61	0.15	0.56	0.07	0.52	0.08
		25	0.70	0.26	0.59	0.15	0.58	0.10
419	95	5	0.53	0.12	X	X	X	X
		15	0.55	0.11	0.60	0.13	0.51	0.10
		25	0.61	0.28	0.64	0.13	0.54	0.05
	115	5	0.52	0.13	X	X	X	X
		15	0.54	0.13	0.56	0.10	0.54	0.08
		25	0.66	0.25	0.58	0.10	0.56	0.06
	135	5	0.54	0.13	X	X	X	X
		15	0.53	0.20	0.53	0.11	0.51	0.10
		25	0.63	0.18	0.59	0.13	0.58	0.10

X – Data not acquired for the combination

### 3.6.1 Relationship between the backrest contact force and seated posture

The magnitudes of the measured backrest contact force show significant variations with the seated posture, as evident from the relatively high standard deviations (Table 3.14). A multifactor within subject ANOVA revealed that only the factors H and B have strong statistical significance ( $p < 0.001$ ) and only the two-way interaction between S and K (S\*K) becomes fairly significant ( $p < 0.05$ ). A multiple regression model relating the backrest contact force with the significant factors is formulated as:

$$F_c = \beta_0 + \beta_1(W) + \beta_2(H) + \beta_3(B) + \beta_4(S * K) \quad (3.11)$$

where  $\beta_0$ ,  $\beta_1$ ,  $\beta_2$ ,  $\beta_3$  and  $\beta_4$  are the coefficients of the regression model. The model coefficients obtained for the three seats are summarized in Table 3.18 together with the correlation coefficient,  $R^2$ . The model coefficients suggest that heavier subjects tend to generate higher contact forces but that the effect of body weight is not as significant as the backrest angle. Conversely, seat height shows a negative trend on the contact force of the backrest which means that higher seats promote reduced contact force, which may be due to the subject's tendency to shift more weight on the legs when seated on a high seat thereby less contact at the backrest. The two-way interaction between S and K (S\*K) suggests that both the knee angle and the cushion characteristics significantly affect the magnitudes the of contact force. Thus, for seat 1, the combination of higher knee angle and stiffer backrest results in higher backrest contact force, while the opposite trends are observed for seats 2 and 3. The interactions between S and K, S\*K, would suggest that seats with greater contouring and stiffer backrest in the lower lumbar area reduces the body weight transferred to the backrest. The regression model however, provides poor accuracy in the prediction of backrest CFR, as evident from the correlation factors,  $R^2$ , in Table 3.18 and Figure 3.16.

Table 3.18: Regression coefficients and correlation factors for the backrest contact force

Seat	$R^2$	$\beta_0$	$\beta_1$	$\beta_2$	$\beta_3$	$\beta_4$
1	0.114	133.17	$-6.22 \times 10^{-5}$	-0.11	1.73	$1.63 \times 10^{-5}$
2	0.534	3.12	0.27	-0.17	2.48	$-3.59 \times 10^{-5}$
3	0.299	80.37	0.12	-0.12	1.20	$-7.27 \times 10^{-7}$

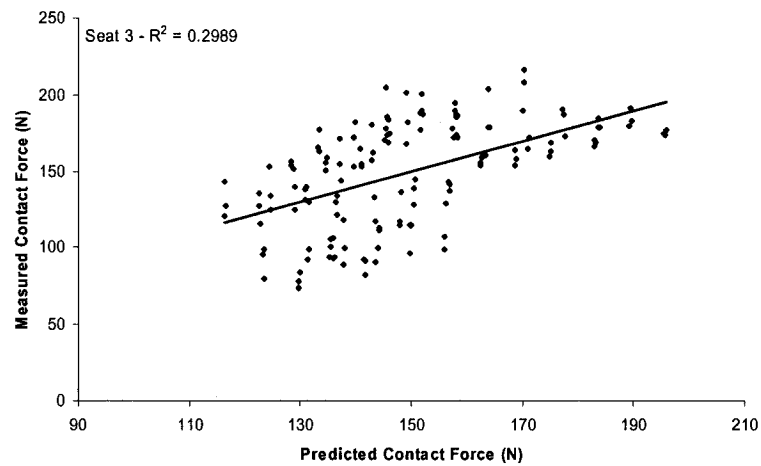
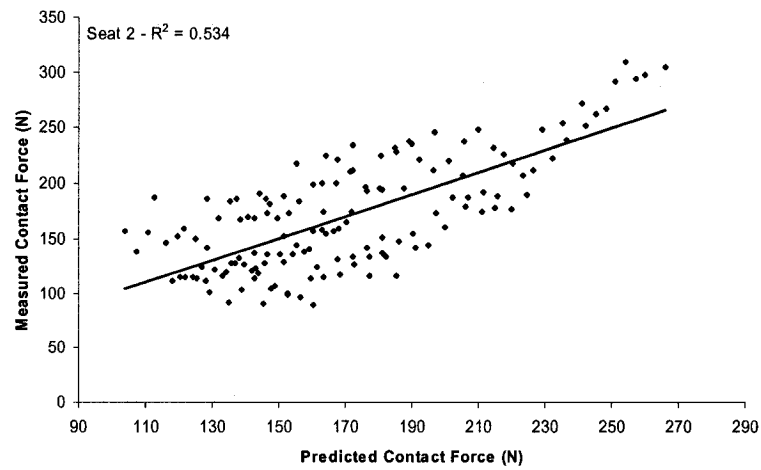
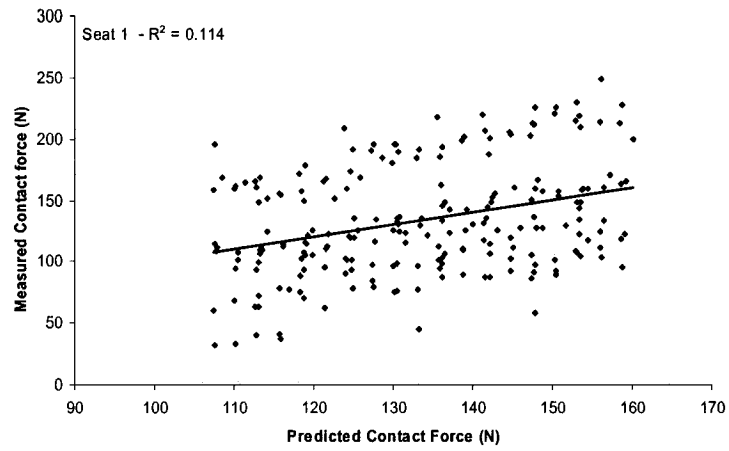


Figure 3.16: Correlations between the measured and estimated backrest mean contact force for the three candidate seats

The Contact Force Ratios (CFR) of the backrests are further derived by normalizing the measured contact force with the subject weight. The resulting values directly relate to the body weight supported by the backrest as functions of the various posture and seat-related parameters. Figures 3.17, 3.18 and 3.19 illustrate the backrest CFR for seats 1, 2 and 3, respectively. The results show that the backrest CFR generally decreases with increasing seat height for all test seats. Higher backrest angles, on the other hand, cause higher CFR for all the test seats. The variations in knee angle setting do not show a clear trend in the CFR at the backrest. The ratio of the body weight supported by the backrest is also significantly affected by the amount of cushion contouring, as evident from the differences in CFR values for each seat. Figure 3.15 suggests, for seat 1, that the mean CFR and thus the total body weight transferred to the backrest ranges from 13 to 26 % for the postural variations considered. The backrest CFR for seats 2 and 3 range from 19 to 26 % and 19 to 23 %, respectively. Considering the large standard deviations, the CFR for seat 1 was observed to be as low as 6% for the 5° backrest angle and as high as 30% for the 25° backrest angle. Similarly for seat 2, the lowest and highest values of CFR were obtained as 14% and as high as 30%, respectively, while those for seat 3, as 13% and 27%. The higher standard deviations of seat 1 further suggest that the backrest contouring helps minimize the variations in the contact force and pressure, as it tends to limit the effects of the variations caused by individuals preferred sitting posture by forcing the upper body to follow the contours of the backrest cushion.

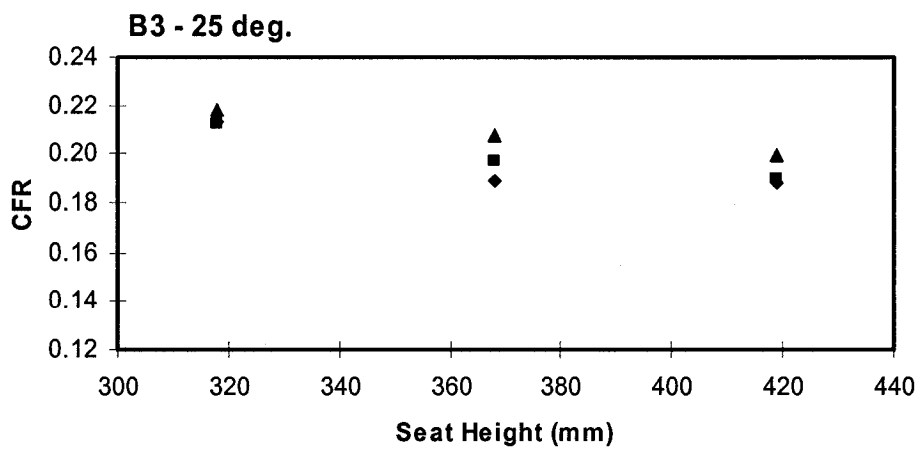
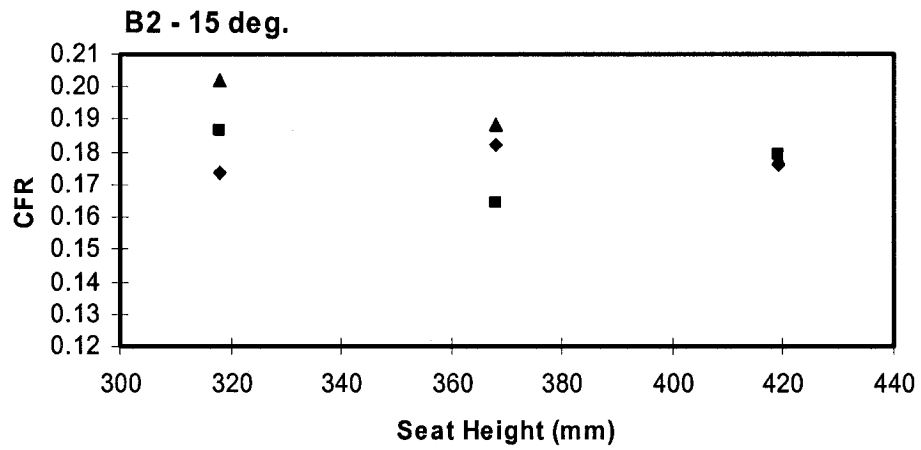
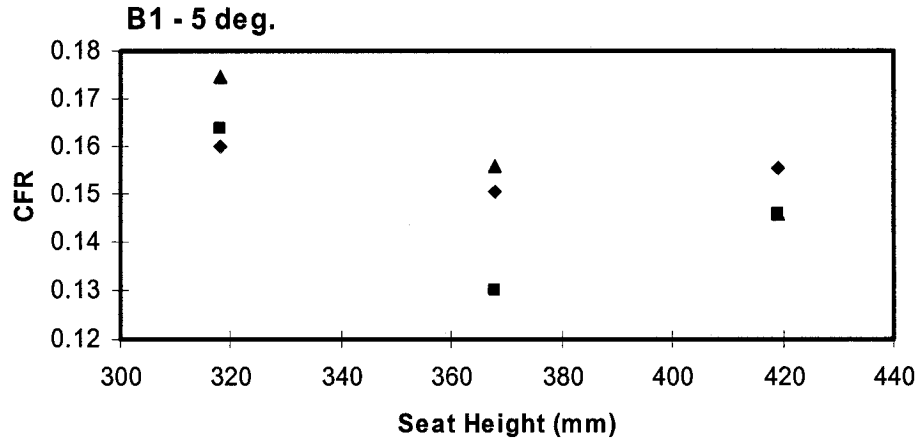


Figure 3.17: Variations in the CFR of the backrest of seat 1: ◆ K1 - 95°; ■ K2 - 115 °; ▲ K3 - 135°.

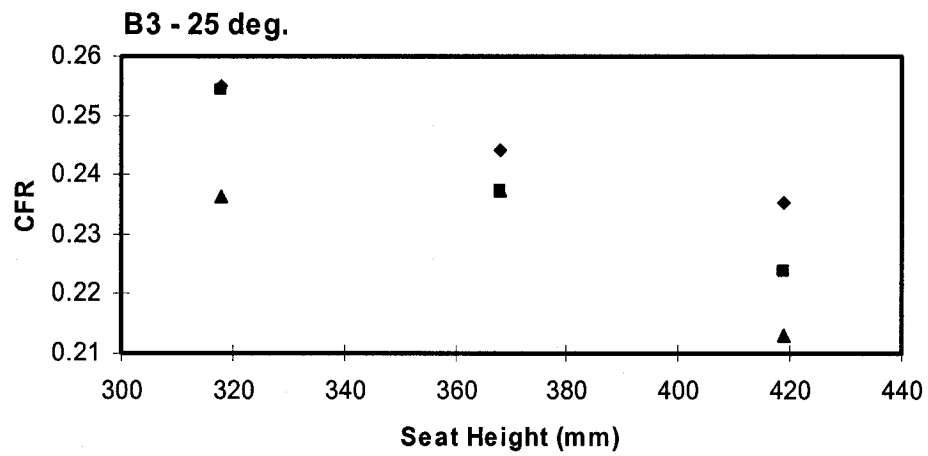
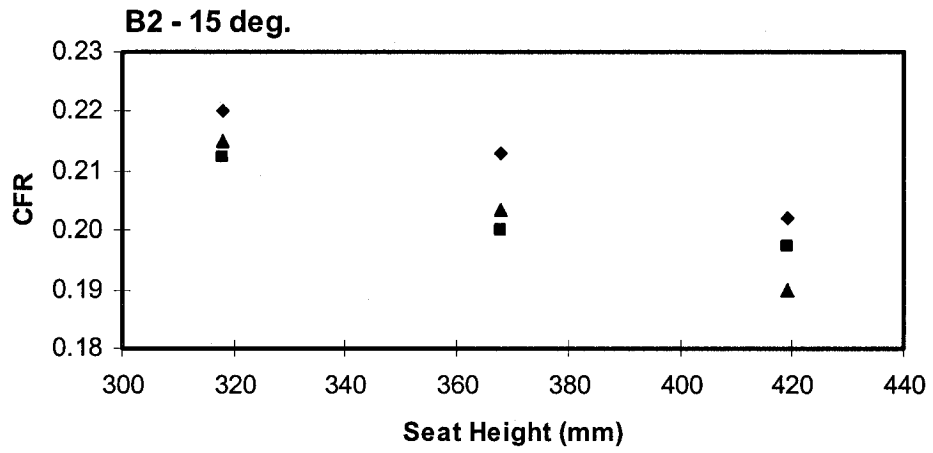


Figure 3.18: Variations in the CFR of the backrest of seat 2: ♦ K1 - 95°; ■ K2 - 115 °; ▲ K3 - 135°.

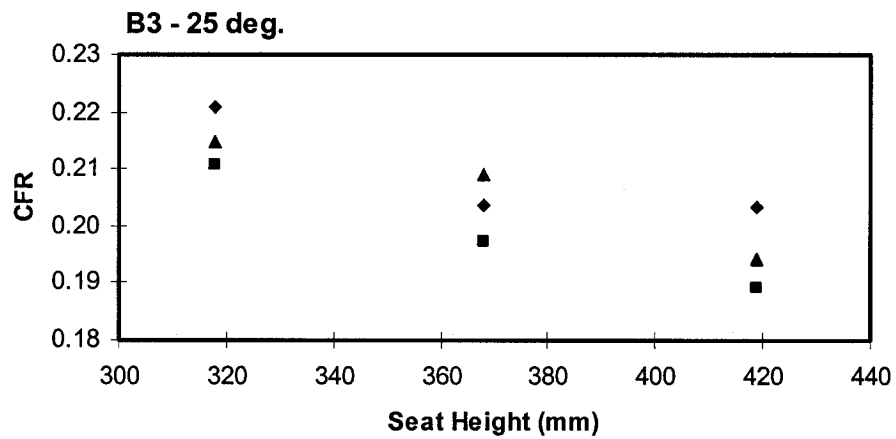
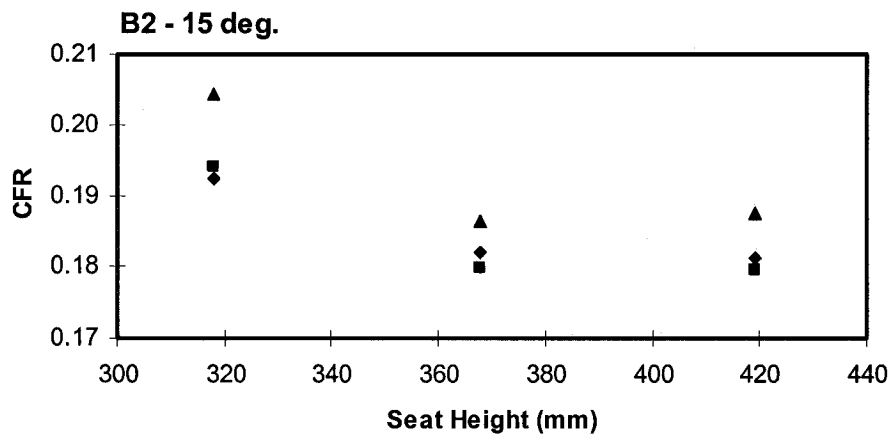


Figure 3.19: Variations in the CFR of the backrest of seat 2: ♦ K1 - 95°; ■ K2 - 115 °; ▲ K3 - 135°.



### 3.6.2 Relationship between interface pressure and seated posture.

A multi factor ANOVA on the peak and mean pressures as well as the contact area of the backrest revealed that only the backrest angle is significant ( $p < 0.001$ ) for the peak and mean pressure, while the factors H, K and B are also fairly significant ( $p < 0.05$ ) on the backrest contact area. The results are applied to formulate the following regression models in peak pressure (PP), mean pressure (MP) and the contact area:

$$PP = \beta_0 + \beta_1(W) + \beta_2(B) \quad (3.12)$$

$$MP = \beta_0 + \beta_1(W) + \beta_2(B) \quad (3.13)$$

$$A_c = \beta_0 + \beta_1(W) + \beta_2(H) + \beta_3(K) + \beta_4(B) \quad (3.14)$$

Table 3.19: Regression coefficients and correlation factors for the backrest peak pressure

Seat	R <sup>2</sup>	$\beta_0$	$\beta_1$	$\beta_2$
1	0.109	0.33	0	0.005
2	0.075	0.725	0	0.003
3	0.262	0.27	0	0.004

Table 3.20: Regression coefficients and correlation factors for the mean pressure

Seat	R <sup>2</sup>	$\beta_0$	$\beta_1$	$\beta_2$
1	0.091	0.31	0	0.005
2	0.062	0.67	0	0.002
3	0.232	0.25	0	0.004

Table 3.21: Regression coefficients and correlation factors for the contact area

Seat	R <sup>2</sup>	$\beta_0$	$\beta_1$	$\beta_2$	$\beta_3$	$\beta_4$
1	0.226	225.37	0.71	-0.40	-0.52	6.54
2	0.702	-15.25	1.27	-0.39	-1.61	7.77
3	0.215	442.07	0.55	-0.41	-0.07	4.33

Tables 3.19, 3.20 and 3.21 summarize the regression and correlation coefficients for the peak and mean pressures, and the contact area respectively. The results show extremely poor correlation between the measured and predicted values of peak and mean pressures, and the contact areas on the backrests of all the candidate seats. The subject weight is shown to have zero contribution to the prediction of the pressure at the backrest. This suggests that the pressure variations are far more sensitive to cushion contours and stiffness and that subject weight does not provide an accurate indication of the level of loading at the backrest. In terms of the contact area, both heavier subjects and higher backrest angles lead to increased contact between the subject and the seat, while higher seats and knee angles contribute to a reduction in the contact between the subject and the seat.

### **3.7 Summary of Backrest Analysis**

The statistical analyses of the contact forces and areas as well as the peak and mean pressures of the backrest of the three candidate seats have shown that higher backrest angles create higher magnitudes of contact area and force between the occupant and the seat. The large standard deviations associated with all the measured responses suggest that anthropometry and postural variations do inevitably cause differences in pressure distributions at the backrest, while the backrest cushion contours and stiffness have a more significant effect on creating zones of localized high pressure, irrespective of the subject anthropometry and posture. The analysis of the pressure distribution on the backrest of the three automotive seats has shown that while some mildly significant trends are observable with respect to anthropometry and the posture, excessive inter-

subject variability or standard deviations exist, which are attributed to preferred sitting postures which cannot be easily quantified. Furthermore, the pressure profiles of the backrest cushion are significantly affected by the cushion geometry and require much larger test populations and considerable investigation into a more suitable method of comparison to draw any significant conclusions pertaining to the assessment of the comfort performance of automotive seats.

### 3.8 Summary of Generalized Seat-Pan and Backrest Pressure Analyses

The pressure profiles acquired at the seat-pan and backrest for three different automotive seats have been analyzed with respect to anthropometry, posture and cushion stiffness. It was found that the amount of body weight supported by the seat-pan varied with posture and anthropometry but generally varied in the 60% to 79% range, irrespective of the cushion properties, which correlates well with the data reported in more extensive studies in automotive seating [50,55,62]. The backrest was found to support up to 27% of the body weight and as low as 11% for seats allowing a more erect posture. The ratio of body weight transferred to the seat-pans and backrests of automotive seats have been found to be a complex function of anthropometry, posture and cushion properties. Table 3.22 summarizes the overall seat-pan and backrest contact force ratios for each test seat; these values reflect the total means and do not correspond to a particular subject or posture.

Table 3.22: Mean values and standard deviations (SD) of seat-pan and backrest CFR

	SEAT 1		SEAT 2		SEAT 3	
	Seat-Pan	Backrest	Seat-Pan	Backrest	Seat-Pan	Backrest
MEAN	0.70	0.18	0.68	0.22	0.66	0.20
SD	0.09	0.07	0.06	0.05	0.06	0.04

## CHAPTER 4

### DISTRIBUTED CONTACT FORCES AND PRESSURE ANALYSES AT THE HUMAN-SEAT INTERFACE OF AUTOMOTIVE SEATS

#### 4.1 Introduction

The ratio of the total body weight supported by the seat-pan and the backrest is found to vary from seat to seat, depending on its stiffness and cushion geometry. The seat-pan of automotive seats is reported to carry up to 76% of the total body weight [4, 28,55], while the remainder of the body weight is transferred to the backrest and the feet. The results obtained from the generalized pressure analyses, presented in chapter 3, show that the amount of body weight supported by each section of a seat is also a complex function of anthropometry and the sitting posture. Specific areas of the body, namely: the IT, the fleshy area of the thighs just above the knees and the lower lumbar area of the back are known to be sensitive to excessive pressure loading [10,27]. The sensation of comfort, fatigue and pain in specific segments of the biological system could be related to the high localized pressure and contact forces in the vicinity of the specific body segments.

The interface pressure distribution attained for a seat could be analyzed to derive peak pressures and contact forces occurring over different body segments. The knowledge gained from such analysis could provide guidelines for contouring of the seat-pan and the backrest to redistribute the contact pressure. The data attained from the interface pressure measurements are therefore further analyzed in this chapter to investigate the localized pressure concentrations and contact forces in the zones known to be more sensitive to pressure loading. The effect of body weight on the distribution of

forces and pressures at the seat-pan and backrest are shown, and a zonal analysis of the interface pressure is performed with respect to the three experimental factors namely, the seat height, knee angle and the backrest angle. The data are analyzed to determine the combinations of factors that could help reduce the levels of loading on the sensitive areas of the body. The data are analyzed with the group-mask evaluation software module of the *PLIANCE* system to derive the zonal contact forces, areas, and peak and mean pressures.

#### **4.2 Analysis of Distributed Seat-Pan Forces and Pressures**

The surface areas of the seat-pan and the backrest of each candidate seat are divided into different zones to study the contact force and interface pressure imparted on specific body segments in contact with the seat. The seat-pan is divided into 5 zones referred to as 'Zone 1' to 'Zone 5', as illustrated in Figure 4.1. The figure presents a generalized description of the zones that could be applied to all the candidate seats. Zone 1 encompasses the region surrounding the IT, which is known to support the major portion of the body weight and exhibits higher concentration of interface pressure. It has been reported that the two IT bones are approximately 16 to 25 cm apart [4]. The zone is thus defined by a 25.4 cm x 14.8 cm area of the sensing mat enveloping 10 columns and 7 rows of sensors, with a total area of 451.61 cm<sup>2</sup>. Zone 2 is defined to measure the contact force between the sacro-iliac region and the seat surface. This zone comprises 10 columns and 3 rows of sensors with a total surface area of 195.55 cm<sup>2</sup>. It has been reported that soft thigh tissues may undergo rapid fatigue under high contact pressure[1,4,10], Zone 3 is thus defined to measure the contact forces between the thighs and the seat surface, and it envelopes 10 columns and 6 rows of the sensor mat with a

total area of 387.10 cm<sup>2</sup>. The side wings of a seat-pan, when elevated, could cause high loading of the

<b>ZONE 5</b> <b>RIGHT</b> <b>LATERAL</b> 3 Columns x 16 Rows 48 Sensors 309.68 cm <sup>2</sup>	<b>ZONE 2</b> <b>SACRO-ILLIAC</b> 10 Columns x 3 Rows 30 Sensors 195.55 cm <sup>2</sup>	<b>ZONE 4</b> <b>LEFT</b> <b>LATERAL</b> 3 Columns x 16 Rows 48 Sensors 309.68 cm <sup>2</sup>
	<b>ZONE 1</b> <b>ISCHIAL TUBEROSITIES</b> 10 Columns x 7 Rows 70 Sensors 451.61 cm <sup>2</sup>	
	<b>ZONE 3</b> <b>THIGHS</b> 10 Columns x 6 Rows 60 Sensors 387.10 cm <sup>2</sup>	

Figure 4.1: Zone definitions for the seat-pan cushion.

femur bone leading to increased sensation of discomfort and fatigue. The localized contact forces arising from the side supports are thus evaluated by defining left-lateral (Zone 4) and right-lateral (Zone 5) regions, as shown in Figure 4.1. It is anticipated that the leading portions of these zones surrounding Zone 2 may encounter negligible interface pressure. Each of these zones envelopes 3 columns and 16 rows of sensors with a total area of 309.68 cm<sup>2</sup>.

The interface pressure distributions acquired at the seat-pan under different seat heights and sitting postures are analyzed to derive the contact force, peak and mean pressures, and the effective contact area for each zone. The effects of various experimental factors on the zonal response parameters are then evaluated and discussed in the following sub-sections.

#### 4.2.1 Postural effects on the distribution of seat-pan contact forces

The results presented in the previous chapter clearly show that the body weight supported by the seat-pan significantly influences the contact force and peak pressure. The body weight is thus expected to affect the zonal contact force and pressure in a similar manner. The effect of body weight, therefore, needs to be isolated in order to study the effects of the postural factors alone. For this purpose, the resulting forces developed in the various zones are normalized by the total body weight to derive the zonal CFRs, such that:

$$CFR_n = \frac{F_{cn}}{W_i} \quad (4.1)$$

where  $CFR_n$  is the contact force ratio of Zone 'n' and  $F_{cn}$  is the corresponding zonal contact force. The zonal CFR data could yield knowledge on the proportion of body weight supported by different segments of the seat-pan. The zonal pressure and force data may further provide guidelines with respect to contouring and localized cushion stiffness requirements. The data acquired for all the test subjects for specific seat and postural factors are analyzed to compute the mean values of zonal contact forces, interface pressures, and effective contact areas.

Figures 4.2 to 4.4 show the variations in the mean values of the zonal CFR for seats 1, 2 and 3, respectively, as functions of the seat height, knee angle and the backrest angle. The figures show that the ratio of the body weight supported by different zones of the seat-pan is not only a function of anthropometry and posture, but significant variations are also attributed to the differences in cushion contours and stiffness. The Zone 1, surrounding the IT, supports the largest portion of the body weight, irrespective

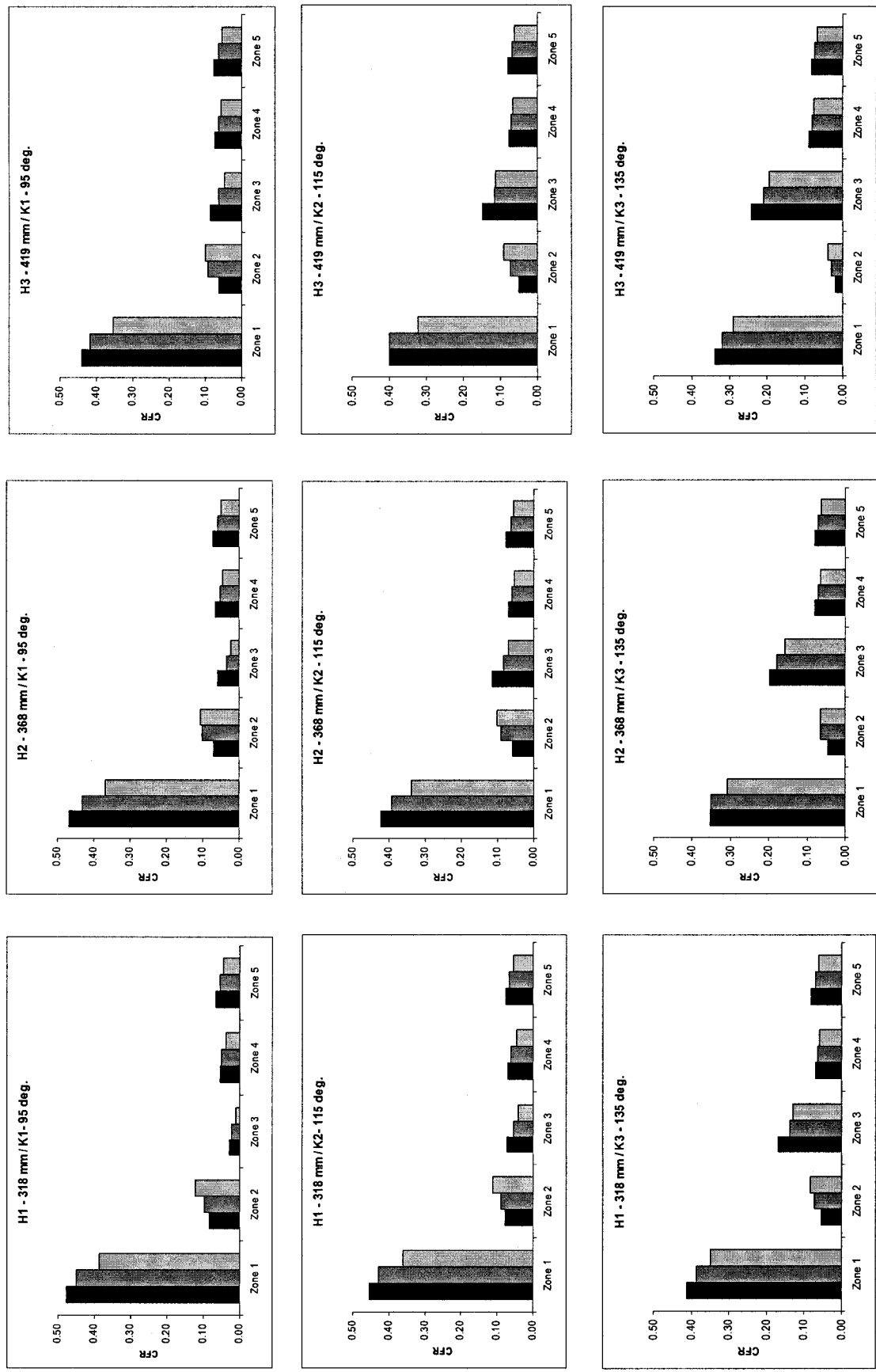


Figure 4.2: Effect of seat height, knee angle and backrest angle on the zonal CFR variations of the seat-pan of seat 1 (Backrest angle)



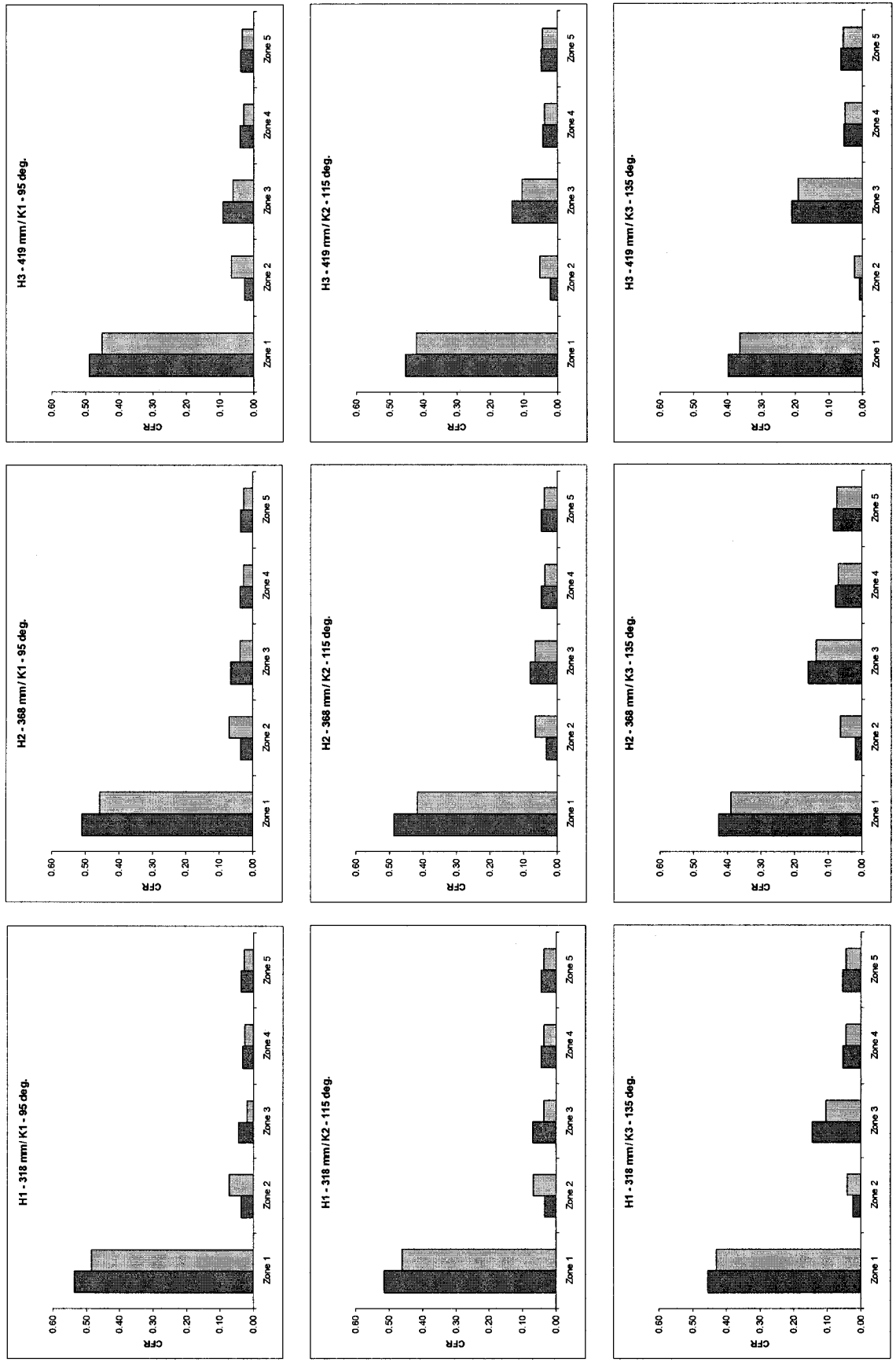


Figure 4.3: Effect of seat height, knee and backrest angle on the zonal CFR variations on the seat-pan of seat 2 (15° 25° Backrest angle)

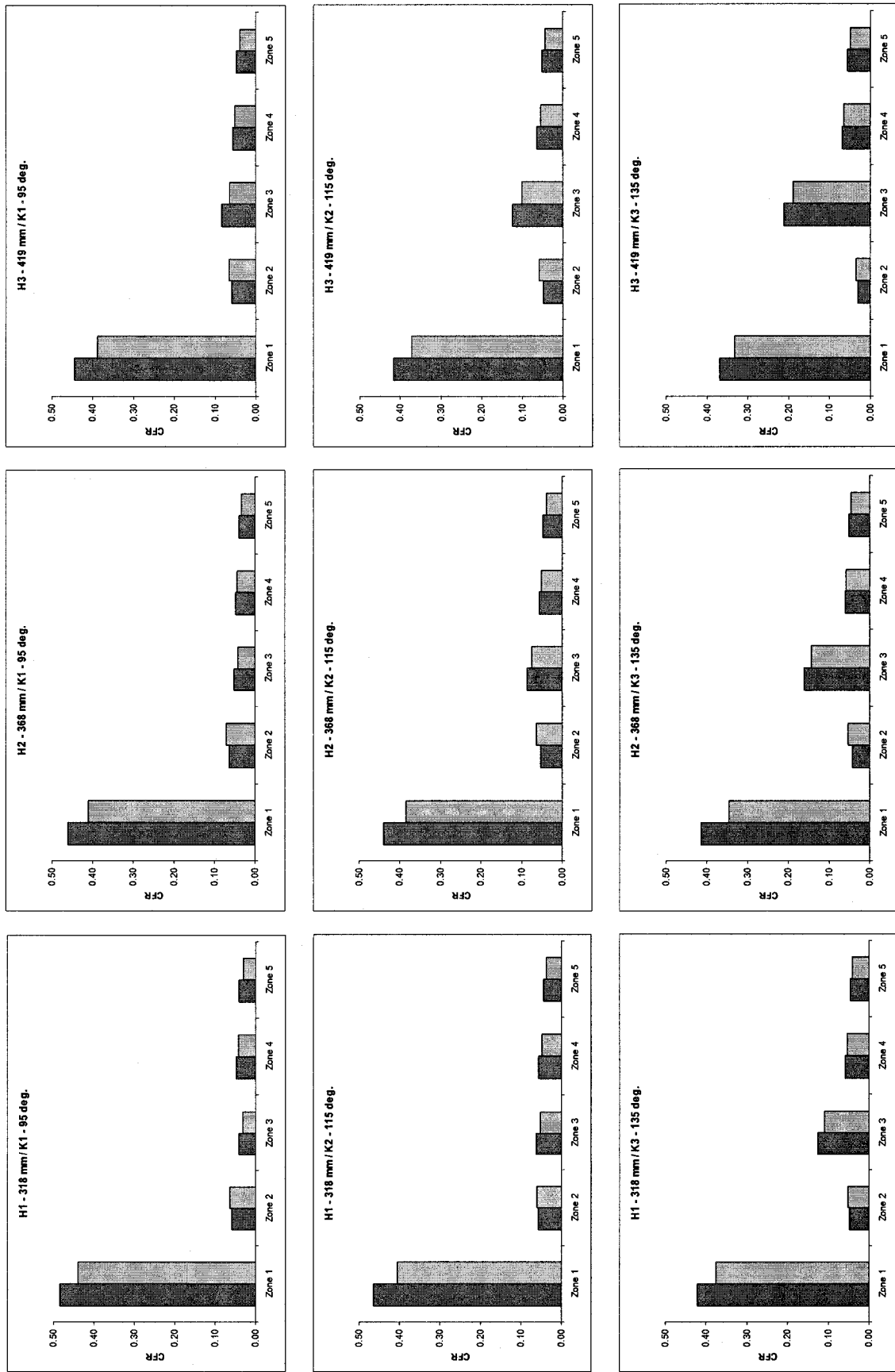


Figure 4.4 Effect of seat height, knee and backrest angle on the zonal CFR variations on the seat-pan of seat 3 (15° 25° Backrest angle)

of the subject-seat-posture combinations. The results suggest that 32 to 54 % of the total body weight is supported by Zone 1, while significant variations occur with variations in the seat design and posture related factors. The body weight supported by this zone is followed by that of Zone 2, surrounding the sacro-iliac region specifically under postures of low knee angle. On the basis of the CFR data, it was concluded that this zone supports 3 to 11 % of the total body weight when all three seats and seat heights are considered with a knee angle of 95°. An increase in the knee angle tends to shift the body weight from Zones 1 and 2 onto Zone 3, surrounding the thighs, indicating increased contact between the thighs and the seat, for all seats. The results suggest that a higher knee angle could impose increased loads on the soft tissues and may potentially impede blood flow and cause fatigue in that area of the body.

The portion of body weight supported by different zones is also strongly influenced by the seat height. A higher seat coupled with large knee angles causes far more contact with the thighs, as evident from the high contact force ratio in Zone 3 for all the candidate seats. A higher seat, however, tends to lower the concentration of high pressures and thus the contact force in the IT region (Zone 1) and the sacro-iliac zone (Zone 2). An increase in the backrest angle also helps to reduce the contact force around the IT (Zone 1) and the thighs (Zone 3), while it tends to increase the contact with the sacro-iliac zone and the seat for seats with less backrest curvature. For seat 1, the mean contact force attained for each height-knee-backrest combination suggests that increasing the backrest angle from 5° to 15° to 25° systematically reduces the ratio of body weight supported by the IT (zone 1), the thighs (Zone 3) and both the lateral zones (Zones 4 and 5) as evident in Figure 4.2. Furthermore, increasing the knee angle and seat height also

individually contribute to reductions in the CFR in Zones 1 and 2 but significantly increase the loading onto the thighs both beneath the knees (Zone 3) and on each lateral portion of the legs (Zones 4 and 5). The results further show strong interaction between the seat height (H) and the knee angle (K), where increasing the level of both factors simultaneously leads to a more significant reduction in CFR surrounding the IT and sacrum but transfers the body weight onto the thighs and lateral zones. The similar trends are also observed for seats 2 and 3, as shown in Figures 4.3 and 4.4, respectively. All the three seats tend to support similar proportions of the body weight in Zone 1, while more significant variations are observed for Zones 3, 4 and 5 with the experimental factors.

To determine the effects of each experimental factor on the variations in the seat-pan  $CFR_n$  and to verify the statistical significance of the factors, ANOVA and multiple linear regression analyses are performed on the data for each zone. The analysis also revealed fair to high significance of the seat height (H), knee angle (K) and the backrest angle (B);  $p < 0.05$ . A multiple linear regression formulation is thus obtained to describe the relationship between the  $CFR_n$  and the seat height, the knee angle and the backrest angle, such that:

$$CFR_n = \beta_0 + \beta_1(H) + \beta_2(K) + \beta_3(B); n = 1,2, \dots,5 \quad (4.2)$$

where  $\beta_0$ ,  $\beta_1$ ,  $\beta_2$  and  $\beta_3$  are the regression coefficients.

Table 4.1 summarizes the regression coefficients attained for each zone of the seat-pan. The regression based relationships revealed a high degree of correlation with the mean measured data with  $R^2$  values in excess of 0.8 for all cases. The results in general support the conclusions derived from the generalized force analysis of the previous chapter and the observations made from the mean data presented in Figures 4.2

Table 4.1: Regression coefficients for the zonal contact force ratios for seats 1, 2 and 3

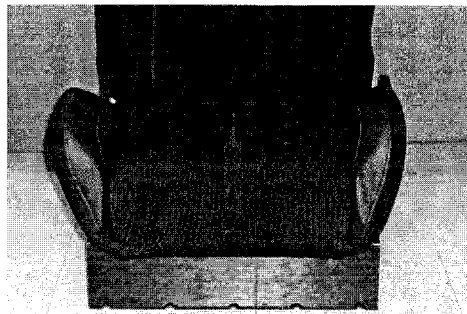
ZONE	SEAT	R <sup>2</sup>	$\beta_0$	$\beta_1$	$\beta_2$	$\beta_3$
1	1	0.92	0.832	0	-0.002	-0.004
	2	0.95	0.949	-0.001	-0.002	-0.004
	3	0.98	0.85	0	-0.002	-0.005
2	1	0.89	0.263	0	-0.001	0.002
	2	0.86	0.088	0	-0.001	0.003
	3	0.84	0.129	7.8 E -5	-0.001	0.001
3	1	0.97	-0.488	0.001	0.003	-0.002
	2	0.93	-0.374	0.001	0.003	-0.003
	3	0.93	-0.329	0.001	0.003	-0.002
4	1	0.96	-0.027	0	0	-0.001
	2	0.75	-0.032	3.6 E -5	0.001	-0.001
	3	0.92	-0.002	9.1 E -5	0	-0.001
5	1	0.97	0.024	0	0	-0.001
	2	0.75	-0.046	6.9 E -5	0.001	-0.001
	3	0.95	0.001	7.2 E -5	0	-0.001

to 4.4. The effect of backrest inclination is again obvious and shows that for the range of angles considered, increasing the value from 5° to 15° to 25° significantly reduces the amount of body weight carried by the ischials (Zone 1) by transferring the weight backwards onto the sacro-iliac zone (Zone 2) and onto the backrest. All the seats indicate similar contributions of the backrest angle to the CFR in the lateral zones (Zones 4 and 5). The contributions due to the variations in the knee angles to the CFR in the lateral zones are also quite small, which is further evident from Figures 4.2 to 4.4. Variations in the seat height show very little effect on the variations in the CFR of Zones 1, 2, 4 and 5, but are found to be considerably significant in increasing the contact force in Zone 3 surrounding the thighs.

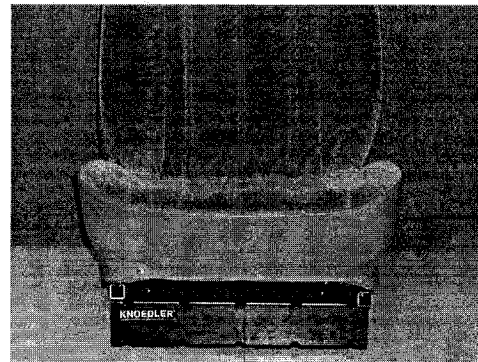
#### 4.2.2 Distribution of seat-pan contact pressure

The peak contact pressures and their concentration have been shown to vary with respect to the anthropometric and postural factors. The cushion contour and the effective

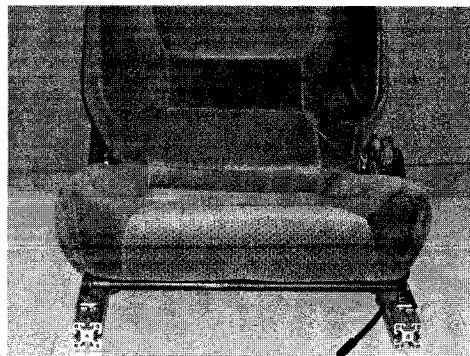
stiffness of the seat have also been shown to be important in view of the contact pressure variations. Figure 4.5 shows the differences in the contours of the seat-pan cushions of seats 1, 2 and 3, considered for this study. The figures clearly illustrate major differences in the lateral wings of the three seats. The seat-pan of seat 1, Figure 4.5 (a), is very narrow and shows very high wings when compared to those of seats 2 and 3 as illustrated in Figures 4.5 (b) and (c), respectively. The seat-pan of seat 2, Figure 4.5 (b), is relatively flat when compared to seats 1 and 3. While the seat-pans of each seat are generally considered flat, the differences in the wing's height, shape and the stiffness are expected to generate significant variations in peak pressure.



(a)



(b)



(c)

Figure 4.5: Comparisons of seat-pan contours of seats 1 (a), 2 (b) and 3 (c)

The pressure distribution data acquired at the body-seat-pan interface are analyzed to derive the pressure maps for each zone. The peak pressures within different zones are then identified for each subject-seat-posture combination using the multi-mask analysis module available within the *PLIANCE* software. The peak pressure data obtained for each subject are then grouped to derive the mean values of peak pressure within each zone. Table 4.2 shows the variations in the mean peak pressures within the five different zones together with the standard deviations (SD) of the means as a function of the posture-related factors for seat 1. Comparing Zones 1, 2 and 3 clearly shows that the IT are subjected to higher magnitudes of pressure. The mean data further shows the strong effects of the posture related factors, namely the knee and backrest angles. The mean pressure of Zone 1 tends to decrease with increasing knee angle, backrest angle and seat height, while that of Zone 2 increases with backrest angle and decreases with increasing knee angle and seat height. Zones 4 and 5 are of particular significance to seat 1 because they include the lateral wings of the seat-pan and clearly show higher peak pressures regardless of the posture. This further suggests that seat-pan contouring has a significant effect on creating hard-points, which may lead to significant pressure loading and increased discomfort in subjects of heavier stature.

Seats 2 and 3 on the other hand, show somewhat opposite trends; a comparison of the mean pressures of Zones 4 and 5, of both seats, to those of seat 1 clearly highlights the effect of the wings. For seats 2 and 3, the location of the peak pressure invariably occurs within Zone 1 surrounding the IT, as seen in Tables 4.3 and 4.4, respectively. Similarly, comparing the peak pressure of Zones 4 and 5 for seats 2 and 3 further highlights the effects of the lateral wings in generating higher peak pressures.

Significantly large standard deviations are also observed for Zones 2, 4 and 5 for all seats. These are mainly attributed to the lack of contact within these zones for postures with lower seat heights and knee angle settings for subjects of smaller stature.

Table 4.2: Zonal mean peak pressure and standard deviations (SD) variations for seat 1

Seat Height (mm)	Knee Angle (deg.)	Back Angle (deg.)	ZONE 1		ZONE 2		ZONE 3		ZONE 4		ZONE 5	
			Mean	SD	Mean	SD	Mean	SD	Mean	SD	Mean	SD
318	95	5	1.33	0.26	0.91	0.29	0.38	0.25	1.27	0.38	1.36	0.19
		15	1.19	0.16	1.01	0.23	0.35	0.26	1.07	0.32	1.11	0.22
		25	1.09	0.13	1.15	0.25	0.27	0.21	0.88	0.34	0.92	0.26
	115	5	1.15	0.16	0.80	0.37	0.55	0.21	1.30	0.33	1.39	0.21
		15	1.06	0.12	0.91	0.26	0.48	0.20	1.11	0.26	1.12	0.26
		25	0.98	0.07	1.10	0.24	0.41	0.20	0.93	0.28	0.95	0.25
	135	5	1.01	0.13	0.70	0.33	0.70	0.14	1.16	0.35	1.31	0.26
		15	0.92	0.12	0.83	0.30	0.60	0.15	1.02	0.29	1.11	0.31
		25	0.90	0.07	0.88	0.33	0.63	0.18	0.88	0.22	0.95	0.27
368	95	5	1.22	0.20	0.78	0.35	0.54	0.22	1.30	0.32	1.31	0.15
		15	1.09	0.11	1.05	0.25	0.40	0.26	1.01	0.36	1.10	0.25
		25	0.97	0.12	1.08	0.32	0.34	0.21	0.91	0.28	0.92	0.26
	115	5	1.06	0.19	0.72	0.32	0.60	0.15	1.23	0.35	1.30	0.23
		15	0.99	0.12	0.94	0.34	0.52	0.15	1.02	0.22	1.06	0.22
		25	0.90	0.12	1.03	0.27	0.49	0.16	0.89	0.26	0.97	0.20
	135	5	0.92	0.14	0.62	0.30	0.77	0.14	1.20	0.35	1.30	0.30
		15	0.90	0.11	0.78	0.40	0.69	0.14	1.02	0.29	1.09	0.30
		25	0.79	0.10	0.75	0.39	0.66	0.16	0.89	0.23	1.00	0.27
419	95	5	1.09	0.10	0.74	0.32	0.59	0.19	1.28	0.23	1.40	0.21
		15	1.02	0.05	0.94	0.24	0.48	0.16	1.02	0.26	1.11	0.24
		25	0.92	0.07	1.00	0.26	0.43	0.14	0.96	0.20	0.90	0.14
	115	5	0.97	0.13	0.65	0.30	0.71	0.13	1.15	0.21	1.32	0.25
		15	0.94	0.06	0.85	0.24	0.58	0.09	1.02	0.22	1.15	0.21
		25	0.85	0.09	0.89	0.34	0.54	0.13	0.97	0.27	0.92	0.20
	135	5	0.87	0.05	0.38	0.24	0.84	0.12	1.23	0.27	1.35	0.29
		15	0.78	0.06	0.52	0.27	0.78	0.16	1.07	0.28	1.16	0.29
		25	0.77	0.09	0.58	0.29	0.78	0.17	0.95	0.24	1.05	0.22



Table 4.3: Zonal mean peak pressure and standard deviations (SD) variations for seat 2

Seat Height (mm)	Knee Angle (deg.)	Back Angle (deg.)	ZONE 1		ZONE 2		ZONE 3		ZONE 4		ZONE 5	
			Mean	SD	Mean	SD	Mean	SD	Mean	SD	Mean	SD
318	95	15	1.48	0.29	0.66	0.32	0.54	0.18	0.67	0.26	0.64	0.18
	95	25	1.33	0.23	0.90	0.29	0.38	0.22	0.59	0.24	0.56	0.11
	115	15	1.31	0.27	0.62	0.30	0.60	0.15	0.74	0.21	0.73	0.17
	115	25	1.22	0.20	0.90	0.32	0.48	0.11	0.64	0.22	0.60	0.14
	135	15	1.09	0.25	0.51	0.30	0.70	0.21	0.67	0.22	0.69	0.18
	135	25	1.06	0.22	0.66	0.34	0.63	0.30	0.62	0.18	0.55	0.13
368	95	15	1.39	0.20	0.60	0.34	0.56	0.18	0.71	0.18	0.68	0.16
	95	25	1.29	0.18	0.84	0.37	0.46	0.15	0.58	0.15	0.55	0.16
	115	15	1.29	0.29	0.56	0.31	0.62	0.13	0.71	0.21	0.69	0.15
	115	25	1.13	0.19	0.80	0.35	0.51	0.09	0.62	0.15	0.56	0.15
	135	15	1.52	1.23	0.51	0.36	1.09	0.95	0.88	0.82	0.98	0.98
	135	25	1.42	1.03	0.99	0.80	0.92	0.58	0.86	0.82	0.79	0.60
419	95	15	1.32	0.32	0.59	0.29	0.62	0.15	0.65	0.19	0.65	0.25
	95	25	1.19	0.18	0.83	0.34	0.53	0.11	0.55	0.18	0.57	0.13
	115	15	1.18	0.27	0.53	0.27	0.70	0.13	0.62	0.18	0.69	0.23
	115	25	1.15	0.19	0.75	0.32	0.63	0.15	0.54	0.20	0.57	0.12
	135	15	1.04	0.10	0.26	0.25	0.93	0.23	0.62	0.25	0.71	0.13
	135	25	0.99	0.12	0.50	0.24	0.87	0.24	0.55	0.25	0.67	0.07

Table 4.4: Zonal mean peak pressure and standard deviations (SD) variations for seat 3

Seat Height (mm)	Knee Angle (deg.)	Back Angle (deg.)	Zone 1		Zone 2		Zone 3		Zone 4		Zone 5	
			Mean	SD	Mean	SD	Mean	SD	Mean	SD	Mean	SD
318	95	15	1.42	0.31	0.71	0.20	0.48	0.18	0.71	0.15	0.61	0.12
	95	25	1.27	0.24	0.75	0.15	0.47	0.16	0.73	0.15	0.49	0.09
	115	15	1.23	0.27	0.70	0.16	0.56	0.10	0.76	0.11	0.61	0.09
	115	25	1.11	0.24	0.76	0.20	0.51	0.12	0.72	0.16	0.55	0.10
	135	15	1.07	0.23	0.58	0.14	0.67	0.13	0.68	0.15	0.59	0.10
	135	25	0.95	0.20	0.69	0.16	0.60	0.16	0.66	0.13	0.53	0.12
368	95	15	1.26	0.26	0.74	0.16	0.55	0.11	0.73	0.14	0.55	0.11
	95	25	1.15	0.10	0.75	0.18	0.52	0.12	0.69	0.17	0.52	0.08
	115	15	1.13	0.28	0.66	0.15	0.61	0.07	0.72	0.13	0.58	0.12
	115	25	1.03	0.18	0.66	0.16	0.53	0.11	0.69	0.13	0.53	0.12
	135	15	1.03	0.27	0.61	0.17	0.74	0.12	0.69	0.18	0.66	0.17
	135	25	0.90	0.16	0.63	0.17	0.67	0.15	0.70	0.14	0.58	0.11
419	95	15	1.17	0.25	0.69	0.17	0.62	0.14	0.78	0.15	0.60	0.15
	95	25	1.02	0.11	0.68	0.15	0.56	0.13	0.69	0.10	0.53	0.08
	115	15	1.05	0.16	0.66	0.19	0.71	0.14	0.76	0.15	0.63	0.15
	115	25	0.95	0.12	0.70	0.13	0.64	0.13	0.65	0.12	0.53	0.08
	135	15	0.92	0.13	0.48	0.18	0.87	0.23	0.75	0.32	0.65	0.12
	135	25	0.85	0.09	0.50	0.22	0.80	0.21	0.70	0.28	0.59	0.11

### 4.3 Analysis of Distributed Backrest Contact Forces and Pressures

Similar to the seat-pan, the backrest area was also divided into different zones to study the contact forces and pressures imparted on specific body segments of the back in contact with the seat. The backrest is divided into 4 different zones, referred to as 'Zone 1' to 'Zone 4', as illustrated in Figure 4.6. The figure presents a generalized description of the zones that could be applied to each candidate seat. Zone 1 encompasses the region including all the lumbar vertebrae of the spine. Zone 1 is defined by an area of 25.4 cm x 20.3 cm on the sensing mat, which contains 10 columns and 8 rows of sensors, with a total area of 516.13 cm<sup>2</sup>. Zone 2 is defined to measure the contact force between the thoracic region of the back and the backrest support surface of the seats. This zone includes 10 columns and 8 rows of sensors with a total surface of 516.13 cm<sup>2</sup>; it is anticipated that this zone will exhibit higher contact forces and concentrations of peak pressure at higher backrest angles.

<b>ZONE 3</b> Right Lateral 3 Columns x 16 Rows 48 Sensors 309.68 cm <sup>2</sup>	<b>ZONE 2</b> Thoracic Zone 10 Columns x 8 Rows 80 Sensors 516.13 cm <sup>2</sup>	<b>ZONE 4</b> Left Lateral 3 Columns x 16 Rows 48 Sensors 309.68 cm <sup>2</sup>
	<b>ZONE 1</b> Lumbar Zone 10 Columns x 8 Rows 80 Sensors 516.13 cm <sup>2</sup>	

Figure 4.6: Zone definitions for the backrest cushion

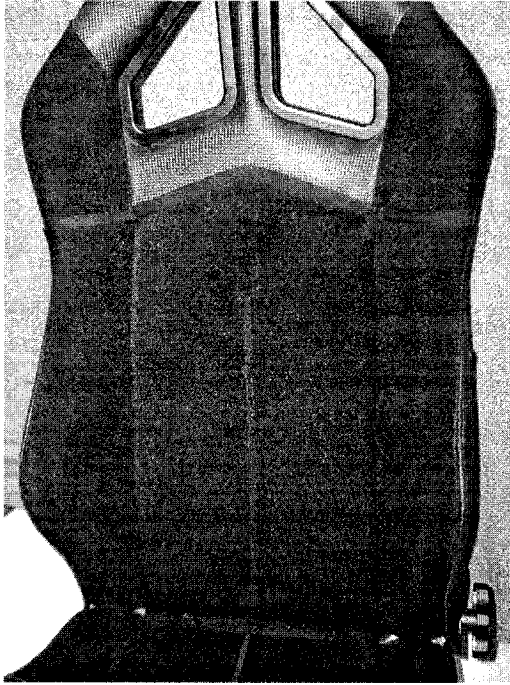
The wings located on the backrest provide an effective way to create significant contouring of the backrest support. Similar to the seat-pan, higher and stiffer wings of the backrest can significantly increase loading on the lateral segments of the body leading to increased discomfort. The localized contact forces and pressures in these areas are thus evaluated by defining Zones 3 and 4 to include the right (Zone 3) and left (Zone 4) lateral wings of the test seats, as shown in Figure 4.6. Each of these zones includes 3 columns and 16 rows of the sensor matrix for a total area of 309.68 cm<sup>2</sup>.

The backrest interface pressure distributions acquired under different seat-height-knee-back combinations are analyzed to derive the mean zonal contact forces, peak and mean pressures, and the effective contact areas for each zone. The effects of the various experimental factors on the response of the zonal parameters are then evaluated and discussed in the following sub-sections.

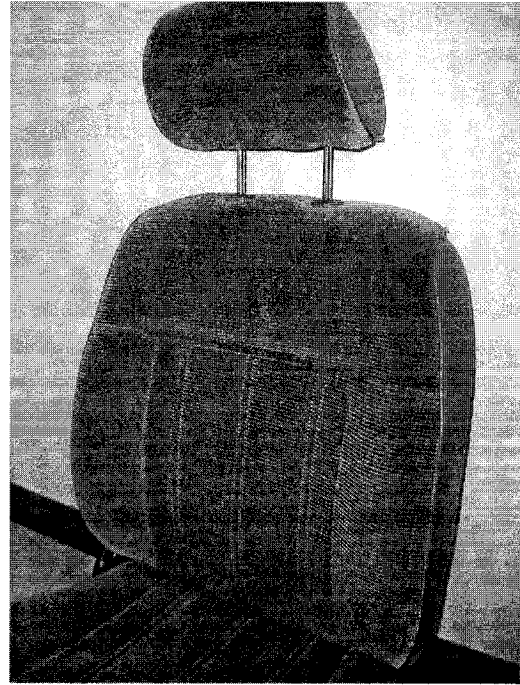
#### **4.3.1 Postural effects on the distribution of backrest contact forces**

As it has been observed in the previous chapter, significant variations in the backrest contact forces and pressures have been attributed to the various experimental factors as well as to the inter-subject variability. However, the poor correlation factors attained for the backrest regression analyses in chapter 3 further suggest that the backrest contouring is also a very significant factor causing large variations in the backrest contact forces and pressures, irrespective of the anthropometric and postural factors. Similar to the seat-pan, significant contouring is achieved by adding wings to the lateral portions of the backrest support and is accounted for by Zones 3 and 4 on the backrest. In addition, significant contouring is also achieved by adding curvature along the vertical axes of the

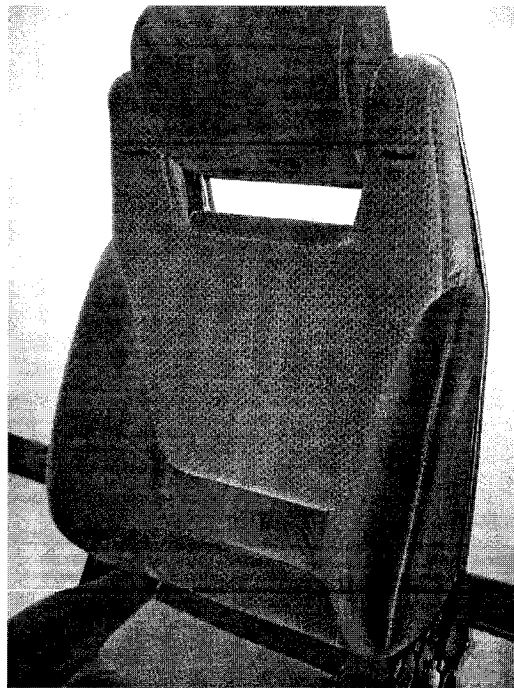
backrest to provide support for the natural curvature of the spine. The differences between the backrest supports of the three test seats are shown in Figure 4.7. It is anticipated that significant variations in the contact forces will arise due to the different curvatures of the backrests. Figure 4.7 (a) shows that the backrest of seat 1 has no curvature along the vertical axes of the cushion, but has wings of considerable size that are anticipated to create high pressures in Zones 3 and 4 when compared to seats 2 and 3. Seats 2 and 3 on the other hand, exhibit considerable curvature along the vertical axis of the backrest, as shown in Figures 4.7 (b) and (c), respectively. With respect to the lateral wings on the backrest, seat 2 provides very little lateral support (Figure 4.7(b)), while seat 3 (Figure 4.7(c)), exhibits much larger wings similar to but smaller than seat 1. The backrest zonal CFRs are thus derived to study the behavior of the distribution of total body weight over the surface of the backrest as functions of the subject anthropometry, seated postures, the cushion stiffness and the backrest contouring.



(a)



(b)



(c)

Figure 4.7: Comparison of the backrest contouring of seats 1 (a), 2 (b) and 3 (c)

Figures 4.8 to 4.10 show the variations in the mean values of the zonal backrest CFR for seats 1, 2 and 3, respectively, as functions of the seat height, knee angle and the backrest angle. The figures show that the ratio of the body weight supported by different zones of the backrest is not only a function of anthropometry and posture, but significant variations can be attributed to the differences in cushion contours and stiffness, as observed for the seat-pan.

Figure 4.8 shows the zonal CFR variations for the backrest of seat 1, which exhibits very little contouring along the vertical axis of the backrest. For this seat, Zone 2 carries significantly higher portions of the body weight, up to 12 %, while the CFR for Zone 1 was observed to be only as high as approximately 7.5 %. The figure further suggests that the backrest angle has a higher effect on the CFR of Zone 1 when compared to Zone 2. The amount of body weight supported by Zone 1 is further affected by the seat height, where higher seats produced lower CFR; this effect becomes more pronounced at higher knee angles suggesting a significant interaction between the seat height and the knee angle. Zones 1 and 2 exhibit an inverse relationship with respect to the knee angle, where higher knee angles tend to cause body weight transfer from Zone 1 onto Zone 2. This behavior is also shown to be significantly affected by the seat height, where the combination of higher seat heights and knee angles caused higher portions of the body weight to be transferred onto Zone 2 from Zone 1. Zones 3 and 4 are significantly affected by the backrest angle, where higher backrest inclinations caused higher contact between the body and the seat irrespective of the height-knee combination.

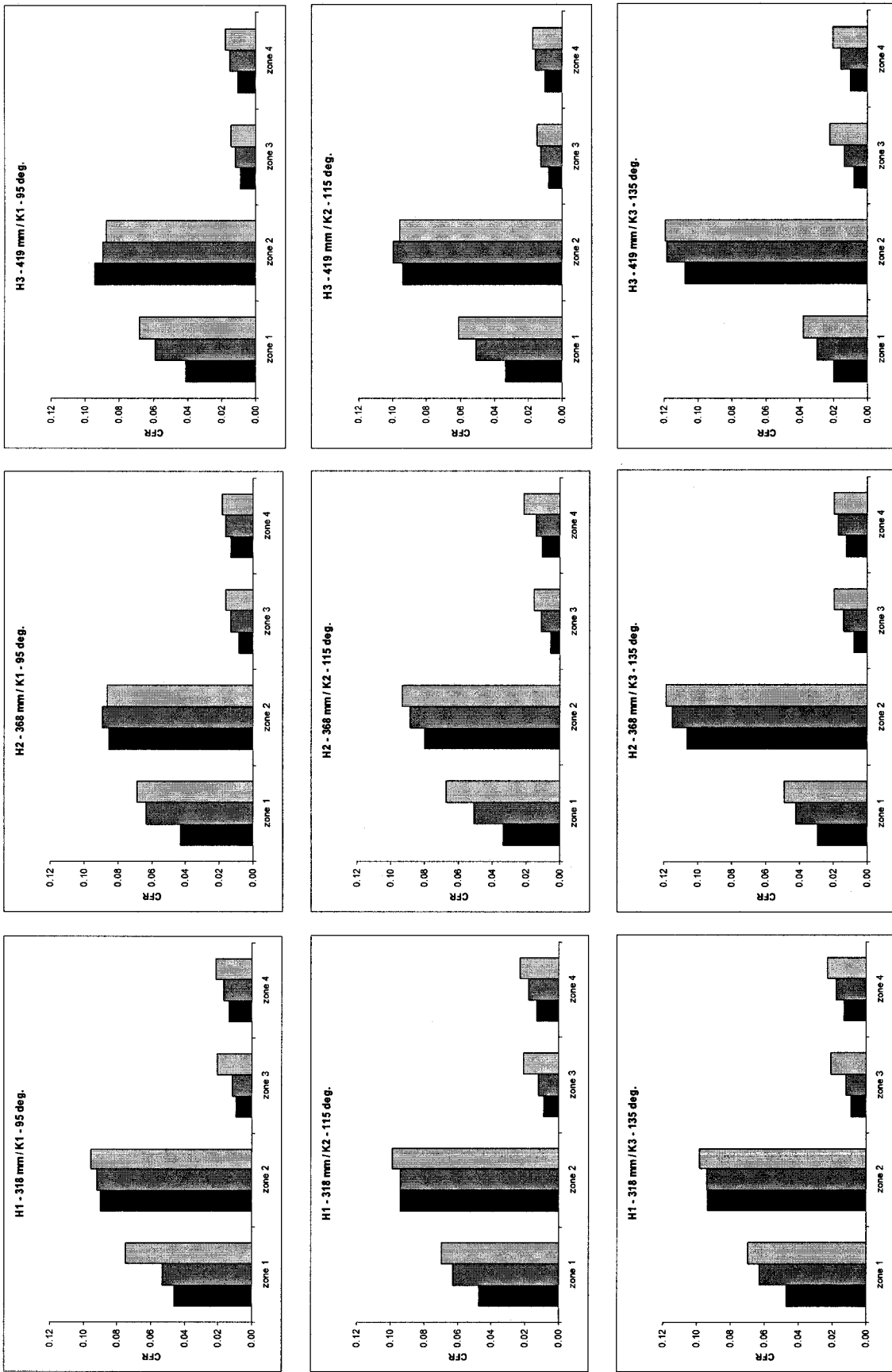


Figure 4.8: Effect of seat height, knee and backrest angle on the zonal CFR variations on the backrest of seat 1 (Backrest angle)

Figure 4.9 shows the variations in zonal CFR for the backrest of seat 2. The ratio of body weight carried by Zones 1 and 2 are observed to have smaller variations with respect to all the experimental factors, when compared to seat 1. Zones 1 and 2 each carry between 8 and approximately 11.5 % of the total body weight for all the height-knee-back combinations, while Zones 3 and 4 carry no more than approximately 2.5 % of the total body weight within their respective zones. Some small trends, however, are observed with respect to the backrest where higher values of backrest angle generally caused higher contact between the subject and all the backrest zones.

Figure 4.10 shows the variations in zonal CFR for seat 3. The backrest contour of this seat exhibits some curvature along the vertical axis within the lumbar area (Zone 1) and is considered flat in the thoracic area (Zone 2). Zone 1 carries between 9 and 12 % of the total body weight for this seat, while Zone 2 carries up to approximately 5 %. The contact force variations in Zone 1 are mildly affected by the knee angle where higher knee angles caused small increases in contact between the body and the backrest. Zone 2 also shows some variation with respect to the knee angle where higher knee angle were also observed to cause slight increases in the CFR.

In light of the dependence of the CFR on seat height, knee angle and the backrest angle, a multi factor within subject ANOVA was performed on the backrest zonal CFRs to verify the statistical significance of the experimental factors. The ANOVA was also used to identify any significant interactions between the experimental factors. Table 4.5 summarizes the results attained for the ANOVA for both the 99.9% and the 95% Confidence Intervals (CI). The results revealed that the factors S and H are very significant on the variations within Zone 1 ( $p < 0.001$ ), while Zone 2 is only



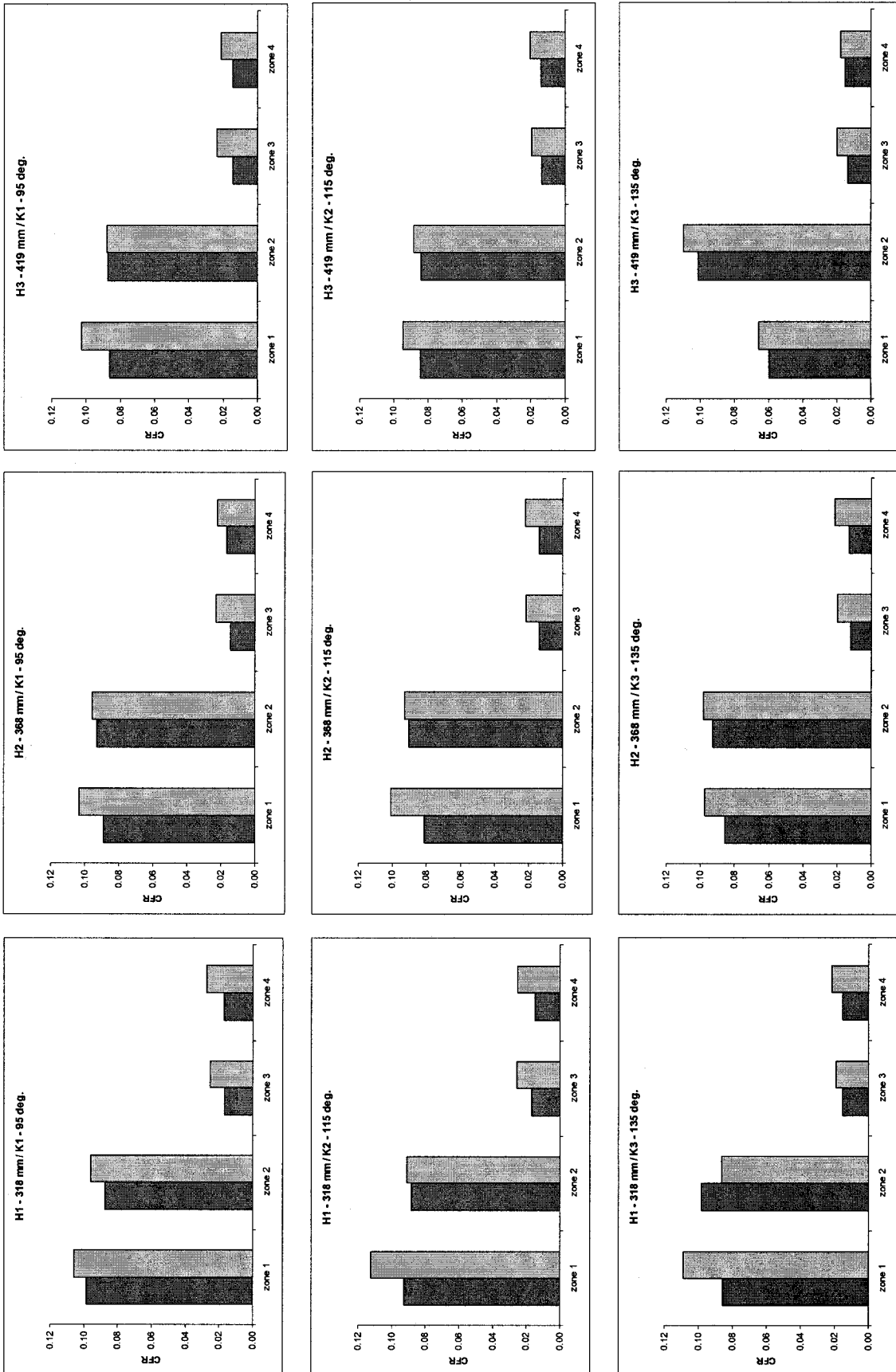


Figure 4.9: Effect of seat height, knee and backrest angle on the zonal CFR variations on the backrest of seat 2 (15° 25° Backrest angle)

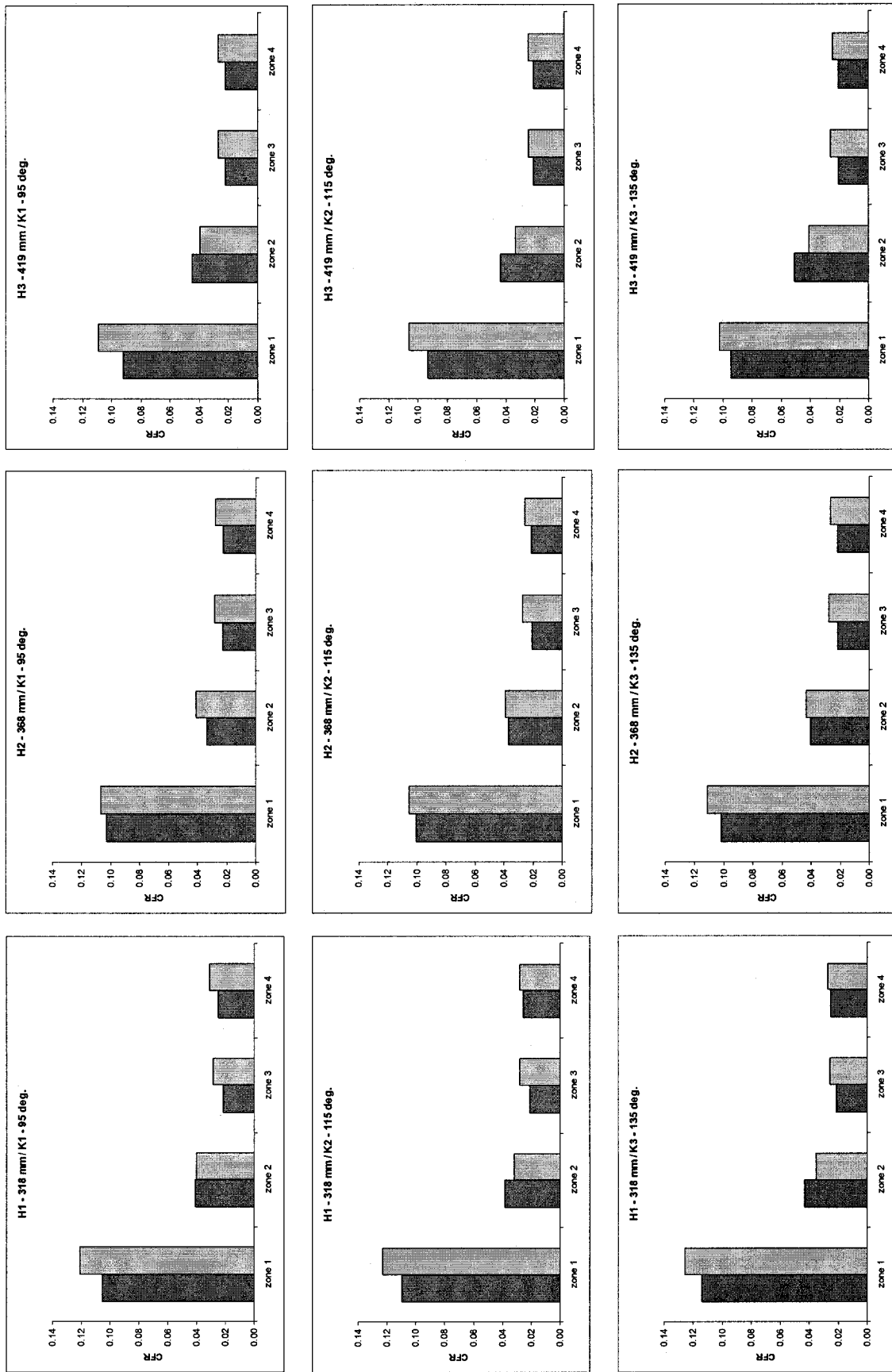


Figure 4.10: Effect of seat height, knee and backrest angle on the zonal CFR variations on the backrest of seat 3  
 ( 15° 25° Backrest angle

mildly affected by the factors S, K, and the two-way interaction between S and K, (S\*K) ( $p < 0.05$ ). The factors B and S\*K are also found to have a strong statistical significance ( $p < 0.001$ ) on the CFR variations of Zones 3 and 4. The results attained from the ANOVA further suggest that the cushion stiffness alone is not sufficient to compare the distribution of contact forces, but that the amount of contouring is also significant and should be considered in the analysis of the backrest contact force variations.

Table 4.5: Summary of ANOVA results for the backrest zonal CFR for 99.9% and 95% Confidence Intervals (CI)

ZONE	99.9 % CI ( $p < 0.001$ )	95 % CI ( $p < 0.05$ )
1	S, H	S, H, K, B, S*K, H*K
2	-	S, K, S*K
3	B, S*K	H, B, S*K, H*K, H*K*B
4	B, S*K	H, B, S*K, S*B,

A multiple regression was formulated similar to Equation (4.2) to investigate the contribution of seat height, knee angle and the backrest angle on the variations in the backrest CFR, where  $\beta_0$ ,  $\beta_1$ ,  $\beta_2$  and  $\beta_3$  are the regression coefficients relating H, K and B to the CFR and are summarized in Table 4.6. The results suggest that for all seats, the ratio of total body weight within Zone 1 is decreased for higher seat heights and higher knee angles, while higher backrest inclinations cause increased contact in the lumbar region. The weaker correlation coefficients,  $R^2$ , for Zone 2 on seats 2 and 3 further suggest that postural factors are not as significant as the cushion contouring and stiffness in causing contact variations. Higher seats also reduced the interface contact between the subjects and Zones 3 and 4, while higher backrest angular settings again increased loading within these zones.

Table 4.6: Regression and correlation coefficients for the backrest CFR.

ZONE	SEAT	R <sup>2</sup>	$\beta_0$	$\beta_1(10^{-5})$	$\beta_2(10^{-5})$	$\beta_3(10^{-3})$
1	1	0.880	0.124	-11.5	-44.1	1.240
	2	0.774	0.172	-19.7	-29.2	1.330
	3	0.904	0.147	-18.0	0	1.330
2	1	0.744	0.026	-2.1	60.9	0.237
	2	0.205	0.070	0	12.5	0.444
	3	0.169	0.028	1.7	8.3	-0.222
3	1	0.854	0.006	-1.6	4.5	0.500
	2	0.805	0.035	-8.2	-4.2	0.889
	3	0.819	0.013	-1.6	0	0.889
4	1	0.921	0.018	-2.7	1.4	0.427
	2	0.547	0.026	-4.9	-4.2	0.778
	3	0.605	0.038	-6.6	0	0.556

The relationship between the zonal CFRs have been shown to be a complex functions of the seated posture and the cushion characteristics, which are generally expressed in terms of the effective stiffness. It has also been found, based on the zonal analyses, that seats with cushion contouring along the vertical axis of the backrest generally exhibit lower contact forces in the lumbar region which is mainly attributed to the increased structural support of the spine and the reduced spinal deformation normally associated with poorly supported postures.

#### 4.3.2 Distribution of backrest contact pressure

The magnitudes of peak pressure in the various backrest zones are again found to be significantly affected by the shape of the cushion. The contours of the backrests for each seat have been shown in Figure 4.7. Both seats 2 and 3 have a significant amount of curvature along the vertical axis of the cushion, while seat 1 exhibits none. The wings of the three seats are also observed to be significantly different. Tables 4.7 to 4.9 summarize

the mean zonal peak pressure magnitudes as functions of the posture for seats 1, 2 and 3 respectively. The magnitudes of peak pressure for zone 1 are highest for seat 3 and are attributed to the significant amount of lumbar curvature located lower along the height of the backrest as shown in Figure 4.7 (c), when compared to those of seats 1 and 2. While the peak pressure magnitudes are significantly different for each seat within Zone 1, they show little variation with respect to the postural factors. Zone 2 however, shows higher variations with respect to backrest angle, where higher backrest inclinations generate higher peak pressures in the thoracic zone. The values of peak pressure within zone 2 are opposite to the trends found for Zone 1, which suggests that the thoracic zone supports significantly larger contact as a result of the higher backrest angles. Seat 3 shows the lowest magnitudes within Zone 2, while seat 2 was observed to have the highest. Seat 1 has the least amount of backrest curvature and exhibits almost equal magnitudes of peak pressure for both zones 1 and 2 with more variations attributed to posture, which further suggests that seats with less backrest contouring are more prone to pressure variations due to anthropometric and posture related factors, when compared to those with contouring. Both seats 2 and 3 exhibit similar peak contact pressures within Zones 3 and 4, which is mainly attributed to the backrest contouring that provides a greater amount of structural support to the spine, whereas seat 1, which has no curvature, exhibits asymmetric pressure loading of Zones 3 and 4. The lack of appropriate backrest support, as in the case of seat 1, also increases the muscle activity required to maintain an insufficiently supported posture, which may also lead to rapid fatigue of the back muscles and an overall higher sensation of discomfort in the seat.

Table 4.7: Zonal peak pressure variations for seat 1

Seat Height (mm)	Knee Angle (deg.)	Back Angle (deg.)	Zonal Peak Pressures (N/cm <sup>2</sup> )							
			ZONE 1		ZONE 2		ZONE 3		ZONE 4	
			Mean	SD	Mean	SD	Mean	SD	Mean	SD
318	95	5	0.45	0.19	0.42	0.12	0.30	0.27	0.42	0.26
		15	0.46	0.21	0.47	0.13	0.32	0.18	0.49	0.31
		25	0.47	0.20	0.47	0.14	0.39	0.14	0.59	0.39
	115	5	0.44	0.17	0.46	0.12	0.31	0.24	0.45	0.31
		15	0.45	0.26	0.48	0.17	0.27	0.21	0.51	0.29
		25	0.45	0.18	0.52	0.15	0.44	0.14	0.60	0.32
	135	5	0.43	0.13	0.50	0.16	0.30	0.26	0.40	0.24
		15	0.48	0.15	0.52	0.17	0.34	0.19	0.49	0.27
		25	0.46	0.20	0.52	0.21	0.45	0.11	0.61	0.34
368	95	5	0.44	0.18	0.43	0.12	0.28	0.19	0.48	0.33
		15	0.45	0.23	0.45	0.15	0.37	0.15	0.49	0.31
		25	0.45	0.17	0.47	0.18	0.38	0.14	0.56	0.41
	115	5	0.44	0.18	0.44	0.17	0.26	0.21	0.40	0.27
		15	0.42	0.16	0.44	0.15	0.35	0.17	0.51	0.31
		25	0.47	0.16	0.48	0.20	0.37	0.18	0.60	0.42
	135	5	0.36	0.14	0.49	0.15	0.29	0.22	0.40	0.22
		15	0.36	0.12	0.48	0.15	0.34	0.16	0.49	0.28
		25	0.43	0.15	0.52	0.24	0.43	0.15	0.59	0.34
419	95	5	0.38	0.16	0.45	0.15	0.28	0.24	0.28	0.25
		15	0.39	0.17	0.49	0.15	0.34	0.17	0.44	0.25
		25	0.49	0.16	0.45	0.21	0.38	0.17	0.52	0.37
	115	5	0.36	0.10	0.46	0.16	0.27	0.20	0.30	0.27
		15	0.37	0.12	0.51	0.14	0.32	0.19	0.42	0.25
		25	0.47	0.15	0.49	0.23	0.38	0.17	0.57	0.39
	135	5	0.26	0.15	0.52	0.12	0.27	0.20	0.30	0.25
		15	0.31	0.09	0.51	0.19	0.34	0.14	0.42	0.21
		25	0.37	0.13	0.55	0.21	0.42	0.15	0.49	0.24

Table 4.8: Zonal peak pressure variations for seat 2

Seat Height (mm)	Knee Angle (deg.)	Back Angle (deg.)	Zonal Peak Pressures (N/cm <sup>2</sup> )							
			ZONE 1		ZONE 2		ZONE 3		ZONE 4	
			Mean	SD	Mean	SD	Mean	SD	Mean	SD
318	95	15	0.28	0.07	0.52	0.19	0.28	0.17	0.31	0.14
	95	25	0.41	0.10	0.54	0.18	0.41	0.22	0.40	0.15
	115	15	0.30	0.09	0.53	0.11	0.30	0.19	0.31	0.11
	115	25	0.41	0.11	0.53	0.15	0.41	0.23	0.31	0.12
	135	15	0.26	0.08	0.59	0.16	0.26	0.17	0.31	0.13
368	135	25	0.34	0.09	0.52	0.20	0.34	0.18	0.40	0.16
	95	15	0.26	0.09	0.52	0.15	0.26	0.17	0.33	0.15
	95	25	0.37	0.09	0.52	0.19	0.37	0.20	0.34	0.12
	115	15	0.28	0.06	0.52	0.17	0.28	0.16	0.30	0.15
	115	25	0.36	0.08	0.50	0.12	0.36	0.21	0.38	0.14
419	135	15	0.24	0.06	0.53	0.13	0.24	0.17	0.28	0.15
	135	25	0.30	0.08	0.55	0.20	0.30	0.16	0.37	0.15
	95	15	0.30	0.12	0.53	0.17	0.30	0.17	0.27	0.11
	95	25	0.38	0.12	0.56	0.18	0.38	0.23	0.36	0.13
	115	15	0.26	0.10	0.54	0.15	0.26	0.18	0.29	0.10
	115	25	0.35	0.08	0.54	0.14	0.35	0.18	0.33	0.12
419	135	15	0.26	0.11	0.52	0.15	0.26	0.19	0.30	0.12
	135	25	0.33	0.08	0.59	0.18	0.33	0.18	0.35	0.11

Table 4.9: Zonal peak pressure variations for seat 3

Seat Height (mm)	Knee Angle (deg.)	Back Angle (deg.)	Zonal Peak Pressures (N/cm <sup>2</sup> )							
			Zone 1		Zone 2		Zone 3		Zone 4	
			Mean	SD	Mean	SD	Mean	SD	Mean	SD
318	95	15	0.50	0.10	0.32	0.13	0.39	0.22	0.44	0.22
	95	25	0.52	0.12	0.31	0.10	0.45	0.26	0.47	0.23
	115	15	0.51	0.09	0.32	0.17	0.36	0.23	0.44	0.21
	115	25	0.52	0.11	0.29	0.12	0.44	0.28	0.48	0.22
	135	15	0.50	0.14	0.35	0.13	0.37	0.21	0.42	0.21
368	95	15	0.52	0.11	0.27	0.09	0.37	0.22	0.48	0.22
	95	25	0.49	0.10	0.33	0.12	0.44	0.25	0.46	0.18
	115	15	0.53	0.08	0.31	0.10	0.36	0.23	0.46	0.23
	115	25	0.49	0.10	0.32	0.13	0.43	0.28	0.45	0.18
	135	15	0.50	0.10	0.32	0.12	0.35	0.26	0.45	0.20
419	95	15	0.46	0.11	0.35	0.15	0.35	0.22	0.43	0.18
	95	25	0.50	0.10	0.34	0.16	0.41	0.22	0.46	0.20
	115	15	0.48	0.10	0.34	0.18	0.37	0.22	0.41	0.20
	115	25	0.52	0.10	0.29	0.13	0.41	0.26	0.43	0.17
	135	15	0.49	0.10	0.38	0.19	0.36	0.21	0.37	0.16
	135	25	0.45	0.08	0.35	0.11	0.43	0.27	0.43	0.15

#### 4.4 Distribution of Total Body Weight

The distribution of the body weight at the human-seat interface has been found to be a complex function of subject anthropometry, seated posture and cushion characteristics, which include the contour shapes and static stiffness of the cushions. The characterization of the cushions has been performed following two different methods outlined by the SAE J1051 [50] and JASO B407 [51] standards respectively. The results have been found to vary considerably for both methods, and for the purposes of this study, the point of application was taken as the aggregate center of pressure for each seat for both the seat-pan and the backrest. The loads and deflections observed during the characterization of the cushions were found to be excessive, when compared to the deflections observed during the BPD acquisition. The subsequent pressure analyses of chapter 3 has been found to correlate well with the recent studies published regarding the total amount of body weight supported by both the seat-pan and the backrest cushions [31,53,60]. The cushion stiffness was derived corresponding to 76% and 24% of the total

body weight for the seat-pans and backrests, respectively. The point of application for the characterization of the seat-pan was inside the ischial zone (zone 1) and in the lumbar zone (Zone 1) for the backrest. The zonal analysis of chapter 4 has further shown that the total body weight carried by these same zones only reaches a maximum of 52% and 14% on the seat-pan and backrest, respectively. Therefore, application of forces up to 76% and 24 % of the total body weight on the seat-pan and backrest is inaccurate and provides an over-estimation of the stiffness of the cushion in those specific zones.

Figure 4.11 shows the overall mean distributed contact force ratios between the seat-pan and the backrest cushions for each of the test seats. The large standard deviations for each seat accounts for the anthropometric and postural variations. The values strongly suggest that a more accurate characterization of the cushion properties can be performed by considering the results of the zonal analyses as limits regarding the loads applied to the various areas of the cushions for characterization of the static stiffness. As a result, the characterization of the cushions could inevitably provide more accurate information regarding the true foam properties instead of the combined foam and seat sub-frame. The characteristics of the seat properties in different areas, similar to those derived in [60], could also provide more insight into the localized stiffness requirements for the alleviation of high contact pressures.



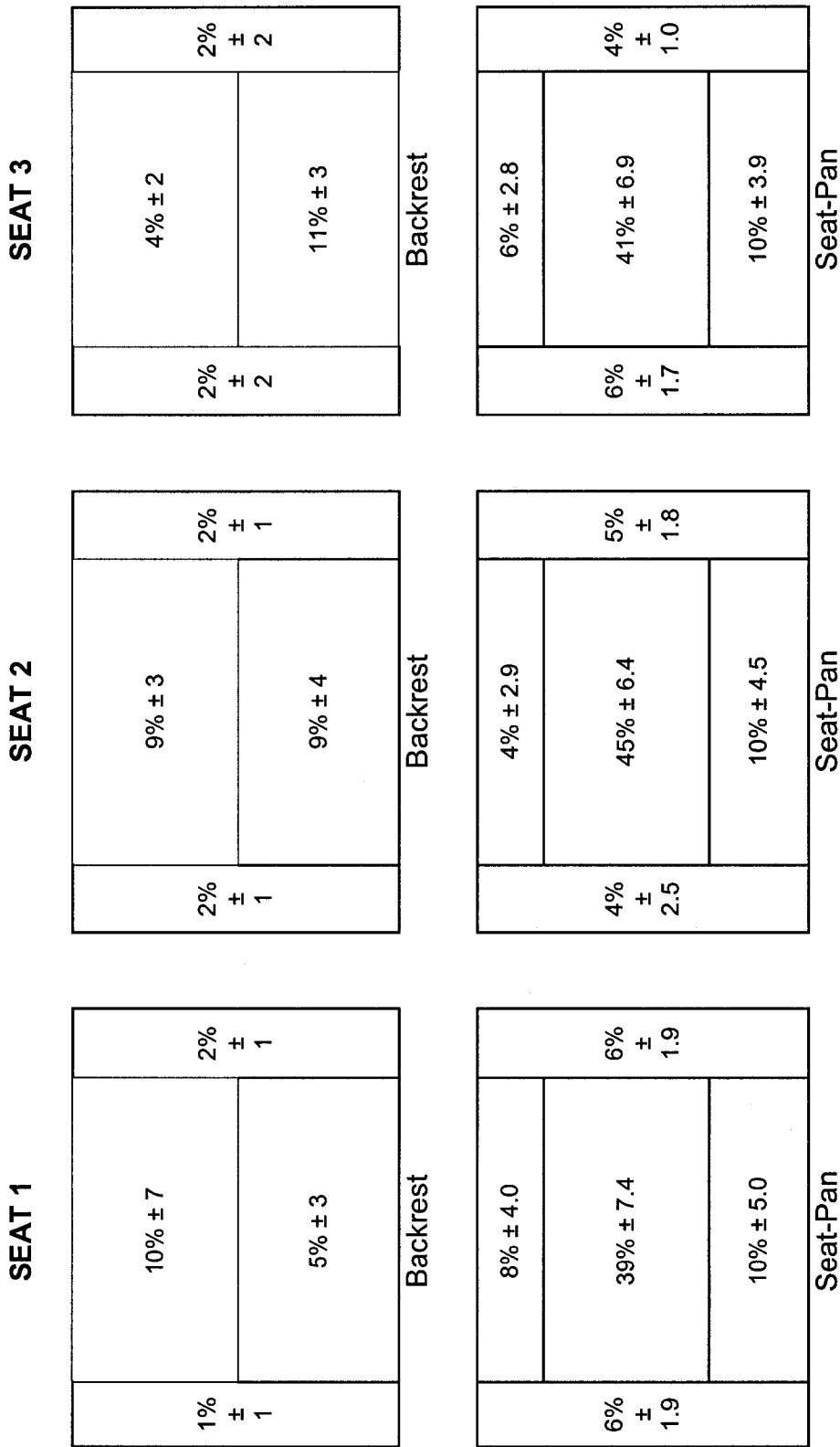


Figure 4.1.1: Percentage of total body weight on the seat-pan and backrest of seats 1, 2 and 3 (Mean ± 1 standard deviation)

## 4.5 Summary

The pressure distribution at the human-seat interface of three different automotive seats was acquired with a flexible sensor matrix under static conditions. The seat-pan and backrest cushions were divided into anatomical zones which are known to be sensitive to pressure loading. The contact forces and peak pressures within each zone were analyzed as a function of anthropometry and posture. The study revealed that the load supported by the various anatomical zones are a complex function of anthropometry, posture and cushion properties. The backrest angle was found to have the most significant effect on the variations of contact force for both the seat-pan and backrest. Higher levels of backrest inclination lead to greater reductions in contact force for all the seat-pan zones except for the sacro-iliac zone (Zone 2), which tended to support higher loads for higher backrest angles. The knee angle was found to have a similar effect on the weight distribution of zones 1 and 2 and also generated significantly higher levels of loading along the outer thighs (Zones 4 and 5) as well as Zone 3 beneath the thighs above the knees. The seat height was only found to have a positive influence on zone 3 where higher seat heights generated more contact within that zone but had little effect on the variations within the other zones. With respect to the backrest measurements, the trends were opposite. Higher values of backrest angle generated higher values of contact over the entire surface of the back. Both seat height and knee angle had very little effect on the overall backrest force variations but higher seats and knee angles did contribute to reducing the contact in the lateral zones of the backrest.

The peak pressure have also been found to vary with respect to anthropometry and posture, but the most significant factor affecting the peak pressure was the cushion

geometry and stiffness, which suggests that anthropometric measures such as weight and BMI alone, do not necessarily provide an accurate indication regarding the pressure loading. Seats with high lateral wings generated peak pressure magnitudes similar to, and in some cases, greater than those attained beneath the IT and lumbar areas.

The results of the zonal analyses have shown that while contact forces with weight and posture, the mean total load carried by the various anatomical areas was found to be approximately 45 % for the IT, 10 % for the thighs beneath the knees, 9% on the sacrum and 5% for each lateral zone. On the backrest, much smaller magnitudes were observed, where the lumbar area carries up to approximately 14% and the thoracic zone carried up to 10%, while each lateral zone carried no more than 2% of the total body weight.

## CHAPTER 5

### CONCLUSIONS AND RECOMMENDATIONS FOR FUTURE WORK

#### 5.1 HIGHLIGHTS OF THE STUDY

The comfort performance of a seat is a complex function of multiple seat design factors such as: cushion geometry and contouring, stiffness and damping properties, sitting posture and individual preferences. The assessments of comfort performance of automotive seats are mostly performed through subjective evaluations. In this study, the body-seat interface pressure is explored as an objective measure of the seating comfort. A comfort study of automotive seats was carried out through structured experiments involving human subjects and different automotive seats in a static environment. The study involved consideration of resiliency of the PUF materials of the seat-pan and backrest; sitting posture as realized by varying seat height, knee and backrest angle; three different seats with significantly different contouring of the pan and backrest; and eight different subjects. The total body seat interface contact force at the pan and backrest, and pressure distributions in different localized zones are investigated to study the pressure loading influenced by the different design and postural factors.

The static stiffness of the test seats were investigated using two different standards; the two methods resulted in significantly different results suggesting that the manner in which the load is applied has a significant effect on the characterization of the cushion. Discrete loading of the PUF over timed intervals allows the cushion material to undergo stress relaxation, which reduces the cushion force for a given deflection thereby underestimating the static stiffness of the cushion. Stiffness derived from continuous loading functions, on the other hand, is more representative of the instantaneous stiffness

and is more suitable for the characterization of the dynamic properties of the PUF. The foam deflections observed during the characterization of the cushions were found to be excessive when compared to those observed during the BDP measurements with human occupants. The contact force analysis further revealed that the ratios of the total body weight in specific areas of the seat reach maximum values irrespective of the occupant-posture combinations.

The pressure distribution at the human-seat interface of the seat-pan is investigated under varying postural conditions for a range of subjects. The variations in the pressure distribution have been found to be significantly affected by the subject weight, the seated posture and the cushion characteristics. The data are analyzed to determine the contact force and localized pressure peaks at different segments of the body that may provide measures of comfort performance and design guidance with respect to contouring, PUF material and seat geometry. Although body size and mass have a definite effect on the interactions at the seat-pan of automotive seats in terms of contact force and contact pressures, the changes in the seated posture and the cushion characteristics cause the most significant variations in the measured responses.

Similar to the analysis of the seat-pan pressure distributions, the measured responses were also analyzed for the backrests of automotive seats. Again, body weight and size generated significant differences in the measured responses, but it is the characteristics of the backrest, namely, the stiffness and the cushion contouring that had the most significant effect on the variations of force and pressure.

## 5.2 CONCLUSIONS

Based on the analysis of the pressure distribution at the human-seat interface, the following conclusions regarding the assessment of comfort performance of automotive seats are drawn:

- The cushion stiffness is highly dependent upon the pre-load and the cushion construction, which affects the distribution of body pressure at the human-seat interface.
- The cushion characterization performed in this research was found to cause excessive deflections of the cushion material and in some cases the application of the recommended loads in SAE and JASO Standards caused deflections in the seat substructure.
- It is concluded, on this basis, that more an accurate characterization of the cushion properties may be attained by significantly reducing the magnitudes of force applied to the cushions and by deriving the force-deflection characteristics in multiple areas of the cushion based on the limiting force values derived from the zonal analysis.
- Stiffer seat-pans caused less deformation of the cushion leading to decreased contact area, but significantly higher contact forces and peak interface pressures. Softer seats, on the other hand, provide higher amounts of pressure redistribution, leading to higher contact areas and mean pressures but beneficially lower peak pressures.
- Variations in the knee angle and the backrest angle were found to be most significant in changing the seat-pan contact force. Higher knee angles caused higher contact at the seat-pan, while higher backrest angles decreased the seat-pan contact force.
- Seat height was found to have a smaller effect compared with those of the knee and the backrest angles but generally, higher seats caused higher seat-pan contact forces.
- The overall ratio of body weight supported by the seat-pan is also strongly influenced by the seat height, the knee angle. Higher knee angles and higher seats generally decreased the body weight supported by the seat-pan.
- The ratio of body weight supported by the seat-pan correlates well with the reported literature, and varies between 60 and 79% of the total body weight with significant standard deviations attributed to variations in anthropometry, posture and cushion characteristics.
- Heavier subjects have been found to generate higher interface contact forces and areas but generally benefited from lower values of peak pressure owing to a higher degree of soft tissue deformation. Conversely, lighter and leaner subjects were

observed to generate higher peak contact pressures surrounding the Ischial Tuberosities and lumbar zones.

- The location of the peak contact pressures of the seat-pan were invariably found to be in the area of the ischial tuberosities, with some exceptions occurring on narrower seat-pans with high lateral wings where peak pressure magnitudes exceeded the peak Ischial pressure for heavier subjects in extended leg postures.
- Reductions in peak Ischial pressures were achieved by increasing the knee and backrest angles, which lead to a redistribution of the total body weight over a larger area on the seat-pan and transferred portions of the body weight onto the backrest.
- The measures of seat-pan contact area and mean pressure were found to be significantly affected by all the experimental factors, but can generally be increased by providing softer cushions and more contouring.
- The zonal analysis of the seat-pan indicates that higher seats and knee angles transfer the seated body weight from the IT and the sacrum onto the thighs and the cushions with significantly less contouring produce lower peak interface pressures in the thigh and lateral regions.
- Lower knee angles generate increased contact at the sacrum for lower seats
- Seat height and backrest angle were observed to be the most significant factors causing differences in the backrest contact forces. Higher seats decreased the contact at the backrest while higher backrest angles significantly increased the loading at the backrest interface.
- The ratio of body weight supported by the backrest was also found to be strongly affected by seat height and backrest, and is observed to be between 11 and 27 % with large standard deviations attributed to anthropometric, postural and cushion variations.
- The peak and mean contact pressures at the backrest were found to be only significantly affected by the subject weight and the backrest angle. The contact areas were further affected by the knee angle where higher knee angles decreased the contact in the lumbar region.
- The regression analysis of the peak and mean pressure indicate that body weight has little to no significance when compared to the backrest angle. The poor correlation coefficients for peak and mean pressure further indicate that the variations are strongly affected by the contouring.
- Seats with a significant amount of backrest contouring along the vertical axis provide more structural support to the spine reducing the occurrence of excessive peak pressures on the backrest.

- Seats with a higher degree of contouring along the vertical axis of the backrest were found to provide more support for the body, thereby reducing the occurrence of localized high pressures.

The above conclusions with respect to the analysis of body pressure distribution at the human-seat interface can be interpreted to derive fundamental guidelines for the design of automotive seats with enhanced comfort. Based on the results of this research thesis, it is suggested that increased comfort can be attained by eliminating or reducing the occurrence of high localized pressures and providing the seated body with adequate structural support. Therefore the following design guidelines are proposed:

- As the force-deflection characteristics of PUF have been found to be highly non-linear, selecting a foam material that is soft enough to deflect under lighter subjects but stiff enough to support heavier subjects without bottoming-out is of primary importance.
- Owing to the large variations in occupant anthropometry among automobile users, wider seat-pans with lower and softer lateral wings would be desirable to accommodate smaller and larger occupants alike without creating hard-points or points of localized high pressure along the lower extremities.
- If the height of the seat presents a design constraint within the vehicle interior, then the alleviation of high pressure surrounding the tuberosities can be achieved by allowing sufficient leg room so that the occupant may increase/decrease the knee angle accordingly. This is implicitly related to the adjustability of the seat in the longitudinal direction with respect to the location of the pedals.
- Similar reductions in the pressure loading around the tuberosities can also be achieved by increasing the backrest angle for the same height-knee combinations. Increasing the backrest angle, however, increases the distance between the upper body and the steering wheel highlighting the need for adjustable steering wheels.
- Owing to the large variations in upper body anthropometry among automobile users, wider backrests with smaller wings reduces the occurrence of high pressure.
- Providing adjustable lumbar support in the vertical direction provides added flexibility for accommodating occupants of varying stature, and also provides good structural support to the spine which reduces spinal deformation and pelvic rotation thereby decreasing muscle activity required to maintain unstable posture.



### 5.3 RECOMMENDATIONS FOR FUTURE WORK

The assessment of the comfort performance of automotive seats has been investigated by the objectives measures in terms of body pressure distribution; the following recommendations for future work may provide more advanced and reliable conclusions and design guidelines for automotive seats with enhanced comfort.

- A more in depth study into the factors affecting the characterization of the seat mechanical properties. The behavior of the PUF used in the design of automotive seats exhibits highly non-linear force-deflection characteristics, which depend on pre-load, cushion thickness and foam chemistry. Important advances in the accuracy of the cushion characterization can be accomplished and would thus provide a more accurate representation of the actual PUF behavior under loading.
- The current characterization methods use flat, solid, circular indentors to impose a force on the cushion material and do not account for the soft tissue deformations occurring at the human-seat interface. Developing force indentors which replicate the actual shape of the human body may be validated with the pressure distributions attained in this study. Selecting indenter materials that could account for the soft tissue deformation would further enhance the accuracy of the cushion characterization.
- A more accurate seat cushion model, which incorporates the variations caused by the different postures, can be developed.
- Comprehensive criteria need to be developed to define a measure that would quantify the seat cushion contour so that seat features on different seats may be compared to one another, this would yield more substantial conclusions regarding the influence of the cushion on the pressure variations and thus the comfort performance of the seat.
- While the analysis of the pressure distribution at the human-seat interface in this study has provided insightful information regarding its behavior as a function of posture, comfort studies using a significantly higher number of subjects representing the complete range of intended occupants is recommended. This may reduce the standard deviations attributed to anthropometry and posture.
- Further study the interactions at the human-seat interface under simulated driving conditions to investigate the effects of a realistic driving environment.

## REFERENCES

1. Osborne, D.J., Ergonomics at Work, John Wiley and Sons, 1982, 165-179
2. Kumar, A., Bush, N. J., Thakurta, K., "Characterization of Occupant Comfort in Automotive Seats" IBEC' 94
3. Griffin, M.J., 1990 Handbook of Human Vibrations, Academic Press, London.
4. Dempsey, C.A., Chapter 9: Posture and Sitting, pp. 165-180, McGraw-Hill, New York, 1963
5. McCormick, E.J., Sanders, M.S., Human Factors in Engineering and Design, McGraw-Hill, USA, 1982
6. Woodson, W.E., Conover, D.W., Human Engineering Guide, University of California Press, Berkeley, 1966
7. Domey, R.G., Mcfarland, R.A., Chapter 14: The Operator and Vehicle Design, pp.247 - 267
8. Judic, J-M., Cooper J.A., Truchot, P., Van Effenterre, P., Duchamp, R., "More Objectives Tools for the Integration of Postural Comfort in Automotive Seat Design", SAE Paper No. 930113
9. Weichenrieder, A., Haldenwanger, H. G., "The Best Function for the Seat of a Passenger Car", SAE Paper No. 850484
10. Sember III, J.A., the Biomechanical Relationship of Seat Design to the Human Anatomy. *Hard Facts about Soft Machines: The Ergonomics of Seating*. Taylor and Francis: London, 1994, 221-28
11. Osborne, D.J., "Vibration and Passenger Comfort: Can Data from Subjects be Used to Predict Passenger Comfort?" Applied Ergonomics, 9 (1978a), 155-161
12. Society of Automotive Engineers, 1987. Devices for Use in Defining and Measuring Vehicle Seating Accommodation. SAE J 826. May 1987.
13. Society of Automotive Engineers, 1990. Driver Selected Seat Position. SAE J1517. March 1990.
14. Society of Automotive Engineers, 1990. Driver Hand Control Reach (A). SAE J1517. June 1988.
15. Society of Automotive Engineers, 1990. Motor Vehicle Driver's Eye Range. SAE J1517. October 1985.

16. Gibson, L.J., Ashby, M.F. Cellular Solid Structure and Properties, Pergamon Press, New York, 1988.
17. Apatsidis, D.P., Solomonidis, S.E., Micheal, S.M., "Pressure Distribution at the Seating Interface of Custom Molded Wheelchair Seats: Effects of Various Materials". Archives of Physical Medicine and Rehabilitation Vol. 83 Aug. 2002
18. Ebe, K., " Effect of Thickness on Static and Dynamic Characteristics of Polyurethane Foam"
19. Gurram, R., Veritz, A.M., "The Role of Automotive Seat Cushion Deflection in Improving Ride Comfort" SAE Paper No. 970596, Detroit, Michigan, 1997
20. Hostens, I. Papaioannou, G., Spaepen, A., Ramon, H., "Buttock Distribution Tests on Seats of Mobile Agricultural Machinery". Applied Ergonomics 32 (2001) 347-355
21. Blair, G.R., Milivojevich, A., Van Heumen, J.D., "Automotive Seating Comfort: Investigating the Polyurethane Foam Contribution - Phase I" SAE Paper No. 980656, Detroit, Michigan, 1997
22. Webster's Ninth New collegiate Dictionary, 1988 Merriam-Webster
23. Osborne, D.J., Clarke, M. J., (1973) the development of questionnaire surveys for the investigation of passenger comfort. *Ergonomics*, 16, 855 – 869
24. Griffin, M. J., (1995) the ergonomics of vehicle comfort. *Proceedings of the 3<sup>rd</sup> International Conference on Vehicle Comfort and Ergonomics*. March 29-31, Bologna, Italy. Paper No. 95A1026, 213-221
25. Reynolds, H. M., (1993) Automotive Seat Design for Sitting Comfort. *Automotive Ergonomics* (Edited by Peacock, B and Karwoski, W), 99-116, London: Taylor and Francis.
26. Branton, P., (1969) Behavior, body mechanics and discomfort. *Ergonomics*, 12, 316-327.
27. Bower-Carnahan, R., Carnahan, T., Tallis-Crump, R., Crump, R., Faulkner, D., Martin, D., Sanford, L., Walters, J., "User Perspectives on Seat Design", SAE Paper No. 952679
28. Gross, C.M., Goonetilleke, R.S., Menon, K.K., Banaag, J.C.N., Nair, C.M., The Biomechanical assessment and prediction of seat comfort. *Hard Facts about Soft Machines: The Ergonomics of Seating*. Taylor and Francis: London, 1994, 231-53

29. Thakurta, K., Koester, D, Bush, N., Bachia, S, “Evaluating Short and Long Term Seating Comfort”. SAE Paper No. 950144
30. Demontis, S., Giacoletto, M., “Prediction of Car Seat Comfort from Human-Seat Interface Pressure Distribution”. SAE Paper No. 2002-01-0781, SAE 2002 World Congress, Detroit, Michigan, March 4 – 7.
31. Wang, W., Rakheja, S., Boileau, P.E., “Effects of Sitting Posture on Biodynamic Response of seated occupants under vertical vibration”, *International Journal of Industrial Ergonomics*, **34**(4), Oct. 2004, 289-306
32. Bioleau, P.E., Wu, X., Rakheja, S., “Definition of a Range of Idealized Values to Characterize Seated Body Biodynamic Response Under Vertical Vibration”, *Journal of Sound and Vibration*, **215**(4), Aug. 1998, 841-862
33. Brienza, D.M., Karg, P.E., Jo Goyer, M., Kelsey, S., Trefler, E., “The Relationship Between Pressure Ulcer Incidence and Buttock-Seat Cushion Interface Pressure in At-Risk Elderly Wheelchair Users”, *Arch Phys Med Rehabil* Vol. 82, April 2001
34. Kernozek, T.W., Wilder, P.A., Amundson, A., Hummer, J., “The Effects of Body Mass Index on Peak Seat-Interface Pressure of Institutionalized Elders”, *Arch Phys Med Rehabil* Vol. 83, June 2002
35. Frusti, M.T., Hoffman, D.J., “Quantifying the Comfortable Seat Developing Measureable Parameters Relating to Subjective Comfort” IBEC 1991
36. Oudenhuijzen, A., Tan, K., Morsch, F., “The Relationship between Seat Comfort and Pressure Distribution”. SAE Paper No. 2003-01-2213
37. Kamijo, K., Tsujimura, H., Obara, H., Katsumata, M., “Evaluation of Seating Comfort”. SAE Paper No. 820761
38. Gyi, D. E., Porter, J.M., “Interface Pressure and the Prediction of Car Seat Discomfort”. *Applied Ergonomics* **30**, 99 - 107
39. Swearingen, J.J., Wheelwright, C.D., Garner, J.D., 1962. An analysis of the sitting areas and pressures of man (Report 62-1). Oklahoma City, OK: Civil AeroMedical Research Institute.
40. Lindan, O., Greenway, R.W., Piazza, J.M., (1965). Pressure distribution on the surface of the human body: I. Evaluation in lying and sitting positions using a bed of spring and nails. *Arch Phys Med Rehabil*, May. 378 – 385.

41. Gyi, D. E., Porter, J.M., Robertson, N.K.B., (1997) "Seat Pressure Measurement Technologies: Considerations for Their Evaluation", *Applied Ergonomics* 27(2), 81-91
42. Ferguson-Pell, M.W., Design Criteria for the Measurement of Pressure at Body/Support Interface. *Eng. Med.* 1980; 9(4): 209 – 214
43. Ashruf, C.M.A., Thin Flexible Pressure Sensors. *Sensor Review*, 2002, Vol.22 No. 4 pp.322-27
44. Ferguson-Pell, M.W., Hagsiawa, S., Bain, D., Evaluation of a Sensor for Low Interface Pressure Applications. *Medical Engineering and Physics*, 2000, 22, 657 - 663
45. Grant, L.J., Interface Pressure Measurement between a Patient and a Support Surface. *CARE Br J Rehab Tissue Viability*. 1985; 1 (1): 7 – 9
46. Reed, M.P., Saito, M., Kakishima, Y., Lee, N.S., Schneider, L.W., "An Investigation of Driver Discomfort and related seat design factors in extended-duration driving". SAE Conference 1996, SAE Paper No. 960478.
47. Park, S.J., Kim, C.B., "The Evaluation of Seating Comfort by the Objective Measures". SAE Conference 1997, SAE Paper No. 970595.
48. Park, S.J., Lee, Y.S., Nahm, Y.E., Lee, J.W., Kim, J.S., "Seating physical Characteristics and Subjective Comfort". SAE Conference, SAE Paper No. 980653
49. Milivojevich, A., Stanciu, R., Russ, A., Blair, G.R., Van Heumen, J.D., "Investigating Psychometric and body Pressure Distribution Responses to Automotive Seating Comfort". SAE Conference 2000, SAE Paper No. 2000-01-0626
50. Wu, X, "Study of Driver-Seat Interactions and Enhancement of Vehicular Ride Vibration Environment", *Ph.D. Thesis, Concordia University*, Montreal, 1998.
51. Tchermnychouk, V. "Objective assessment of Static and Dynamic Seats Under Vehicular Vibrations", *Master's Thesis, Concordia University*, Montreal, 1999
52. "Static and Dynamic Characterization of automotive Seats", CONCAVE Research Center, Concordia University, January 1997
53. Society of Automotive Engineers, 1988. Force-Deflection Measurements of Cushioned components of Seats for Off-Road Work Machines. SAE J1051. December 1988. Society of Automotive Engineers

54. Japanese Automobile Standards Organization, 1982. Test Code of Seating Comfort for Automobile Seats. JASO B407-82. The Society of Automotive Engineers of Japan, Inc.
55. Rakheja, S., Stiharu, I., Boileau, P.-É., “Seated Occupant Apparent Mass Characteristics under Automotive Postures and Vertical Vibration”, *Journal of Sound and Vibration* (2002) **253** (1), 57 – 75.
56. Hughes, E.C., Shen, W., Vézitz, A., “The Effects of Regional Compliance and Instantaneous stiffness on the Seat Back Comfort”. SAE Conference 1998, SAE Paper No. 980658.
57. Rao, S. S., *Mechanical Vibrations*, 3<sup>rd</sup> Ed., Addison-Wesley, Reading MA, 1993.
58. Neter, J., Wasserman, W., *Applied Linear Statistical Models*, Richard D. Irwin, Inc. Homewood IL, 1974.
59. Tabachnick, B. G., Fidell, L.S., *Using Multivariate Statistics*, 4<sup>th</sup> Ed., Allyn and Bacon, Needham Heights MA, 2001.
60. Neter, J., Kutner, M.H., Nachtsheim, C.J., Wasserman, W., *Applied Linear Statistical Models*, 4<sup>th</sup> Ed., McGraw Hill, 1996.
61. Hawkins, C.A., Weber, J.E., *Statistical Analysis; Applications to Business and Economics*, Harper & Row, New York, 1980.
62. Verver, M., “Numerical Tools for the Analysis of Automotive Seating”. *Ph.D. Thesis, Technical University of Eindhoven*, Eindhoven, 2004.

## **APPENDIX - A**

### **SEAT-PAN DATA PLOTS**

## **APPENDIX - A1**

### **SEAT-PAN CONTACT FORCE VARIATIONS**



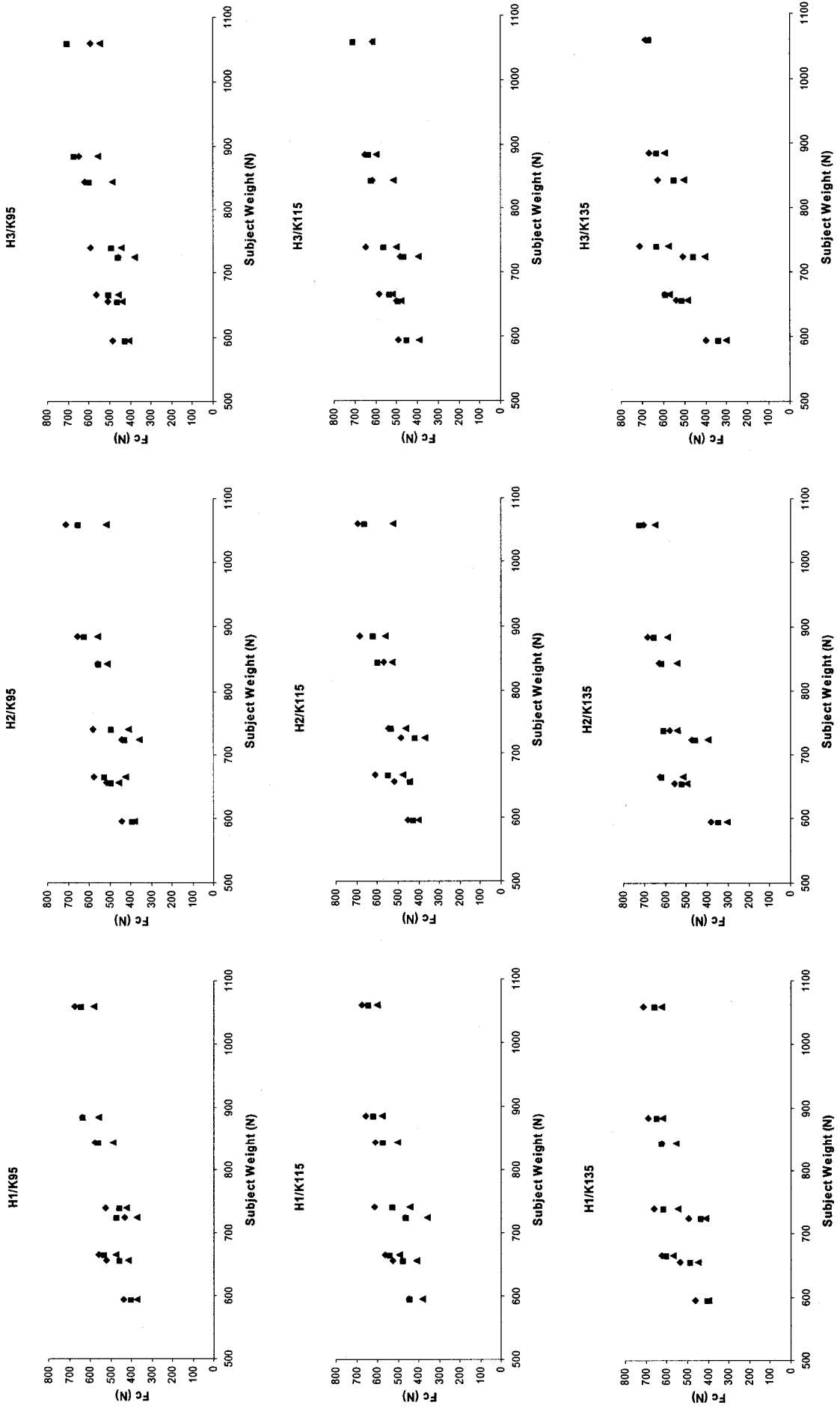


Figure A1.1: Effect of backrest angle on the seat-pan contact force of seat 1 ◆ B1 - 5° ■ B2 - 15° ▲ B3 - 25°

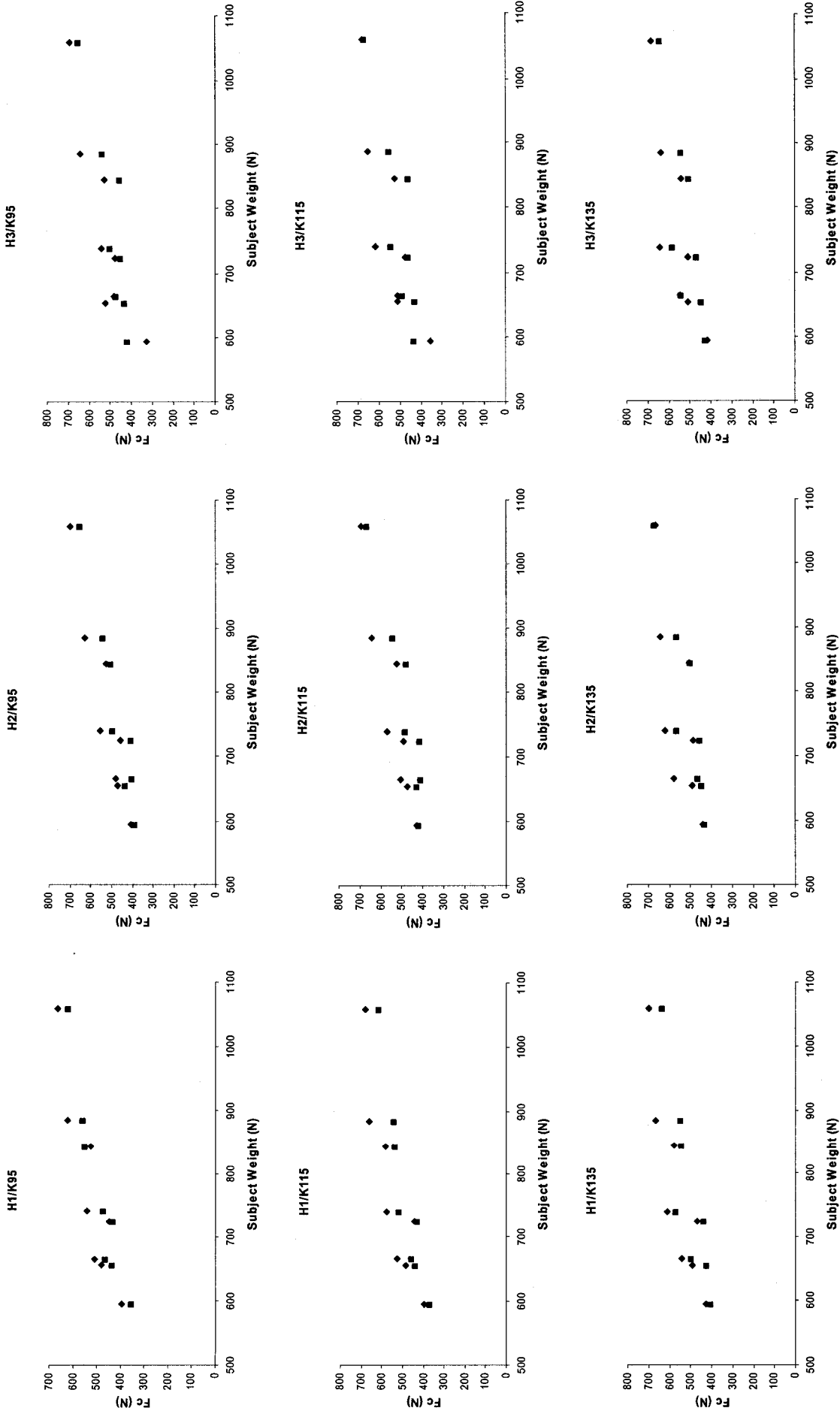


Figure A1.2: Effect of back angle on the seat-pan contact force of seat 2 ◆ B2 - 15° ■ B3 - 25°

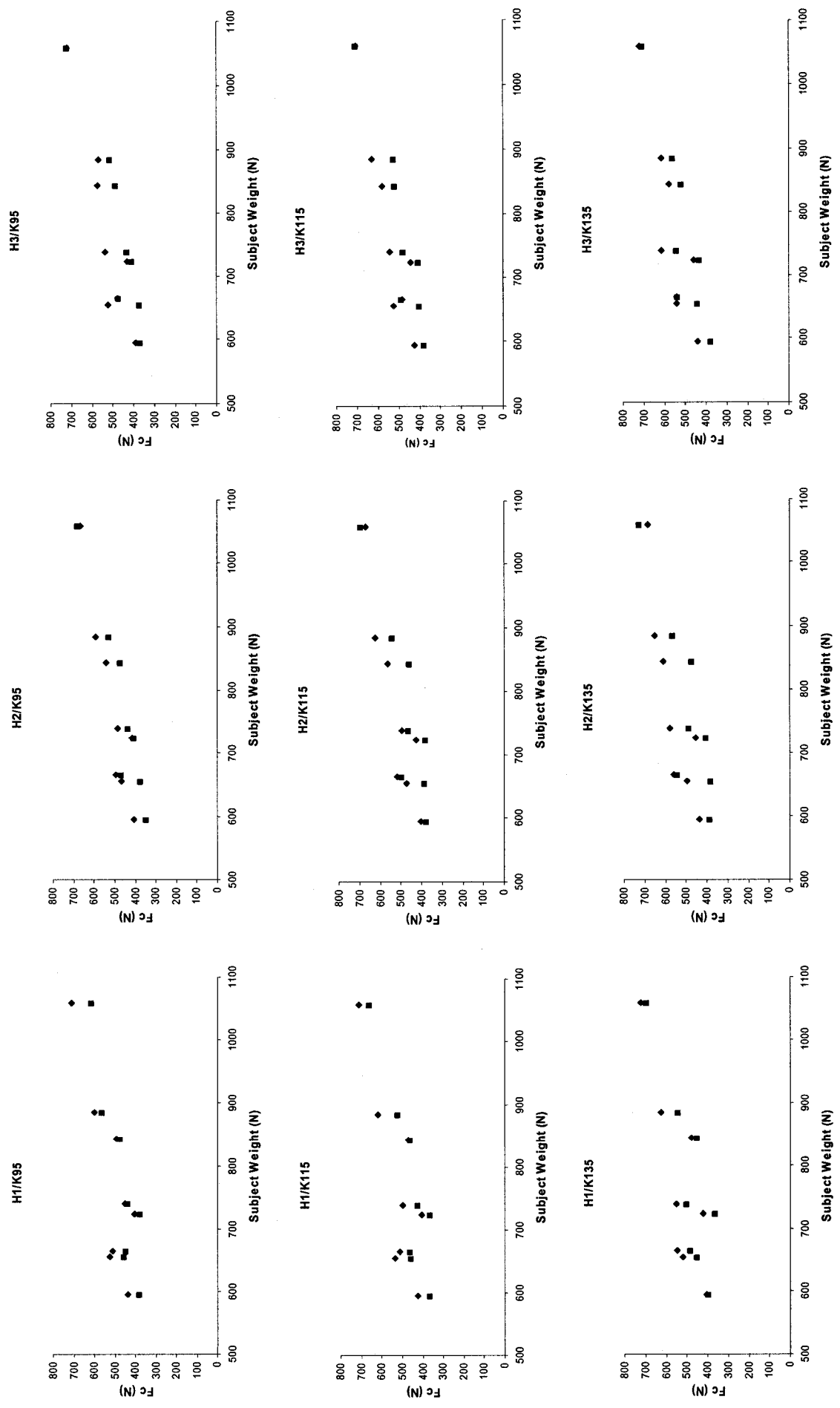


Figure A1.3: Effect of back angle on the seat-pan contact force of seat 3 ♦ B2 - 15° ■ B3 - 25°

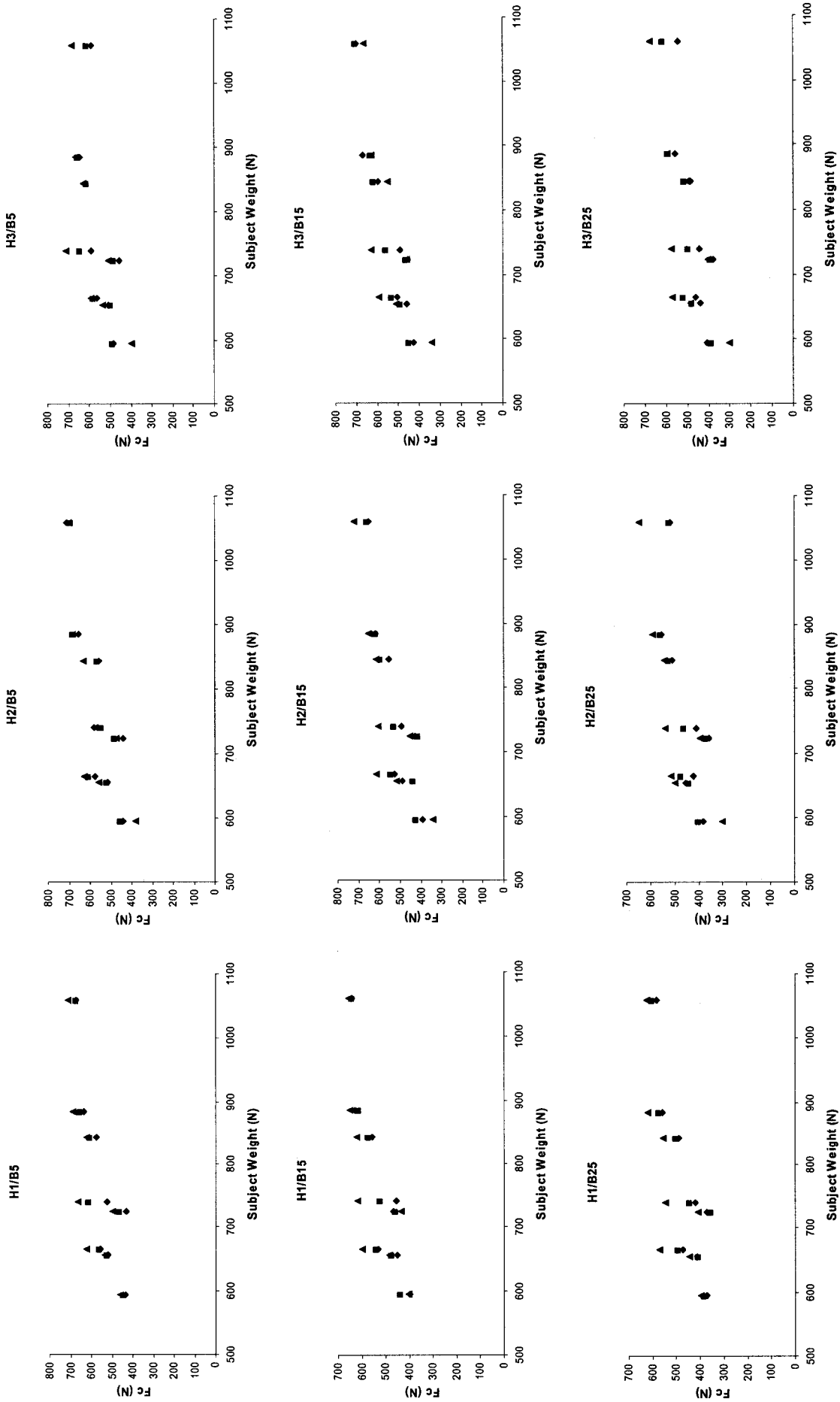


Figure A1.4: Effect of knee angle on the seat-pan contact force of seat 1 ◆ K1 - 95° ■ K2 - 115° ▲ K3 - 135°

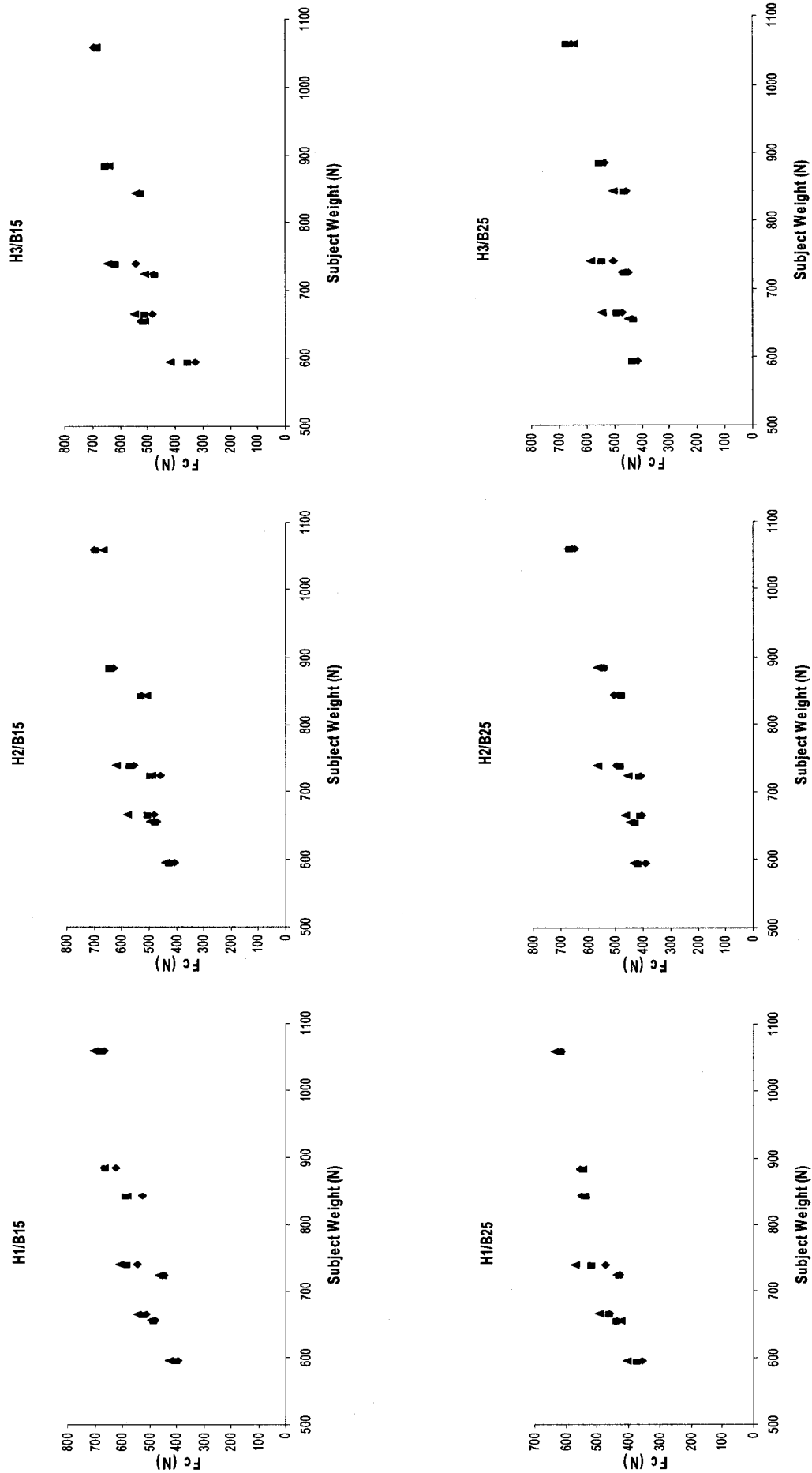


Figure A1.5: Effect of knee angle on the seat-pan contact force of seat 2 ◆ K1 - 95° ■ K2 - 115° ▲ K3 - 135°

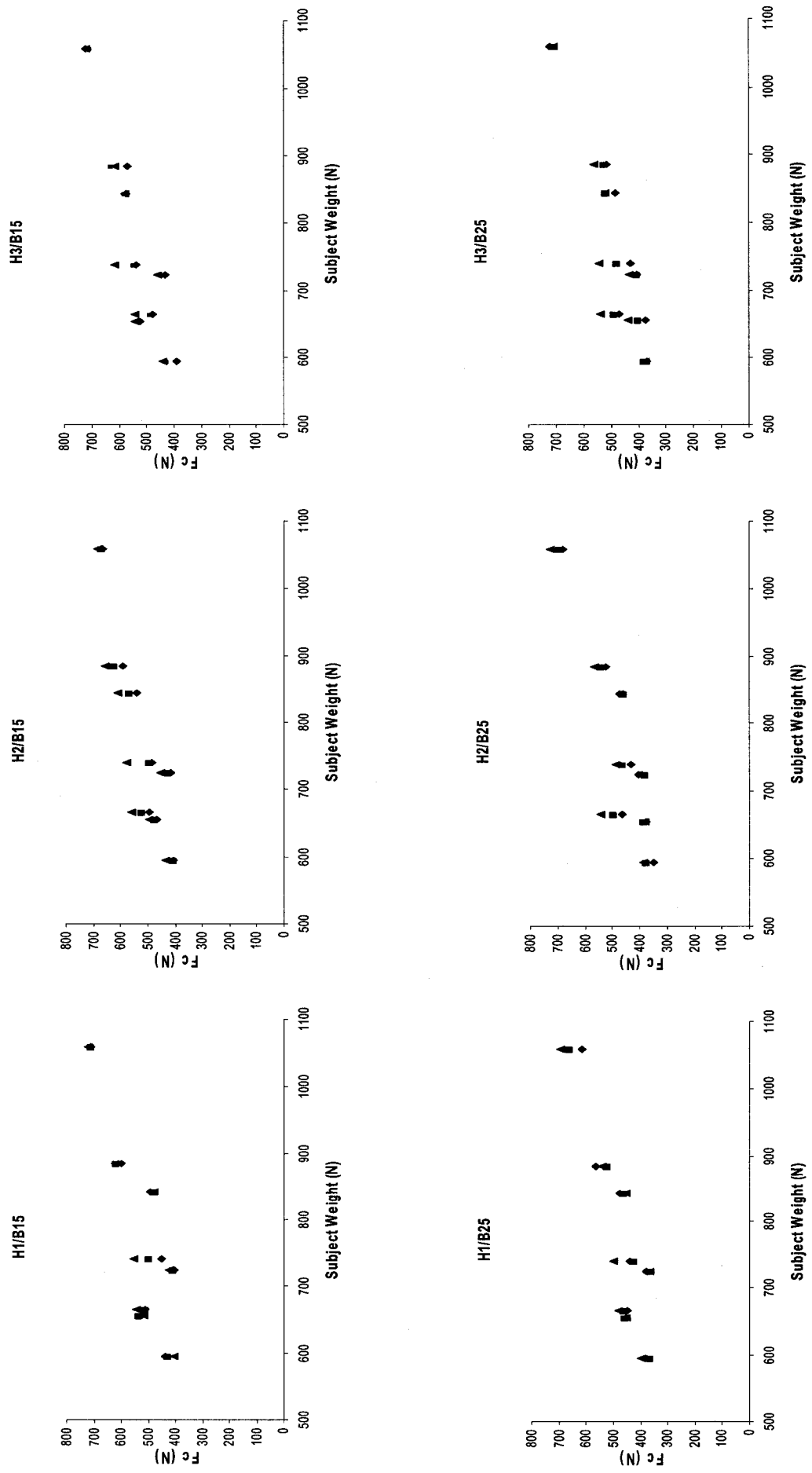


Figure A1.6: Effect of knee angle on the seat-pan contact force of seat 3 ♦ K1 - 95° ■ K2 - 115° ▲ K3 - 135°

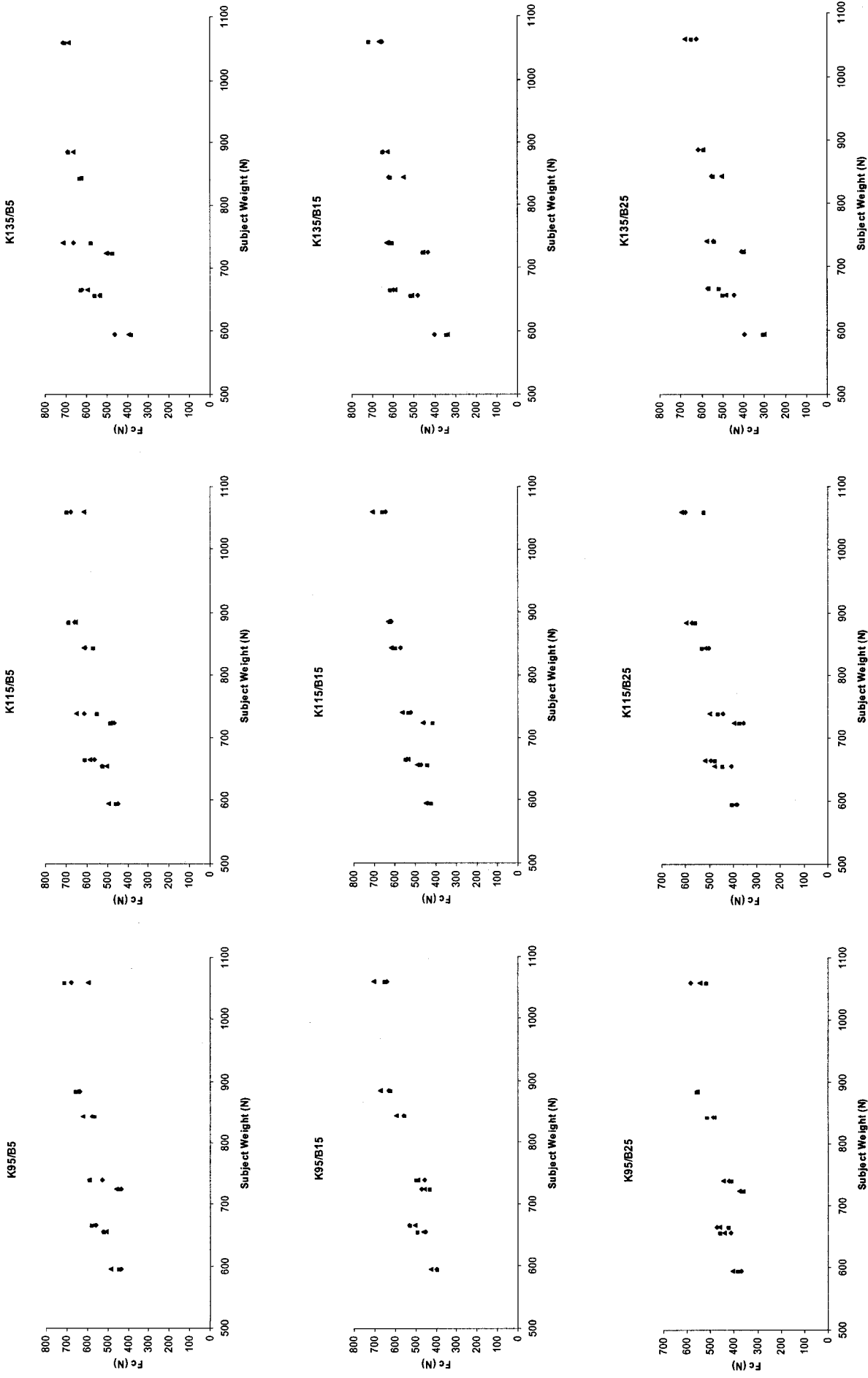


Figure A1.7: Effect of seat height on the seat-pan contact force of seat 1 (◆H1 – 318mm ■ H2 – 368 mm ▲ H3 – 419 mm)

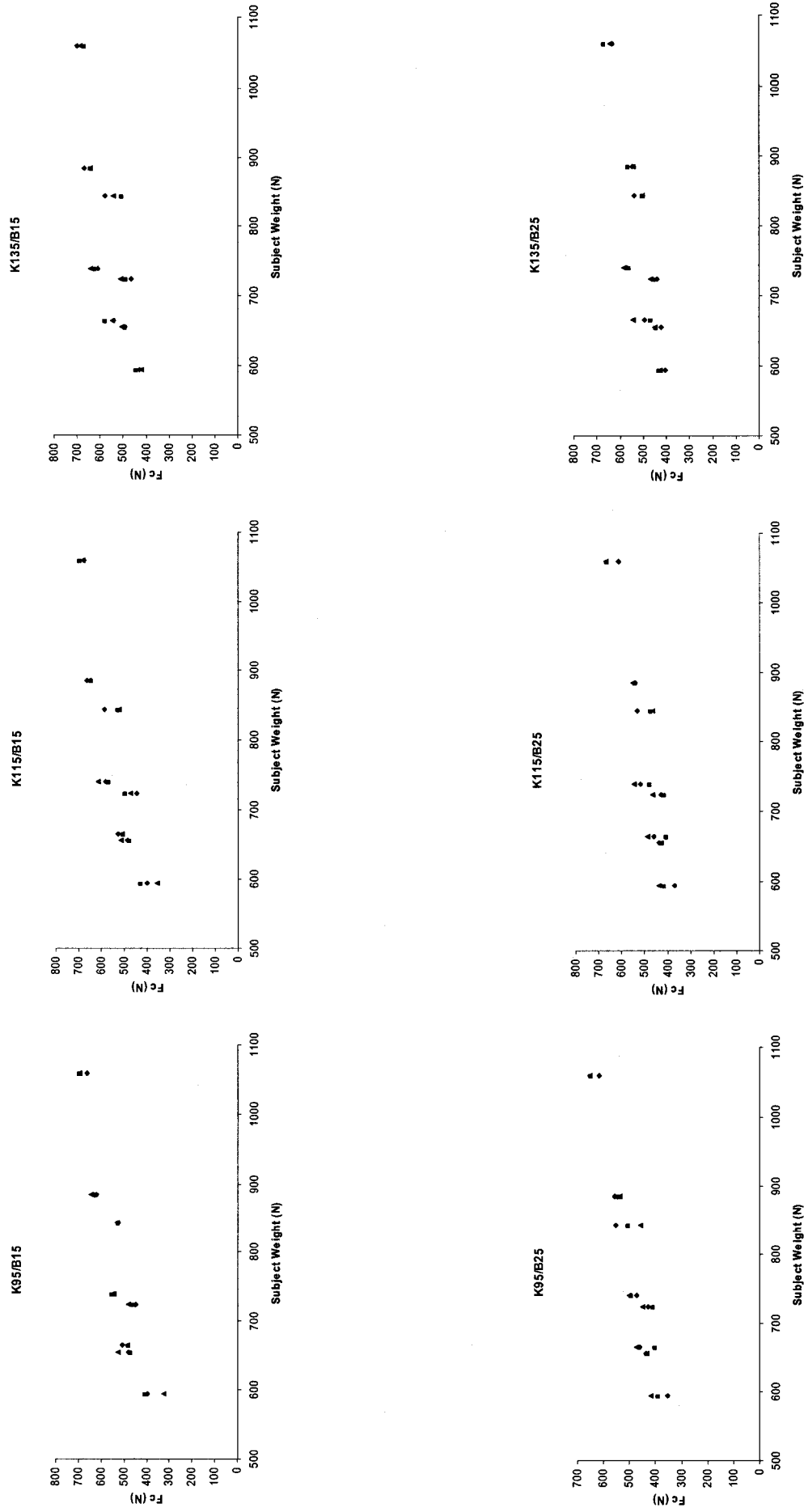


Figure A1.8: Effect of seat height on the seat-pan contact force of seat 2 (◆H1 – 318mm ■ H2 – 368 mm ▲H3 – 419 mm)



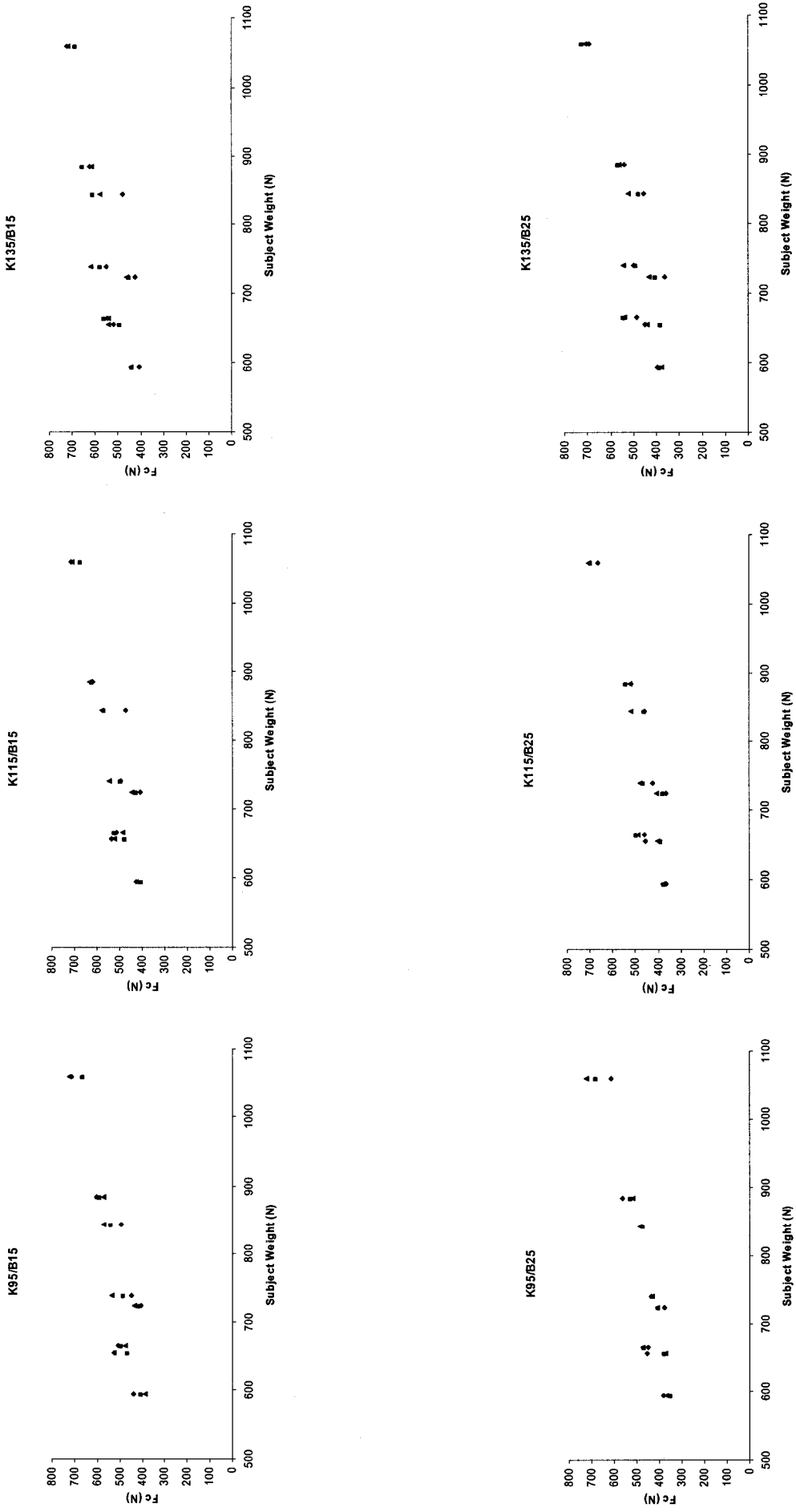


Figure A1.9: Effect of seat height on the seat-pan contact force of seat 3 (♦ H1 – 318mm ■ H2 – 368 mm ▲ H3 – 419 mm)

## **APPENDIX – A2**

### **SEAT-PAN PEAK PRESSURE VARIATIONS**

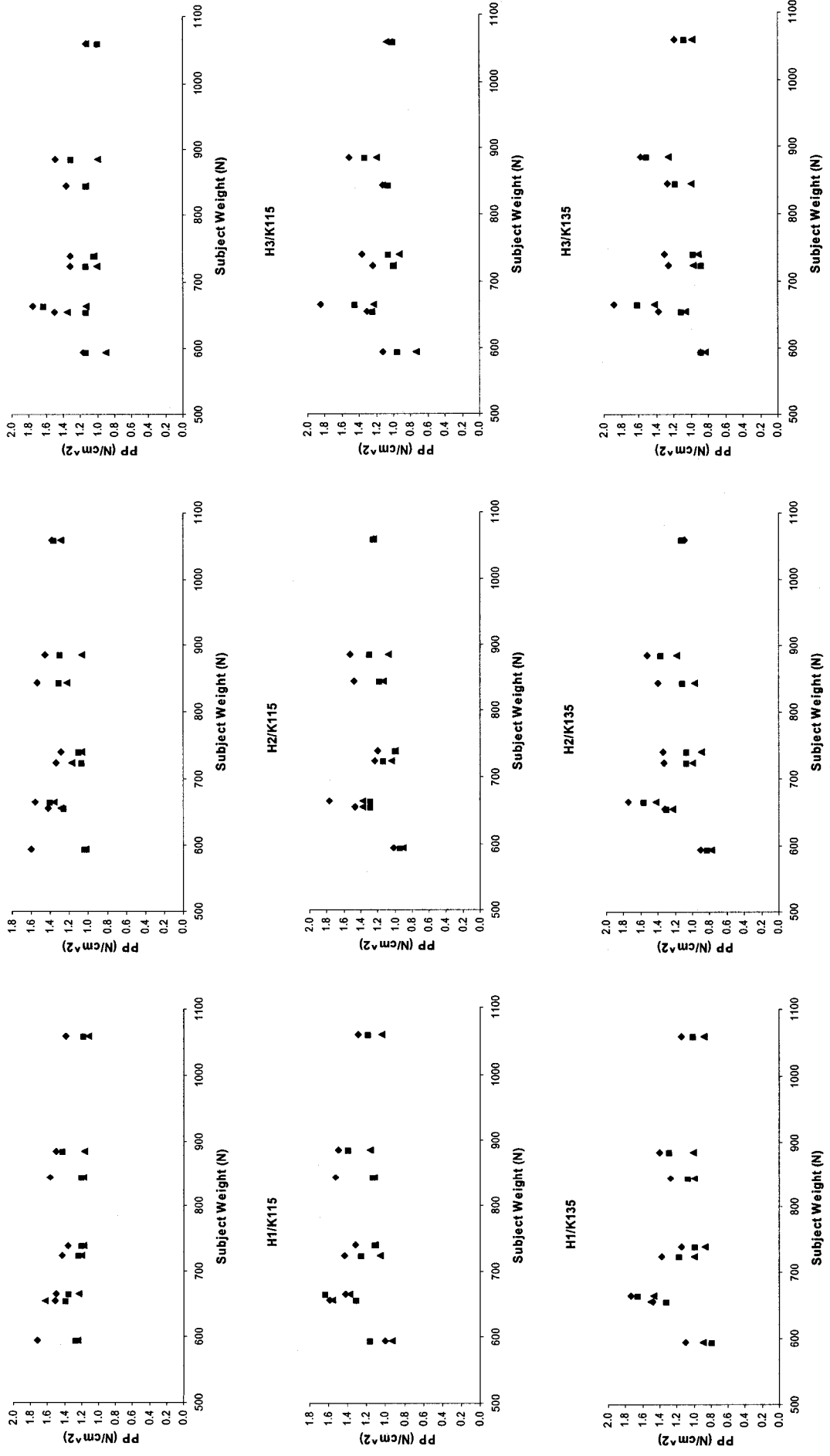


Figure A2.1: Effect of backrest angle on Peak Pressure seat 1 ◆ B1 - 5° ■ B2 - 15° ▲ B3 - 25°

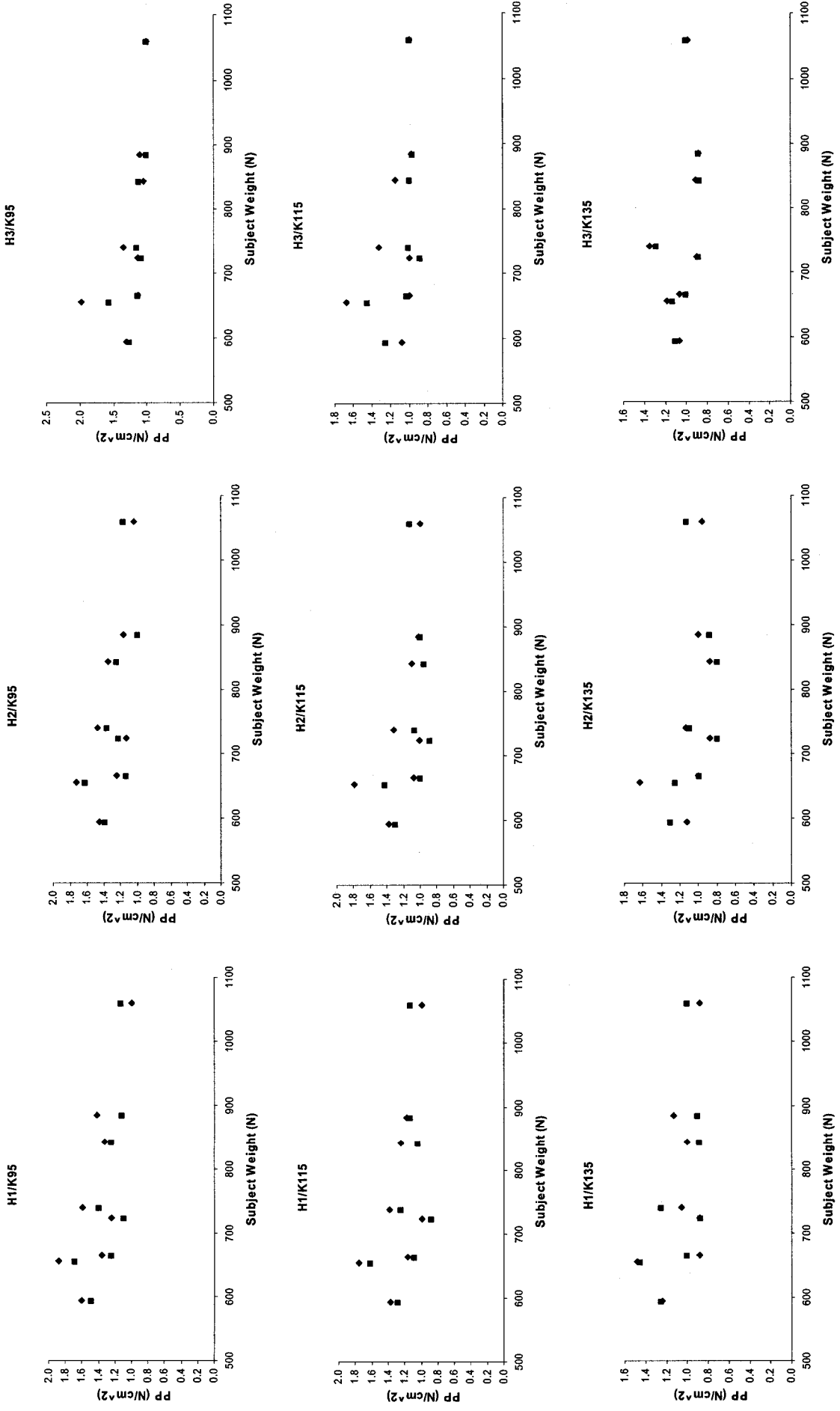


Figure A2.2: Effect of backrest angle on Peak Pressure seat 2    ♦ B2 - 15°    ■ B3 - 25°

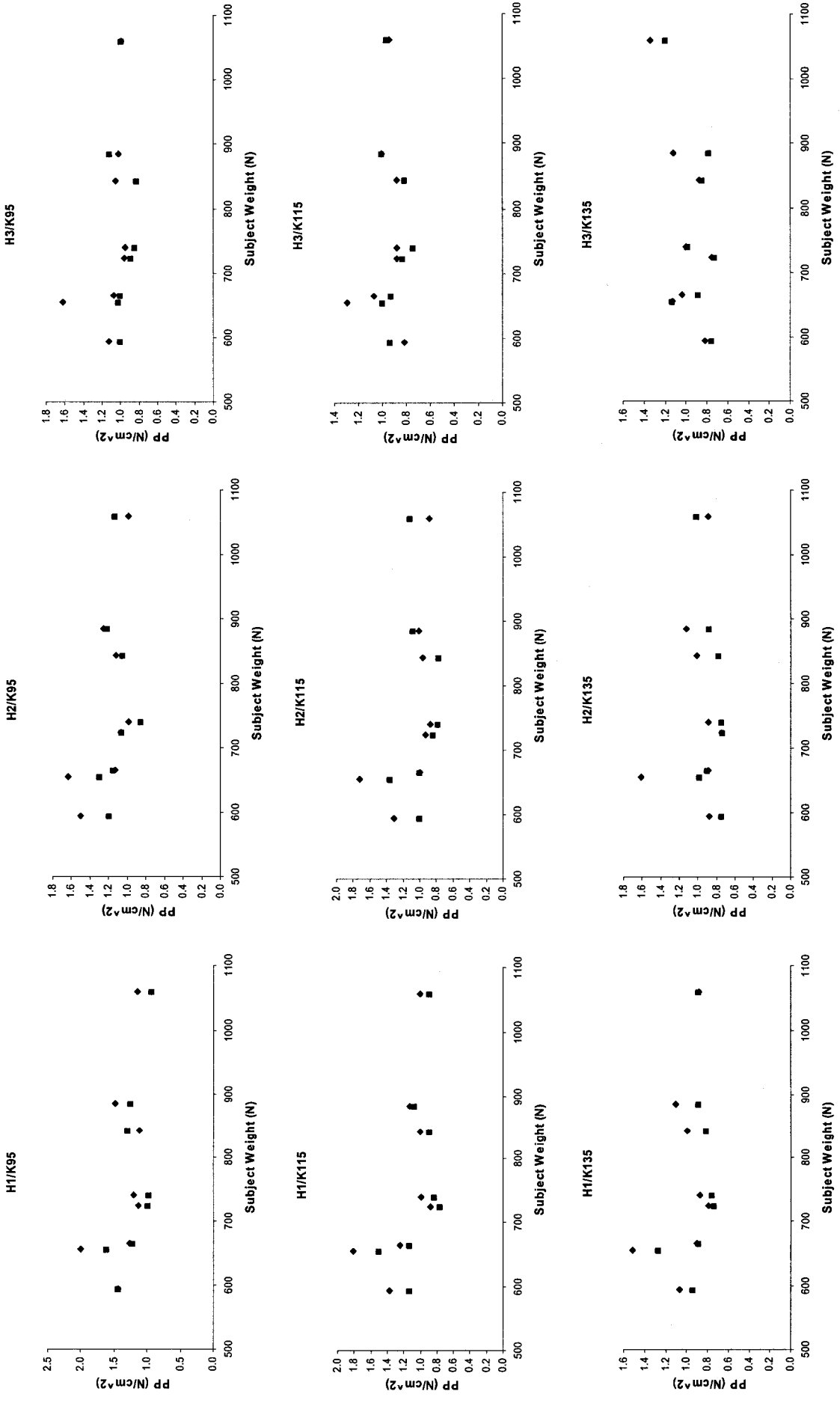


Figure A2.3: Effect of backrest angle on Peak Pressure seat 3 ◆ B2 - 15° ■ B3 - 25°

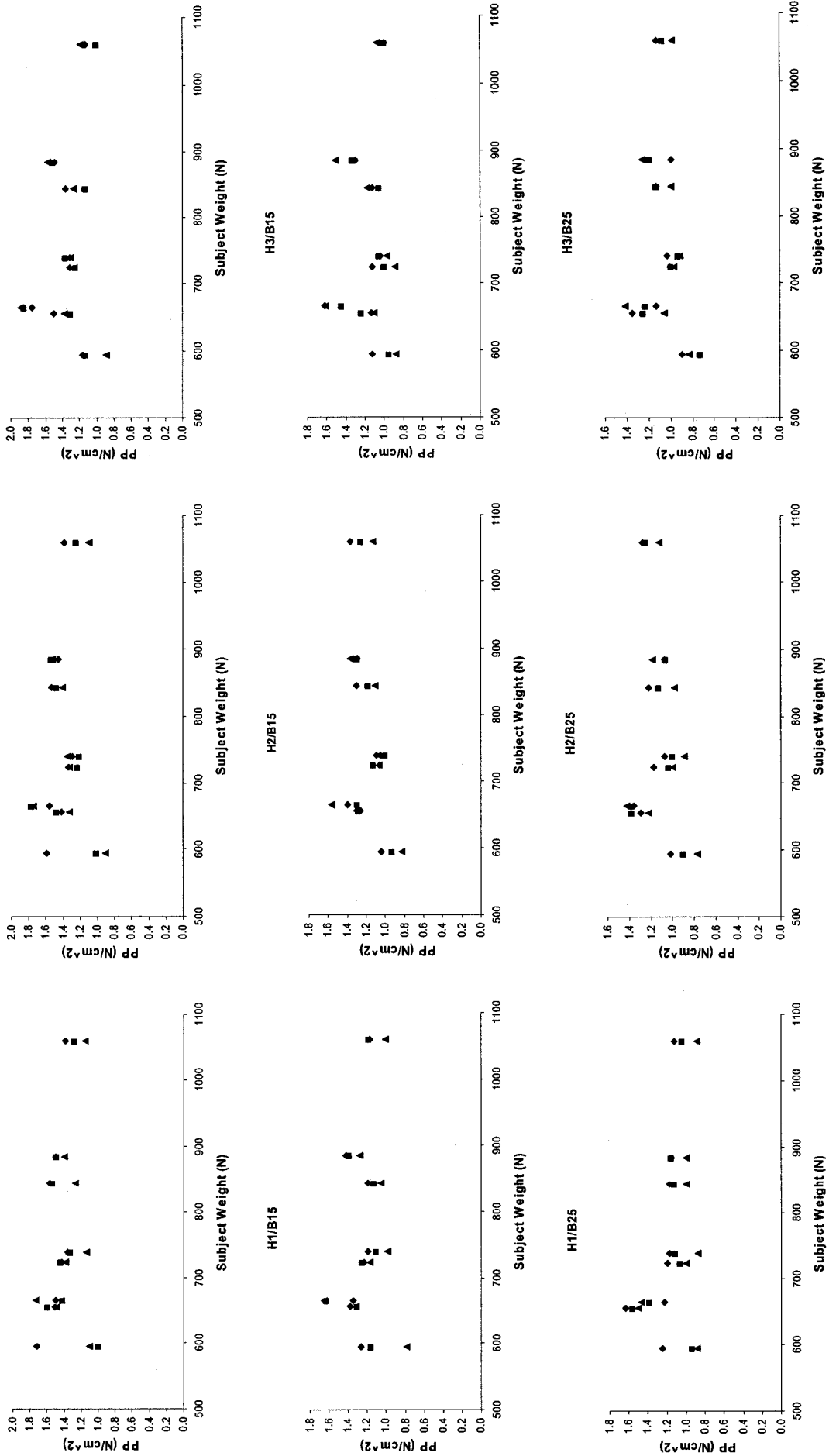


Figure A2.4: Peak pressure variations as a function of seat height for seat 1 ♦ K1 - 95° ■ K2 - 115° ▲ K3 - 135°

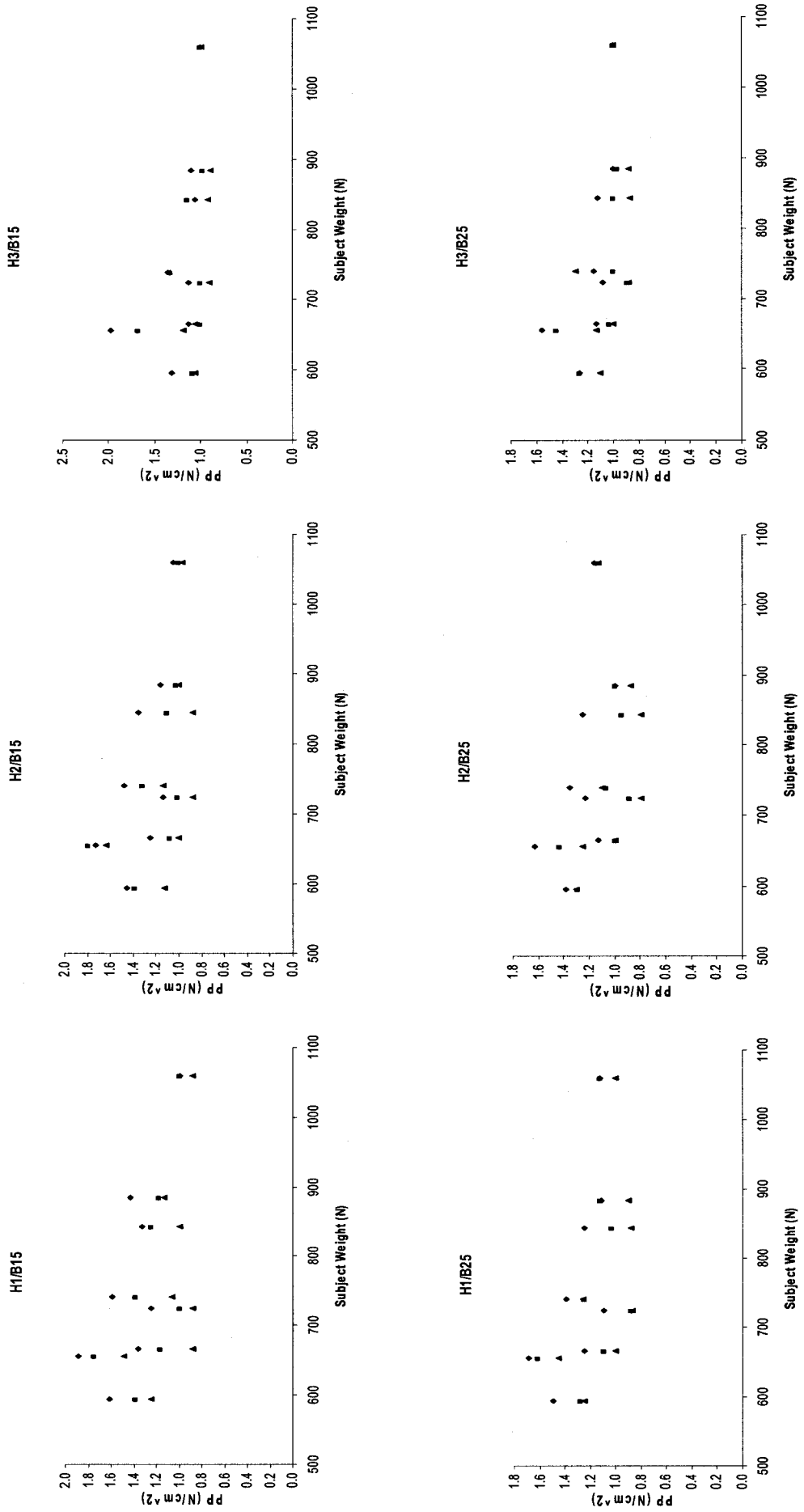


Figure A2.5: Effect of knee angle on the seat-pan peak pressure of seat 2 ◆ K1 - 95° ■ K2 - 115° ▲ K3 - 135°

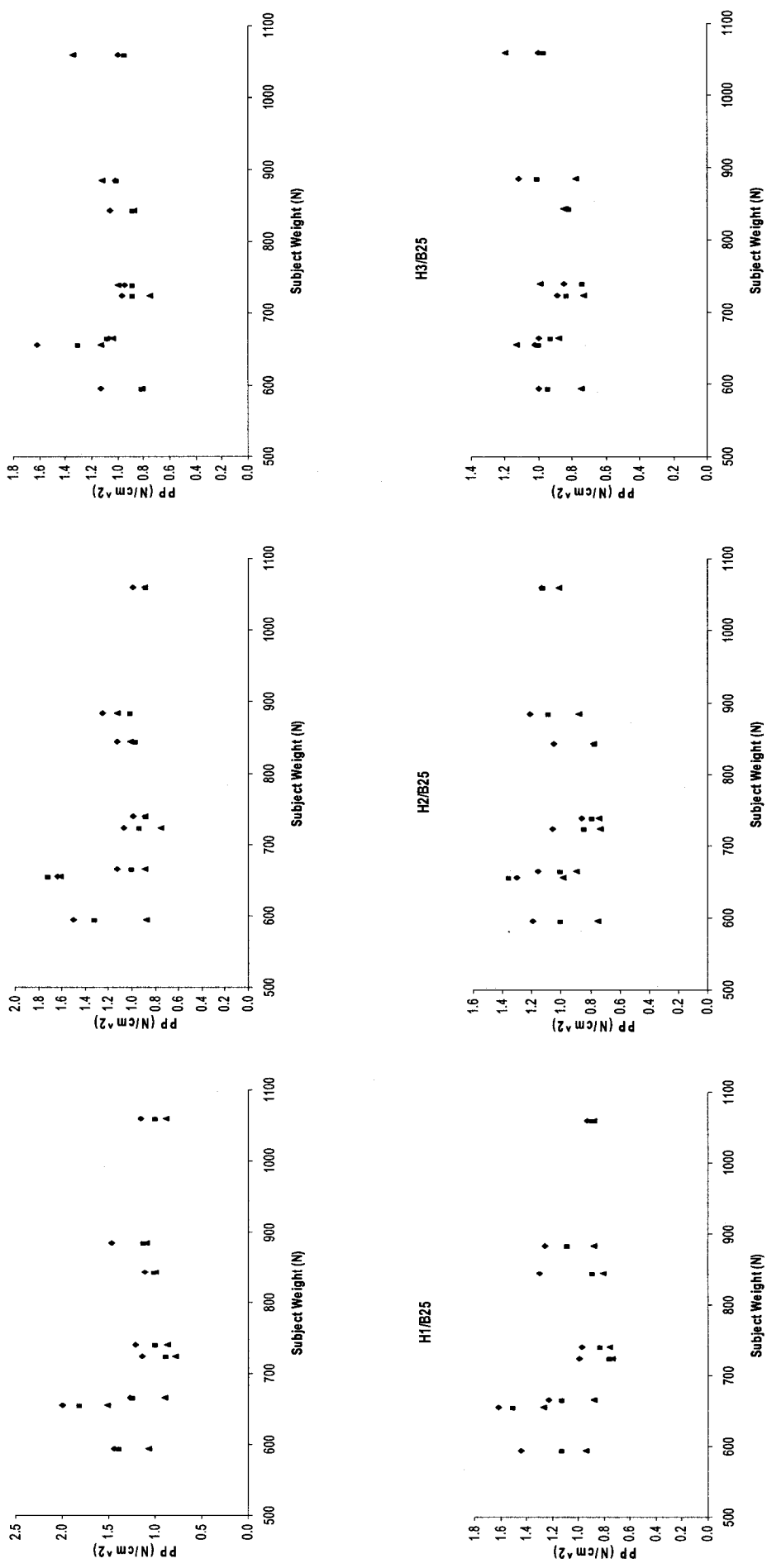


Figure A2.6: Effect of knee angle on the seat-pan peak pressure of seat 3 ♦ K1 - 95° ■ K2 - 115° ▲ K3 - 135



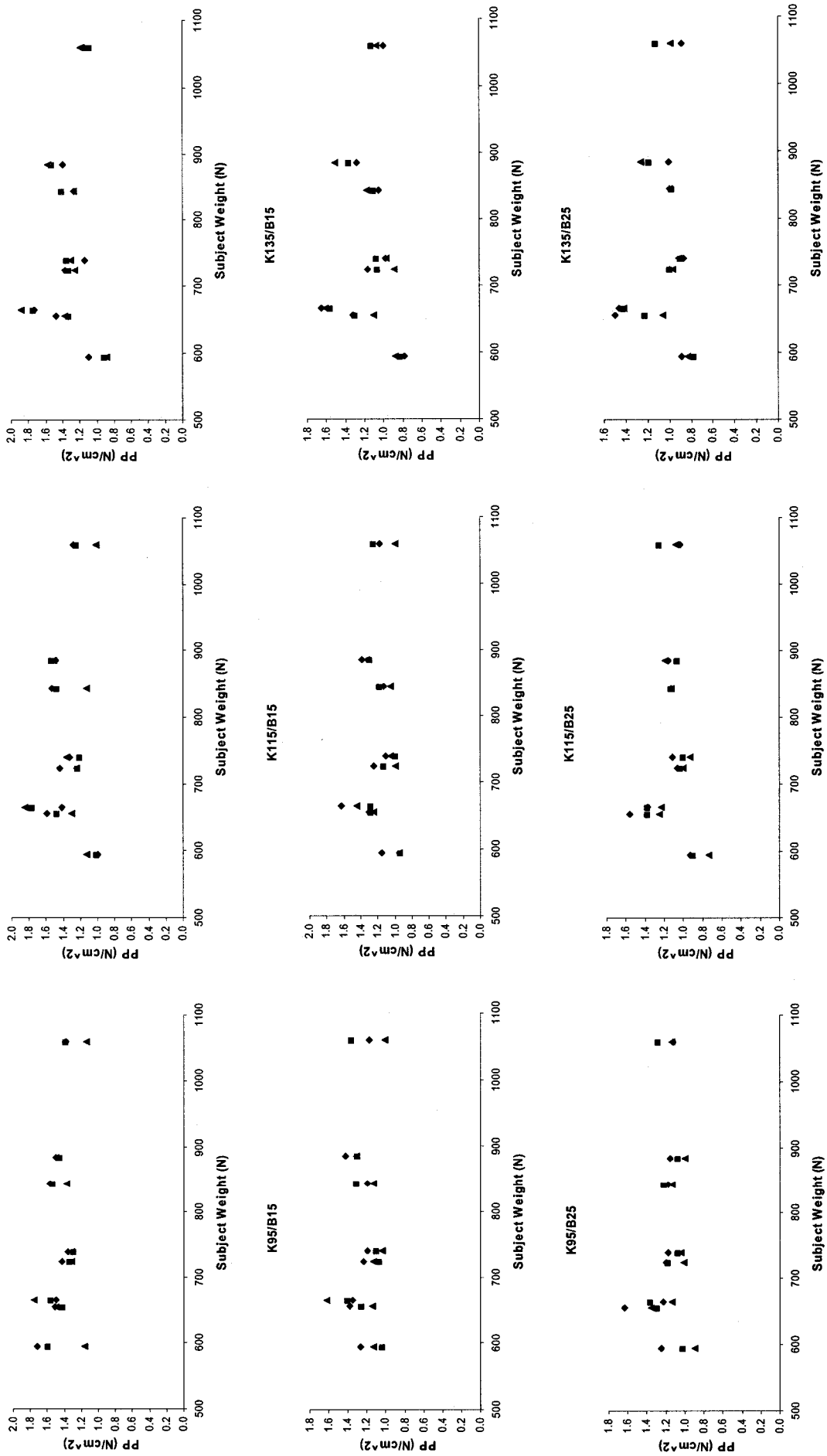


Figure A2.7: Peak pressure variations as a function of seat height for seat 1 ◆ H1 - 318 mm ■ H2 - 368 mm ▲ H3 - 419 mm

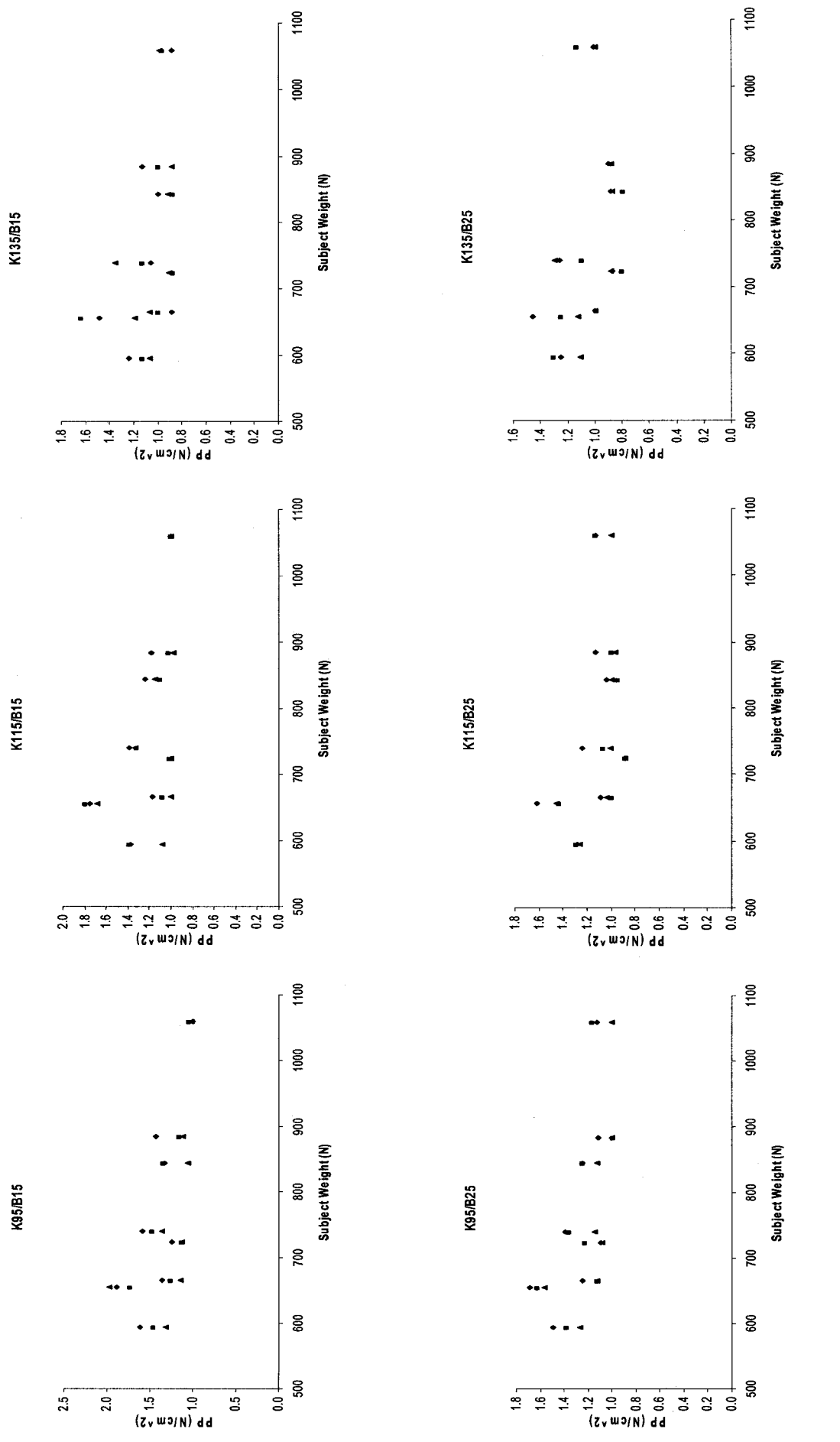


Figure A2.8: Peak pressure variations as a function of seat height for seat 2 ♦ H1 - 318 mm ■ H2 - 368 mm ▲ H3 - 419 mm

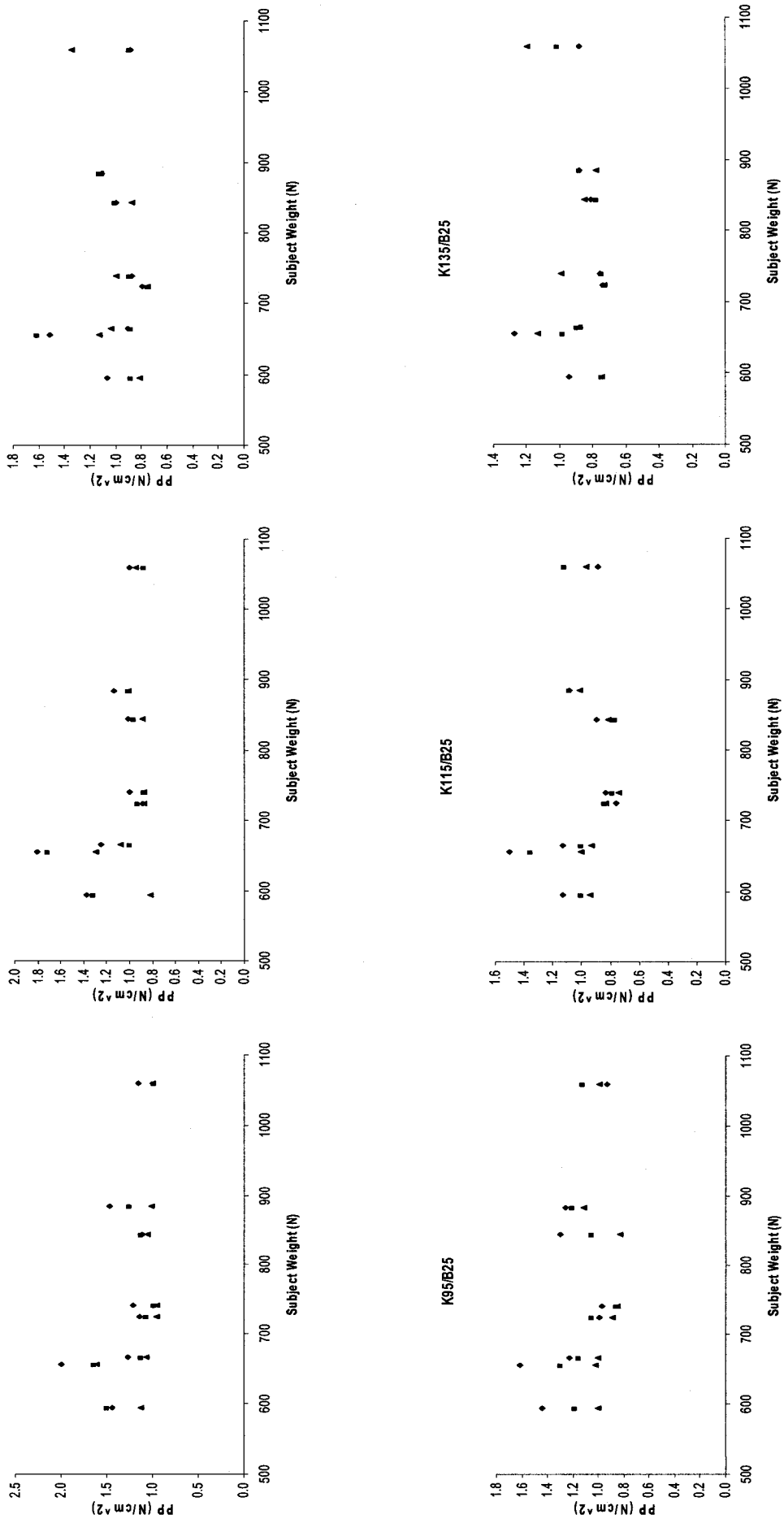


Figure A2.9: Peak pressure variations as a function of seat height for seat 3 ♦ H1 - 318 mm ■ H2 - 368 mm ▲ H3 - 419 mm

## **APPENDIX - B**

### **STATISTICAL ANALYSES**

## **APPENDIX – B1**

### **Sample SPSS Output of the Analysis of Variance for the Measured Seat-Pan Contact Force for Seats 1, 2 and 3**

Table B1-1: Within-Subject ANOVA for the Seat-Pan Contact Force

Tests of Within-Subjects Effects

Measure: Seat-Pan Contact Force

Source		Type III Sum of Squares	df	Mean Square	F	Sig.
SEAT	Sphericity Assumed	10872.462	2	5436.231	.655	.535
	Greenhouse-Geisser	10872.462	1.959	5548.701	.655	.532
	Huynh-Feldt	10872.462	2.000	5436.231	.655	.535
	Lower-bound	10872.462	1.000	10872.462	.655	.445
Error(SEAT)	Sphericity Assumed	116142.846	14	8295.918		
	Greenhouse-Geisser	116142.846	13.716	8467.551		
	Huynh-Feldt	116142.846	14.000	8295.918		
	Lower-bound	116142.846	7.000	16591.835		
HEIGHT	Sphericity Assumed	14273.734	2	7136.867	5.991	.013
	Greenhouse-Geisser	14273.734	1.296	11015.693	5.991	.031
	Huynh-Feldt	14273.734	1.467	9732.213	5.991	.025
	Lower-bound	14273.734	1.000	14273.734	5.991	.044
Error(HEIGHT)	Sphericity Assumed	16678.787	14	1191.342		
	Greenhouse-Geisser	16678.787	9.070	1838.826		
	Huynh-Feldt	16678.787	10.267	1624.577		
	Lower-bound	16678.787	7.000	2382.684		
KNEE	Sphericity Assumed	92207.943	2	46103.971	9.083	.003
	Greenhouse-Geisser	92207.943	1.072	86051.605	9.083	.017
	Huynh-Feldt	92207.943	1.109	83174.478	9.083	.016
	Lower-bound	92207.943	1.000	92207.943	9.083	.020
Error(KNEE)	Sphericity Assumed	71065.444	14	5076.103		
	Greenhouse-Geisser	71065.444	7.501	9474.386		
	Huynh-Feldt	71065.444	7.760	9157.611		
	Lower-bound	71065.444	7.000	10152.206		
BACK	Sphericity Assumed	291570.423	1	291570.423	84.115	.000
	Greenhouse-Geisser	291570.423	1.000	291570.423	84.115	.000
	Huynh-Feldt	291570.423	1.000	291570.423	84.115	.000
	Lower-bound	291570.423	1.000	291570.423	84.115	.000
Error(BACK)	Sphericity Assumed	24264.212	7	3466.316		
	Greenhouse-Geisser	24264.212	7.000	3466.316		
	Huynh-Feldt	24264.212	7.000	3466.316		
	Lower-bound	24264.212	7.000	3466.316		
SEAT * HEIGHT	Sphericity Assumed	2653.623	4	663.406	.364	.832
	Greenhouse-Geisser	2653.623	2.277	1165.390	.364	.727
	Huynh-Feldt	2653.623	3.433	772.869	.364	.805
	Lower-bound	2653.623	1.000	2653.623	.364	.565
Error(SEAT*HEIGHT)	Sphericity Assumed	51045.795	28	1823.064		
	Greenhouse-Geisser	51045.795	15.939	3202.537		
	Huynh-Feldt	51045.795	24.034	2123.873		
	Lower-bound	51045.795	7.000	7292.256		

SEAT * KNEE	Sphericity Assumed	2150.333	4	537.583	.441	.778
	Greenhouse-Geisser	2150.333	1.231	1746.267	.441	.565
	Huynh-Feldt	2150.333	1.361	1579.960	.441	.583
	Lower-bound	2150.333	1.000	2150.333	.441	.528
Error(SEAT*KNEE)	Sphericity Assumed	34155.004	28	1219.822		
	Greenhouse-Geisser	34155.004	8.620	3962.427		
	Huynh-Feldt	34155.004	9.527	3585.062		
	Lower-bound	34155.004	7.000	4879.286		
HEIGHT * KNEE	Sphericity Assumed	3300.447	4	825.112	2.769	.047
	Greenhouse-Geisser	3300.447	2.596	1271.237	2.769	.078
	Huynh-Feldt	3300.447	4.000	825.112	2.769	.047
	Lower-bound	3300.447	1.000	3300.447	2.769	.140
Error(HEIGHT*KNEE)	Sphericity Assumed	8342.855	28	297.959		
	Greenhouse-Geisser	8342.855	18.174	459.061		
	Huynh-Feldt	8342.855	28.000	297.959		
	Lower-bound	8342.855	7.000	1191.836		
SEAT * HEIGHT * KNEE	Sphericity Assumed	6838.962	8	854.870	2.233	.038
	Greenhouse-Geisser	6838.962	2.337	2926.259	2.233	.133
	Huynh-Feldt	6838.962	3.581	1909.909	2.233	.100
	Lower-bound	6838.962	1.000	6838.962	2.233	.179
Error(SEAT*HEIGHT*KN EE)	Sphericity Assumed	21441.434	56	382.883		
	Greenhouse-Geisser	21441.434	16.360	1310.625		
	Huynh-Feldt	21441.434	25.065	855.418		
	Lower-bound	21441.434	7.000	3063.062		
SEAT * BACK	Sphericity Assumed	1797.363	2	898.681	.339	.718
	Greenhouse-Geisser	1797.363	1.768	1016.615	.339	.693
	Huynh-Feldt	1797.363	2.000	898.681	.339	.718
	Lower-bound	1797.363	1.000	1797.363	.339	.579
Error(SEAT*BACK)	Sphericity Assumed	37107.787	14	2650.556		
	Greenhouse-Geisser	37107.787	12.376	2998.388		
	Huynh-Feldt	37107.787	14.000	2650.556		
	Lower-bound	37107.787	7.000	5301.112		
HEIGHT * BACK	Sphericity Assumed	782.973	2	391.487	.402	.676
	Greenhouse-Geisser	782.973	1.523	514.110	.402	.625
	Huynh-Feldt	782.973	1.859	421.100	.402	.662
	Lower-bound	782.973	1.000	782.973	.402	.546
Error(HEIGHT*BACK)	Sphericity Assumed	13628.663	14	973.476		
	Greenhouse-Geisser	13628.663	10.661	1278.393		
	Huynh-Feldt	13628.663	13.015	1047.112		
	Lower-bound	13628.663	7.000	1946.952		
SEAT * HEIGHT * BACK	Sphericity Assumed	1173.361	4	293.340	.309	.870
	Greenhouse-Geisser	1173.361	2.381	492.763	.309	.774
	Huynh-Feldt	1173.361	3.691	317.871	.309	.856
	Lower-bound	1173.361	1.000	1173.361	.309	.596
Error(SEAT*HEIGHT*BA CK)	Sphericity Assumed	26592.717	28	949.740		
	Greenhouse-Geisser	26592.717	16.668	1595.406		
	Huynh-Feldt	26592.717	25.839	1029.162		

	Lower-bound	26592.717	7.000	3798.960		
KNEE * BACK	Sphericity Assumed	903.092	2	451.546	1.496	.258
	Greenhouse-Geisser	903.092	1.285	702.767	1.496	.262
	Huynh-Feldt	903.092	1.449	623.292	1.496	.262
	Lower-bound	903.092	1.000	903.092	1.496	.261
Error(KNEE*BACK)	Sphericity Assumed	4226.290	14	301.878		
	Greenhouse-Geisser	4226.290	8.995	469.830		
	Huynh-Feldt	4226.290	10.142	416.698		
	Lower-bound	4226.290	7.000	603.756		
SEAT * KNEE * BACK	Sphericity Assumed	2926.546	4	731.637	2.933	.038
	Greenhouse-Geisser	2926.546	2.903	1008.249	2.933	.059
	Huynh-Feldt	2926.546	4.000	731.637	2.933	.038
	Lower-bound	2926.546	1.000	2926.546	2.933	.131
Error(SEAT*KNEE*BAC K)	Sphericity Assumed	6984.277	28	249.438		
	Greenhouse-Geisser	6984.277	20.318	343.745		
	Huynh-Feldt	6984.277	28.000	249.438		
	Lower-bound	6984.277	7.000	997.754		
HEIGHT * KNEE * BACK	Sphericity Assumed	1631.428	4	407.857	1.619	.197
	Greenhouse-Geisser	1631.428	1.454	1121.788	1.619	.241
	Huynh-Feldt	1631.428	1.737	939.064	1.619	.237
	Lower-bound	1631.428	1.000	1631.428	1.619	.244
Error(HEIGHT*KNEE*BA CK)	Sphericity Assumed	7052.524	28	251.876		
	Greenhouse-Geisser	7052.524	10.180	692.770		
	Huynh-Feldt	7052.524	12.161	579.927		
	Lower-bound	7052.524	7.000	1007.503		
SEAT * HEIGHT * KNEE * BACK	Sphericity Assumed	2371.459	8	296.432	1.352	.238
	Greenhouse-Geisser	2371.459	3.073	771.776	1.352	.284
	Huynh-Feldt	2371.459	5.750	412.427	1.352	.259
	Lower-bound	2371.459	1.000	2371.459	1.352	.283
Error(SEAT*HEIGHT*KN EE*BACK)	Sphericity Assumed	12275.187	56	219.200		
	Greenhouse-Geisser	12275.187	21.509	570.697		
	Huynh-Feldt	12275.187	40.250	304.973		
	Lower-bound	12275.187	7.000	1753.598		



## **APPENDIX – B2**

### **Sample SPSS Output of the Multiple Regression Analyses for the Seat-Pan Contact Force of Seat 1**

Figure B2-1: Multiple Regression Output for the Seat-Pan Contact Force of Seat 1

**Variables Entered/Removed(b)**

Model	Variables Entered	Variables Removed	Method
1	S_K_B, HEIGHT, KNEE, BACK, WEIGHT, S_H_K, H_K(a)		Enter

a All requested variables entered.  
b Dependent Variable: SP\_FORCE

**Model Summary**

Model	R	R Square	Adjusted R Square	Std. Error of the Estimate
1	.826(a)	.682	.671	54.65101

a Predictors: (Constant), S\_K\_B, HEIGHT, KNEE, BACK, WEIGHT, S\_H\_K, H\_K

**ANOVA(b)**

Model		Sum of Squares	df	Mean Square	F	Sig.
1	Regression	1330727.478	7	190103.925	63.649	.000(a)
	Residual	621240.416	208	2986.733		
	Total	1951967.894	215			

a Predictors: (Constant), S\_K\_B, HEIGHT, KNEE, BACK, WEIGHT, S\_H\_K, H\_K  
b Dependent Variable: SP\_FORCE

**Coefficients(a)**

Model		Unstandardized Coefficients		Standardized Coefficients	t	Sig.
		B	Std. Error	Beta		
1	(Constant)	-255.650	258.815		-988	.324
	WEIGHT	.621	.134	.925	4.622	.000
	HEIGHT	.708	.638	.309	1.110	.268
	KNEE	3.017	2.037	.518	1.482	.140
	BACK	-4.496	.822	-.386	-5.473	.000
	H_K	-.005	.006	-.381	-.849	.397
	S_H_K	-6.256E-08	.000	-.238	-1.120	.264
	S_K_B	7.052E-08	.000	.015	.151	.880

a Dependent Variable: SP\_FORCE